Advances in Soft Computing Algorithms

Research in Computing Science

Series Editorial Board
Comité Editorial de la Serie

Volume 54
Volumen 54

Advances in Soft Computing Algorithms

Volume Editors:

Ildar Batyrshin
Grigori Sidorov

Preface

The purpose of this volume is to reflect the new directions of investigation in the areas of Computer Science related to Artificial Intelligence (AI), and more specifically, this issue is focused on algorithms that are based on AI in different ways.

Papers for this volume were carefully selected by volume editors on the basis of the blind reviewing process performed by editorial board members and additional reviewers. The main criteria for selection were their originality and technical quality.

This issue of the journal Research in Computing Science can be interesting for researchers and students in computer science, especially in areas related to artificial intelligence, and also for persons who are interested in cutting edge themes of the computer science. Each submission was reviewed by three independent members of the editorial board of the volume or additional reviewers.

This volume contains revised versions of 25 accepted papers. The papers are structured into the following six sections:

- Image Processing and Pattern Recognition (6 papers),
- Ontologies, Logic and Multi-agent Systems (3 papers),
- Natural Language Processing (3 papers),
- Evolutionary Algorithms and Process Optimization (4 papers),
- Bioinformatics and Medical Applications (4 papers),
- Robotics, Planning and Scheduling (5 papers).

As usual, the main topics of the papers reflect the tendencies in the current state of art in Artificial Intelligence, or we can say that they represent the research lines that are "in fashion" or have major demand in the area of practical applications.

This volume is a result of work of many people. In the first place, we thank the authors of the papers included in this volume for the technical excellence of their papers that assures the high quality of this publication. We also thank the members of the International Editorial Board of the volume and the additional reviewers for their hard work consisting in selection of the best papers out of many submissions that were received.

The submission, reviewing, and selection process was performed on the basis of the free system EasyChair, www.EasyChair.org.

November, 2011

Ildar Batyrshin
Grigori Sidorov

Table of Contents
Índice

Natural Language Processing

Evolutionary Algorithms and Process Optimization

Bioinformatics and Medical Applications

Robotics, Planning and Scheduling

Image Processing and Pattern Recognition

Automatic Recognition of Human Activities under Variable Lighting

Jaime R. Ruiz[1], Leopoldo Altamirano[2], Eduardo F. Morales[3], Adrián León[4], and Jesús A. González[5]

{jrruiz[1] ,robles[2] ,emorales[3] ,enthe[4] ,jagonzalez[5] }@ccc.inaoep.mx

Department of Computer Science
National Institute of Astrophysics, Optics, and Electronics
Luis Enrique Erro #1, Sta. Maria Tonantzintla,C.P. 72840
Puebla, Mexico.
Tel.:+52 222 266 3100, ext, 8303; Fax: +52 222 266 3152.

Abstract. The recognition of activities plays an important role as part of the analysis of human behavior in video sequences. It is desirable that monitoring systems may accomplish their task in conditions different to the training ones. A novel method is proposed for activity recognition on variable lighting. The method starts with an automatic segmentation procedure to locate the person. It takes the advantage of Harris and Harris-Laplace operators of capturing information in spite of extreme changing lighting to locate corners along the human body. Corners are followed through the images to generate a set of trajectories that represent the behavior of the human. The method shows its effectiveness recognizing behaviors by a comparison procedure based on dynamic time warping, and also working well with examples of activities under different lighting.

1   Introduction

The analysis of human behavior has taken great importance in modern surveillance systems, due to its application for video analysis, elderly care, video retrieval, among others.

In the last decade, the demand for systems capable of interpret human behavior in video sequences and capable of operating correctly under variable lighting conditions has been an unsolved challenge.

This capability depends directly on the performance of an algorithm to determine the location of a person on the scene and to follow it through the next images in the video sequence. This tracking information is not enough for determining what the person does at the place. If the algorithm can obtain consistent information, we need after that a learning phase that defines how the information will be represented, and how a model will be constructed to represent the individuals' activities, and in later steps to identify similar activities.

A big effort has been dedicated, and a lot of works have been proposed to accomplish this work. Some of the methods involve to determine activities based

in the human body's form, principally based on silhouettes, to determine what the person did at the place of analysis [15,8,1], or if the activity is normal or not, [12,6]. These approaches do not work on scenes with variable lighting.

Other works like [16,2,5] are able to recognize activities according to the person's movements and consider gradual changes in environment lighting. However, these approaches consider the tracked person as a whole region. As a consequence of this simplification, they cannot distinguish activities where articulations as individuals are involved. Considering both trends, our work can do the recognition of activities based on the human body articulations taking into account a scene with variable illumination.

The method use local feature operators as a tool to segment and follow the person inside a scene. From these operators, we calculate space-time information derived from the tracking of interest points. After that the algorithm builds an activity model using the tracked points in a compact form. We choose b-splines to represent the trajectories over the scene. Once the models have been constructed, the activities are evaluated with a test set of activity sequences taken in different lighting conditions. The results show that the method can be used to recognize activities in this kind of environments.

The organization of the paper is as follows. In the section 2, the method of feature extraction and the segmentation used are described. In the section 3, we detail the representation of the trajectories obtained based on b-splines. The generation of the model and how to recognize the activities are explained in section 4. Experiments and results are presented in section 5, and conclusions are exposed in section 6.

2   Feature extraction method

2.1   Features

Follow a person under changes of illumination in a scene represents a challenge for tracking algorithms. In spite of this, there are algorithms that can be used for this purpose. These approaches works by taking into account the spatial information of the object of interest in an initialization step. Then, in subsequent frames, the algorithms calculates the new object position in the scene using data from the previous frame.

Finding out the location in the scene of the tracked person is not a hard task if we need only to know where the person is situated [16,2]. However, if we need to make an analysis based on the human body parts is essential not only to know its position in the environment but also to determine the area that it occupies in the scene with the purpose of obtaining information from different parts of its body. With these data it is possible to make an analysis using the pose of the person.

Taking into account the idea explained above,and knowing the complexity involved to do this on variable lighting conditions. We perform an exhaustive

evaluation of some interest points algorithms reported in the literature. We evaluate SIFT, Hessian-Laplace and Harris-Laplace algorithms under different degrees of illumination; the results have been showed in the table 1. According with the results, we have proposed the use of Harris-Laplace detector [11] to obtain a set of points located on several parts of the human body, and capture motion information of these. This can be seen in figure 1. An analysis about the detector Harris-Laplace allows us to know that some corners have been removed by the operator because they do not pass the selection criteria for multiples scales —[11]— therefore there is information not considered that may be helpful. As a result, to compensate this loss, we propose to use the original Harris detector [7] for getting a greater number of points on the region of interest.

	SIFT	Five Activities Harris-Laplace	Hessian-Laplace
Morning	168.6	274.4	209.6
Evening	34.8	175.4	53.6
Night	12.4	109.2	16.2

Table 1: Points number average calculated for each detector under three lighting conditions.

Fig. 1: Example of Harris-Laplace points calculated with the proposed method.

2.2   Segmentation

For exploiting the robustness of the Harris points to extreme lighting, we use them in the segmentation procedure to locate the person in scene. The method starts by applying the detectors of Harris and Harris-Laplace on the first frame, to obtain a set of points.

After that, we examine the behavior of this collection of points during the next nine frames, with the purpose of finding regions with high movement.

To do this, we work with tracking methods based on predictions capable of operating with variable lighting. In this direction, the algorithm initially proposed by Lucas and Kanade in [10], which was later fully developed by Tomasi and Kanade in [14], is used as our tracking module.

It allows the tracking of multiple points in a sequence of images as shown in [14]. There are several variants of the Kanade-Lukas-Tomasi tracker (KLT), and we use in this work its pyramidal implementation.

Once the points have been tracked, we need to determinate the regions of interest. In this case we define a threshold α to identify zones with high motion. During the frames, the algorithm accumulates the displacement calculated by the KLT tracker for each point obtained in the initial stage. If the points displacement is higher or equal to the threshold α after ten frames, then they are considered in the next phase as moving objects in the scene.

Next, to situate the person on the scene and discriminate it of others objects in movement, we employ the basic idea of the traditional segmentation methods. We suppose a minimum size β of the person as a new threshold to eliminate regions below it. After that, we can know where the person is. The general idea of segmentation procedure can be seen in the figure 2.
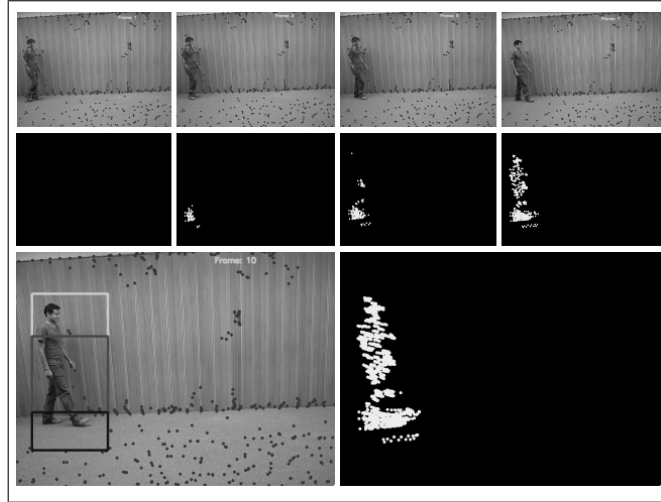
Fig. 2: Example of the segmentation procedure. First row: Motion of the points over the 1,3,5,7 frames. Second row: Points higher or equal to threshold α for 1,3,5,7 frames. Third row, left: Region of interest after ten frames (three rectangles box) and right: set of points higher or equal to threshold α after ten frames.

2.3   Tracking

Once the person position and size are determined, the next is to determine which strategy is useful to capture the motion of the body of the person being tested.

On the same line, the KLT algorithm uses Harris points calculated at the initial step to find the new location of these points on the next frames, after a period of time. This results in a set of trajectories that are taken as motion information of the human body parts. In this way, the trajectories can reflect what the person performs in the scene. The behavior of the points along the sequences is depicted in figure 3.
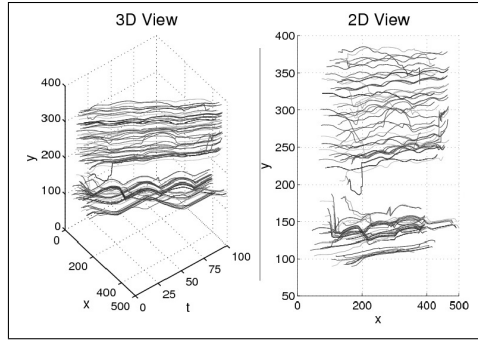
Fig. 3: Example of Harris points trajectories in the "Walk" activity. Left: spatio-temporal view for tracked points with KLT algorithm, and right: 2D projection to x and y components for tracked points.

Notice that the number of trajectories obtained from this approach may contain redundant information of different areas of the body. For this reason, we established three major regions of analysis on the size of the person, top, middle and bottom. These regions are defined at the beginning of the algorithm.

Defined the three regions, we need to determine the points that are within the limits of these to create three sets of points, $Top = \{P_1, \ldots, P_L\}$, $Middle = \{P_{L+1}, \ldots, P_M\}$ and $Bottom = \{P_{M+1}, \ldots, P_N\}$. Where N is the total of Harris points calculated when the algorithm starts.

Subsequently, the algorithm creates a central point. It can be viewed like an average of all points in each one of the sets, according to each new prediction of the tracking algorithm until the time T in which the activity ends. It is calculated through the following expressions:

$$topCP(x_t, y_t) = (\max_{i=1,\ldots,L} x_i, \sum_{i=1}^{L} y_i/L) \tag{1}$$

$$middleCP(x_t, y_t) = (\max_{i=L+1,\ldots,M} x_i, \sum_{i=L+1}^{M} y_i/(M-L)) \tag{2}$$

$$bottomCP(x_t, y_t) = (\max_{i=M+1,\dots,N} x_i, \ \sum_{i=M+1}^{N} y_i/(N-M))$$ (3)

Note that in the expressions $(1, 2, 3)$. $t = 1, \dots, T$, the position x_t is the coordinate farther in the x axis. This is the direction in which the person is moving. This is done to preserve as much detail in the trajectory generation as possible. The y_t position is the simple average of the y-coordinates of the points within each set.

Once a sequence of T frames was analyzed, we obtain three resulting curves that encode the trajectories generated by the tracking algorithm to this instant, see figure 4. In this way, the information of the different parts of the body can be processed. Based on this information we can determine the activity that the person is carrying on.
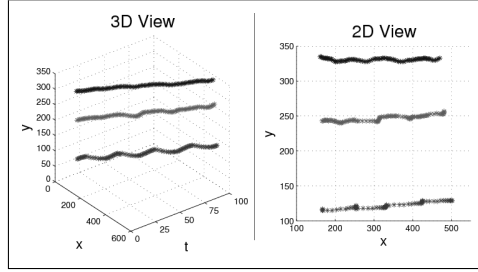
Fig. 4: Example of the central points for "Walk" activity after $T = 100$ frames. Left: spatio-temporal view for tracked points with KLT algorithm, and right: 2D projection to x and y components for tracked points.

3   Representation of trajectories

As shown in figure 4 there are variations in the resulting paths due to errors in the predictions of the tracking algorithm as a consequence of changes in lighting. Therefore, in order to have consistent information and somehow eliminating these variations in the curves produced, we propose the use of uniform cubic b-spline curves [3]. In this way we can generate a compact model based on curves, avoiding the storing of all information corresponding to the trajectories.

According to its definition, a b-spline can approximate and smooth a collection of points with the combination of a set of size P of basic polynomial functions and a collection of size P of coefficients. The b-spline provides an adjustment for the original curves.

In our study, each of the curves is parameterize by time. The algorithm generates a b-spline for all X components with respect to t and a b-spline for

Y with respect to t. At the end, the information is combined to generate the resulting curve that encodes the trajectory of each of the zones established for the analysis. As an uniform b-spline is used, we need a knot vector -[3]- evenly distributed to make the adjustment.

The procedure can be summarized as follows: The central points of each area identified -top, middle and lower- are stored in the curves $TopCurve$, $MiddleCurve$ and $BottomCurve$, respectively.

Each of these curves is then approximated and smoothed with b-spline, as previously established. In this way models are built for the top, middle and bottom zones of the person for each of the activities by eliminating the effects of different lighting conditions on the scene. The resulting curves can be seen in figure 5a.

Once patterns of activity are generated and the effects of lighting changes are eliminated, see figure 5, we must define how a new activity will be identified with respect to the activities stored.

4   Recognition of activities

Each activity consists of a set of three curves, resulting from the approximation to b-spline of the components X y Y of each curve. Due to the nature of the people's activities, an activity can be re-executed at diverse speeds either by the same person or by a different person. Therefore we must use a method that allows us to compare the shape of two curves which have different proportions. It should determine a degree of similarity between them. In this case, we use the dynamic time warping algorithm (DTW) [13] to do this comparison.

The DTW was developed for comparing two time series of different lengths and find out the similarity grade between them [13]. This technique is widely used in mathematical field [4,9]. Using these algorithms is possible to find similarities between signatures and person activities based on sensors.

It is worth to mention that it is necessary to follow the same procedure that was used for the generation of the stored models in the moment of the comparison of an unknown activity with the stored activities models. This means that we need to generate a model with three curves that represents the new behavior. For a better adjustment in the comparison step, the models and the activities to be evaluated are moved to one common point that we will call origin.

Then, we compare one by one the curves corresponding to each zone of the person. We compare the top curve of the activity that we attempt to recognize with each of the top curves of the activities that were stored as models using DTW. With this action, we obtain a degree of similarity between them. The procedure is the same for middle and lower curves.

At the end of comparison of the zones, the recognized activity will be the activity with the highest fit, i.e., activity with the highest average measure of similarity of the three zones. Thus the method can recognize activities through DTW as a measure of similarity between the models.

(a) Walk

(b) Fall

(c) Crouch

(d) Sitting Front

(e) Sitting Sideways
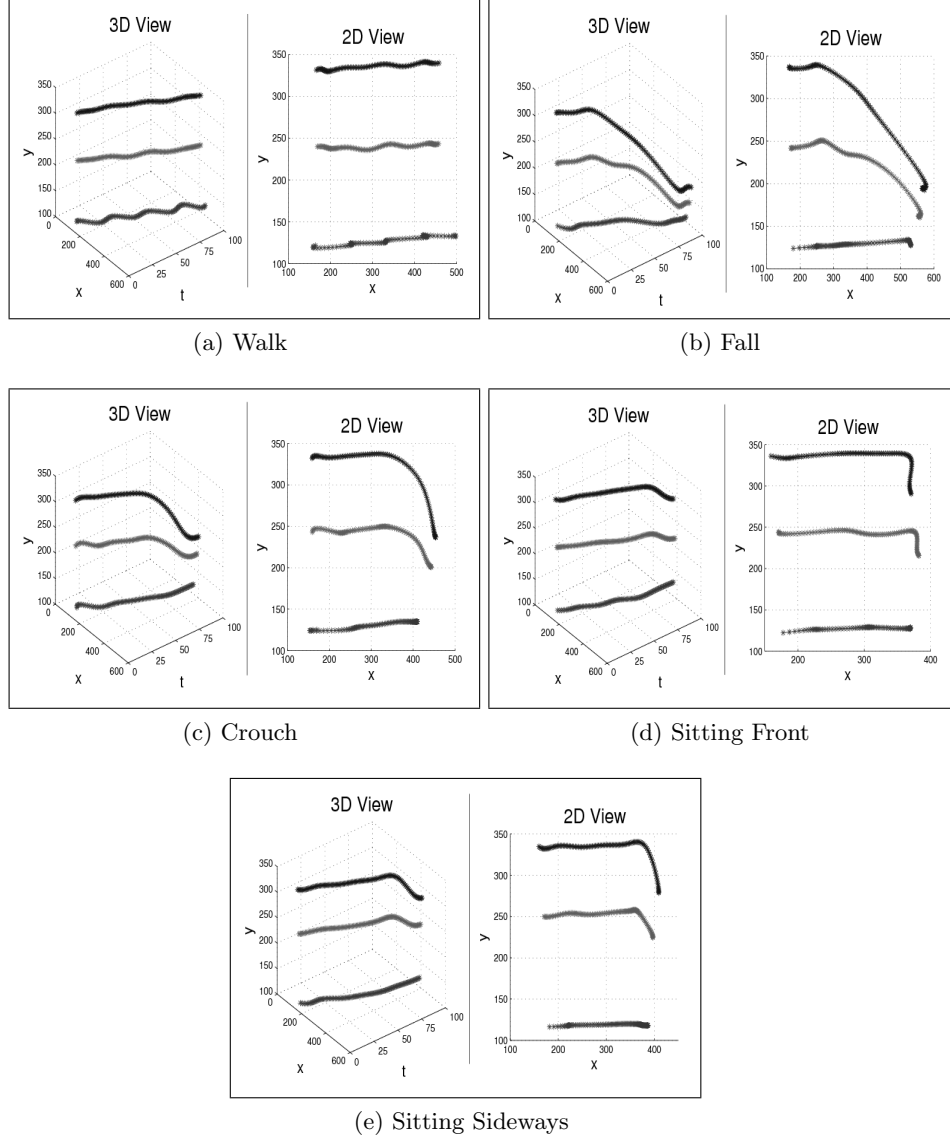
Fig. 5: Activity models generated by the b-splines curves. For each image, the left side shows the spatio-temporal view for b-spline curves, and right side shows the 2D projection to x, y axis for each b-spline curve.

5 Experiments and results

This section details the experiments performed to test the proposed method. In our case, five people were employed with different anatomy and clothing as objects of study. Five basic activities were carried on in a static background and a fixed camera with front sight to the scene and three different lighting changes to test the method were tagged as, Morning, Evening and Night, as can be seen in figure 6. Finally, every single person reproduced the five activities under different lighting conditions to generate a total of 15 analysis sequences for each of the activities.

(a) Walk	(b) Crouch	(c) Fall	(d) Sitting Sideways	(e) Sitting Front
(f) Walk	(g) Crouch	(h) Fall	(i) Sitting Sideways	(j) Sitting Front
(k) Walk	(l) Crouch	(m) Fall	(n) Sitting Sideways	(o) Sitting Front
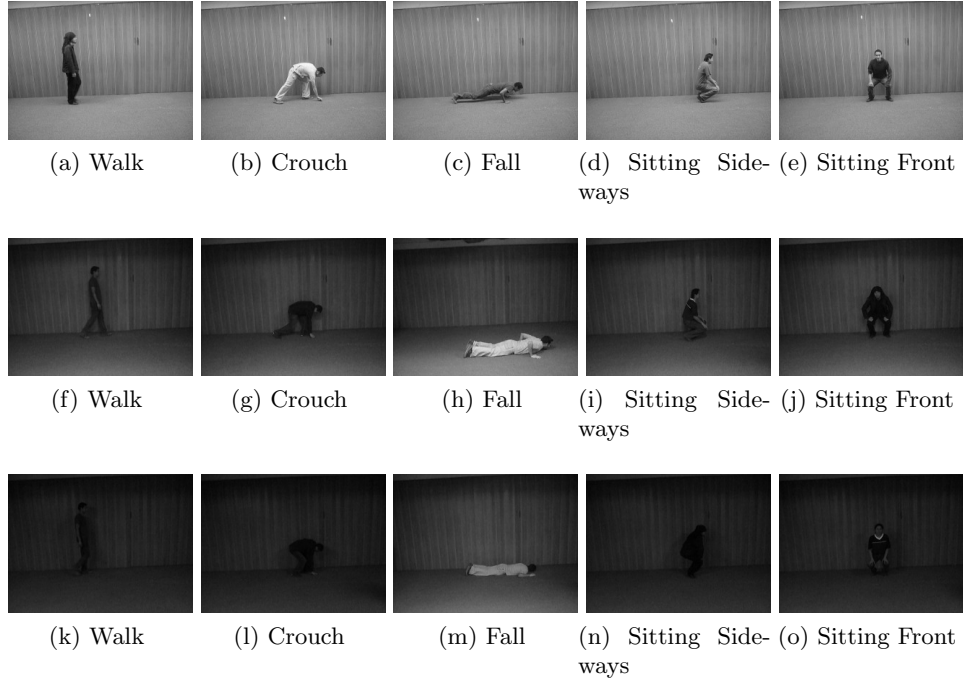
Fig. 6: Examples of sequences used to test the proposed method. First row: Morning. Second row: Evening. Third row: Night.

The training phase was done using the morning sequence, and the model base was generated by showing a single sequence of each activity. The method was tested using 75 sequences of activities that included sequences of the morning, evening and night. The thresholds considered in this phase are $\alpha = 50\,pixels$ and $\beta = 45,000\,pixels^2 (150\,pixels\ X\ 300\,pixels)$.

For the generation of models, interpolations and smoothing by b-spline were made with a knot vector uniformly distributed according to the interval in which

each curve was evaluated. We used 10 control points and therefore, 10 basic functions, and 10 coefficients were used to adjust the curves that were analyzed.

For the purpose of comparison we use other approach. A human operator localize and establish the area of the person manually in the beginning of the method.

The results of the proposed method are summarized in the confusion matrix in table 2. The results of the method assisted by a human operator are concentrated in the confusion matrix in table 3, both results show the average score of repeating the experiment five times.

At the end a recognition rate of 88% in average was reached for all activities for the proposed method in comparison with a recognition rate of 89.33% for the manual method.

	Walk	Crouch	Fall	SF	SS
Walk	15				
Crouch		14			1
Fall		1	14		
SF				14	1
SS		5		1	9

Table 2: Confusion matrix with the results from the recognition of activities using the automatic proposed method.

	Walk	Crouch	Fall	SF	SS
Walk	15				
Crouch		14			1
Fall		1	14		
SF				14	1
SS		3		2	10

Table 3: Confusion matrix with the results from the recognition of activities using the method assisted by a human operator.

6   Discussion

The percentage of correct classification of the results presented in table 2 may seem low compared with other approaches reported in the literature. However, the proposed method is evaluated in a scenario with different levels of illumination. Furthermore, compared to other jobs with uncontrolled lighting, this project, in very similar activities such as "Crouch" and "Sit", had good results. But, the activity "Sitting sideways" was confused with the activities of "Crouch"

and "Sitting front" because sometimes it was impossible to obtain a set of curves to make a clearer distinction between activities. By contrast, in "Walk" activity, the method has no problems extracting the curves to make the distinction between "Walk" and other activities. Comparing the method proposed with the manual approach, even though we get a better percentage in the correct classification with the human assisted method, the results show that only one example correctly classified in the "Sitting Sideways" activity makes the difference.

7   Conclusions

The proposed method is useful for recognition of activities under different lighting conditions, using a simple technique for comparison.

The procedure in the same way, gives evidence that Harris operator can locate important body parts for the analysis of behavior, in our case, the head, torso, legs and feet, and these features can be detected even though there is a change in lighting conditions. The algorithm is also able to recognize activities based on the human body that are similar and can be easily confused between them.

As future work, we plan to test the method performance with abrupt changes in lighting when the activities are performed in outdoor scenarios.

Acknowledgment

References

1. Ali, S., Shah, M.: Human action recognition in videos using kinematic features and multiple instance learning. IEEE Transactions on Pattern Analysis and Machine Intelligence 32, 288–303 (2010)
2. Arasanz, P.B.: Modeling Human Behavior for Image Sequence Understanding and Generation. Ph.D. thesis, Universidad Autónoma de Barcelona, España (2009)
3. Deboor, C.: A Practical Guide to Splines. Springer-Verlag Berlin and Heidelberg GmbH & Co. K (dec 1978), `http://www.worldcat.org/isbn/3540903569`
4. Efrat, A., Fan, Q., Venkatasubramanian, S.: Curve matching, time warping, and light fields: New algorithms for computing similarity between curves. J. Math. Imaging Vis. 27, 203–216 (April 2007), `http://portal.acm.org/citation.cfm?id=1265122.1265128`
5. Fernández Tena, C., Baiget, P., Roca, X., González, J.: Natural language descriptions of human behavior from video sequences. In: KI 2007: Advances in Artificial Intelligence, pp. 279–292 (2007)
6. Goya, K., Zhang, X., Kitayama, K., Nagayama, I.: A method for automatic detection of crimes for public security by using motion analysis. In: Proceedings of the 2009 Fifth International Conference on Intelligent Information Hiding and Multimedia Signal Processing. pp. 736–741. IIH-MSP '09, IEEE Computer Society, Washington, DC, USA (2009), `http://dx.doi.org/10.1109/IIH-MSP.2009.264`

7. Harris, C., Stephens, M.: A combined corner and edge detection. In: Proceedings of The Fourth Alvey Vision Conference. pp. 147–151 (1988)
8. Lao, W., Han, J.: Flexible human behavior analysis framework for video surveillance applications. International Journal of Digital Multimedia Broadcasting 2010, 1–10 (2010)
9. Liu, J., Wang, Z., Zhong, L., Wickramasuriya, J., Vasudevan, V.: uWave: Accelerometer-based personalized gesture recognition and its applications. Pervasive Computing and Communications, IEEE International Conference on pp. 1–9 (2009), `http://dx.doi.org/10.1109/PERCOM.2009.4912759`
10. Lucas, B.D., Kanade, T.: An iterative image registration technique with an application to stereo vision. In: IJCAI81. pp. 674–679 (1981), `http://citeseerx.ist.psu.edu/viewdoc/summary?doi=10.1.1.49.2019`
11. Mikolajczyk, K., Schmid, C.: An affine invariant interest point detector. In: Proceedings of the 7th European Conference on Computer Vision, Copenhagen, Denmark. pp. 128–142. Springer (2002), `http://perception.inrialpes.fr/Publications/2002/MS02`, copenhagen
12. Nater, F., Grabner, H., Gool, L.V.: Exploiting simple hierarchies for unsupervised human behavior analysis. Computer and Robot Vision (CRV2010) (2010)
13. Sakoe, H.: Dynamic programming algorithm optimization for spoken word recognition. IEEE Transactions on Acoustics, Speech, and Signal Processing 26, 43–49 (1978)
14. Tomasi, C., Kanade, T.: Detection and tracking of point features. Tech. rep., International Journal of Computer Vision (1991)
15. Wang, Y., Mori, G.: Human action recognition by semilatent topic models. IEEE Transactions on Pattern Analysis and Machine Intelligence 31(10), 1762–1774 (2009), `http://www.ncbi.nlm.nih.gov/pubmed/19696448`
16. Zhou, Z., Chen, X., Chung, Y.C., He, Z., Han, T.X., Keller, J.M.: Activity analysis, summarization, and visualization for indoor human activity monitoring. Circuits and Systems for Video Technology, IEEE Transactions on 18(11), 1489–1498 (2008), `http://dx.doi.org/10.1109/TCSVT.2008.2005612`

A Study on How the Training Data Monotonicity Affects the Performance of Ordinal Classifiers

Carlos Milian[1], Rafael Bello[2], Carlos Morell[2], and Bernard de Baets[3]

[1] Universidad de las Ciencias Informáticas, Cuba
[2] Computer Science Department, Universidad Central "Marta Abreu" de Las Villas, Cuba
[3] Department of Applied Mathematics, Biometrics and Process Control, Ghent University, Coupure links 653, B-9000 Gent, Belgium

Abstract. Some classification problems are based on decision systems with ordinal-valued attributes. Sometimes ordinal classification problems arise with monotone datasets. One important characteristic of monotone decision systems is that objects with better condition attribute values cannot be classified in a worse class. Nevertheless, noise is often present in real-life data, and these noises could generate partially non-monotone datasets. Several classifiers have been developed to deal with this problem but its performance is affected when faced with real data that are only partially monotone. In this paper are studied two monotonicity measures for datasets and it is analyzed its correlation with several ordinal classifiers performance. The results allow to a priori estimate the ordinal classifier behavior when faced with partially monotone ordinal decision system.

Keyword:. Ordinal classification, monotonicity, data complexity.

1   Introduction

The problem of the ordinal classification, also called ordinal regression has attracted the interest of the machine learning field due to the fact that many prediction problems or decision taking have present the ordinal values on the decision features [1, 2, 3], and [4]. An ordinal dataset is one with an ordinal variable output. In this case, the classification could be seen as a ranking, with a preference of the type 'higher values are better'.

In the ordinal classification, there is a dataset $D = \{O_1, O_2, \dots, O_n\}$, where each object is described by a group of features $A = \{a_1, a_2, \dots, a_n\}$; each feature a_i has a domain with an order relation which establishes an order among the domain's values; this kind of feature is frequently called criterion. Also, each object O_i has a decision feature d, which is also a criterion; therefore the decision values have also an order which defines a preference degree. Two objects O_i and O_j can be compared on the basis of their feature vectors $(O_{i1}, O_{i2}, \dots, O_{im})$ and $(O_{j1}, O_{j2}, \dots, O_{jm})$ or their decision values $d(O_i)$ and $d(O_j)$.

One important aspect in this topic is the data's monotony. Because of this concept, it is established the following relation:

$$O_i \leq O_j \Rightarrow d(O_i) \leq d(O_j) \,. \tag{1}$$

which means that if the object O_j is selected over the O_i therefore the class of the object O_j must be as good as the one of the object O_i This means that if only the value of one feature a_i increase (or decrease), while the rest is un-changed; the value of the decision feature d can only increase (decrease) or remain unchanged. An object is called monotone if it does not make up a non-monotone couple with any other object, and a dataset monotone if it contains no non-monotone objects. That is, monotone classification of multi-criteria data simply means that for improving criterion scores, the rank assigned by the ranking algorithm will never get worse. Non-monotonicity is present if there exist O_i and O_j in the dataset for which $O_i < O_j$ and $d(O_i) > d(O_j)$, such instances are said to be 'non-monotone'. Monotone ordinal problems, in which monotonicity constraint is imposed on the relationship between the input variables and the ordinal output is a special, yet common, type of ordinal problem [5].

Nevertheless, noise is often present in real-life data, and these noises could generate partially non-monotone datasets. Data can contain inaccurate rank or criterion values or can be an amalgam of various sources ranked by different experts; this then leads to a training set where a 'better' instance has received a lower rank than a 'worse' instance, when training a ranking algorithm on such a training set, contradictory information will be supplied to the ranking algorithm [6]. Non-monotonicity is in conflict with the domain knowledge where not only two objects with identical feature scores should have identical labels, but additionally, that increasing scores should not lead to a decrease in label; in other words, an object should receive a label at least as good as the best label received by any object that is worse than it [7].

There are many investigations about how monotony affects the way learning algorithms work. Some of the already existent algorithms are unable to be trained by using these partially non-monotone data sets. However, there are other algorithms that select the examples suitable for learning the concepts needed, during the learning process, eliminating those examples with monotonic inconsistencies.

One alternative to face this problem has been to drop the non-monotonicity grade by means of a method for relabeling the datasets, authors in [6] and [8] studied the consequences of a non-monotone training and test a set for a general monotone classification algorithm, to discuss some ways of cleaning up a non-monotone training set and determine whether it is useful in general to do such a thing. In [7], a single-pass optimal ordinal relabeling algorithm is formulated; other algorithm was presented in [9]. Also, other method was formulated in [1].

Algorithms for this kind of classification have been developed, some of which require monotone datasets. Because a monotone instance-based ranking algorithm will classify any new instance in a way monotone w.r.t. the dataset, not all instances will be able to be

classified 'correctly' [6]; therefore the need of the methods for relabeling the datasets. Some classifiers guarantee the monotonicity of subsequent predictions, while others do not; ordinal classifiers also differ from each other by the way they handle non-monotone datasets [5]. For a non-monotone classification algorithm, no such 'handicap' exists; therefore, the accuracy might misleadingly be reported higher.

The method of construction of decision trees for ordinal classification in [10] also requires monotone datasets. In other work, a method was formulated to construct monotone ordinal decision trees [11] for the case of partially non-monotone datasets, though it has to relabel some of the noisy objects during the construction of the trees. The TOMASO algorithm [12] does not accept a (partially) non-monotone training set. There are some other algorithms which are mentioned and used in other parts of this work.

In this work, has been studied the relation between the grade of non-monotonicity and the performance of some classifiers. To establish this relation there are considered some measures for measuring the non-monotonicity grade. The rest of the paper is organized as follows. In section 2, we briefly describe a set of data complexity measures which will be used to develop the experimental analysis. Section 3 presents the experiments carried out over several training sets and discusses the relation between the measures and the performance of the some ordinal classifiers. Finally, the conclusions are outlined.

2   Measures of Data Complexity

The monotonicity constraint is so important that some monotone classification algorithms cannot be trained on datasets containing this kind of noise. Research on more flexible algorithms is increasing, but the basic question that if non-monotonicity of a dataset affects the learning process, remains valid. Authors in [6], showed the grade of non-monotonicity present in two datasets, quantified by the number of nonmonotone instances, and the maximum attainable accuracy for a monotone classification algorithm (OSDL); also, the effect of relabeling the instances is presented.

The purpose of this work is showing by means of an experimental study and statistical analysis the relation between monotonicity (non-monotonicity) and the performance of the algorithm. In order to do that, some measures to measure the monotonicity of the datasets are employed, and several classifiers are used.

The problem of characterizing data by means of different measures is present in machine learning, the central idea is that high-quality data characteristics or meta-features provide enough information to differentiate the performance of a set of given learning algorithms. Different studies have been done on data complexity and meta-learning, such as [13, 14, 15 and 16]. To address this problem it is necessary to use data describing the characteristics of the datasets and the performance of the algorithms, which are called meta-data. In this work, are used some measures to characterize the grade of monotonicity

(or non-monotonicity) of the datasets, and two measures about the performance of the classifiers.

Two measures are used in this study, *DgrMon* y *OM*. The first one was presented in [4] and the second is proposed by us in this paper. The degree of monotonicity *DgrMon* of a dataset *D* is defined by expression (2):

$$DgrMon = \frac{\# \, Monotone \, pairs \, (D)}{\# \, Comparable \, pairs \, (D)} \, . \tag{2}$$

The pair $(O_1; O_2)$ is called comparable if $O_1 \leq O_2$ or $O_1 \geq O_2$, according to features in *A*; and if the relationship defined in (1) holds, it is also a monotone pair. If all comparable pairs are monotone then $DgrMon = 1$ and the dataset is called monotone (non-decreasing by assumption).

The other degree of monotonicity *OM* of a dataset *D* is defined by expression (3):

$$OM(D) = \frac{\# Monotone \, Objects(D)}{\# \, Objects(D)} \, . \tag{3}$$

As it was stated before, an object is called monotone if it does not make up a non-monotone couple with any other object.

It was studied the performance of the following classifiers: **OLM, OSDL, B-OSDL, 2B-OSDL,** and **OCC.** The ordinal learning model (OLM) is a simple algorithm that learns ordinal concepts by eliminating non-monotonic pairwise inconsistencies [17]; the learning process is based on a rule-based, which is generated during the learning. The Ordinal Stochastic Dominance Learner (OSDL) is an instance-based monotone ranking algorithm based on the concept of ordinal stochastic dominance of which several variants exist [2] and [18]; according to [7], it (really some of its extensions such as B-OSDL, this algorithm reduces to the OSDL when the stochastic training dataset is monotone) is able to use non-monotone training sets to perform a monotone interpolation, without the need of deletion or relabelling of non-monotone samples. The Ordinal class classifier (OCC) is a meta-classifier, because it uses some other classifier, such as C4.5, k-nearest neighbor, Naive bayes, etc., as a base classifier [19], in the experiments developed in this work was used as a base classifier J48, although there were used others obtaining similar results as it will be showed afterwards.; OCC does not guarantee monotonic classifications even when it learns from monotonic data.

3   Experimental Results

In the experimental study were used nine datasets whose dimensions are described in Table1.

In Tables 2-6 is described the measures' value for each dataset and the performance reached by the algorithms using the Weka platform, as measures, the Accuracy and coefficient Kappa. Accuracy (often called Confidence*)* is the number of instances that it predicts correctly, expressed as a proportion of all instances to which it applies.

Table 1. Ordinal datasets.

Dataset	Number of features in A	Number of objects	Number of classes
Car	6	1728	4
Nursery	8	12960	5
Contraceptive	9	1473	3
ERA	4	1000	9
ESL	4	488	9
LEV	4	1000	5
Monks-3	6	432	2
SWD	10	1000	4
Balance	4	625	3

Table 2. Classifier OLM and degree of monotonicity.

Dataset/Classify	OLM			OM	DgrMon
	Correctly	Incorretly	Kappa		
Car	94.85%	05.15%	0.8827	0.9890	0.9996
Nursery	97.88%	02.12%	0.9687	0.9997	0.9999
Contraceptive	44.13%	55.87%	0.0797	0.3985	0.7375
ERA	18.30%	81.70%	0.0647	0.096	0.8237
ESL	56.14%	43.85%	0.4534	0.5819	0.9867
LEV	37.10%	62.90%	0.175	0.318	0.9472
Monks-3	43.51%	56.48%	-0.1002	0.5254	0.5426
SWD	42.20%	57.80%	0.1697	0.418	0.9294
Balance	54.88%	45.12%	0.2021	0.4608	0.3875

Table 3. Classifier OSDL and degree of monotonicity.

Dataset/Classify	OSDL			OM	DgrMon
	Correctly	Incorretly	Kappa		
Car	96.18%	03.82%	0.9181	0.9890	0.9996
Nursery	98.79%	01.21%	0.9823	0.9997	0.9999
Contraceptive	30.96%	69.04%	0.055	0.3985	0.7375
ERA	23.60%	76.40%	0.0975	0.096	0.8237
ESL	68.24%	31.76%	0.6016	0.5819	0.9867
LEV	63.10%	36.90%	0.4665	0.318	0.9472
Monks-3	52.55%	47.45%	-0.0046	0.5254	0.5426
SWD	58.70%	41.30%	0.3636	0.418	0.9294
Balance	12.32%	87.68%	0.0266	0.4608	0.3875

Table 4. Classifier B-OSDL and degree of monotonicity.

Dataset/Classify	B-OSDL			OM	DgrMon
	Correctly	Incorretly	Kappa		
Car	96.35%	03.65%	0.9212	0.9890	0.9996
Nursery	98.69%	01.31%	0.9808	0.9997	0.9999
Contraceptive	42.16%	57.84%	0.0882	0.3985	0.7375
ERA	23.50%	76.50%	0.0967	0.096	0.8237
ESL	69.26%	30.74%	0.6157	0.5819	0.9867
LEV	63.00%	37.00%	0.4658	0.318	0.9472
Monks-3	38.43%	61.57%	-0.2366	0.5254	0.5426
SWD	58.80%	41.20%	0.3677	0.418	0.9294
Balance	57.92%	42.08%	0.2678	0.4608	0.3875

Table 5. Classifier 2B-OSDL and degree of monotonicity.

Dataset/Classify	2B-OSDL			OM	DgrMon
	Correctly	Incorretly	Kappa		
Car	96.35%	03.65%	0.9212	0.9890	0.9996
Nursery	98.68%	01.31%	0.9808	0.9997	0.9999
Contraceptive	42.16%	57.84%	0.0882	0.3985	0.7375
ERA	23.50%	76.50%	0.0967	0.096	0.8237
ESL	69.26%	30.74%	0.6157	0.5819	0.9867
LEV	63.00%	37.00%	0.4658	0.318	0.9472
Monks-3	38.43%	61.57%	-0.2366	0.5254	0.5426
SWD	58.80%	41.20%	0.3677	0.418	0.9294
Balance	57.92%	42.08%	0.2678	0.4608	0.3875

Table 6. Classifier OCC (J48) and degree of monotonicity.

Dataset/Classify	OCC (J48)			OM	DgrMon
	Correctly	Incorretly	Kappa		
Car	92.19%	07.81%	0.8319	0.9890	0.9996
Nursery	97.04%	02.96%	0.9565	0.9997	0.9999
Contraceptive	49.83%	50.17%	0.2561	0.3985	0.7375
ERA	27.30%	72.70%	0.1399	0.096	0.8237
ESL	65.78%	34.22%	0.5685	0.5819	0.9867
LEV	61.40%	38.60%	0.4433	0.318	0.9472
Monks-3	100 %	00.00 %	1	0.5254	0.5426
SWD	58.00%	42.00%	0.3505	0.418	0.9294
Balance	75.84%	24.16%	0.5884	0.4608	0.3875

The Kappa statistic is used to measure the agreement between predicted and observed categorizations of a dataset, while correcting for agreement that occurs by chance [20].

In the following Tables 7 and 8 is shown a review of the statistic correlation between measures OM y $DgrMon$, and the performance of the algorithms, measured, by using the precision and the coefficient Kappa.

This statistical analysis was carried out using bivariate correlations in the Kendall´s tau-b correlation coefficient that is used to analyze data not following a normal distribution. This coefficient establishes that for values smaller than 0.05 the significance between the data is high.
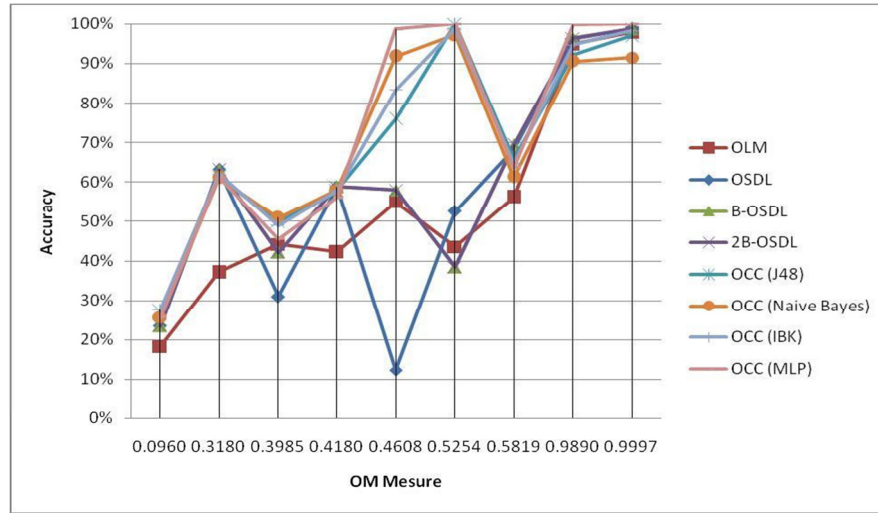
Fig. 1. Algorithms performance vs. Monotonicity measured by OM.

Table 7. Correlation between OM and the algorithms

Ordinal Classifiers	Correlation OM and precision	Correlation OM and Kappa
OLM	Significant 0.002	Significant 0.022
OSDL	Significant 0.037	Not Significant 0.211
B-OSDL	Significant 0.037	Not Significant 0.95
2B-OSDL	Significant 0.037	Not Significant 0.95
OCC(J48)	Significant 0.012	Significant 0.012

In the case of the OCC other experiments were performed using as a base classifier, classification methods k-NN and Naive Bayes, obtaining a performance similar to that

obtained with the base classifier J48; Figures 1 and 2 show the performance of the algorithms.

Table 8. Correlation between DgrMon and the algorithms.

Ordinal Classifiers	Correlation DgrMon and precision	Correlation DgrMon and Kappa
OLM	Not Significant 0.211	Significant 0.012
OSDL	Significant 0.002	Significant 0.000
B-OSDL	Significant 0.007	Significant 0.002
2B-OSDL	Significant 0.007	Significant 0.002
OCC(J48)	Not Significant 0.297	Not Significant 0.297
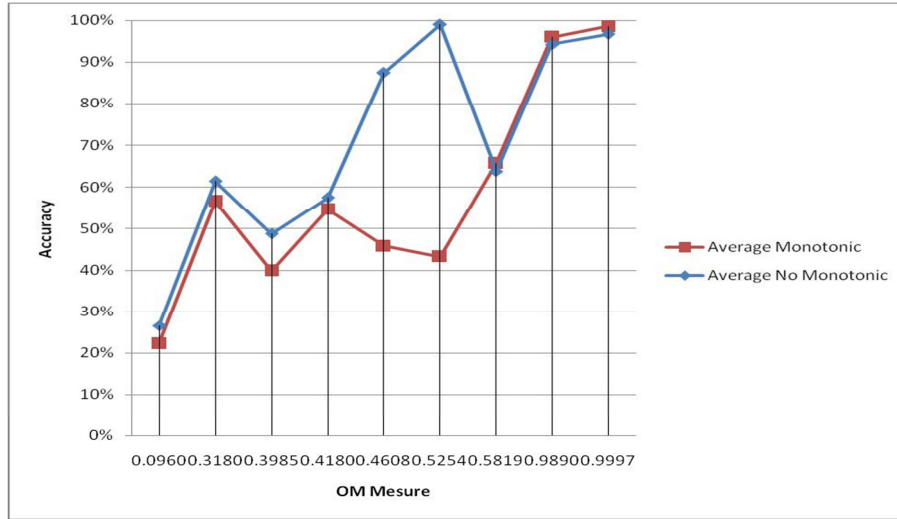
Fig. 2. Monotone and non-monotones algorithms performance vs. Monotonicity

As can be seen from the results shown in Tables 7 and 8 there is a significant statistical correlation between the measures considered to calculate the degree of monotony of the datasets and the performance of the algorithms, especially the monotony extent OM proposed in this work and the performance measure Accuracy, which is also shown in Figures 1 and 2.

The correct correlation existing between the proposed measure OM and the accuracy shown by classifiers is due to the fact that this measure is more sensible to the degree of monotony present in the datasets than the measure DgrMon because the former is more rigorous in selecting the objects to be compared.

4   Conclusions

The study on the relationship between the degree of monotony of ordinal datasets and the performance of some classifiers showed a significant correlation. The degree of monotony of the datasets was calculated by using two measures, one of which is proposed in this work and it showed a stronger relationship. This relationship allows that given a new dataset, can be estimated, by using the measures, its degree of non-monotonicity and to estimate the potential performance of the classifiers.

References

1. H. Daniels and M. Velikova.: Derivation of monotone decision models from noisy data, IEEE Trans. Syst. Man Cybern. Part C Appl. Rev., pp. 705–710 (2006)
2. S. Lievens, S., De Baets, B., and Cao-Van, K.: A probabilistic framework for the design of instance-based supervised ranking algorithms in an ordinal setting, Annals of Operations Research. 163, pp. 115–142 (2008)
3. Ben-David, A., Sterling, L., Tran, T.: Adding monotonicity to learning algorithms may impair their accuracy, Expert Systems with Applications 36, pp 667–66 (2009)
4. Velikova, M. and Daniels, H.: On Testing Monotonicity of Datasets. Ad Feelders and Rob Potharst (eds) Proceedings of MoMo2009, ¨Learning monotone models from data¨, at ECML PKDD 2009, pp. 11–22. September 7, Bled, Slovenia. (2009)
5. Potharst, R., Ben-David, A., and van Wezel, M.: Two algorithms for generating structured and unstructured monotone ordinal datasets. Engineering Applications of Artificial Intelligence 22, pp. 491–496 (2009)
6. Rademaker, M., De Baets, B., and De Meyer, H.: On the Role of Maximal Independent Sets in Cleaning Data Sets for Supervised Ranking. In Proc. of IEEE International Conference on Fuzzy Systems, Vancouver, BC, Canada. July 16-21 (2006)
7. Rademaker, M., De Baets, B., and De Meyer, H.: Optimal monotone relabelling of partially non-monotone ordinal data. Optimization Methods and Software, iFirst, pp. 1–15 (2010)
8. Rademaker, M., De Baets, B., and De Meyer, H.: Loss optimal monotone relabeling of noisy multi-criteria data sets. Information Sciences 179, pp. 4089–4096 (2009)
9. Rademaker, M., De Baets, B.: Optimal restoration of stochastic monotonicity with respect to cumulative label frequency loss functions. Information Sciences 181, 747–757. (2011)
10. Potharst, R. and Bioch, JJ.C.: Decision trees for ordinal classification, Intell. Data Anal. 4 (2), pp. 97–111 (2000)
11. Bioch, J. and Popova, V.: Monotone decision trees and noisy data, Tech. Rep. ERS-2002-53-LIS, Department of Computer Science, Erasmus University Rotterdam (2002)
12. Marichal, J.-L., Meyer, P. and Roubens, M.M.: Sorting multi-attribute alternatives: The TOMASO method, Computational Oper. Research. 32, pp. 861–877 (2005)
13. T. Ho, M. Basu.: Complexity measures of supervised classification problems, IEEE Transactions on Pattern Analysis and Machine Intelligence 24, pp. 289–300 (2002)
14. S. Singh.: Multiresolution estimates of classification complexity, IEEE Transactions on Pattern Analysis and Machine Intelligence 25 (12), pp. 1534–1539 (2003)
15. Brazdil, P. et al.: Metalearning: Applications to Data Mining. Springer, ISSN: 1611–2482, ISBN: 978-3-540-73262-4 (2009)

16. Caballero, Y., Bello, R., Arco, L., and Garcia, M.: Knowledge Discovery using Rough Set Theory, Capitulo en el libro Advances in Machine learning I Dedicated to the memory of Professor Ryszard S. Michalski in Series: Studies in Computational Intelligence Vol 262; Koronacki J., Ras Z.W., Wierzchon S.T.; Kacprzyk J (Eds), ISBN 978-3-642-05176-0 (2010)
17. Ben-David, A.: Automatic Generation of Symbolic Multiattribute Ordinal Knowledge-Based DSSs: methodology and Applications. Decision Sciences. 23:1357–1372 (1992)
18. Lievens, S., De Baets, B.: Supervised ranking in the WEKA environment, Information Sciences 180 (24), 4763–4771 (2010)
19. Frank, E. and Hall, M.: A Simple Approach to Ordinal Classification. In: 12th European Conference on Machine Learning, 145–156 (2001)
20. Witten, I. H. and Frank E.: Data mining: practical machine learning tools and techniques-2nd ed. Elsevier, ISBN: 0-12-088407-0 (2005)

An Information Fusion Architecture
for Situation Assessment of Ground Battlefield

Huimin Chai and Baoshu Wang

School of Computer Science and Technology, Xidain University, Xi'an, China
{chaihm@mail.xidian.edu.cn, bswang@xidian.edu.cn}

Abstract. The information fusion architecture for situation assessment is designed in the paper, which is divided into three stages: perception, comprehension and projection. The process of force structure classification is an important part which includes target aggregation region partition, command post recognition and force structure classification. The algorithm of template matching is proposed for the recognition of command post and force structure. Thus, the ground situation assessment is made in terms of concepts that can be computed. Finally, the simulation system of situation assessment is developed, a seaboard defense scenario is simulated and the situation assessment for the seaboard is analyzed to illustrate the functionality of the proposed model.

Keywords: Situation assessment, ground battlefield awareness, template matching.

1 Introduction

In recent years, decision-making in real-time dynamic battlefield is becoming increasingly complex due to the nature and diversity of threats and tactics that may be encountered. With enormous amounts of information available for command decisions, C4ISR system is required of the capability for situation assessment, which can help commanders form appropriate perception, timely and exactly understanding of battlefield situation. Situation assessment (SA) is the process of inferring relevant information about forces of concern in a battlefield, including location, movement and deployment of enemy forces, which is needed by the campaign commanders or analysts to support decision-making [1, 2].

Situation assessment is belonging to high-level information fusion, which goals include identifying the meaningful events and activities, deriving higher order relations among objects and inferring the intension. Over the course of the last two decades there have been several definitions of situation assessment proposed. The most widely accepted definitions are Dr. Mica Endsley's [3] and the Joint Development Laboratory (JDL) fusion model [4, 5]. Endsley's view is based on cognitive principles, which divides SA into three levels: perceiving elements in the environment within a volume of space and time; comprehending what they mean in context; and predicting their status in the near

future. On the other hand, the JDL model provides a function data centric approach, which has 5 levels: Level 0-Sub-Object Identification; Level 1-Object Identification; Level 2-Situation Assessment; Level 3-Threat Assessment; Level 4-Process Refinement. With the JDL data fusion model, situation assessment falls in level 2 and accepts the results from level 1.

Situation assessment is a complex domain, especially for ground battlefield. Today, the modern battlefield is characterized by an overwhelming volume of information collected from a vast networked array of increasingly more sophisticated sensors and technologically equipped troops. There remains a significant need for higher levels of information fusion such as those required for generic situation assessment, prediction of enemy coursed of action (COA) and potential threat. For roughly 10 years, the research community has been recognizing the need for significant progress in this domain. Some researchers have proposed a few of methods and models for situation assessment, which includes fuzzy reasoning and theory [6, 7], Bayesian networks [8, 9, 10], template matching [11, 12], case-based reasoning [13, 14], ontology-based system [15, 16, 17], etc. Some researchers [18, 19, 20] have advocated the considerations of the battlefield intelligence in situation assessment, which provides some good illustrations of the complexity of gathering and processing intelligence in the practical applications.

In this paper, the problem of ground battlefield awareness is discussed. The rest of the paper is organized as follows. Section 2 provides an overview of the information fusion architecture for ground battlefield. Section 3 presents the process of force structure and deployment recognition, and the template matching algorithm is given. Section 4 illustrates a demonstration scenario of the coastal defense plan, and the results of situation assessment are given. Section 5 concludes this paper and presents some prospects for future work.

2   Overview of the Information Fusion Architecture

The process of situation assessment for ground battlefield is complex, nonlinear and replete with human interpretation and judgment. Therefore, the construction of computational models that infers the enemy courses of action (COA) and comprehends what have happened in the context is an extremely challenging task. In this section, we will provide an overview of the information fusion architecture for ground battlefield. The architecture is based on Endsley's model of SA with stages for perception, comprehension and projection. In Fig.1, the fusion architecture of ground battlefield awareness is presented.

(1) Event extraction: In the battlefield, there are various sensors deployed to scan an area of stationary or moving targets. Based on the output of sensors, we can obtain the different intelligence of ground battlefield. With the characteristics of the raw intelligence data, we can identify meaningful events and activities, such as appearance of important target, radio signal, fortification, force activity and so on. This is the first fusion level of

the architecture, which can be viewed as the phase of perceiving elements in the battlefield. Fuzzy theory and template matching are used in this level.
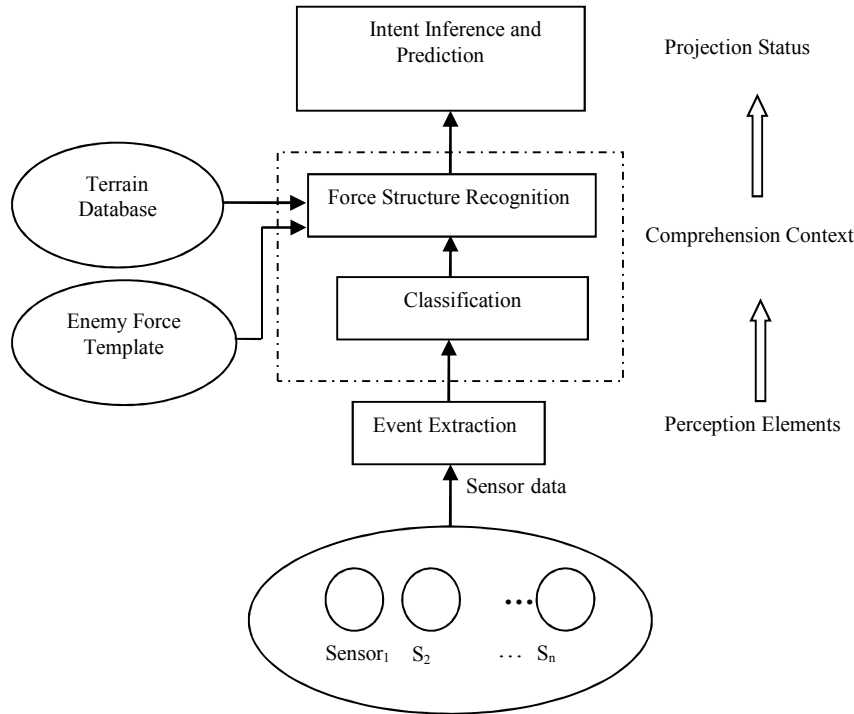
Fig.1. The architecture of ground battlefield awareness.

(2) Force structure recognition: To make awareness of ground battlefield, not only the individual targets should be identified, but also higher order relations among the different objects must be derived. Force group classification and recognition can explain the force composition, dynamic deployment and its intension, which is of great importance in the military decision making process. With the information on targets as well as terrain characteristics, the process of force structure recognition can interpret the relations among objects. Under force structure recognition, our effort is to obtain the results which can explain the following problems: ①who is there? ②what is their organizational group structure and posture? ③what are relative relations between group and its neighbors? ④what are their intensions?

(3) Intent inference and prediction: The process of intent inference and prediction is termed as the third level of fusion architecture, which predicts enemy force status in the near future. It takes as input the result of force structure recognition, some additional intelligence and infers enemy intension according to enemy doctrinal templates. In the

ground battlefield, the enemy intent inference is a very challenging problem, for the high degree uncertainty of observations. Most computational approaches to the intent inference are based on artificial intelligence, for example, D-S theory, dynamic Bayesian networks, fuzzy reasoning, etc. In the paper, this part is not discussed in the following.

(4) Enemy structure template: An enemy structure template depicts the composition and deployment of various types of sub-echelons or forces. For example, a brigade of artillery consists of several battalions, artillery. The expert knowledge base should be constructed for different level of force structure, which is used to recognize the enemy force structure.

(5) Terrain database: The terrain data is stored in the terrain database, which represents the terrain characteristics and traffic facilities: elevation, slopes, down-country, vegetation, body of water, road, railway, etc. The terrain data, used by force structure recognition, can make our analytical approach and methods available to the ground battlefield. The format of terrain data is based on a sampling of every N meters of terrain from a reference map, a rectangular mesh that includes significant information: elevation, road, river, and so on. Terrain analysis is essential in the process of determining enemy force group, including tactically important terrain characteristics, traffic ability patterns, and key terrain.

3   Force Structure Recognition

3.1   Intelligence Report

One of the challenges at the heart of this paper is analyzing large volumes of battlefield intelligence with the intention of figuring out what the enemy is doing and what type of threat such activities might represent. The intelligence reports are derived from various forms of physical sensors as well as by direct human observations. In the process of intelligence report analysis, some questions can be explained, for example, "what the enemy unit is doing?", "where are the important fortification in the ground battlefield?", and so on.

As intelligence reports come from the battlefield, the information it contains needs to be analyzed in the context, which is very important for situation assessment in ground battlefield. After event extraction from intelligence reports, we can identify some meaningful battlefield events. We now turn attention to the dimensions or attributes of the event from intelligence data, which includes: (1)Object: the object described in intelligence report, for example, command car, radio signal, fortification; (2)Size: the number of observed vehicles, the level of enemy force which can be equated with echelon level(e.g., squad, platoon, company); (3) Location: the location of the observed units in terms of latitude/longitude; (4) Time: the time of the observation; (5) Features: the

features of target, such as a list of all the observed equipment the enemy is occupied, activity which denotes what the enemy force is doing, parameters of radio signal.

For different type of intelligence report, it can be represented by the formulation:

$$Intel_i = (K_i, S_i, T_i, F_i) \qquad\qquad (1)$$

where K_i represents the observed object in intelligence report, such as enemy force, fortification, radio signal. S_i denotes the size of enemy force or the number of vehicles, and T_i represents the time of intelligence. F_i denotes the feature of the observed object. For the different type of object, the representation of feature is different.

3.2   Processing of Force Classification

According to the characteristics of ground battlefield, we give the process of force structure classification in the following:
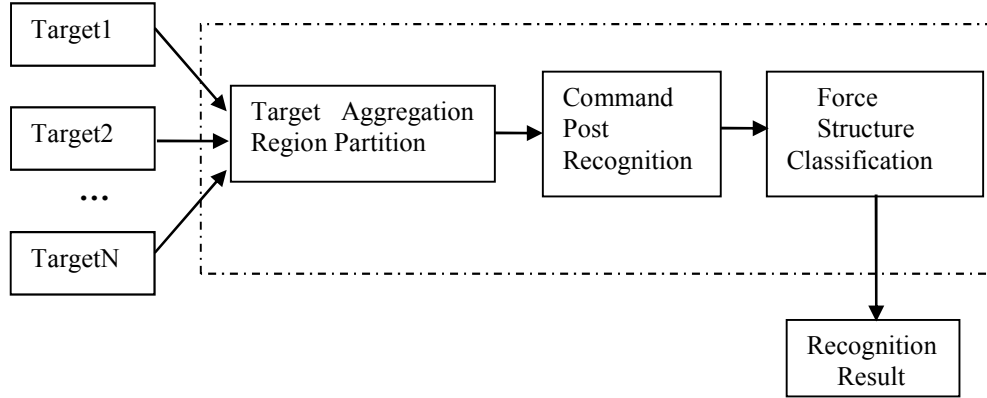
Fig.2. The process of force structure recognition.

(1) Target aggregation region partition: In the process of force structure recognition, we firstly divide the region of war into several parts based on military rules and battlefield target. For example, the region partition for the brigade command post is shown in Fig. 3.

According to general military rules, the brigade command post locates rectangular region (abcd) shown in Fig. 3. To get the position of the command post, the region (abcd) is partitioned into grid cell by 500*500(meter). Based on the twenty-four grid cells, the analysis can be made of the command post existence in the partitioned region (abcd). During the command post analysis process, the following information is utilized: terrain feature of a sampled cell, battlefield intelligence, and military rules.

(2) Command post recognition: After the partition of war region, we can analyze whether there is command post based on the military rules in the region. If the analysis shows the existence of command post, then the type of enemy force should be identified, e.g. tank platoon, company. Otherwise, the recognition of enemy force will be not performed in the partitioned region.
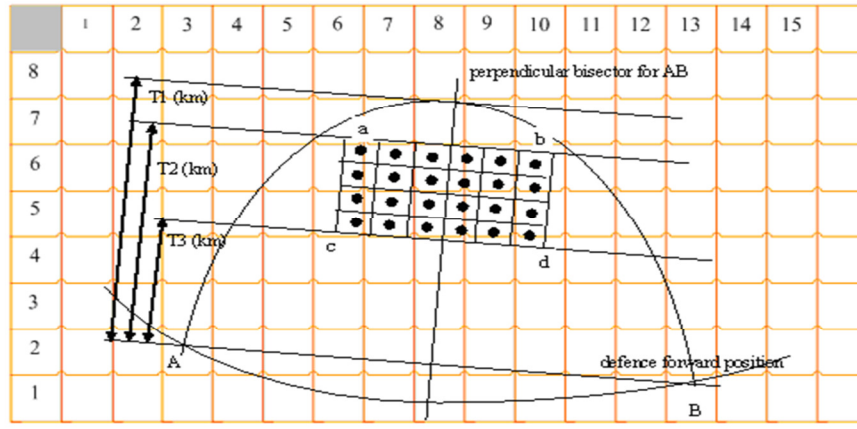
Fig.3. The region partition for the brigade command post.

On the process of recognizing the command post, the knowledge model is utilized to identify the type of command post. The knowledge model is based on some military knowledge, which is comprised of three parts: Position rule, Terrain characteristic, Intelligence symptom. For illustrative purpose, the knowledge model of brigade command post is described concisely in Fig.4.
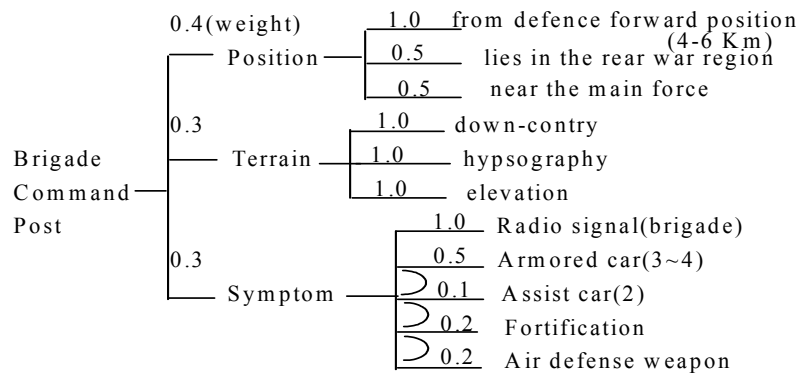
Fig.4. The knowledge model for the brigade command post.

According to the knowledge model, we can calculate the belief of the type of command post, which is defined by

$$Belief = W_1 \times Pbelief + W_2 \times Tbelief + W_3 \times Sbelief \tag{2}$$

where *Pbelief* denotes the belief of position according to corresponding military rules, *Tbelief* is the belief of terrain characteristic, *Sbelief* is the belief of intelligence report, W_1, W_2, W_3 are the weights that are standardized to sum to unity.

(3) Force structure classification: To make useful predictions about the enemy intension, we should cluster the battlefield entities into higher level force aggregates based on the result of command post recognition. Similarly, expert knowledge model for force structure are used to match the various clusters so as to classify the aggregates into known classes of force structure. In the paper, the template matching method is utilized to classify the force structure.

3.3 Algorithm for Template Matching

A doctrinal template of force structure depicts the characteristic and deployment of various types of sub-echelons or vehicles. For example, a brigade consists of several battalions and some weapons. In general, a brigade should be deployed in the suitable area. So the template of brigade is comprised of three parts: terrain characteristics, the position of battalion, and intelligence reports for force, weapons and fortification, which is similar to knowledge model shown in Fig.4. Then the template of brigade can be represented as:

$$T = \{Rule, Terrain, Intel\} \tag{3}$$

where *Rule* is the military rules for the brigade deployment, *Terrain* denotes the terrain characteristics, and *Intel* is the intelligence reports for the brigade.

For different levels of force, the constituent structure of each template is the same as the template of brigade. We can identify the type of force structure based on the force template matching. The algorithm of template matching includes: position rules matching, terrain characteristic matching and the matching of intelligence report. The matching process attempts to maximize the matching degree between a template and the enemy force. The process returns the template with the maximum matching degree.

For the two parts in the template: terrain characteristics, rule for the position of force, the matching algorithm is simple. We assume that for a given location *L*, there are enemy forces, e.g., two platoons. If the given location *L* is correspondent with the i-th rule in the template, the matching degree for part rule *Rule* is calculated as:

$$Bel_R = Bel_R + W_{Ri} \times 1.0 \tag{4}$$

where W_{Ri} is the weight value of the i-th rule in the template and all the weights are standardized to sum to unity. Similarly, the matching degree for terrain characteristic Bel_T can be calculated by (4). For example, the force deployment area contains the features, such as a river, road, and elevation. And if the area terrain features is correspondent with the terrain characteristic in the template, then $Bel_T = Bel_T + W_{Ti} \times 1.0$.

In the intelligence part of force structure template, the fuzzy number is utilized to describe the number of target, e.g., approximate three command cars, approximate two platoon of enemy force. Then, fuzzy theory is used to match the ground intelligence report with the force template.

We assume that the membership function of the fuzzy number $\underset{\sim}{n}$ in the template can be defined as:

$$\mu_{\underset{\sim}{n}}(x) = \begin{cases} x - t_1, & t_1 \le x \le n \\ t_2 - x, & n < x \le t_2 \end{cases} \tag{5}$$

where t_1 can be given as $n-1$ or $n-2$, then t_2 is given $n+1$ or $n+2$. The membership function is represented by Fig.4.
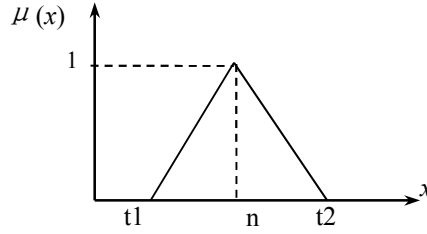
Fig.4. The fuzzy member of $\underset{\sim}{n}$.

If the target type in the intelligence report $Intel_i$ is matched with the type in the intelligence part of template T_k, then we can calculate the degree of match $\delta(Intel_i, T_k)$ between $Intel_i$ and T_k as

$$\delta(Intel_i, T_k) = w_1 \times m\_Bel_i + w_2 \times \mu_{\underset{\sim}{n}}(m) \tag{6}$$

where m_Bel_i is the mean belief value for the type of target in the $Intel_i$, m is the number of target in the intelligence report, $\mu_{\underset{\sim}{n}}$ is the member function of $\underset{\sim}{n}$ in the template, w_1, w_2 respectively denote the importance weight of target type, number in the template T_k.

Algorithm1 describes the process of matching with force structure template, where the matching degree δ is initialized as '0'. The template with the maximum matching degree which is greater than the threshold value σ is returned by the matching process. The algorithm can also be used to match command post, e.g. a command post of brigade.

<div align="center">

Algorithm 1. Template Matching Algorithm.
</div>

1: Initialize $\delta_k = 0$, and the templates for matching: $\{T_1, T_2, ..., T_n\}$

2: For rules of force deployment(position), the matching degree is calculated as:
$\delta(Location_i, T_k) = W_{Ri} \times 1.0$

3: For terrain characteristic, $\delta(Terrain_j, T_k) = W_{Tj} \times 1.0$

4: For intelligence report: $\delta(Intel_p, T_k) = w_{11} \times m\_Bel_p + w_{12} \times \mu_n(m)$

5: Update the total matching degree as necessary:
$\delta_k = W_R \sum \delta(Location_i, T_k) + W_T \sum \delta(Terrain_j, T_k) + W_I \sum \delta(Intel_p, T_k)$

where $W_R + W_T + W_I = 1$. If the value of $\sum \delta(Intel_p, T_k)$ is greater than '1', then the value is set '1'.

6: Determine the δ_k is maximum matching degree and greater than the threshold

σ, then return template T_k.

4 Simulation and Results

The simulation system, the essential part of information fusion project, is developed to demonstrate the process of ground battlefield awareness, which is comprised of four parts: intelligence editor, command post recognition, force structure analysis, template database and terrain database. The relation of the different parts in the simulation system is shown in Fig. 5.

We developed the intelligence editor in order to add the ground battlefield intelligence report into the simulation system. The type of intelligence includes force activity, fortification, vehicles, radio signal and so on. The intelligence data is comprised of the type of object, the size or number of object, the position, the object feature and the received time. The data of terrain characteristic is stored in the terrain database. The corresponding database editor is also developed for terrain data maintenance. The results of situation assessment are displayed on a traditional map.

For the purpose of showing the simulation process of situation assessment, let's consider the following scenario: there is a conflict in the sea, and the enemy attempt to attack our domain. They deployed some force in the seaboard. To destroy their plan, we should analyze the enemy force deployment and the force structure. According to the

terrain features, received intelligence report and other sensor data, the situation assessment for the seaboard can be analyzed.
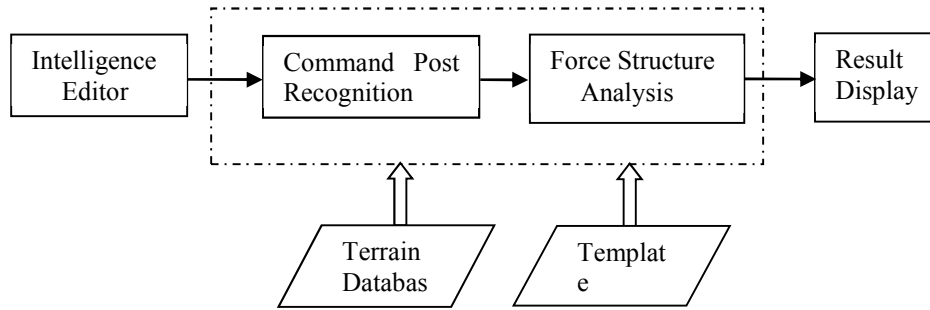
Fig.5. The structure of simulation system.
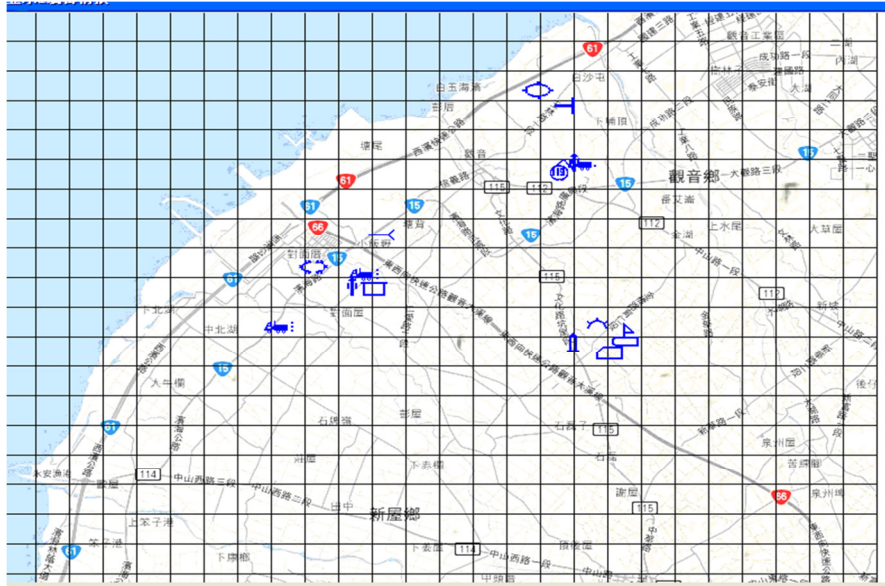
Fig.6. The result of intelligence edition for situation assessment.

4.1   Intelligence Editor

The intelligence editor is used to demonstrate the fusion of ground battlefield intelligence report. It is a software tool that can edit the intelligence for ground battlefield awareness.

An example edition result of the tool is shown in Fig.6. We can add, delete, or update an intelligence object which is shown by blue color on the map, such as command car, fortification. Then the intelligence report can be generated according to the edition result, and saved in a file by defined data format. While the simulation of battlefield situation assessment, the intelligence report is read from the corresponding file and sent to the module of command post recognition or force structure analysis by the order of the received time.

Similarly, some intelligence reports are edited for the simulation scenario. Table 1 describes the object of each intelligence report and the number or size of the object.

Table 1. The intelligence reports in the simulation scenario.

Intelligence No.	Target	Size/number	Position(x,y)
1	Armored car	3~4	(9233,5466)
2	Air defense rocket	2	(6366,2600)
3	Fortification		(8933,5350)
4	Assist car	3~5	(9033,5750)
5	Grenade launch base		(3833,5216)
6	Air defense rocket	2	(3933,4166)
7	Assist car	4~5	(9450,2850)
8	Fortification		(9283,3066)
9	Radio signal(battalion)		(5450,5400)
10	Air defense weapon		(9150,2800)
11	Fortification		(7200,3583)

Fig.7. The results of target aggregation region partition

4.2   Command post Recognition

The command post recognition is the first step in the ground situation assessment. It includes region partition for command post, and data fusion of sensors, intelligence, terrain etc. According to military rules, the war region in the seaboard can be partitioned into two results, which is shown in Fig.7.

a: partition 1   **b:** partition 2

In Fig. 7, the rectangular grid cell is used to recognize the command post. In the front, the grid cells are used for battalion command post. And in the rear region, the grid cell is used for brigade command post. According to the brigade and battalion command post knowledge models, we can use the template matching algorithm to identify whether there exits command post. In the process of template matching, the sensor data, terrain characteristic, intelligence report are fused. If the degree of template matching is greater than the threshold σ , we can identify the type of command post. Otherwise, we can infer there does not exit command post. The threshold σ for command post template matching is set by 0.7.

In this simulation scenario, the templates for brigade and battalion command post are respectively utilized. The results show that the command post matching degrees of Fig. 7(a) are greater than Fig. 7(b). Furthermore, the matching degrees of both battalion and brigade command post in Fig. 7(a) are all greater than threshold σ (0.7). Table 2 describes the matching degree of each command post in Fig. 7(a).

Table 2. The result of template matching for command post in Fig. 7(a).

Command Post	Position rule	Terrain characteristic	Intelligence symptom	Matching degree
Brigade command post 1	1.0	1.0	0.77	0.93
Brigade command post 2	1.0	1.0	0.68	0.90
Brigade command post 3	1.0	1.0	1.0	1.0
Battalion command post	1.0	1.0	0.85	0.95

(The sequence of brigade command post 1,2,3 is from right to left.)

In table 2, the columns of position rule, terrain characteristic, intelligence symptom respectively denotes position rules matching, terrain characteristic matching and the matching of intelligence report. The last column represents the total matching degree which is a tradeoff for the three template matching part.

4.3 Force Structure Analysis

In the next step, we can analyze the force structure according to the results of command post recognition. Thus, the analysis is made based on the result of Fig. 7(a). The force structure templates are used in this step, and the template matching algorithm described as section 4.3 is implemented. In this simulation example, the result of force structure analysis is shown in Fig. 8.
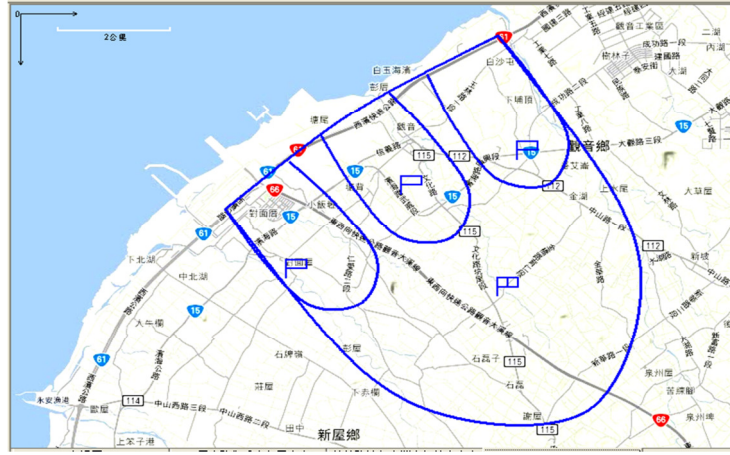
Fig.8. The result of force structure analysis.

The deployment of enemy force is approximately illustrated in Fig.8, which template matching degree is great than 0.60. There are three battalions in the forward position which is represented by blue arc, and each battalion command post is located which is shown by blue flag. In the rear area, the blue flag represents the brigade command post. Furthermore, the analysis can give the detail features of the deployment, such as the location of battalion or brigade, the width value and depth value.

5 Conclusion

We presented architecture and its implemented computational embodiment for situation assessment of ground battlefield. The architecture can fuse intelligence from sensor data, terrain characteristic, and military knowledge in a coherent system. The force structure is analyzed and computed, which can be shown in the simulation system of situation assessment.

In the future work, we plan to explore the model of tactical goal hypothesis generation and inference. In addition, we will extend our architecture of situation assessment to predict the future significant feature of battlefield.

References

1. Blasch, E., Plano, S.: DFIG Level 5 issues supporting Situation Assessment Reasoning, Proceedings of Information Fusion. (2005)
2. Salerno, J.J.: Where's Level 2/3 Fusion- a Look Back over the Past 10 Years. Proceedings of Information Fusion, pp.1-4 (2007)
3. Endsley, M.R.: Toward a Theory of Situation Awareness in Dynamic Systems. Human Factors Journal. 37(1), pp. 32-64 (1995)
4. Hall, D.L., Llinas, J.: Handbook of Multisensor Data Fusion. Washington DC, NY: CRC Press (2001)
5. Linas, J., Bowman, C.,: Revisiting the JDL Data Fusion Model II. Proceedings of Information Fusion, pp.1-13 (2004)
6. Stover, J. A., Hall, D.L., Gibson, R.E.: A Fuzzy-logic Architecture for Autonomous Multisensor Data Fusion. IEEE Transaction on Industrial Electronics, 43(3), pp.403-410 (1996)
7. Huimin, C., Baoshu, W.: A Fuzzy Logic Approach for Force Aggregation and Classification in Situation Assessment. Proceedings of the International Conference of Machine Learning and Cybernetics, pp. 1220-1225 (2007)
8. Das, S., Grey, R., Gonsalves, P.: Situation Assessment via Bayesian Belief Networks. Proceedings of the Fifth International Conference on Information Fusion, 1, pp. 664–671 (2002)
9. Das, S., Lawless, D.: Trustworthy Situation Assessment via Belief Networks. Proceedings of Information Fusion, 1, pp. 543–549 (2002)
10. Qiang, J.: Information Fusion for High Level Situation Assessment and Prediction. Report:OMB No. 3, pp. 074-0188 (2007)
11. Noble, D.F.: Schema-Based Knowledge Elicitation for Planning and Situation Assessment Aids. IEEE Trans. on Systems, Man and Cybernetics, Part A, 19(3): pp. 473-482(1989)
12. Huimin, C., Baoshu, W.: A Template-based Method for Force Group Classification in Situation Assessment. IEEE Symposium on Computation Intelligence in Security and Defense Application, pp. 85-91 (2007)
13. Looney, C.G., Liang, L.R.: Cognitive situation and threat assessment of ground battlespaces, Information Fusion, 4, pp. 297-308 (2003)

Unsupervised Learning Objects Categories using Image Retrieval System

Karina Ruby Perez Daniel, Enrique Escamilla Hernandez,
Mariko Nakano Miyatake, and Hector Manuel Perez Meana

National Polytechnic Institute IPN, ESIME Culhuacan, Av. Santa Ana No. 1000 Col.
San, Francisco Culhuacan, Del. Coyoacan, Zip Code 04430, Mexico City
`krperezd@hotmail.com,eescamillah@ipn.mx,mariko@infinitum.com.mx,`
`hmpm@prodigy.net.mx`
`http://www.posgrados.esimecu.ipn.mx`

Abstract. Since several years ago artificial intelligent systems have become in a big challenge and learning of object categories is one of the most important parts in this field. Unsupervised learning of object categories provides the considerably high intelligence to apply several ambitious tasks, such as robot vision and powerful image retrieval engine, etc. In the learning object categories, a fast and accurate unsupervised learning model is required. In this paper we propose an unsupervised learning method to categorize the objects using images retrieved by Internet, in which a keyword is introduced as input data. For this purpose, all retrieved images are described using the Pyramid of Histogram of Oriented Gradients (PHOG) algorithm and the resultant PHOG vector is clustered to get a dataset for learning object categories. Two clustering methods are used in the proposed method, which are K-means and Chinese Restaurant Process (CRP), to make the learning method more efficient and simple.

Key words: Unsupervised learning objects, PHOG, k-means, Chinese restaurant process.

1 Introduction

Learning Object Categories is a very important tool in computer vision systems, which has attracted the researchers' attention during the last several years. Most of currently learning object methods are based on the manually gathered and labeled images [1–3]. However recently, with the fast developing of internet and fast growing users number, the requirement of more efficient methods have stimulated the developing of new learning methods to handle the images retrieved by internet [4–7]. Because of that it is a fast developing field in which many researchers around the world are concentrating their efforts, given as a result the developing of learning objects methods to be used with internet connection based on labels or word annotations [8], complex images training to classify them [9] or probabilistic methods using text and images. However, when used in internet such methods still retrieve several images unrelated with the keyword.

To reduce this problem, a learning object method in which the Chinese Restaurant Process CRP is used as a clustering method for learning object purposes is proposed since, as shown in [10–12], CRP is very simple and efficient for clustering data making it possible the unsupervised learning of objects and the image classification according to their vector features. Thus, the learning object method proposed in this paper is based on a simple techniques that let us building a visual model from a query (word) given by the user, where the main the aim is to construct a visual representation of any object without previous knowledge about it.

Is well known that is almost impossible to store an image database large enough to represent all the existing objects related to a given keyword provided for a given user, thus the web appears to be a desirable alternative and then the internet connection is fundamental for the proposed system. To search the image associated to the given keyword avoids the construction of an extensive database, however many images obtained from internet may have few relation with the desired object and then these images must be filtered out. In order to filter the image database obtained from internet to achieve the acquisition of objects concept, all images must be clustered according to the similarity existing among their main features. This process, if it is possible, must be carried out in an unsupervised way. To this end several unsupervised and semi-supervised clustering algorithms have been proposed in the literature. Among them, one of the most widely used is the k-means algorithm. The K-means [13] is easy to implement, simple and efficient, however this method needs the number of clusters as an input. To solve this problem, this paper proposes to use "Chinese Restaurant Process" (CRP) [12] as clustering method. CRP implements a model-based Bayesian clustering algorithm, in which the cluster assignment procedure can be regarded as an iterative Chinese restaurant process. The CRP, unlike the K-means, is a probabilistic method and do not need the number of clusters as an input.

Taking in account the above mentioned issues, this paper proposes a learning object algorithm in which, all gathered images from Internet are transformed into vectors features which are clustered using CRP according to the similarities existing among their main features. To this end, firstly the feature extraction is done using PHOG (Pyramid of Histogram of Oriented Gradients) [14, 15] method. Then the PHOG, CRP and color segmentations are combined to achieve the Learning Object Category. Here as first step the K-means algorithm is used and next the CRP is used in order to get a successful method at learning from Google images. Finally the "Ground Trut" test was used as evaluation criteria. The rest of this paper is organized as follows, in Section 2 a brief description of PHOG, K-means, color segmentation and CRP is given, in Section 3 provides the proposed algorithm. Section 4 provides the experimental results and finally in section 5 the conclusion of this work is given.

2   Basic Concepts used in the Proposed Algorithm

In the proposed algorithm, several important tools, such as Pyramid of Histogram of Oriented Gradient (PHOG), K-means clustering algorithm, object segmentation and Chinese Restaurant Process (CRP) are used. In this section we describe basic concept of the before mentioned algorithms in general manner.

2.1   Pyramid of Histogram of Oriented Gradient (PHOG)

PHOG is a global feature descriptor based on distribution of the edge direction of the image, then using PHOG the global shape of each object in the image can be extracted as a vector representation. Therefore recently PHOG is considered as adequate tool for the image classification [4, 7, 9, 14]. PHOG extracts an image description based on hierarchical representation which consists of several levels of descriptions. In the first level, Histogram of Oriented Gradients (HOG) is applied into the original whole image, while in the subsequent levels, the image or sub-image is segmented into four non-overlapped sub-images and a HOG is applied to each of them. Once the HOG vectors of sub-images of each level are obtained, the final PHOG vector is obtained concatenating each single HOG vector. The detail operation of PHOG is described below.

Firstly, the edge contours of the entry image must be extracted using the Canny edge detector. The resultant edge image is split into four non-overlapped sub-images called cell in the first level of pyramid, in the second level of pyramid each cell of first level of pyramid moreover is split into four non-overlapped cells. Consecutively this operation is done until L level of PHOG. The HOG operation is applied to each cell of each level of pyramid, getting histogram of the direction of existent edges in each cell. This operation is performed using Sobel operator of 3 x 3 without Gaussian smoothing filter. The edges direction is divided into N intervals, which forms N bins of a histogram of a single cell. The values of all bins of the histogram of a single cell form a vector of N elements, called HOG vector. Once HOG vectors of all cells are obtained, these are concatenated at each pyramid level, which means the HOG vector of 0-level pyramid is concatenated with four HOG vectors of 1-level pyramid, and so on. The concatenated vectors form the PHOG vector, which introduces the spatial information of the image, giving the ability of detection of global shape and also local features of the object, which corresponds to human learning mechanism of objects [14, 15]. The number of elements (vector size) of PHOG vector is determined by number of bins of each cell, which is given by 1.

$$PHOG\ vector\ size = N \sum_{l \in L} 4^l \qquad (1)$$

Where N is the number of bins, l is number of bins used in each cell and L is total pyramid levels. If we use $L = 0$ (only original whole image is used) and $N = 20$, PHOG vector is a 20-dimentioanl vector. Thus if $L = 1$, and $N = 20$, PHOG vector has 100 elements, when $L = 2$ and $N = 40$, the size of PHOG

vector is 840. Worth noting that if the HOG quantize 20 edge direction ($N = 20$), the range of orientation angle $[0, 180]$ is divided by 20 and if $N = 40$, the angle range is $[0, 360]$, but the interval of each angle is same with $N = 20$.

2.2 K-means

The K-means clustering algorithm [13] is an unsupervised method to cluster input feature vectors into some meaningful subclasses, i. e., the members of the same cluster share similar features while the members from different clusters are sufficiently different each other. Considering that each input feature vector x_i is d-dimension vector, the data set X is given by 2.

$$X = \{x_i \mid x_i \in R^d, \ i = 1, 2, \ldots M\} \tag{2}$$

where M is number of input vectors.

The K-means clustering algorithm [16] is described as follows:

1. *Initialization:* k-centroids $(c_1, c_2, \ldots, c_k)$ of k clusters $C_1, C_2, \ldots, C_k$ are randomly selected from data set X. These centroids are initial cluster centers of each cluster.
2. *Assignment:* Each elements $x_i(i = 1 \ldots M)$ of the data set X is assigned to a cluster with closest centroid from x_i which is determined taking account of minimum distance between and all centroids. That is if $d(x_i, c_j) < d(x_i, c_m)$ for all $m = 1, \ldots, k;\ j \neq m$ then x_i is assigned to the cluster C_j.
3. *Updating:* Recalculate the centroids $c_1^*, c_2^*, \ldots, c_k^*$ of clusters, using members of clusters.
4. *Iteration:* Repeat steps 2 and 3 until the centroids no longer move. That is if $c_i^* = c_i$ for all $i = 1, \ldots, k$ then the current $c_1^*, c_2^*, \ldots, c_k^*$ are considered as the final *cluster centroids*, otherwise assign $c_i = c_i^*$ and then repeat steps 2 and 3.

Finally all elements of data set X are classified into k clusters. A principal inconvenience of the K-means algorithm is that the number of cluster must be determined in advance. In the many applications, this number is unknown.

2.3 Object Segmentation

In almost all image processing techniques, complex background in image causes several difficulties an adequate process. Then the complex background must be discarded using image segmentation method, before the principal processing. The image segmentation is typically used to locate objects and boundaries in the images. A segmented region of an image should be uniform and homogeneous with respect to some characteristic such as color, intensity or texture. Therefore the image segmentation provides homogeneous regions.

Although according to Lucchese and Mitra [17], the object segmentation algorithms can be divided into feature-space, image-domain and physics based

techniques, all these techniques use a same assumption that color is a constant property of the surface of each object. The formal definition of the object segmentation is given as following way [18].

Let $\mathcal{I}$ denote an image and let $\mathcal{H}$ define a color homogeneity; then the image $\mathcal{I}$ is segmented into $\mathcal{N}$ regions $\mathcal{R}_n$, $n = 1, 2, \ldots, \mathcal{N}$ such that

1. $\bigcup_{n=1}^{N} \mathcal{R}_n = \mathcal{I}$ with $\mathcal{R}_n \cap \mathcal{R}_m \neq \emptyset$, $n \neq m$, i.e., states that the union of all region cover the whole image.
2. $\mathcal{H}(\mathcal{R}_n) = $ true $\forall\, n$ states that each region has to be color homogeneous, and
3. $\mathcal{H}(\mathcal{R}_n \cup \mathcal{R}_m) = $ false $\forall\, \mathcal{R}_n$ and $\mathcal{R}_m$ adjacent, i.e., two adjacent region cannot be merged into a single region that satisfies the color homogeneity $\mathcal{H}$

Nowadays, there are several color-spaces used in different applications, although the RGB color-space is most commonly used color-space, it doesn't represent the color perception of human visual system. In this sense, the color-space HSV (Hue, Saturation and Value) is considered as better color-space than RGB [17–19], because HSV is more intuitive than RGB. For example, the variation of the saturation (S) presents the variation of perceptual color intensity and the variation of value (V) presents the perceptual illumination intensity. Taking account of the property of the HSV color-space , a circular histogram HSV color segmentation was proposed [19]. Then HSV color-space can be obtained from the RGB color-space, performing as follows.

$$
\begin{aligned}
H &= \tan^{-1}\left(\sqrt{3(G - B)}, (2R - G - B) \right) \\
S &= 1 - \min\left(R, G, B\right)/I \\
V &= \max(R, G, B)
\end{aligned}
$$

2.4 Chinese Restaurant Process

Chinese Restaurant Process [11, 12] refers to an analogy with a real Chinese restaurant where the number of tables is infinite. The first customer sits down at a table. The ith customer sits down at a table with a probability that is proportional to the number of people already sitting at that table or if a new table is opened up with a probability proportional to the hyperparameter α. Because of exchangeability, the order in which customers sit down is irrelevant and we can draw each customers table assignment z_i by pretending they are the last person to sit down. Let K be the number of tables and let n_k be the number of people sitting at each table. For the ith customer, then is defined a multinomial distribution over table assignments conditioned on z_{-i}, i.e. all other table assignments except the ith:

$$
p(z_i = k \mid z_{-i}, \alpha) \propto \begin{cases} n_k & \text{if } k \leq K \\ \alpha & \text{if } k = K + 1 \end{cases} \tag{3}
$$

Given the cluster assignment each data point is conditionally independent of the other ones. The exchangeability assumption in this process holds for some datasets but not in others. While several special models for spatial and temporal

dependencies have been proposed, the distance-dependent CRP offers an elegant general method to modeling additional features and non-exchangeability. For example if 10 customers are clustered using the CRP method, the first customer choosed the firts table with $p = \frac{\alpha}{\alpha} = 1$. The second customer chooses the first table with probability $\frac{1}{1+\alpha}$ and the second table with probability $\frac{\alpha}{1+\alpha}$. After the second customer chooses the second table, the third customer chooses the first table with probability $\frac{1}{2+\alpha}$, the second table with probability $\frac{1}{2+\alpha}$, and the third table with probability of $\frac{\alpha}{2+\alpha}$. This process continues until all customers have seats, defining a distribution over allocations of people to table or object to classes.

This method employed as a clustering algorithm shows an advantage compared with K-means clustering algorithm. In the K-means algorithm, the number of clusters must be determined in advance, while in the CRP algorithm, an adequate number of clusters can be determined though the process.

3   Proposed Algorithm

In the proposed algorithm, to cluster successfully the retrieved images from Internet, a PHOG, K-means clustering, object segmentation and CRP algorithms are employed in the cascade structure with 4-stages. This proposed 4-stages approach is shown by figure 1. Firstly using keyword introduced by user, the Google image retrieval engine "Google Image Search$^{\text{TM}}$" extracts the corresponding images from Internet to generate a database, which becomes the input of the proposed 4-stages clustering algorithm. The dataset consist of 64 images for each keyword. The use of Internet is convenient, because it allows uploading the dataset for any object at any time. In this section process of each stage is described.

3.1   Image Clustering using PHOG and K-means

The data set generated using any image search engine contains many junk images which is not related to the introduced keyword. Firstly in the proposed algorithm junk images are discarded using PHOG and K-means clustering algorithm. The PHOG is applied to all images retrieved by a specific keyword to get M PHOG vectors, where M is number of retrieved images. Figure 2 shows some retrieved image together with the PHOG vector (level 0) represented by histogram form. From the figure, the images which share similar object shape yield quite similar PHOG vector. For instance the PHOG vector shown in figure 2b is very similar to figure 2b. On the other hand, the representation of figures 2f and 2h are significantly different, indicating that two images 2e and 2g are different. The pyramid levels of the PHOG used for this task is one, that is level-0 PHOG vectors is used. Thus, in order to get the most common group of the images retrieved by the same keyword, K-means clustering algorithm is used.

K-means algorithm requires the number of clusters as one of input data. After previous test, the clustering performance cannot be improved using more
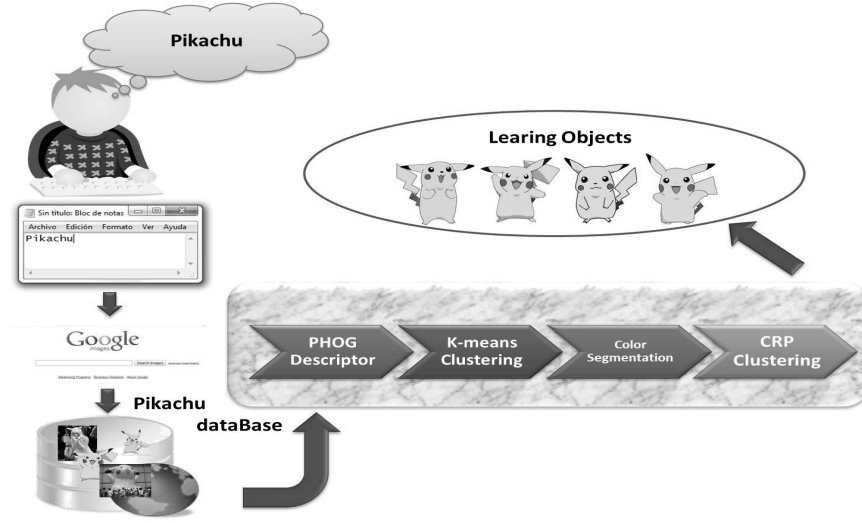
Fig. 1: Outline of the proposed learning object method.

than three clusters, so adequate number of cluster is considered as three ($k = 3$). Actually using three clusters, 64 retrieved images using same query (keyword) can be clustered correctly according with image appearance.

When K-means algorithm is converged, we analyze the number of elements of three clusters. The cluster with largest number of elements (images) is considered as winner and is kept for further process, while other two clusters are discarded, because images in these clusters are junk images whose relation with the query is very low.

3.2   Object Segmentation

In this section, all images in the winner cluster obtained in the previous stages are analyzed. When an image which contains a specific object is classified using this object, the background of the image can be interfered with the classification process causing an error. As mentioned in section 2.3, to segment the object from the background, we use color property of the surface of the object in HSV color-space.

The color reference is randomly selected from the center region of the image, which is defined as Region of Interest (ROI). The segmentation is done using a HSV color filter inspired on the circular filter introduced in [19]. If extracted area (object region) is less than the pre-established threshold, then the image is considered as a junk image, in other words, the image does not contain the object indicated by keyword, otherwise the image is considered as useful image and it is analyzed furthermore. The junk images are discarded in this stage.

(a)

(b)

(c)

(d)

(e)

(f)

(g)

(h)
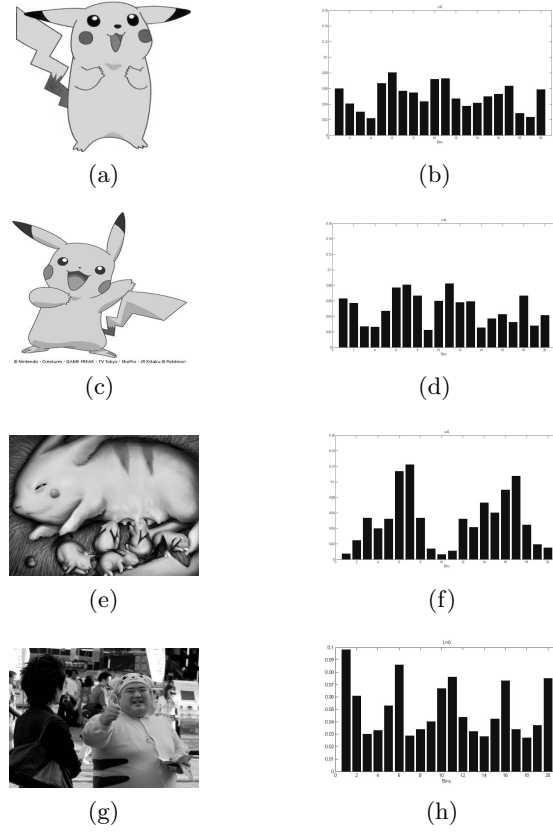
Fig. 2: Example of retrieved images and their PHOG representation (L=0).

The threshold value is established by a heuristic way, retrieving more than 1000 images using 50 keywords indicating cartoon's characters, animals and several objects. Fig. 3 shows an example of useful images and discarded images through the segmentation process, when a word "Pikachu" is given as keyword.

3.3   Chinese Restaurant Process (CRP)

Once the most of junk images were discarded, the most representative images (cluster of images) with the desired object indicated by keyword, can be selected using the CRP. CRP is implemented by a model-based Bayesian clustering algorithm with two input parameters n and α (see 2.4). The first parameter n is the maximum number of elements of each cluster and another parameter α determines the probability that a new table is opened up.

According with the total number of the retrieved images and the number of the discarded images during the previous stages, we determine these two
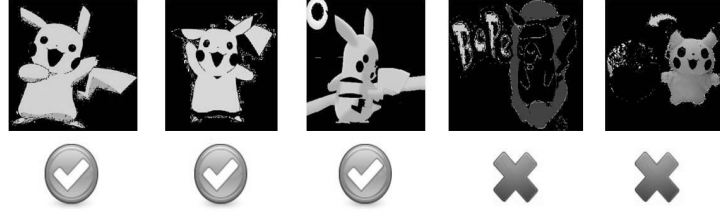
Fig. 3: Segmentation results.

parameters as $n = 5$ and $\alpha = 0.2$. These values guarantee that the highest probability is assigned to the most popular cluster. The final cluster obtained by this process is called as "Learning Object Category"

4 Experimental Results

To evaluate the proposed algorithm, in this section some experimental results are shown. The evaluation criteria used here is "Ground truth", which indicate if the elements of final cluster obtained through the proposed algorithm are corresponded to the query (keyword) or not. The figure 4 shows the number of well-classified objects after all four stages on the proposed algorithm. Worth noting that for each keyword, 64 images are retrieved and finally only five images are allowed as the most popular cluster of the CRP algorithm.

The two graphs shown by Fig. 4 depict the level of well-classified objects according to the Ground Truth test. Although the values of the Ground Truth test of some objects such as teapot and chair are not sufficiently high compared with other objects, this situation can be improved if more specific keywords are used. This refers to a semantic problem. When the user query implies an ambiguous concept, for instance, "mouse", in the 64 retrieved images, 52 images contains computer mouse, 10 of them are an animal mouse and only 2 images are Mickey Mouse. In this case, the most of the retrieved images regards to a "computer mouse", therefore the learning object by the proposed algorithm is obviously a computer mouse. If a user desires to retrieve "animal mouse" in place of "computer mouse", he has to specify the query specifying his keyword as "animal mouse" or "mouse animal". Figure 5 shows the PHOG vectors obtained from given three images with the three different "mouse" object. From the figure, we can observed that three PHOG vectors are considerably different among them.

The learning objects obtained, are similar images to each other, i.e., this method can be used as similar-images retrieval system.

(a)

(b)
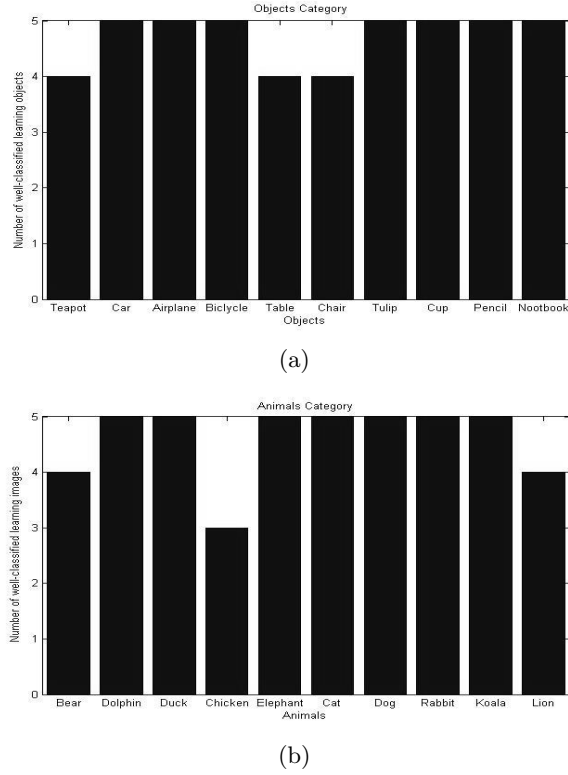
Fig. 4: Number of well-classified objects. a) Varied Objects. b) Animals.

5   Conclusions

In this paper, we proposed learning object category algorithm, which is composed by the following four stages: Pyramid of Histogram of Oriented Gradient (PHOG), K-means clustering algorithm, image segmentation on HSV color filter and Chinese Restaurant Process (CRP). From the experimental results, we conclude that the rate of the wrong classified objects in the final cluster (learning objects) is very low according to the figure 4. Due to the shape description capacity of PHOG, K-means algorithm and moreover efficient CRP classifier allow improving the learning methodology. Since CRP is a non parametric clustering method, the proposed algorithm can be combined with other techniques for some applications in which the learning of object category is important. Furthermore, since the proposed algorithm can use the huge image database of Internet, it can be an alternative method to learn any object at any time without a prior stored database. Even though the totally unsupervised learning object category task is still far, we consider that this work contributes to achieve this goal.

(a)

(b)

(c)

(d)

(e)

(f)
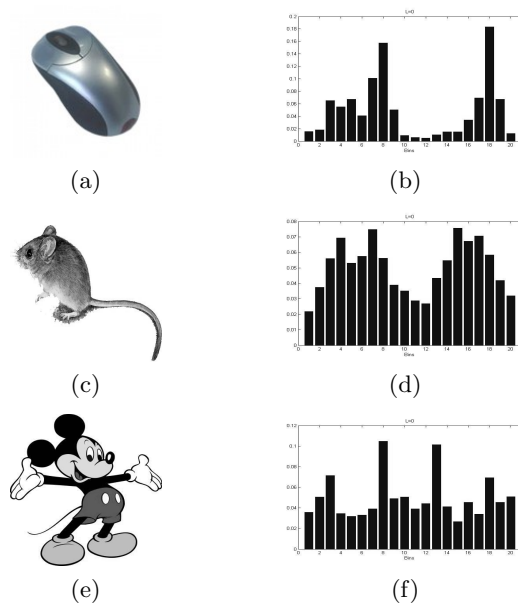
Fig. 5: Example of retrieved images by the "mouse" querry and their PHOG representation.

References

1. S. Agarwal, A. Awan, and D. Roth: Learning to detect objects in images via a sparse, part-based representation. IEEE PAMI, Vol. 20, Number 11, pp. 1475–1490 (2004)
2. K. Barnard, P. Duygulu, N. de Freitas, D. Forsyth, D. Blei, and M. Jordan: Matching words and pictures. JMLR, Vol. 3, pp. 1107–1135 (2003)
3. A. Berg, T. Berg, and J. Malik: An improved cluster labeling method for support vector clustering. Pattern Analysis and Machine Intelligence, IEEE Transactions, Vol. 27, pp. 461–464 (2005)
4. R. Fergus, L. Fei-Fei, P. Perona, and A. Zisserman: Learning Object Categories from Google's Image Search. In Proc. of ICCV, Vol. 2, pp. 1816–1823 (2005)
5. F.Schroff, A.Criminisi, A.Zisserman: Harvesting Image Database from the Web. in Proc. of International Conference on Computer Vision, pp. 1–8 (2007)
6. B. C. Russell, A. Torralba, K. P. Murphy, and W. T. Freeman: Labelme: a Database and Web Based Tool for Image Annotation. IJCV, Vol. 77, Number 1, pp.1453–1466 (2010)
7. R. Fergus, L. Fei-Fei, P. Perona, and A. Zisserman: Learning Object Categories from Internet Image Search. JPROC. of IEEE, Vol. 98, pp. 1453–1466 (2010)
8. J. Liu, R. Hu, M. Wang, Y. Wang and E. Chang: Web-Scale Image Annotation. Proceedings of the 9th Pacific Rim Conference on Multimedia, pp. 663–674 (2008)
9. F.Schroff, A.Criminisi, A.Zisserman: Harvesting Image Database from the Web. In Proc. of International Conference on Computer Vision, pp. 1–8 (2007)

10. D. M. Blei and P. I. Frazier: Distance dependent Chinese restaurant processes. In ICML 2010 (2010)
11. D. M. Blei, T. L. Griffiths, M. I. Jordan and J.B. Tenenbaum: Hierarchical Topic Models and the Nested Chinese Restaurant Process. In Neural Information Processing Systems(NIPS) (2003)
12. R. Socher, A. Maas and Christopher D. Manning: Spectral Chinese Restaurant Processes: Nonparametric Clustering Based on Similarities. In Fourteenth International Conference on Artificial Intelligence and Statistics (AISTATS) (2011)
13. K. Jain: Data clustering: 50 years beyond K-means. Pattern Recognition Letters. Elseiver Journal. Vol.31, pp. 651–666 (2010)
14. A. Bosch, A. Zisserman, and X. Munoz: Representing shape with a spatial pyramid kernel. In Proceedings of the International Conference on Computer Vision, pp. 401–408 (2007)
15. A. Bosch, A. Zisserman, and X. Munoz: Image Classification using Random Forests and Ferns. In Proceedings of the International Conference on Image and Video Retrieval, pp. 1–8 (2007)
16. J. Meng, H. Shang and L. Bian: The Application on Intrusion Detection Based on K-means Cluster Algorithm. In Proceedings of the 2009 International Forum on Information Technology and Applications, Vol.1, pp. 150–152 (2007)
17. L. Lucchese and S.K. Mitra: Image Segmentation A State-Of-Art Survey for Prediction. In Advanced Computer Control, 2009. ICACC '09., pp. 420–424 (2009)
18. N.R. Pal and S.K. Pal: A Review on Image Segmentation Techniques. Pattern Recognition, Vol. 26, Number 9, pp. 1277–1294 (1993)
19. Din-Chang Tseng, Yao-Fu Li, and Cheng-Tan Tung: Circular histogram thresholding for color image segmentation. Pattern Recognition, Vol. 2, pp. 673–676, (1995) Current version: 2002

Video Processing on the DaVinci Platform

Alejandro A. Ramírez-Acosta[2], Mireya S. García-Vázquez[1],
and Gustavo L. Vidal-González[1]

[1] Centro de Centro de Investigación y Desarrollo de Tecnología Digital (CITEDI),
Av. del Parque No. 1310, Mesa de Otay,
Tijuana, Baja California, C.P. 22510,
México
[2] MIRAL R&D, Imperial Beach,
USA
{mgarcia, vidal}@citedi.mx, ramacos10@hotmail.com

Abstract. Nowadays, the complexity of embedded systems has increased dramatically, making design process more complex and time consuming. This situation has caused significant delays in introducing new products to market and serious economic problems for several companies. Thus, the integrated circuit manufacturers have revised; redesigned or abandoned the traditional paradigms of the design of electronic circuits and systems. This effort allows the emergence of applications based on design platforms (platform-based design, PBD). This paper describes the implementation of a MPEG-4 Advanced Simple Profile video encoder prototype based on Xvid software, which is ported to the ARM9 platform-based architecture of the evaluation development DaVinci platform DVEVM355 of Texas Instruments (TI). Our encoder implementation is under eXpressDSP Digital Media (xDM) standard of TI. The importance of our work is that the implemented encoder based on xDM standard can be integrated with other software to build a multimedia system based on either DVEMs platform in a very short time. The experimental evaluation of our MPEG-4 ASP-Xvid encoder's performance demonstrate high performance and efficiency compared to the MPEG-4 Simple Profile video encoder of TI.

Keywords: Video, embedded system, DaVinci platform, platform-based design, MPEG-4 codecs, DVEVMs.

1 Introduction

Thanks to the advent of microprocessor technology, the applications based on platform-based design [1] and the emergence of standards bodies in the area of video coding such as ISO/IEC [2] and ITU-T [3], the multimedia embedded systems are a reality. For instance, recently, embedded multimedia system based on advanced digital media processors (DMP) have been integrated into commercial products to implement coding

tools in MPEG-4 real time environment [4]. The MPEG-4 includes many standard coding tools [5, 6].

Texas Instruments (TI) as an industry leader has generated DaVinci technology for embedded application development [7]. This includes hardware, software and development tools. DaVinci technology belongs to development applications platform-based design [1]. The design platforms from TI, called Digital Video Evaluation Module (DVEVM) under DaVinci technology [7], allow to create a SoC (System on Chip, [8]) for video applications such as videophones, IP set-top-box, digital cameras, IP cameras, DVRs, portable media players, media gateways, medical images, etc.

Nowadays, the complexity of embedded systems has increased dramatically, making design process more complex and time consuming. Therefore the use of standardized tools and methodologies such as DaVinci technology significantly help designers, developers, integrators and researchers to develop complex embedded systems in shorter times. In this paper we describe the use of standardized tools and DaVinci technology for the implementation of a MPEG-4 Advanced Simple Profile video encoder prototype based on Xvid software, which is ported to the ARM9 platform-based architecture of the evaluation development DaVinci platform DVEVM355 of Texas Instruments (TI). Our encoder implementation is under eXpressDSP Digital Media (xDM) standard of TI. The importance of our work is that the implemented encoder based on xDM standard can be integrated with other software to build a multimedia system based on either DVEMs platform in a very short time.

The paper is organized as follows: In section 2 the main features of the MPEG-4 standard and ASP profile are presented. In section 3, DaVinci development environment is described. The methodology for integrating a modular MPEG-4 ASP Xvid encoder in DaVinci architecture DVEVM355 is given in section 4. The results of the performance of MPEG-4 ASP-Xvid encoder ported to the ARM9 platform-based DaVinci architecture of DM355 are set out in section 5. Conclusions are drawn in section 6.

2   MPEG-4 ASP

The MPEG-4 standard and the rapid proliferation of the existing IP (Internet Protocol) networks present new opportunities and challenges to the scientific community. The MPEG-4 standard provides standardized technological elements enabling the integration of production, distribution and access to content. Examples of this are: digital television, graphic interactive applications and interactive multimedia. In addition, the standard tries to avoid a multitude of formats and owner players, which do not have interoperability capability. The MPEG-4 standard is organized into multiple parts, two of these parts define the video coding schemes: Part 2 (ISO/IEC 14496-2) [5] define the MPEG-4 visual and Part-10 (ISO/IEC 14496-10) [6] define MPEG-4 AVC (Advanced Video Coding). The MPEG-4 part-2, offers a variety of tools for visual coding. These tools are combined in subgroups called Profiles. The most common profiles for video coding are: *Simple*

Visual Profile (SP) and the *Advanced Simple Visual Profile (ASP)*. These profiles are the best choice for coding an entire image. The standard also defines Levels. These levels subdivide the profiles in terms of complexity as the image resolution, bitrates or buffer requirements. The Simple Visual Profile provides efficient, error resilient coding of rectangular video objects, suitable for applications on mobile networks, such as IMT2000 [9]. The *Advanced Simple Profile* looks much like Simple in that it has only rectangular objects, but it has a few extra tools that make it more efficient: B-frames, ¼ pel motion compensation, extra quantization tables and global motion compensation.

3   DVEVM355 Evaluation Module

DaVinci technology [7] is a signal processing based solution tailored for digital video applications that provides video equipment manufacturers with integrated processors, software, tools and support to simplify the design process and accelerate innovation. DaVinci technology refers to the *DM* platform of media processors with their associated development tools, software components, and support infrastructure including third party companies.

The DM3x generation, including DM355 processors [10], is ideal for applications compliant to MPEG-4 standard (video-playback devices such as IP cameras, video doorbells, video conferencing, digital signage, portable media players and more). This processor, due to its parallelism, it can be used to process multiple blocks of an image simultaneously. This improves system performance and overall performance compared to the serial processors.

The DVEVM355 evaluation module [11] is based on the TI TMS320DM355 processor [10]. DM355 is a multimedia processor with ARM9EJ processor and hardware video accelerator (fixed function co-processor, MJCP) and a set of peripherals for multimedia products. To harness the processing power of the DM355, we integrate MPEG-4 ASP encoder for the DM355 ARM processor.

The following figure shows the software components used for application development with the DVEVM kit.

In Figure 1, everything runs on the ARM. The application handles I/O and application processing. To process video, image, speech, and audio signals, it uses the VISA APIs provided by the Codec Engine. The Codec Engine, in turn, uses xDM-based codecs (enCOders/DECoders).

xDM, which stands for xDAIS for Digital Medial [12] is a standard API (Application Programmer Interface) that is wrapped around all signal processing functions, especially encoders/decoders. In the figure, this is represented as a container that holds a codec in VISA API. The container, which represents the code interconnections in the xDM standard and the Codec Engine negotiate the execution stages and the resources required by the encoder/decoder. VISA API (Video, Imaging, and Speech & Audio) abstracts the details of signal processing functionality, and allows an application developer to leverage

the benefits of these functions without having to know their details. The API VISA allows managing a common format to call the encoder/decoder through the codec engine. Codec Engine (CE) [13] is a piece of software of the technology DaVinci that manages the system resources and translates VISA calls into xDM calls.
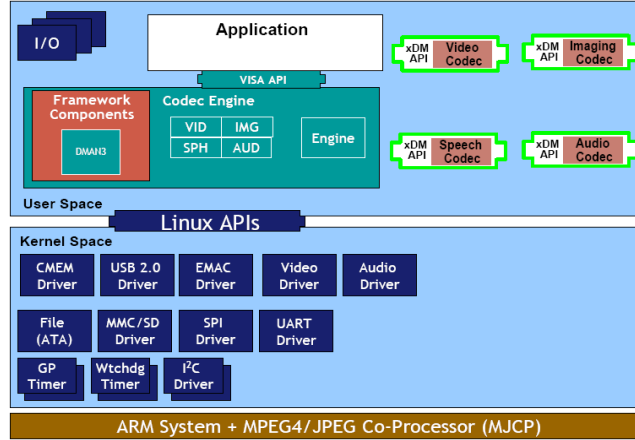
Fig. 1. Software components.

4   MPEG-4 ASP Encoder in DVEVM355

DaVinci technology consists of modular software components, which perform various tasks for an application. The encoders/decoders are called in the application using standard APIs. These APIs provide the interface with different modules that contain the encoder/decoder instructions [14] (cf. section 3). To evaluate the performance of our MPEG-4 encoder ported in the embedded platform, we develop an application in DVEVM355 that encodes a video sequence with the MPEG-4 ASP-Xvid encoder. This application is based on standards VISA, xDM and codec engine of the DaVinci technology to develop embedded software.

The Xvid encoder [15] is an implementation non-compliant to standard MPEG-4 part-2 [5]. This encoder is under open source license known as GNU GPL (General Public License) [15]. We performed the integration of the Xvid 1.3.0-rc1 encoder in the ARM9 platform-based architecture under TI DaVinci standards [10-13]. The operating system used is MontaVista's embedded Linux distribution Pro v4.0.1.

The Xvid encoder was developed in *ANSI C* code following a modular structure [15]. The modularity of the code allows the reuse of software components in certain operating systems and processor architectures. The Xvid encoder has many tools [15] that are not covered by the MPEG-4 ASP encoder. Thus, we can say that Xvid encoder is close to

compliant, but no really compliant. For this reason, one of our contributions in this work is the Xvid encoder adaptation being compliant to the MPEG-4 ASP [5] standard. With this, we only integrate the tools provided in the standard for MPEG-4 ASP encoder. The coding tools of the Xvid encoder that satisfy the MPEG-4 ASP profile are: ASP@Level 1 (ASP@L1), ASP@L2, ASP@L3, ASP@L4, ASP@L5; I-Frames/Keyframes, P-Frames/directional encoding, B-Frames/Bi-directional encoding, Quarter Pixel Motion Estimation search precision (QPEL), Global Motion Compensation (GMC), Interlace coding, and H.263/MPEG/Custom Quantization.

Another interesting contribution of our work is the porting of the Xvid encoder to the ARM9 CPU; this porting takes advantage of the TI DaVinci standards and the DaVinci TI DVEVM355 platform. The method to porting the Xvid encoder in the ARM9 platform-based architecture of DM355 is divided in two parts:

− Xvid encoder configuration to the ARM9 platform-based architecture.
− Porting of Xvid encoder to the xDM TI standards.

4.1 Xvid Encoder Configuration to the ARM9 Platform-based Architecture

The Xvid encoder is configured to be executed on the ARM9 processor architecture into the DM355 of TI. The parameters for the set up are: target platform *"ARM generic"*; type of compiler *"ARM_V5T_LE-GCC"*, the company Montavista Linux; host platform *"x86_64-pc-linux"*.

4.2 Porting of Xvid Encoder to the xDM TI Standards

Once that the Xvid encoder is integrated with the coding tools under the MPEG-4 ASP profile and its configurations to be executed in the DM355 ARM processor, we develop the MPEG-4 ASP-Xvid encoder implementation under DaVinci TI standards. The methodology is based on the recommendations of R. Pawate [14]. We used the APIs VISA, xDM and the Codec Engine for the management of MPEG-4 ASP-Xvid encoder being compatible with the software components of the DVEVM355 platform. The implementation is described in the following lines:

Figure 2 shows the outline to follow to implement an encoder/decoder under DaVinci technology. The codec engine software basically translates these *create*, *control*, *process* and *delete* APIs to their respective xDM APIs, while managing the system resources and inter-processor communication.

The process and control API of VISA are a direct reflection of the low-level process and control functions of the xDM algorithm (codec1). As a result, Texas Instruments providing low-level control of codecs along with high level abstraction of the details. The figure 3 shows the specific VISA and xDM APIs for the video encoder/decoder. For a

given class, say Video, the signature of these APIs is held constant. This enables an integrator and developer to easily replace one encoder/decoder with another.
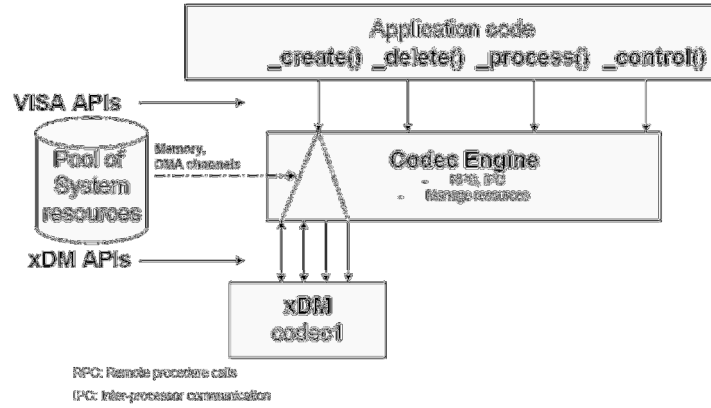
Fig. 2. Management of an encoder/decoder under DaVinci technology.
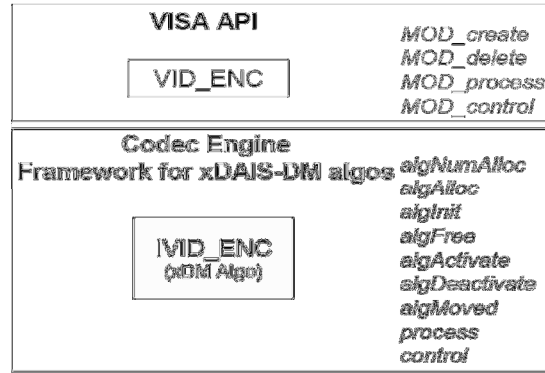
Fig. 3. VISA Abstracts details of xDM algorithms for video encoder/decoder.

To use the followings APIs: VISA, xDM and of the Codec Engine, the application is divided into four logical blocks:

−   Parameter setup,
−   Algorithm instance creation and initialization,
−   Process call – xDM 1.0,
−   Algorithm instance deletion.

4.2.1 Parameter Setup

The video encoder/decoder requires various configuration parameters to be set at initialization. Our application obtains the required parameters from the encoder configuration. The coding parameters are assigned to *VIDENC1_XVID_PARAMS* structure, which is an extended version of the generic structure *IVIDENC1_Params*. The generic structure is used by video codecs for the API VISA. We verify that the parameters are within the ranges set by the MPEG-4 ASP standard. We also assign memory space E/S for the data of the entry frame and for the data of the coded frame. The allocation of contiguous memory space is done by the function: *Memory_contigAlloc().* After successful completion of the above steps, the application does the algorithm instance creation and initialization.

4.2.2 Algorithm Instance Creation and Initialization

In this logical block, the application accepts the various initialization parameters and returns an algorithm instance pointer. *The VIDENC1_XVID_Create() API* creates an instance of xDM encoder MPEG-4 ASP-Xvid and allocates the required resources for the encoder MPEG-4 ASP-Xvid to run. *VIDENC1_XVID_Create() API*, using the Codec Engine, queries the xDM encoder for the resources that it needs, and based on the encoder requirements, it allocates them. The following APIs are called in sequence:

- *algAlloc()* – to query the algorithm about the memory requirement to be filled in the memory records.
- *xvid_global(XVID_GBL_INIT)* – to initialize the global variables of the algorithm.
- *xvid_encore(XVID_ENC_CREATE)* – to initialize the algorithm.
- *algInit()* – to initialize the algorithm with the memory structures provided by the application.

4.2.3 Process Call – xDM 1.0

After algorithm instance creation and initialization, the application does the following:

- Sets the dynamic parameters (if they change during run time) by calling the *VIDENC1_XVID_control()* function.
- Sets the input and output buffers descriptors required for the *VIDENC1_XVID_process()* function call. The input and output buffer descriptors are obtained by calling the *VIDENC1_XVID_control()* function.
- Call the *VIDENC1_XVID_process()* function to encode a single frame of data. In this function, we call the function *xvid_encore(XVID_ENC_ENCODE)* which coding the frame at the input buffer with MPEG-4 ASP-Xvid encoder. When the process function ends, the output buffer is updated with the encoded picture.

The *VIDENC1_XVID_control()* and *VIDENC1_XVID_process()* functions should be called only within the scope of the *algActivate()* and *algDeactivate() xDAIS* functions which activate and deactivate the algorithm instance respectively. Once an algorithm is

activated, there could be any ordering of *VIDENC1_XVID_control()* and *VIDENC1_XVID_process()* functions. The do-while loop encapsulates frame level *VIDENC1_XVID_process()* call and updates the input buffer pointer every time before the next call. The do-while loop breaks off either when an error condition occurs or when the input buffer exhausts.

4.2.4 Algorithm Instance Deletion
Once encoding is complete, the application must release the resource for the encoder MPEG-4 ASP-Xvid and delete the current algorithm instance.

5   Results

This section presents the evaluation of MPEG-4 ASP-Xvid encoder ported in the embedded Linux operating system under ARM9 platform-based architecture of DM355. In order to evaluate our MPEG-4 ASP-Xvid encoder porting, we develop an application in DVEVM355 that encodes a video sequence with the MPEG-4 ASP-Xvid encoder. In order to have a reference for comparing our encoder's performance, we conducted the evaluation of the MPEG-4 SP encoder of TI for DM355 [16] under the same conditions. The test database consists of three video sequences *(Bus, Foreman and News)*. These sequences are used as reference by the integrators developers, and the scientific community to evaluate the encoder's performance. These sequences have great information in texture, movements ranging from low to high level. Each video has the following parameters: 10 seconds of video, CIF (Common Interface Format) resolutions (352x288), YUV 4:2:0P, 30 fps. The coding scheme was tested with different constant bitrates: CBR: 64kbps, 128Kbps, 384Kbps, 512Kbps and 1024Kbps. The GOP size for both encoders is 12 (frames). The GOP structure for the MPEG-4 ASP-Xvid encoder is IBBPBBPBBPBB, while for the MPEG-4 SP encoder of TI is IPPPPPPPPPPP. According to the above parameters, the three sequences were coded for both encoders under DaVinci platform. Then, the coded sequences were decoded in the host computer. To evaluate the performance of our integration of MPEG-4 ASP-Xvid encoder in the DVEVM355 architecture, according to the standard xDM of TI, we consider Peak Signal to Noise Ratio of the Y-plane of the frame (Y-PSNR) measure. Equation 1 describes Y-PSNR mathematically.

$$d\left(I, I^{'}\right) = 10 \cdot \log_{10} \frac{(Max_I)^2 \cdot m \cdot n}{\sum_{i=0}^{m-1} \sum_{j=0}^{n-1} \left(I(i,j) - I^{'}(i,j)\right)^2} \tag{1}$$

where $d(I, I')$ is the Y-PSNR value, Max_I indicates the largest possible pixel value, I is the original frame and I' is the decoded frame, m,n are the frame size mxn (352x288). The Y-PSNR is obtained of the average of each video sequence. The other evaluation metric used is based on compression ratio.

The figures 4, 5 and 6 depict the result of average Y-PSNR value of Bus, Foreman and News video sequences with different bitrates.

Based on the video quality measure results, the MPEG-4 ASP-Xvid encoder ported to the DM355 maintained better performance than the MPEG-4 SP encoder of TI for the three sequences, which contain different levels of motion.
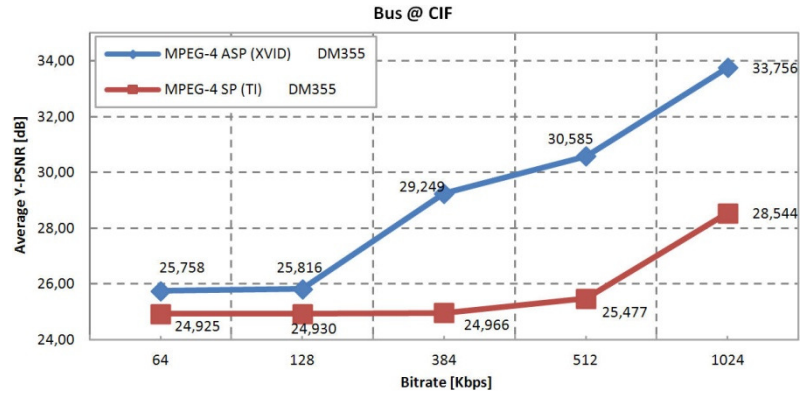
Fig. 4. Coding efficiency: comparison between MPEG-4 SP of TI encoder and our integration of MPEG-4 ASP-Xvid encoder using Bus video sequence.
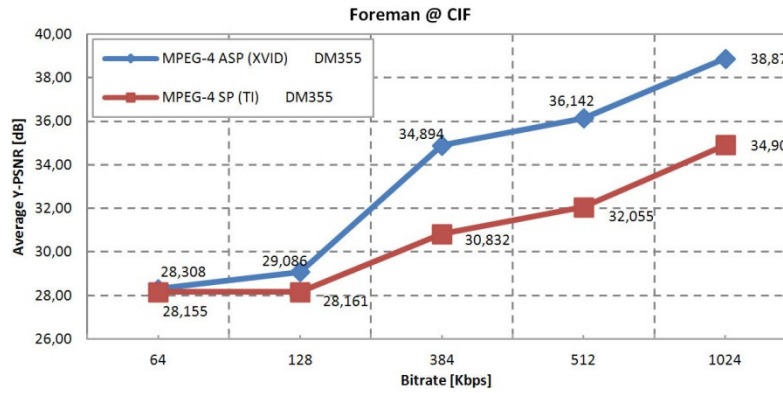
Fig. 5. Coding efficiency: comparison between MPEG-4 SP of TI encoder and our integration of MPEG-4 ASP-Xvid encoder using Foreman video sequence.
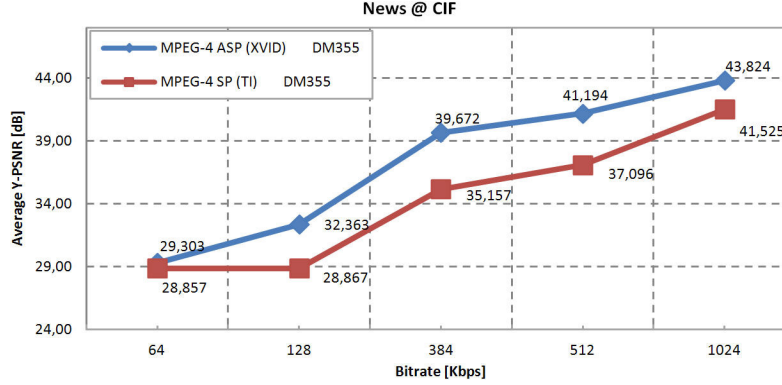
Fig. 6. Coding efficiency: comparison between MPEG-4 SP of TI encoder and our integration of MPEG-4 ASP-Xvid encoder using News video sequence.
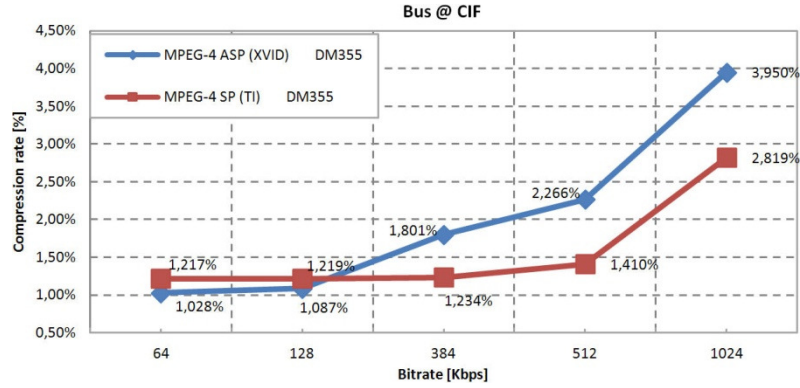
Fig. 7. Compression efficiency: comparison between MPEG-4 SP of TI encoder and our integration of MPEG-4 ASP-Xvid encoder using Bus video sequence.

With respect to overall performance on the three sequences for both encoders, we observe that the best quality is obtained with the News sequence (Fig. 6) behaving with low movement, followed by Foreman (Fig. 5) that presents a middle movement category. Finally, the worst quality is obtained with the Bus sequence (Fig. 4), which presents a high motion category. Based on the compression ratio, figures 7, 8 and 9 show the encoder's performance under different bitrates. The compression ratio represents the size in Kbytes of coded video with respect to the size in Kbytes of the original sequence. The rate of compression is presented as a percentage. With respect to the measure of compression ratio, a value close to zero represents a better performance of the encoder.

With respect to overall performance on the three sequences for both encoders, we can summarize that the best compression is obtained with the News sequence (Fig. 9), then foreman (Fig. 8) and finally, the worst compression is obtained with Bus sequence (Fig. 7).
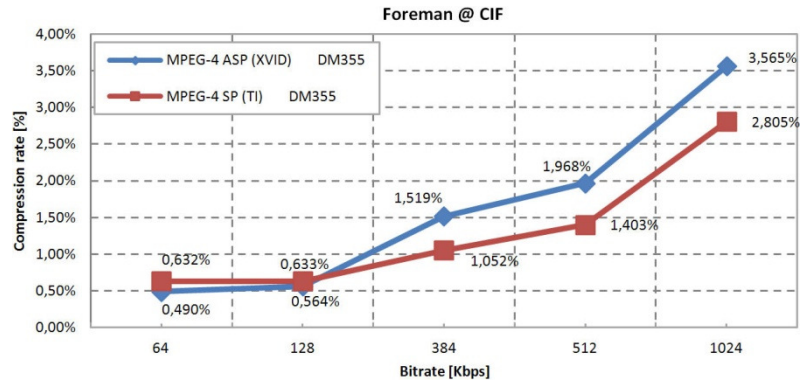
Fig. 8. Compression efficiency: comparison between MPEG-4 SP of TI encoder and our integration of MPEG-4 ASP-Xvid encoder using Foreman video sequence.
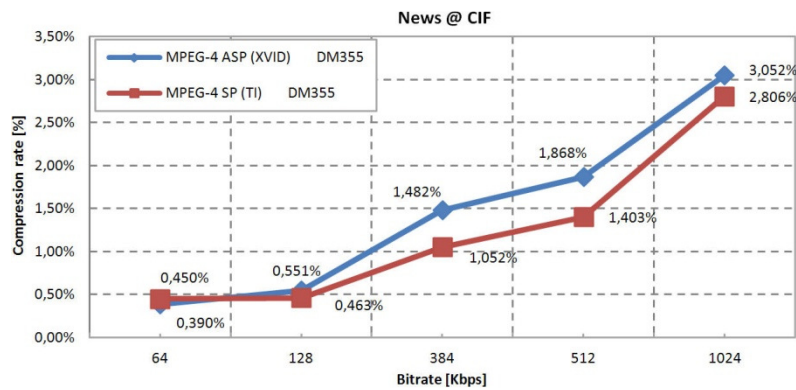
Fig. 9. Compression efficiency: comparison between MPEG-4 SP of TI encoder and our integration of MPEG-4 ASP-Xvid encoder using News video sequence.

6   Conclusions and Future Direction

The main advantage of developing applications platform-based design is the integration of software/hardware components from different manufacturers in a very short time. The

development of a complete software application that constitutes a working embedded system relies on many software components. For this reason, this work leverages the use of an embedded Linux operating system tailored for the DaVinci platform. Based on the analysis of the DaVinci technology, this paper presented a prototype of an MPEG-4 encoder video profile ASP based on Xvid software ported to the architecture ARM9 processor of the DaVinci Platform DVEVM355 of Texas Instruments. We developed an application to evaluate the performance of our MPEG-4 ASP Xvid encoder. This application is based on standards VISA, xDM and codec engine of the DaVinci technology to develop embedded software. The encoder is then evaluated for performance on the platform DVEVM355. Based on testing and performance, the MPEG-4 ASP Xvid encoder ported to the ARM9 platform-based architecture of DM355 is a good candidate to replace the MPEG-4 SP encoder of TI since it shows higher quality video. As future work, we will migrate our algorithm in a fully-programmable DSP to leverage the power of the DSP on the SoC (ARM+DSP) since the co-processor of the DM355 is not a DSP open for programming.

References

1   Sangiovanni-Vincentelli, A., Carloni, L., De Bernardinis, F., Sgroi, M.: Benefits and challenges for platform-based design. In: Proc. DAC, pp. 409–414 (2004)
2   International Organization for Standardization (ISO/IEC). `http://www.iso.org` (2011)
3   International Telecommunication Union (ITU-T). `http://www.itu.int/ITU-T` (2011)
4   Chatterji, S., Narayanan, M., Duell, J., Oliker, L.: Performance evaluation of two emerging media processors: Viram and imagine. In: International Parallel and Distributed Processing Symposium, pp. 229–235 (2003)
5   ISO/IEC 14496-2:2004, Information technology – Coding of audio-visual objects – Part 2: Visual (Approved in 05-24) (2004)
6   Wiegand, T., Sullivan, G. J., Bjontegaard, G., Luthra, A.: Overview of the H.264 / AVC Video Coding Standard. IEEE transactions on circuits and systems for video technology (2003)
7   Texas Instruments, `http://www.ti.com` (2011)
8   Shin, D., Gerstlauer, A., Dömer, R., Gajski, D.: Automatic Network Generation for System-on-Chip Communication Design. In: Proceedings of the International Conference on Hardware/Software Codesign and System Synthesis. Jersey City, New Jersey (2005)
9   IMT-2000.: International Mobile Telecommunications, http://www.itu.int/osg/spu/imt-2000/technology.html (2011)
10 TMS320DM355 Digital Media System-on-Chip (DMSoC) (Rev.G, 24 June). SPRS463G. Texas Instruments (2010)
11 TMS320DM355 Evaluation Module Technical Reference. 509905-0001 Rev. E. Spectrum Digital, Inc. (2008)
12 xDAIS-DM (Digital Media), User Guide. Literature Number: SPRUEC8B. Texas Instruments (2007)

13 Codec Engine Application Developer User's Guide. Literature Number: SPRUE67D, September. Texas Instruments (2007)

14 Pawate, B.I. R.: Developing Embedded Software using DaVinci & OMAP Technology, Synthesis Lectures on Digital Circuits and Systems. Morgan & Claypool Publishers (2009)

15 Xvid Codec. http://www.xvid.org (2011)

16 MPEG-4 Simple Profile Encoder Codec on DM355. User's Guide. Literature Number: SPRUFE4C. Texas Instruments (2008)

Using Signal Processing Based on Wavelet Analysis
to Improve Automatic Speech Recognition
on a Corpus of Digits

José Luis Oropeza Rodríguez, Mario Jiménez Hernández,
and Alfonso Martínez Cruz

Center for Computing Research, National Polytechnic Institute,
Av. Juan de Dios Batiz esq Miguel Othon de Mendizabal s/n, 07038, México DF, Mexico
joropeza@cic.ipn.mx, mjimenezh@ipn.mx, almart001@hotmail.com

Abstract. This paper shows results when we used wavelets in a corpus of digits pronounced by five speakers in Spanish language. One of the most important aspects related to the ASR is to reduce the number of data used. Firstly, we show the results when we used wavelet filters to the speech signal in order to obtain low frequencies only. Secondly, we use the ability of wavelet analysis is to perform data compression, to reduce by half the amount of voice data analyzed. For each of the two previous experiments we obtained new corpus, after that each corpus was used to train an Automatic Speech Recognition System using the technique vector quantization (VQ), being more employed in these corpus, also at final we compare the results obtained with DHMM technique. Finally, we compare our results with respect to the original corpus and found a 3-5% reduction in Word Error Rate (WER) when we use VQ and (1-3%) using CHMM. Daubechies wavelets were used in the experiments, as well as Vector Quantization (VQ) with Linear Prediction Coefficients (LPC) as features to represent the speech signal and DHMM.

Keywords: Wavelets, automatic speech recognition systems (ASRs), Daubechies wavelet, wavelet filters, vector quantization (VQ), discrete hidden Markov models (DHMM), data speech compression.

1 Introduction

Automatic Speech Recognition systems (ASRs) work reasonably well in quiet conditions but work poorly under noisy conditions or distorted channels. For example, the accuracy of a speech recognition system may be acceptable if you call from the phone in your quiet office, yet its performance can be unacceptable if you try to use your cellular phone in a shopping mall. The researchers in the speech group are working on algorithms to improve the robustness of speech recognition system to high noise levels channel conditions not present in the training data used to build the recognizer [Cole et al., 1996]. In this paper we used wavelet filters to avoid high frequencies, where noisy signals regularly are

present. That is very important because of one of the most important aspects that have been studied for the last years is that the important information of the speech signals is contained within low frequencies more than high frequencies. "The schools of thought in speech recognition" describe four different approach researched at today [6], we are going to use template-based approach.

ASR has implemented one stage called "speech analysis". The applications that need voice processing (such as coding, synthesis, and recognition) require specific representations of speech information. For instance, the main requirement for speech recognition is the extraction of speech features, which may distinguish different phonemes of a language. In the template-based approach, the units of speech (usually words, like in this work), are represented by templates in the same form as the speech input itself. Distance metrics are used to compare templates to find the best match, and dynamic programming is used to resolve the problem of temporal variability. Tem-plate-based approaches have been successful, particularly for simple applications requiring minimal overhead. We used this approach in this paper. A variety of techniques have been developed to efficiently represent to speech signals in digital form for either transmission or storage. Since most of the speech energy is contained in the lower frequencies results very important to encode the lower-frequency band with more bits than the high-frequency band. In this paper we based our experiments in the last aspect, we use subband coding which is a method where the speech signal is subdivided into several bands and each band is digitally encoded separately. In subband coding a speech signal is sampled at a rate Fs samples per second. The first frequency subdivision splits the signal spectrum into two equal-width segments, a lowpass signal $0 \leq F \leq F_x/4$, and a highpass signal $F_s/4 \leq F \leq F_s/2$. The second frequency subdivision splits the lowpass signal from the first stage into two equal bands, a lowpass signal $0 \leq F \leq F_s/8$, and a highpass signal $F_s/8 \leq F \leq F_s/4$. Finally, the third fre-quency division splits the lowpass signal from the second stage into two equal band-width signals. Thus the signal is subdivided into four frequency bands, covering three octaves. To perform subband coding we use wavelet analysis as implemented in [7].

1.1   Phonetic and Frequency Analysis

One aspect related with propose mentioned above is that /s/ phoneme, that we can consider as unvoiced fricative sound, contains representative frequencies lower than 3.5 kHz. For that, if the noise components integrated into speech signal were removed using a filter and the response filter were used into Automatic Speech Recognition systems to try to reduce the WER, we can obtain a methodology that can be used in ASR. Now, wavelet filter is newest approach used in digital signal processing, their characteristics are better (in some cases) than techniques employed in classical digital filter.

1.2 Wavelet Compression

Wavelet compression is a form of data compression well suited for image compression (sometimes also video compression and audio compression). The goal is to store image data in as little space as possible in a file. Wavelet compression can be either lossless or lossy (JPEG 2000, for example, may use a 5/3 wavelet for lossless (reversible) transform and a 9/7 wavelet for loss (irreversible transform) [Van Fleet, 2008]. Using a wavelet transform, the wavelet compression methods are adequate for representing transients, such as percussion sounds in audio, or high-frequency components in two-dimensional images, for example an image of stars on a night sky. This means that the transient elements of a data signal can be represented by a smaller amount of information than would be the case if some other transform, such as the more widespread discrete cosine transform, had been used.

1.3 Speech Recognition using Wavelets

Taking into account all that we mentioned above for researcher interested in speech recognition is very interesting analyze how can we use compression properties related with wavelet analysis into a corpus of speech signals that it will be used into Automatic Speech Recognition tasks. The results obtained not only have impact over the task mentioned above, but it could be used for a combination of data compression that it will be used for transmission of information into digital networks, for example. Wavelets was used for one important reason, its computational implementation as digital filter and in compression signal is easy to make and, due to that multi-resolution analysis inherent wavelet systems, a reduced number of coefficients are necessary to be implemented in comparison with digital filters design traditional (FIR) or instability conditions (IIR) [Van Fleet, 2008].

An important amount of works have been realized in this aspect, above all for robust speech recognition task, it refers to the need to maintain good recognition accuracy even when the quality of the input speech is degraded, or when the acoustical, articulatory, or phonetic characteristics of speech in the training and testing environments differ. Obstacles to robust recognition include acoustical degradations produced by additive noise, the effects of linear filtering, nonlinearities in transduction or transmission, as well as impulsive interfering sources, and diminished accuracy caused by changes in articulation produced by the presence of high-intensity noise sources. Even systems, that are designed to be speaker-independent, exhibit dramatic degradations in recognition accuracy when training and testing conditions differ [2]. For these reasons, within others, is necessary to find an alternative that can be used to reduce the conflicts presented here.

2 Wavelet Theory

Fourier analysis, using the Fourier transform, is a powerful tool for analyzing the components of a stationary signal. For example, the Fourier transform is a powerful tool for processing signals that are composed of some combination of sine and cosine signals. The Fourier transform is less useful in analyzing non-stationary data, where there is no repetition within the region sampled. Wavelet transforms (of which there are, at least formally, an infinite number) allow the components of a non-stationary signal to be analyzed. Wavelets also allow filters to be constructed for stationary and non-stationary signals [3].

The statistics of many natural images are simplified when they are decomposed via wavelet transform. Recently, many researchers have found that statistics of order greater than two can be utilized in choosing a basis for images, has shown that the coefficients of frequency subbands of natural scenes have much higher kurtosis than a Gaussian distribution. Daubechies wavelets are a family of orthogonal wavelets defining a discrete wavelet transform and characterized by a maximal number of vanishing moments for some given support [3]. With each wavelet type of this class, there is a scaling function (also called mother wavelet) which generates an orthogonal multiresolution analysis. The selected sub-band was the 3 in all case, because the high level recognition was better for this case. A signal or function $f(t)$ can often be better analyzed, described, or processed if expressed as a linear decomposition by [4].

$$f(t) = \sum_{k \in Z} c_{j,k} \phi_{j,k}(t) \tag{1}$$

Where $\phi_{j,k}(t)$ is an integer index for the sum, is the expansion coefficients and is the set of real-valued functions of t called the expansion set. If the expansion is unique, the set is called a basis for the functions that could be represented. If the basis is orthogonal, then the coefficients can be calculated by the *inner product.* [Walnut, 2001]

$$c_{j,k} = \langle f(t), \phi_{j,k}(t) \rangle = \int_{-\infty}^{\infty} \left| f(t) \phi_{j,k}(t) \right| dt \tag{2}$$

A single $\phi_{j,k}(t)$ coefficient is obtained by substituting (1) into (2) and therefore for the *wavelet expansion,* a two-parameter system is constructed such that (1) becomes

$$f(t) = \sum_{k} \sum_{j} c_{j,k} \phi(t) + \sum_{k} \sum_{j} d_{j,k} \psi(t) \tag{3}$$

Where $\left\{ \psi_{j,k}(t) \mid j,k \in Z \right\}$ and $\phi_{j,k}(t)$ is the wavelet expansion that usually forms an orthogonal basis. The set of expansion coefficients $\psi_{j,k}(t)$ are called the discrete wavelet transform of $f(t)$ and (3) is its inverse.

All wavelet systems are generated from a single scaling function or wavelet by simple scaling and translation. This two-dimensional representation is achieved from the function $\psi_{j,k}(t)$, also called the mother wavelet, by

$$\psi_{j,k}(t) = 2^{\frac{j}{2}} \psi\left(2^j t - k\right) \qquad j,k \in Z \tag{4}$$

Wavelet systems also satisfy multi-resolution conditions. In effect, this means that a set of scaling functions can be determined in terms of integer translates of the basic scaling function by

$$\phi_{j,k}(t) = 2^{\frac{j}{2}} \phi(2^j t - k) \qquad j,k \in Z \tag{5}$$

It can therefore be seen that if a set of signals can be represented by $\phi(t-k)$, a larger set can represented by $\phi(2t-k)$, giving a better approximation of any signal.

Hence, due to the spanning of the space of $\phi(t)$ by $\phi(2t)$, it can be expressed in terms of the weighted sum of the shifted as

$$\phi(t) = \sum_{k \in Z} h(n)\sqrt{2}\phi(2t - k) \tag{6}$$

Where the coefficients *h(n)* may be real or complex numbers called the scaling function coefficients. However, the important features of a signal can better be described, not by $\phi(2t)$, but by defining a slightly different set of functions $\psi_{j,k}(t)$ that span the differences between the spaces spanned by the various scales of the scaling function. These functions are the wavelets and, they can be represented by a weighted sum of shifted scaling function $\phi_{j,k}(t)$ defined in (6) by [Yuan Yan, 2009].

$$\psi(t) = \sum_{k \in Z} \sqrt{2}h(n)\phi(2t - k) \tag{7}$$

The function generated by (7) gives the prototype or mother wavelet $\psi(t)$ for a class of expansion functions of the form given by (4).

$$f(t) = \sum_k \sum_j c_{j,k}\phi(t) + \sum_k \sum_j d_{j,k}\psi(t) \tag{8}$$

The coefficients in this wavelet expansion are called the discrete wavelet transform (DWT), of the signal *f(t)*. For a large class of signals, the wavelet expansion coefficients drop off rapidly as *j* and *k* increase. As a result, the DWT is efficient for image and audio compression

3   Template-Based Approach

The frequency bandwidth of a speech signal is about 16 KHz. However, most of speech energy is under 7 KHz. Speech bandwidth is generally reduced in recording. A speech signal is called orthophonic if all the spectral components over 16 KHz are discarded. A telephonic lower quality signal is obtained whenever a signal does not have energy out of the band 300-3400 Hz. Therefore, digital speech processing is usually performed by a frequency sampling ranging between 8000 samples/sec and 32000 samples/sec. These values correspond to a bandwidth of 4KHz and 16KHz respectively. In this work, we use a frequency sampling 11025 samples/sec [1].

4   Experiments and Results

In the proposal developed in the experiments we used the methodology represented in figure 6, this figure shows the experiment developed using wavelets theory to reduce the amount of noise contained in the speech signal, it was obtained taking into account the frequency allocation in a (conventional, decimated) DWT where we have A1 and D1 frequency allocation to represent such Approximations as Details obtained from wavelet filter used, the actual shape depends of the wavelet filters. Also, figure 6 shows the experiment developed using wavelet theory to applied data compression, DWT decomposition were used with the difference that we token the speech signal from different points.
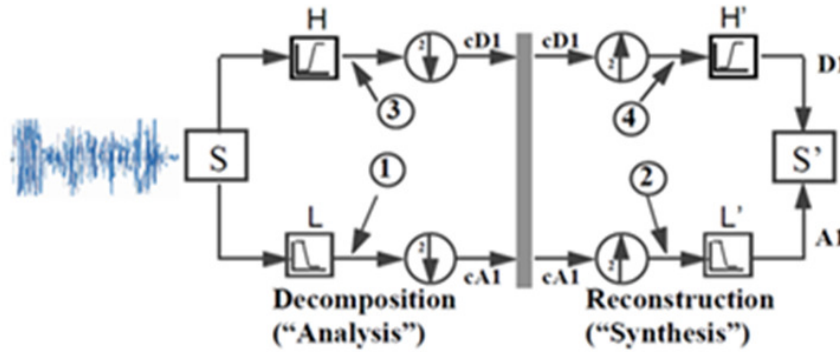
Fig. 1. Analysis wavelet used in the experiments.

For experiments, a Spanish digits database (0-9) was used, it consists of 5 speakers each one of them pronounced 200 sentences of digits, half of them were used to training system and the rest for recognition. Speech signals were recorded at 11025 kHz with 16

bits by sample, using mono-channel with PCM format. As we mentioned before and after to describe the proposal developed in this paper, we obtained a total of 600 sentences for each speaker obtained of a great total of 3000 sentences processed during experiments reported. As we mentioned before and after to describe the proposal developed in this paper, we obtained a total of 600 sentences for each speaker obtained of a great total of 3000 sentences processed during experiments reported.

The signal flow diagram for a single-level conventional DWT is shown in figure 1. The information used to eliminate the noise was taken after of the block denoted as L, while the information used for compression was taken after of the first label cA1 as we shown in the same figure, where down-sampling for 2 was reached. As we mentioned before and after to describe the proposal developed in this paper, we obtained a total of 600 sentences for each speaker obtained of a great total of 3000 sentences processed during experiments reported. The signal flow diagram for a single-level conventional DWT is shown in figure 6. The information used to eliminate the noise was taken after of the block denoted as L, while the information used for compression was taken after of the first label cA1 as we shown in the same figure.

Table 1 shows results obtained using speech signals after to apply wavelet compression, we can see that performance reached was superior using decomposition level 1, for that in all experiments reported here this decomposition level was selected.

In rows we can see wavelet Daubechies order (form 1 to 3) and in the columns we can see the 5 corpus analyzed, the performance reached also is showed. We can see clearly that the best performance was obtained using decomposition level 1 in comparison with decomposition level 2.

Table 1. Results using wavelet filters.

DECOMPOSITION LEVEL 1					
Dbn/corpus	1	2	3	4	5
1	97	93	89	93	100
2	97	93	89	93	100
3	96	97	86	91	100
DECOMPOSITION LEVEL 2					
1	73	89	72	73	92
2	73	89	72	73	92
3	70	86	76	83	92

Another results obtained is illustrated in table 2 which reports obtained using speech signals after to apply lowpass filter, again we can see that the best performance is obtained when we used decomposition level 1.

As we can see, the results obtained using two aspects considered in this paper was successful when we used decomposition level 1, but the best performance occurs and it is most significant using wavelet compression.

Table 2. Results using wavelet filters.

DECOMPOSITION LEVEL 1					
Dbn/corpus	1	2	3	4	5
1	91	98	85	94	100
2	93	97	84	97	100
3	91	98	84	94	100
DECOMPOSITION LEVEL 2					
1	82	99	67	80	97
2	78	99	67	86	96
3	80	100	67	85	95

Finally, we show, in table 3, the performance reached when we used the original corpus for recognition task.

Comparing the results we can conclude that the recognition percentage was better using the compression wavelet with the exception showed for the second corpus because of it had noisy signal.

Table 3 Results using original corpus

ORIGINAL CORPUS					
corpus	1	2	3	4	5
original	97	96	84	92	100

The results previously presented were compared using Discrete Hidden Markov Models (DHMM) with 6 states per model for each word into the corpus. The results obtained demonstrated that DHMM results better than VQ technique in order 3% related with the corpus used.

5   Conclusions and Future Works

Without loss of generality, such as has been demonstrated in ASRs based in VQ, we can to say that the results obtained in these experiments can be extended to others ASRs that employ Continuous Density Hidden Markov Model (CDHMM) and Mel Frequency Cepstrum Coefficients (MFCC) without problem. The main purpose of this paper was to integrate wavelet aspects such as digital filters and compression into ASRs. We showed that the methodology proposed reached out an increase of the 3-5% of the WER for some corpus created. For future works we are going to use the results obtained here to integrate the Automatic Speech Recognition for a system that is focused to speaker and speech recognition wheatear more synthesis in an application that is going to interactively it will respond to anybody people. For that, we must to work in increase the number of the

speakers and programming another splitting algorithm. Though the results reported demonstrated a good and better performance.

References

1. Bechetti, C., Ricoti L.P.: Speech Recognition Theory and C++ Implementation, Fundazione Ugo Bordón. Rome, Italy. John Wiley and Sons, Ltd. (1999)
2. Cole, A.R., Mariani,J., Uszkoreit, H., Zaenen, A., Zue, V.:. Survey of the State of the Art in Human Language Technology, National Science Foundation, CSLU, Oregon Institute.
3. Duran, D.I.: The Wavelet Transform, Time-Frequency Localization and Signal Analysis. IEEE Transactions on Information Theory, Vol. 36, No. 5 (1990)
4. Faundez, P., Fuentes, A.: Procesamiento de señales acústicas utilizando wavelets. Instituto de Matemáticas, UACH.
5. Farnetani, E.: Coarticulation and connected speech processes. In: The Handbook of Phonetic Sciences. W. Hardcastle and J. Laver, 12 . Blackwell, pp. 371-404 (1997)
6. Kirschning, A.I.: Automatic Speech Recognition with the parallel Cascade Neural network, PhD Thesis. Tokyo, Japan (1998)
7. Mallat, S.: A wavelet tour of signal processing. Academic Press, ISBN: 0-12-4666606-X (1999)
8. Nicholas, G.R..: Fourier and wavelet representations of functions, Electronic Journal of Undergraduate Mathematics. Furman University. Volume 6, 1-12 (2000)

Ontologies, Logic and Multi-agent Systems

Methontology-based Ontology
Representing a Service-based Architectural Model
for Collaborative Applications

Mario Anzures-García[1], Luz A. Sánchez-Gálvez[2], Miguel J. Hornos[2],
and Patricia Paderewski[2]

[1] Facultad de Ciencias de la Computación, Benemérita Universidad Autónoma de Puebla,
14 sur y avenida San Claudio. Ciudad Universitaria, San Manuel, 72570 Puebla, Mexico
[2] Universidad de Granada, C/ Periodista Saucedo Aranda, s/n, 18071 Granada, Spain
`{mario.anzures, sanchez.galvez}@correo.buap.mx,`
`{mhornos, patricia}@ugr.es`

Abstract. Nowadays, the usage of ontologies to model systems has been extended to several domains, since ontology facilitates the modeling of complex systems and presents axioms which can be used as rules, policies or constrains to govern the system behavior. This paper presents ontology to represent a Service-based Architectural Model for Collaborative Applications, such as a Conference Management System (CMS), a simple social network, a chat, or a shared workspace. The development process of this ontology is based on *Methontology*, which is a well-structured methodology to build ontologies from scratch that includes a set of activities, techniques to carry out each one, and deliverables to be produced after the execution of such activities using its attached techniques. In order to show the development of the ontology using *Methontology*, the concepts, relations, axioms and instances of this ontology are specified for the collaborative application chosen as a case study, which is a CMS.

Keywords: Ontology, ontology construction process, methontology*,* collaborative application, architectural model.

1 Introduction

Recently, there has been an increase in the use of ontologies to model applications in any domain. Ontology is presented as an organization resource and knowledge representation through an abstract model. This representation model provides a common vocabulary of a domain and defines the meaning of the terms and the relations amongst them.

In a collaborative domain, the ontology provides a well-defined common and shared vocabulary, which supplies a set of concepts, relations and axioms to describe this domain in a formal way. In this domain, the ontologies have mainly been used to model tasks or sessions. Different concepts and terms, such as group, role, actor, task, etc., have been used for the design of tasks and sessions. Moreover, semiformal methods (e.g. UML class

diagrams, use cases, activity graphs, transition graphs, etc.) and formal ones (such as algebraic expressions) have also been applied to model the sessions. There is also a work [1] for modeling cross-enterprise business processes from the perspective of a cooperative system, which is a multi-level design scheme for the construction of cooperative system ontologies. This last work is focused on business processes, and it describes a general scheme for the construction of ontologies. In the literature, there are several papers on ontologies to model collaborative work; however, ontologies to support architectural modeling for developing collaborative applications have not been presented. In this work, the ontology will be used to facilitate the service composition of the architectural modeling by means of a Business Process Modeling (BPM), which is based on the ontological approach. This is the main reason to build the ontology; however, the BPM explanation is outside the scope of this article. Instead, this paper will focus on the ontology construction process using Methontology, since this methodology presents tasks set, which allow us to simplify this construction process and same time the development of collaborative application. These tasks detail each concept, the relations between these, as well as the rules and the axioms that govern its interaction, so it carries out the correspondent tables to these activities facilitate the development of the collaborative applications.

The ontology construction process must be based on methodologies, which specify techniques and methods that drive the development of the corresponding ontology. This allows us to define common and structured guidelines that establish a set of principles, design criteria and phases for building the ontology. *Methontology* [2, 3] is a methodology that supports the ontology construction process from scratch or the reuse of existing ontologies. For this reason, this paper proposes a Methontology-based ontology to represent a Service-based Architectural Model for Collaborative Applications (SAMCA). As a collaborative application example, a Conference Management System (CMS) is modeled by means of this ontology, to show how the CMS construction process is simple when it elaborates the table of each activity of the Methontology.

In the following sections, this paper presents a brief introduction to ontologies (Section 2), a review of the methodologies used in the ontology construction process, and particularly of *Methontology*, which is the one we applied to this work (Section 3), a concise explanation of SAMCA (Section 4), an example taken from the collaborative application CMS to show the use of *Methontology* (Section 5), and finally, the conclusions and future work (Section 6).

2   Introduction to Ontologies

There are several definitions of ontology, which have different connotations depending on the specific application domain. In this paper, we will refer to Gruber's well-known definition [4], where an ontology is an explicit specification of a conceptualization. *Conceptualization* refers to an abstract model of some phenomenon in the world by

identifying the relevant concepts of that phenomenon. *Explicit specification* means that the type of concepts used, and the constraints on their use are explicitly defined.

The ontologies require of a logical and formal language to be expressed. In Artificial Intelligence, different languages have been developed, including First-order Logic-based, Frames-based, and Description Logic-based ones. The first ones provide powerful modeling primitives; the second ones have more expressive power but less inference capacity, while the third ones are more robust in the reasoning power.

Ontology is specified using the following components [4]:

- − *Classes*: Set of classes (or concepts) that belong to the ontology. They may contain individuals (or instances), other classes, or a combination of both with their corresponding attributes.
- − *Relations*: These define interrelations between two or more classes (object properties) or a concept related to a data type (data type properties).
- − *Axioms*: These are used to impose constraints on the values of classes or instances. Axioms represent expressions in the ontology (logical statement) and are always true if they are used inside the ontology.
- − *Instances*: These represent the objects, elements or individuals of ontology.

Based on these components used to represent domain knowledge, the ontology community distinguishes two types of ontologies: lightweight ontologies and heavyweight ontologies [5]. On the one hand, *lightweight ontologies* include concepts, concept taxonomies, relationships between concepts, and properties that describe concepts. On the other hand, *heavyweight ontologies* add axioms and constraints to lightweight ontologies. Axioms and constraints clarify the intended meaning of the terms gathered on the ontology. Heavyweight and lightweight ontologies can be modeled with different knowledge modeling techniques and they can be implemented in various kinds of languages [6]. Ontologies can be highly informal, if they are expressed in natural language; semi-informal, if they are expressed in a restricted and structured form of natural language; formal, if they are expressed in an artificial and formally defined language (i.e. Ontolingua [7], OWL -Web Ontology Language- [8]); and rigorously formal, if they meticulously provide terms defined with formal semantics, theorems and proofs of properties, such as soundness and completeness.

The ontology that models a Service-based Architectural Model for developing Collaborative Applications is a heavy and formal ontology, which has been built using Methontology, defined in OWL, which is a description logic-based language that can define and instantiate Web ontologies using XML (eXtensible Markup Language) and RDF (Resource Description Framework), and published, implemented, validated and documented with the Protégé tool [9]. The ontology validation has been done with the software RACER (Renamed Abox and Concept Expression Reasoner) [10], which can work with Protégé. RACER can verify the consistency of the ontology (i.e. non-contradictory knowledge in it) to infer taxonomy and classify knowledge. Finally, the ontology was implemented with OWL, which allows generating a standalone application in Java.

3   Brief Review of Methodologies for Ontology Construction Process: Why We Use Methontology

The use of terms such as methodology, method, technique, process, activity, etc. on the ontological field is made in accordance to IEEE definitions [11], where it is established that a methodology is made up of methods and techniques, in such a way that the methods include processes and are detailed with techniques, and the processes contain activities. Finally, the activities are made up of a series of tasks.

The absence of common and structured guidelines has slowed the development of ontologies within and between teams. This has led to each development team usually follows their own set of principles, design criteria and phases for manually building the ontology. However, in the last decades, a series of methods and methodologies have been applied to the ontology construction process, such as: some general steps and some interesting points about the Cyc development [12]; the first guidelines for developing ontologies were proposed in the domain of enterprise modeling [5, 13]; a method to build an ontology in the domain of electrical networks was presented in [14]; the Methontology methodology appeared in [2, 3, 5]; a new method was proposed for building ontologies based on the Sensus ontology [15]; and the On-To-Knowledge methodology appeared in [16]. From all of them, only some methodologies were created for the ontology construction process from scratch in any domain, which are: Methontology, Sensus and On-To-Knowledge. In this paper, we use Methontology, since it is a well-structured methodology used to build ontologies from scratch as well as the reuse of existing ontologies. Moreover, this methodology defines different activities related to the ontology development process and its lifecycle, allowing us to adapt these activities to the knowledge representation needs in a domain. In this way, it is possible to modify the knowledge representation in each activity by adding, removing or changing some of the concepts, relations and instances previously presented. One more reason that has influenced the choice of this methodology is that it organizes and converts an informally perceived view of a domain into a semi-formal specification using a set of intermediate representations based on tabular and graphical notations that can be understood by domain experts and ontology developers. All this provides the necessary flexibility and simplicity to the ontology construction process.

Methontology, which was developed within the Ontology group at the Technical University of Madrid, enables the construction of ontologies at the knowledge level, having its roots in the main activities identified by the software development process [17] and in knowledge engineering methodologies [16]. This methodology includes: the identification of the ontology development process, a life cycle based on evolving prototypes (because it allows adding, changing, and removing terms in each new version) and techniques to carry out each activity in the three categories of activities identified in the ontology development process, which are [5]: ontology management, ontology development and ontology support. This process refers to which activities are performed

when building ontologies. Methontology includes a set of tasks (described in Section 5) for structuring knowledge within the conceptualization activity [5].

4 SAMCA

Our architectural model, namely SAMCA, is focused on solving a major problem in the development of collaborative applications, which is their lack to adapt to the different needs and collaborative scenarios that usually arise while these applications are running, i.e. these applications have not enough capability to be reused and adapted to different and dynamic collaborative scenarios. Therefore, a change in the group work objectives, the participants involved, the group structure, etc. can make a previously successful collaborative application unsuitable for the new situation. SAMCA allows us to develop collaborative applications that are both adaptable (the adaptation process adjusts the application functionality by the user's direct intervention) and adaptive (the adaptation process is automatically carried out). In order to achieve both kinds of adaptations, SAMCA considers the adaptation processes are focused on adjusting the architectural model and/or the group organizational structure. In the former case, the fact that the architectural model is based on SOA (Service-Oriented Architecture) [18], allows us to adapt it by replacing or even only modifying one or several application services in order to change solely that part of the application that did not fit the characteristics of the new scenario. In the latter case, such structure is modeled using other ontology (presented in [19]), which supports and manages the necessary dynamic changes and the different working styles of several groups to carry out the group work adequately.

SAMCA have a layered architectural style (see Fig. 1), containing the *Data, Group, Cooperation, Application* and *Adaption* layers. Each of them abstracts the corresponding concerns related to collaborative applications and allows a top-down development, in such a way that the lower layer provides resources to the upper layer, which uses them in accordance with its particular needs.

Data Layer contains different repositories with information, which will be used by the different services of the rest of SAMCA layers. *Application Layer* has only services; while the other layers are made up of modules, which contain services. *Group Layer* supplies a series of modules and services which support the necessary activities for carrying out the group work in a collaborative application. *Cooperation Layer* supports mechanisms that allow users to establish a common context and to coordinate group interactions. *Application Layer* contains the collaborative applications (e.g. CMS, chat, e-mail, etc.) which will be used to carry out the group work. *Adaption Layer* controls how the SAMCA services will be adapted when a state change requiring the modification of the collaborative application takes place, so that the application functionality can be preserved.
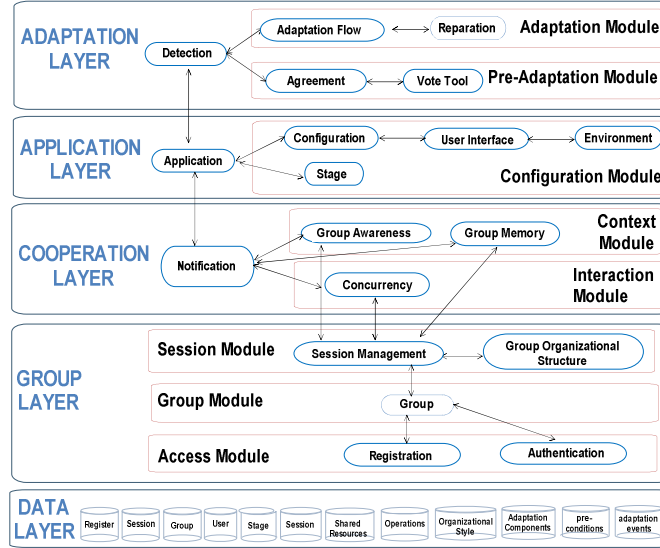
Fig. 1. General scheme of SAMCA

5   Methontology-based Ontology

This section shows how to apply Methontology to build an ontology-based CMS in according to the eleven tasks of this methodology [5]. It presents the tasks and how they are used to build a CMS.

Task 1:   *To build the glossary of terms:* It identifies the concepts and relations to be included in the ontology, as well as the concept instances. Therefore, Table 1 presents the concepts (which are SAMCA services and are represented by an oval in Fig. 2), theirs relations (drawn by arrows joining the ovals in Fig. 2) and theirs instances (for *Group_ Organizational_Style* service, only the corresponding instances to the paper submission stage of the CMS and to the author role are shown, by reason of space limitation).

Task 2:   *To build concept taxonomies:* It builds the concepts that make up the ontology taxonomy to develop the CMS, which is shown in Fig. 2. Note that this hierarchy has its root in the *Application* concept.

Task 3:   *To build ad hoc binary relation diagrams:* It establishes relationships between concepts of different ontologies. Fig. 2 shows how two ontologies (represented with solid and dashed lines respectively) are related.

Task 4:   *To build the concept dictionary:* It specifies the relations that describe each concept of the taxonomy in a concept dictionary (see Table 1).

Task 5:   *To define ad hoc binary relations in detail:* Each binary relation is specified in detail, expressing relation name, source and target concept, and inverse relation, since all ontology relations are symmetrical, for example, the ***makes up*** relationship that as can see in the first row of the Table 1, which describes this relation and specifies that "it application ***is made up*** of Stages" and in the third row it specifies that "Stage ***makes up*** an Application".

Task 6:   *To define instance attributes in detail:* This task describes in detail all the instances included in each concept (see third column of the Table 1).

Task 7:   *To define class attributes in detail:* This task describes in detail all the class attributes included in the concept dictionary.

Task 8:   *To define constants in detail:* This task describes in detail each of the constants defined in the glossary of terms.

Task 9:   *To define formal axioms:* This task identifies the formal axioms needed in the ontology and describes them precisely (see Table 2). Methontology proposes to specify: name, natural language description, logical expression that formally describes the axiom using first order logic, concepts, attributes and ad hoc relations to which the axiom refers and variables used. For example, the first expression in Table 2 shows a formal axiom of our ontology that states that "every application sets up a configuration". The variables used are ?X for *Application* and ?Y for *Configuration*.

Task 10:   To *define rules:* This task identifies which rules are needed in the ontology, and describes them.

Task 11:   *To define instances:* This task defines relevant instances that appear in the concept dictionary.

The definition of these tasks allows us to establish the interactions of the SAMCA services and deduce the phases that make up this interaction. The first phase is *Services Preparation* (see Fig. 3), in which the responsible user to develop the collaborative application must define it and configure it. In this case, the responsible user is the PCC (see Table 1) and the collaborative application to build is a CMS. The services that must be configured are: Application, Stage, GOS, and User Interface. This configuration is carried out in accordance with data shown in Table 1 for the corresponding concepts (i.e. services).

The second phase corresponds to *Service Binding* (see Fig. 3), where the main services are binding to allows the user to use the CMS, e.g. when PCC invokes the CMS. Therefore, when a user invokes the *Application Service* (the CMS, in this case) to organize and/or participate in a conference, its user interface is displayed (using the *User Interface Service*). On the one hand, the CMS is established by means of a session (which defines a set of geographically distributed individuals who share the interest to achieve a common aim), which is established with the *Session Management Service*.
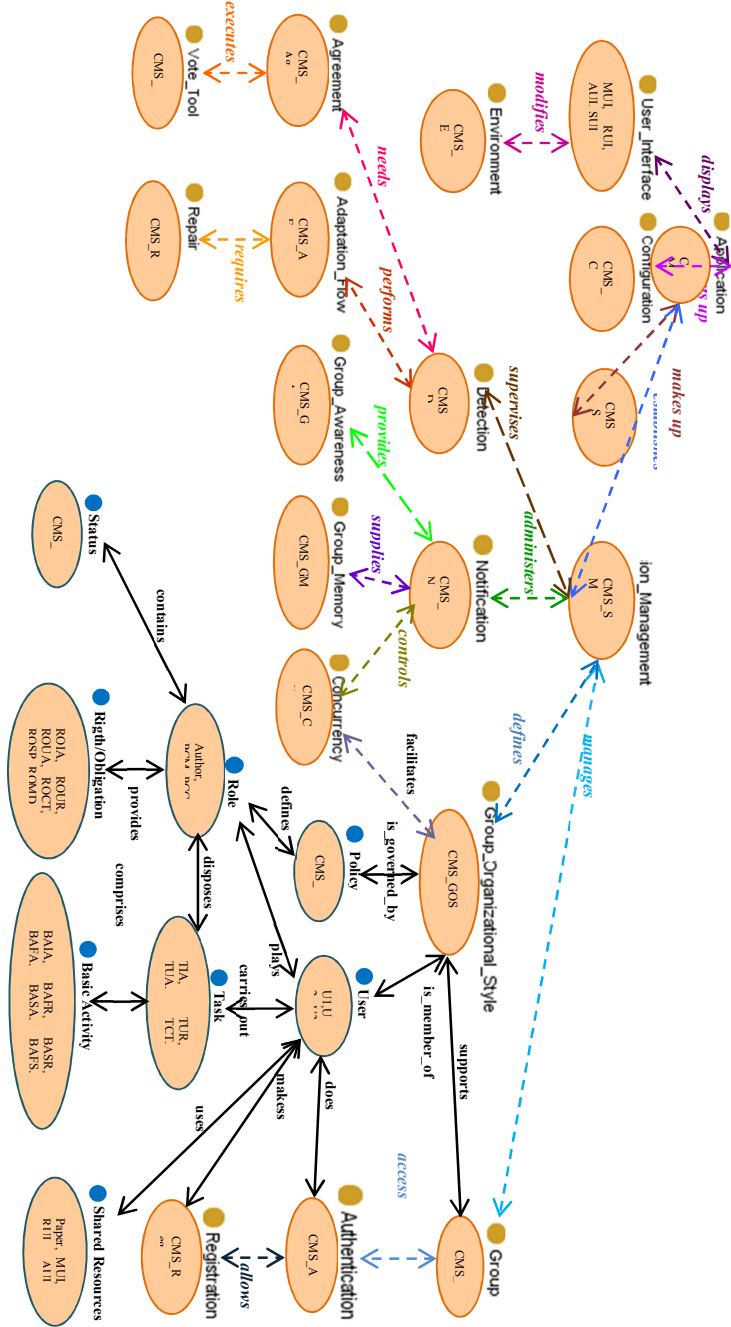
Fig. 2. Ontology developed with Methontology.

Table 1. An excerpt of the *Concept Dictionary* of an ontology to represent SAMCA.

Concept Name	Relations	Instances
Application	It **sets up** a *Configuration*; it is **made up** of *Stages*; it **displays** *User Interface*; it **establishes** *Session Management*	Conference Management System (CMS)
Configuration (C)	It is **set up** by *Application*	CMS_C
User Interface (UI)	It is **displayed** at *Application*; it is **modified** by the *Environment*	Main User Interface (MUI), Registration User Interface (RUI), Authentication User Interface (AUI), Submission User Interface (SUI)
Stage (S)	It **makes up** an *Application*	CMS_S
Session Management (SM)	It is **established** by *Application*; it **manages** a *Group*; it **defines** a *Group Organizational Style (GOS)*	CMS_SM
Detection (D)	It **supervises** a *SM*; it **needs** *Agreement*, it **performs** *Reparation*	CMS_D
Agreement (Ag)	It is **needed** by *SM*; it **executes** *Vote Tool*	CMS_Ag
Adaptation Flow (AF)	It **performs** by *SM*; it **requires** *Reparation*	CMS_AF
Reparation (Rep)	It is **requires** by *Adaptation Flow*	CMS_Rep
Notification (N)	It is **administered** by *SM*; it **provides** *Group Awareness*; it **supplies** *Group Memory*; it **controls** *Concurrency*	CMS_N
Group Awareness (GA)	It is **provided** by *Notification*	CMS_GA
Group Memory (GM)	It is **supplied** by *Notification*	CMS_GM
Concurrency (Cy)	It is **controlled** by *Notification*	CMS_Cy
Group	It is **managed** by a *SM*; it is **supported** by *GOS*; it is **facilitated by** *GOS*	CMG_G
Group_Organizational_Style (GOS)	It is **defined** by *SM*; it **supports** a *Group*; it is **governed by** a *Policy*; it **has** *Users*; it **facilitates** *Concurrency*	CMG_GOS
Authentication	It **gives access to** *Group*; it is **allowed** by *Registration*, it is **done by** *User*	CMS_Aut
Registration	It **allows** *Registration*, it is **made by** *User*	CMS_Reg
Policy	It **governs** a *GOS*; it **defines** *Roles*	CMS_P
User (U)	It is **member of** a *GOS*; it **plays** *Roles*; it **does** *Authentication*; it **makes** *Registration*; it **carries out** *Tasks*; it **uses** *Shared Resources*	U1 U2, U3, U4
Shared Resources	It is **used by** *User*	
Role	It is **played** by *Users*; it is **defined** by a *Policy*, it **contains** a *Status*; it **provides** *Rights/Obligations*; it **disposes** *Tasks*	Author, Program Committee Members (PCM) and Program Committee Chairs (PCC)
Status (St)	It is **contained** in *Role*	Authors, St (U1, U2, U4), PCM_St (U2, U3), PCC_St (U1, U3)
Right/Obligation (RO)	It is **provided** by *Role*	RO Invoking Application (ROIA), RO User Registration (ROUR), RO User Authentication (ROUA), RO Choosing conference Topics (ROCT), RO Submitting Paper (ROSP), RO Modifying Data (ROMD)
Task (T)	It is **carried out** by *User*; it it is **disposed** by *Role*; it is **comprised** by *Basic Activities*	T Invoking Application (TIA), T User Registration (TUR), T User Authentication (TUA), T choosing Conference Topics (TCT), T Submission Papers (TSP), T Modifying Data (TMD)
Basic Activity	It **forms part** of a *Task*	BA Invoking Application (BAIA), BA Filling Registration form (BAFR), BA Sending Registration form (BASR), BA Filling Authentication form (BAFA), BA Sending Authentication form (BASA), BA Filling Submission form (BAFS), BA Sending Submission form (BASS)

Table 2. An excerpt of the *formal axioms* of an ontology to represent SAMCA.

Axiom Name	Description	Expression	Concepts	Binary Relations	Variables
Application Configuration	Every application sets up a configuration	For all(?X, ?Y) ([Application](?X) and ([Configuration](?Y) and [Application](?X) → [sets up Configuration](?Y))	Application Configuration	sets up	?X, ?Y
Establishing of Session	Every application establishes at least one management session	For all(?X, ?Y) ([Application](?X) and ([Management Session](?Y) and [Application](?X) → [establishes Management Session](?Y))	Application Management Session	establishes	?X, ?Y
Administering Notification	Every application administers notifications	For all(?X, ?Y) ([Application](?X) and ([Notification](?Y) and [Application](?X) → [administers Notification](?Y))	Application Notification	administers	?X, ?Y
Making up Application	Every application makes up of stages	For all(?X, ?Y) ([Application](?X) and ([Stage](?Y) and [Application](?X) → [makes up Stage](?Y))	Application Stage	makes up	?X, ?Y
Supervising Detection	Every application supervises the detection mechanism	For all(?X, ?Y) ([Application](?X) and ([Detection](?Y) and [Application](?X) → [supervises Detection](?Y))	Application Detection	supervises	?X, ?Y
Defining Group Organizational Style (GOS)	Every application defines Group Organizational Style	For all(?X, ?Y) ([Application](?X) and ([GOS](?Y) and [Application](?X) → [defines GOS](?Y))	Application GOS	defines	?X, ?Y
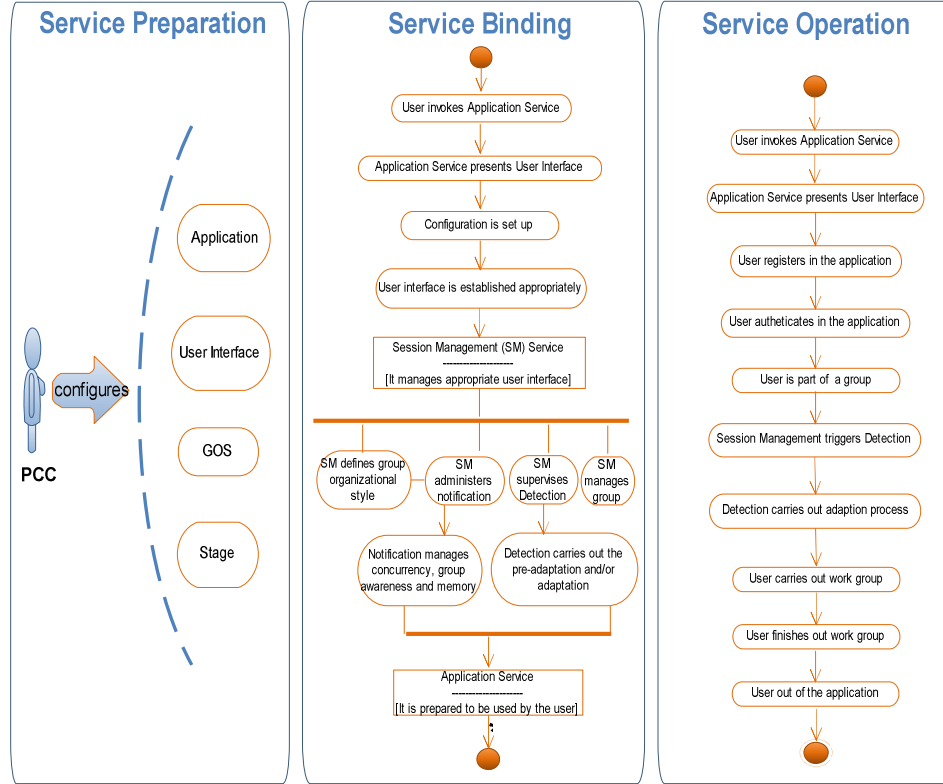
Fig. 3. Interaction phases into SAMCA.

On the other hand, *User Interface Service* is related to tasks to be carried out by a user playing a role according to the defined organizational style (with the *Group Organizational Style Service*). A session represents an execution environment, where the *Notification Service* and the *Detection Service* are always active. The former notifies each event which happens in this environment in order to provide group awareness (*Group Awareness Service*) and memory (*Group Memory Service*), as well as control the concurrency (*Concurrency Service*). The latter is triggered each time that a shared event has occurred, so that it can capture when an adaptation process must be carried out (this is defined by the group). When this process is performed, the *Adaptation Flow Service* is invoked. In case adaptation pre-conditions or pos-conditions are not met, the *Reparation Service* is required. If during the *Services Binding* phase a failure arises, such as unavailability of a requested service, errors in the composition of the collaborative application, missing data or parameters in an execution flow, etc., reconfiguration actions

are carried out, such as duplication (or replication) of services, or substitution of a faulty service. The first case involves addition of services representing similar functionalities; this aims at improving load balancing between services in order to achieve a better adaptation. The second case encompasses redirection between two services; applying this action means the first one is deactivated and replaced by the second one.

The third phase is related with *Services Operation* (see Fig. 3). For example, when an Author wants to send a paper to a conference, s/he has to invoke the CMS, then the registration or authentication user interface (RUI or AUI, see Table 1) is displayed. Supposing that author U4 uses the CMS by first time, s/he must register in it. Once done this, the services *Group* (to add a new user), *Group_Organizational_Style* to assign the Author role, its tasks, its status, etc. – see Fig. 2), *Concurrency* (to manage the new user's permissions), *Group Awareness* (to inform existing users that a new user is in the CMS), *Group Memory* (to the shared resources modified by U4 to the other users or services), *User Interface* (to present the MUI – see Table 1) and *Detection* (to carry out the adaptation process corresponding to having a new user) are notified (*Notification Service*). If these services meet the adaptation pre-conditions and post-conditions, the adaptive process will successfully finish. This is an adaptive process, because it is automatically carried out by the CMS. Methontology facilitates the ontology construction process, since it supplies a set of activities determining its elements (with concepts), the interactions between them (by relations, axioms and rules) and the instances represented. In addition, if different set of instances are specified, different collaborative applications are got. Although a comparison between ontologies and architecture would be interesting, it is outside the scope of this paper.

6   Conclusions and Future Work

This paper has presented an ontology that allows carrying out the development of collaborative applications; a CMS has been used as an example. The ontology construction process is based on Methontology, which allows specifying ontologies from scratch as well as reusing some existent ones. The resultant ontology allows us to specify the services and the relations between them, facilitating the construction of our architectural model in a flexible way. Hence, it allows us to deduce the interactions between the different SAMCA services.

Our future work is orientated to specify a Business Process Management (BPM) based on the ontology proposed in this paper. Its main aim is to control the service composition of SAMCA, facilitating their adaptation in runtime.

References

1. Noguera, M., Hurtado, V, Garrido, J.L.: An Ontology-Based Scheme Enabling the Modeling of Cooperation in Business Processes. In: Meersman, R., Tari, Z., Herrero, P. et al. (eds.) OTM Workshops 2006. LNCS, vol. 4277, pp. 863--872. Springer, Berlin (2006)
2. Fernández-López, M, Gómez-Pérez, A, Pazos, A, Pazos, J.: Building a Chemical Ontology Using Methontology and the Ontology Design Environment. IEEE Intelligent Systems & their Applications. 4(1), 37--46 (1999)
3. Fernández-López, M, Gómez-Pérez, A, Juristo, N.: Methontology: From Ontological Art Towards Ontological Engineering. In: Spring Symposium on Ontological Engineering of AAAI. Stanford University, California, pp 33--40 (1997)
4. Gruber, T.R.: Toward Principles for the Design of Ontologies Used for Knowledge Sharing. In: Guarino, N., Poli, R. (eds.) IWFOCAKR. Padova, Italy. Kluwer Academic Publishers, Deventer (1993)
5. Gómez-Pérez, A., Fernández-López, M, Corcho, O.: Ontological Engineering with Examples from the Areas of Knowledge Management, e-Commerce and the Semantic Web. Springer (2004)
6. Uschold, M., Grüninger, M.: Ontologies: Principles, Methods and Applications. Knowledge Engineering Review 11(2), pp. 93--155 (1996)
7. Farquhar, A., Fikes, R, Rice, J.: The Ontolingua Server: A Tool for Collaborative Ontology Construction. I. J. Human Computer Studies 46(6), pp. 707--727 (1997)
8. Dean, M., Schreiber, G.: OWL Web Ontology Language Reference. W3C Working Draft, http://www.w3.org/TR/owl-ref/ (2003)
9. Protégé Ontology Editor and Knowledge Acquisition System, http://protege.stanford.edu
10. RACER, http://www.sts.tu-harburg.de/~r.f.moeller/racer/
11. IEEE Standard Glossary of Software Engineering Terminology: IEEE Std 610-12. IEEE Computer Society, New York (1990)
12. Lenat, D.B., Guha, R.V.: Building Large Knowledge-based Systems: Representation and Inference in the Cyc Project. Addison-Wesley, Boston, Massachusetts (1990)
13. Uschold, M., King, M.: Towards a Methodology for Building Ontologies. In: Skuce, D. (ed.) IJCAI'95 Workshop on Basic Ontological Issues in Knowledge Sharing. Montreal, Canada, pp. 6.1--6.10 (1995)
14. Bernaras, A., Laresgoiti, I., Corera. J.: Building and Reusing Ontologies for Electrical Network Applications. In: Wahlster W (ed.) European Conference on Artificial Intelligence. John Wiley and Sons, Chichester, United Kingdom, pp. 298--302 (1996)
15. Swartout, B., Ramesh, P., Knight, K., Russ. T.: Toward Distributed Use of Large-Scale Ontologies. In: Farquhar, A., Gruninger, M., Gómez-Pérez, A., Uschold, M., van der Vet, P. (eds.) AAAI'97. Stanford University, California, pp. 138--148 (1997)
16. Staab, S., Schnurr, H.P., Studer, R., Sure, Y.: Knowledge Processes and Ontologies. IEEE Intelligent Systems 16(1) pp. 26--34 (2001)
17. IEEE Standard for Developing Software Life Cycle Processes: IEEE Std 1074. IEEE Computer Society, New York (1995)
18. Erl, T.: Service Oriented Architecture (SOA): Concepts, Technology and Design. Prentice-Hall, Englewood Cliffs (2005)
19. Anzures-García, M., Sánchez-Gálvez, L.A., Hornos, M.J., Paderewski-Rodríguez, P. Ontology-Based Modelling of Session Management Policies for Groupware Applications. LNCS, vol. 4739, pp. 57--64. Springer-Verlag, Berlin (2007)

Consistency and Soundness for a Defeasible Logic of Intention

José Martín Castro-Manzano[1], Axel Arturo Barceló-Aspeitia[1], and
Alejandro Guerra-Hernández[2]

[1] Instituto de Investigaciones Filosóficas, Universidad Nacional Autónoma de México
Circuito Mario de la Cueva s/n Ciudad Universitaria, 04510, México, D.F., Mexico
jmcmanzano@hotmail.com, abarcelo@minerva.filosoficas.unam.mx
[2] Departamento de Inteligencia Artificial, Universidad Veracruzana,
Sebastián Camacho No. 5, 91000, Xalapa, Ver., Mexico
aguerra@uv.mx

Abstract. Defeasible logics have been mainly developed to reason about
beliefs but have been barely used to reason about temporal structures;
meanwhile, intentional logics have been mostly used to reason about in-
tentional states and temporal behavior but most of them are monotonic.
So, a defeasible temporal logic for intentional reasoning has not been
developed yet. In this work we propose a defeasible temporal logic with
the help of some temporal semantics and a non-monotonic framework in
order to model intentional reasoning. We also show the consistency and
soundness of the system.

Keywords: Defeasible logic, temporal logic, BDI logic.

1 Introduction

Intentional reasoning is a form of logical reasoning that uses beliefs and intentions
during time. It has been mainly modeled via BDI logics, for instance [21,23,25];
however, there are two fundamental problems with such approaches: in first
place, human reasoning is not and should not be monotonic [17], and thus, the
logical models should be non-monotonic; and in second place, intentional states
should respect temporal norms, and so, the logical models need to be temporal
as well. Thus, the proof process of intentional reasoning has to have some sort of
control over time and has to take into account a form of non-monotonic reasoning
using beliefs and intentions.

In the state of the art defeasible logics have been mainly developed to reason
about beliefs [19] but have been barely used to reason about temporal struc-
tures [11]; on the other hand, intentional logics have been mostly used to reason
about intentional states and temporal behavior but most of them are monotonic.
In order to solve the double problem mentioned above, our main contribution is
the adaptation and extension for $CTL_{AgentSpeak(L)}$ [13] semantics with a non-
monotonic framework. So, a defeasible temporal logic for intentional reasoning
is proposed. We also show its consistency and soundness.

The relevance of this work becomes clear once we notice that, although intentions have received a lot of attention, their dynamic features have not been studied completely [24]. There are formal theories of intentional reasoning [6,14,21,23,25] but very few of them consider the revision of intentions [24] or the non-monotonicity of intentions [10] as legitimate research topics, which we find odd since the foundational theory guarantees that such research is legitimate and necessary [4]. Recent works confirm the status of this emerging area [10,24,18].

In Section 2 we discuss the case of intentional reasoning as a case of non-monotonic reasoning and we expose a non-monotonic framework for intentional reasoning. In Section 3 we display the system, its consistency and soundness. Finally, in Section 4 we discuss the results and we mention future work.

2   Non-monotonicity of Intentional Reasoning

The BDI models based upon Bratman's theory [4] tend to interpret intentions as a unique fragment [21,23,25] while Bratman's richer framework distinguished three classes of intentions: deliberative, non-deliberative and policy-based. In particular, policy-based intentions are of great importance given their structure and behavior: they have the form of rules and behave like plans. These remarks are relevant because the existing formalisms, despite of recognizing the intimate relationship between plans and intentions, seem to forget that intentions behave like plans.

As Bratman has argued, plans are intentions as well [4]. In this way we can set policy-based intentions to be structures $te : ctx \leftarrow body$ [2] (see Table 1). Now, consider the next example for sake of argument: $on(X,Y) \leftarrow put(X,Y)$. This intention tells us that, for an agent to achieve $on(a,b)$, it typically has to put a on b. If we imagine such an agent is immersed in a dynamic environment, of course the agent will try to put, typically, a on b; nevertheless, a *rational* agent would only do it as long as it is *possible*.

Thus, it results quite natural to talk about some intentions that are maintained typically but not absolutely. And so, it is reasonable to conclude that intentions, and particularly policy-based, allow defeasible intentional reasoning [10]. However, the current BDI models are monotonic and non-monotonic logics are barely used to reason about time [11] or intentional states. Thus, a defeasible temporal logic for intentional reasoning has not been developed yet. So, for example, standard First Order Logic is an instance of monotonic atemporal reasoning; default logic [22] is an instance of non-monotonic atemporal reasoning. In turn, BDI logic [21,23,25] is an example of temporal but monotonic reasoning. Our proposal is a case of temporal and non-monotonic reasoning.

Traditional BDI models formalize intentional reasoning in a monotonic way [6,14,21,23,25], while our proposal aims to do it non-monotonically. As a working example consider the following scenario under the traditional approach: an agent intends to acquire its PhD, $\mathsf{INT}(phd)$, and there is a rule $phd \Rightarrow exam$, then it follows that $\mathsf{INT}(exam)$. It is not hard to notice that this reasoning schema

looks familiar. In knowledge bases it is known as the problem of logical omni-science [15]. Around intentions is it called the problem of collateral effect [4,16]. The schema above, $\mathsf{INT}(\phi) \land \phi \Rightarrow \psi \vdash \mathsf{INT}(\psi)$, is an example of collateral effect that does not allow us to distinguish between intentions that are maintained typically but not absolutely.

Despite great avances in this area, if we take into account the philosophical foundations of rational agency [4], it is not hard to see that most BDI logics fail to grasp all the properties of intentions: functional properties like proactiv-ity, admissibility and inertia; descriptive properties like partiality, hierarchy and dynamism; and of course, the normative properties: internal consistency, strong consistency and means-end coherence. The explanation of these properties can be found in [4]. Following these ideas we propose the next framework:

Definition 1 *(Non-monotonic intentional framework) A non-monotonic inten-tional framework is a tuple* $\langle B, I, F_B, F_I, \vdash, \mid\!\sim, \dashv, \sim\!\mid, \succ \rangle$ *where:*

- B *denotes the belief base.*
- I *denotes the set of intentions.*
- $F_B \subseteq B$ *denotes the basic beliefs.*
- $F_I \subseteq I$ *denotes the basic intentions.*
- $\vdash$ *and* $\dashv$ *are strong consequence relations.*
- $\mid\!\sim$ *and* $\sim\!\mid$ *are weak consequence relations.*
- $\succ \subseteq I^2$ *s.t.* $\succ$ *is acyclic.*

With the help of this framework we can represent the non-monotonic nature of intentional reasoning. We assume a commitment strategy embedded in the agent architecture, i.e. we assume the inertia of intentions by a fixed mechanism that is single-minded [20], because if there is no commitment or the agent is blindly-committed, there is no sense in talking about inertia [12,13], i.e., in reconsidering intentions.

As usual, B denotes the beliefs base, which are literals. F_B stands for the beliefs that are considered basic; and similarly F_I stands for intentions considered as basic. Each intention $\phi \in I$ is a structure $te : ctx \leftarrow body$ where te represents the goal of the intention –so we preserve proactivity–, ctx a context and the rest denotes the body. When ctx or $body$ are empty we write $te : \top \leftarrow \top$ or just te.

We also preserve internal consistency by allowing the context of an intention, $ctx(\phi)$, $ctx(\phi) \in B$ and by letting te be the head of the intention. So, strong consistency is implied by internal consistency (given that strong consistency is $ctx(\phi) \in B$). Means-end coherence is implied by admissibility and the hierarchy of intentions is represented by the order relation, which we require to be acyclic in order to solve conflicts between intentions. Again, all these features can be found in [4]. And with this framework we can arrange a notion of inference where we say that ϕ is strongly (weakly) derivable from a sequence Δ iff there is a proof of $\Delta \vdash \phi$ ($\Delta \mid\!\sim \phi$). And also, that ϕ is not strongly (weakly) provable iff there is a proof of $\Delta \dashv \phi$ ($\Delta \sim\!\mid \phi$), where $\Delta = \langle B, I \rangle$.

3 Formal Model

In this work we adopt AgentSpeak(L) [21] because it has a well defined operational semantics. The problem, however, is that these particular semantics exclude modalities which are important to represent intentional states. To avoid this problem we use $CTL_{AgentSpeak(L)}$ [13] as a logical tool for the formal specification. Of course, initially, the approach is similar to a BDI^{CTL} system defined after $B^{KD45}D^{KD}I^{KD}$ with the temporal operators: *next* ($\bigcirc$), *eventually* ($\Diamond$), *always* ($\Box$), *until* (U), *optional* (E), *inevitable* (A), and so on, defined after $CTL*$ [7,9]. In this section we are going to expose the syntax and semantics of $CTL_{AgentSpeak(L)}$.

3.1 Syntax of AgentSpeak(L)

An agent ag is formed by a set of plans ps and beliefs bs (grounded literals). Each plan has the form $te : ctx \leftarrow h$. The context ctx of a plan is a literal or a conjunction of them. A non empty plan body h is a finite sequence of actions $A(t_1, \ldots, t_n)$, goals g (achieve ! or test ? an atomic formula $P(t_1, \ldots, t_n)$), or beliefs updates u (addition + or deletion −). $\top$ denotes empty elements, e.g., plan bodies, contexts, intentions. The trigger events te are updates (addition or deletion) of beliefs or goals. The syntax is shown in Table 1.

$$
\begin{array}{llll}
ag & ::= bs \quad ps & h & ::= h_1; \top \mid \top \\
bs & ::= b_1 \ldots b_n \ (n \geq 0) & h_1 & ::= a \mid g \mid u \mid h_1; h_1 \\
ps & ::= p_1 \ldots p_n \ (n \geq 1) & at & ::= P(t_1, \ldots, t_n) \ (n \geq 0) \\
p & ::= te : ctx \leftarrow h & a & ::= A(t_1, \ldots, t_n) \ (n \geq 0) \\
te & ::= +at \mid -at \mid +g \mid -g & g & ::= !at \mid ?at \\
ctx & ::= ctx_1 \mid \top & u & ::= +b \mid -b \\
ctx_1 & ::= at \mid \neg at \mid ctx_1 \wedge ctx_1 & &
\end{array}
$$

Table 1. Sintax of AgentSpeak(L) adapted from [2].

3.2 Semantics of AgentSpeak(L)

The operational semantics of AgentSpeak(L) are defined by a transition system, as showed in Figure 1, between configurations $\langle ag, C, M, T, s \rangle$, where:

– ag is an agent program formed by beliefs bs and plans ps.
– An agent circumstance C is a tuple $\langle I, E, A \rangle$ where I is the set of intentions $\{i, i', \ldots, n\}$ s.t. $i \in I$ is a stack of partially instantiated plans $p \in ps$; E is a set of events $\{\langle te, i \rangle, \langle te', i' \rangle, \ldots, n\}$, s.t. te is a *triggerEvent* and each i is an intention (internal event) or an empty intention $\top$ (external event); and A is a set of actions to be performed by the agent in the environment.
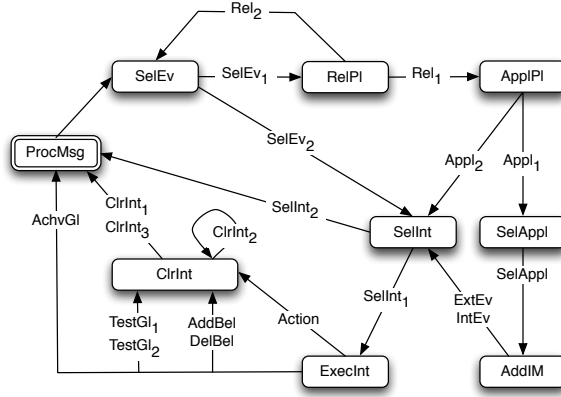
Fig. 1. The interpreter for AgentSpeak(L) as a transition system.

- M is a tuple $\langle In, Out, SI \rangle$ that works as a *mailbox*, where In is the mailbox of the agent, Out is a list of messages to be delivered by the agent and SI is a register of suspended intentions (intentions that wait for an answer message).
- T is a tuple $\langle R, Ap, \iota, \epsilon, \rho \rangle$ that registers temporal information: R is the set of relevant plans given certain *triggerEvent*; Ap is the set of applicable plans (the subset of R s.t. $bs \models ctx$); ι, ϵ and ρ register, respectively, the intention, the event and the current plan during an agent execution.
- The label $s \in \{SelEv, RelPl, AppPl, SelAppl, SelInt, AddIM, ExecInt, ClrInt, ProcMsg\}$ indicates the current step in the reasoning cycle of the agent.

Under such semantics a run is a set $Run = \{(\sigma_i, \sigma_j) | \Gamma \vdash \sigma_i \to \sigma_j\}$ where Γ is the transition system defined by AgentSpeak(L) operational semantics and σ_i, σ_j are agent configurations.

3.3 Syntax of $BDI^{CTL}_{AS(L)}$

$CTL_{AgentSpeak(L)}$ may be seen as an instance of BDI^{CTL}. Similar approaches have been accomplished for other programming languages [8]. The idea is to define some BDI^{CTL} semantics in terms of AgentSpeak(L) structures. So, we need a language able to express temporal and intentional states. Thus, we require in first place some way to express these features.

Definition 2 *(Syntax of $BDI^{CTL}_{AS(L)}$) If ϕ is an AgentSpeak(L) atomic formula, then* BEL(ϕ), *DES(ϕ) and* INT(ϕ) *are well formed formulas of $BDI^{CTL}_{AS(L)}$.*

To specify the temporal behavior we use $CTL*$ in the next way.

Definition 3 *($BDI_{AS(L)}^{CTL}$ temporal syntax) Every $BDI_{AS(L)}^{CTL}$ formula is a state formula s:*

- $s ::= \phi | s \wedge s | \neg s$
- $p ::= s | \neg p | p \wedge p | \mathsf{E}p | \mathsf{A}p | \bigcirc p | \Diamond p | \Box p | p \ \mathsf{U} \ p$

3.4   Semantics of $BDI_{AS(L)}^{CTL}$

Initially the semantics of BEL, DES and INT is adopted from [3]. So, we use the next function:

$$
\begin{aligned}
agoals(\top) &= \{\}, \\
agoals(i[p]) &= \begin{cases} \{at\} \cup agoals(i) & \text{if } p = +!at : ct \leftarrow h, \\ agoals(i) & \text{otherwise} \end{cases}
\end{aligned}
$$

which gives us the set of atomic formulas (at) attached to an achievement goal ($+!$) and $i[p]$ denotes the stack of intentions with p at the top.

Definition 4 *($BDI_{AS(L)}^{CTL}$ semantics) The operators BEL, DES and INT are defined in terms of an agent ag and its configuration $\langle ag, C, M, T, s \rangle$:*

$$
\mathsf{BEL}_{\langle ag,C,M,T,s \rangle}(\phi) \equiv \phi \in bs
$$

$$
\mathsf{INT}_{\langle ag,C,M,T,s \rangle}(\phi) \equiv \phi \in \bigcup_{i \in C_I} agoals(i) \vee \bigcup_{\langle te,i \rangle \in C_E} agoals(i)
$$

$$
\mathsf{DES}_{\langle ag,C,M,T,s \rangle}(\phi) \equiv \langle +!\phi, i \rangle \in C_E \vee \mathsf{INT}(\phi)
$$

where C_I denotes current intentions and C_E suspended intentions.

We have a defeasible framework for intentions that lacks temporal representation; while the BDI temporal model described before grasps the temporal representation but lacks non-monotonicity. The next step is a system denoted by $NBDI$ because it has a non-monotonic behavior. An intention ϕ in $NBDI_{AS(L)}^{CTL}$ is a structure $\langle g : ctx \leftarrow body \rangle$ where g is the head, ctx is the context and $body$ is the body of the rule. We will denote an intention ϕ with head g by $\phi[g]$. Also, a negative intention is denoted by $\phi[g^c]$, i.e., the intention ϕ with $\neg g$ as the head.

The semantics of this theory requires a Kripke structure $K = \langle S, R, V \rangle$ where S is the set of agent configurations, R is an access relation defined after the transition system Γ and V is a valuation function that goes from agent configurations to true propositions in those states.

Definition 5 *Let $K = \langle S, \Gamma, V \rangle$, then:*

- *S is a set of agent configurations $c = \langle ag, C, M, T, s \rangle$.*
- *$\Gamma \subseteq S^2$ is a total relation s.t. for all $c \in \Gamma$ there is a $c' \in \Gamma$ s.t. $(c, c') \in \Gamma$.*
- *V is valuation s.t.:*
    - *$V_{\mathsf{BEL}}(c, \phi) = \mathsf{BEL}_c(\phi)$ where $c = \langle ag, C, M, T, s \rangle$.*
    - *$V_{\mathsf{DES}}(c, \phi) = \mathsf{DES}_c(\phi)$ where $c = \langle ag, C, M, T, s \rangle$.*
    - *$V_{\mathsf{INT}}(c, \phi) = \mathsf{INT}_c(\phi)$ where $c = \langle ag, C, M, T, s \rangle$.*
- *Paths are sequences of configurations $c_0, \ldots, c_n$ s.t. $\forall i (c_i, c_{i+1}) \in R$. We use x^i to indicate the i-th state of path x. Then:*

S1 $K, c \models \mathsf{BEL}(\phi) \Leftrightarrow \phi \in V_{\mathsf{BEL}}(c)$

S2 $K, c \models \mathsf{DES}(\phi) \Leftrightarrow \phi \in V_{\mathsf{DES}}(c)$

S3 $K, c \models \mathsf{INT}(\phi) \Leftrightarrow \phi \in V_{\mathsf{INT}}(c)$

S4 $K, c \models \mathsf{E}\phi \Leftrightarrow \exists x = c_1, \ldots \in K | K, x \models \phi$

S5 $K, c \models \mathsf{A}\phi \Leftrightarrow \forall x = c_1, \ldots \in K | K, x \models \phi$

P1 $K, c \models \phi \Leftrightarrow K, x^0 \models \phi$ where ϕ is a state formula.

P2 $K, c \models \bigcirc \phi \Leftrightarrow K, x^1 \models \phi.$

P3 $K, c \models \Diamond \phi \Leftrightarrow K, x^n \models \phi$ for $n \geq 0$

P4 $K, c \models \Box \phi \Leftrightarrow K, x^n \models \phi$ for all n

P5 $K, c \models \phi \ \mathsf{U} \ \psi \Leftrightarrow \exists k \geq 0$ s.t. $K, x^k \models \psi$ and for all j, k, $0 \leq j < k | K, c^j \models \phi$ or $\forall j \geq 0 : K, x^j \models \phi$

We have four cases of proof: if the sequence is $\Delta \vdash \phi$, we say ϕ is strongly provable; if it is $\Delta \dashv \phi$ we say ϕ is not strongly provable. If is $\Delta \mathrel{|\!\sim} \phi$ we say ϕ is weakly provable and if it is $\Delta \mathrel{\rsim\!|} \phi$, then ϕ is not weakly provable.

Definition 6 *(Proof)* *A proof of ϕ from Δ is a finite sequence of beliefs and intentions satisfying:*

1. $\Delta \vdash \phi$ iff
    1.1. $\Box \mathsf{A}(\mathsf{INT}(\phi))$ or
    1.2. $\Box \mathsf{A}(\exists \phi[g] \in F_I : \mathsf{BEL}(ctx(\phi)) \wedge \forall \psi[g'] \in body(\phi) \vdash \psi[g'])$
2. $\Delta \mathrel{|\!\sim} \phi$ iff
    2.1. $\Delta \vdash \phi$ or
    2.2. $\Delta \dashv \neg\phi$ and
        2.2.1. $\Diamond \mathsf{E}(\mathsf{INT}(\phi) \ \mathsf{U} \ \neg\mathsf{BEL}(ctx(\phi)))$ or
        2.2.2. $\Diamond \mathsf{E}(\exists \phi[g] \in I : \mathsf{BEL}(ctx(\phi)) \wedge \forall \psi[g'] \in body(\phi) \mathrel{|\!\sim} \psi[g'])$ and
            2.2.2.1. $\forall \gamma[g^c] \in I, \gamma[g^c]$ fails at Δ or
            2.2.2.2. $\psi[g'] \succ \gamma[g^c]$
3. $\Delta \dashv \phi$ iff
    3.1. $\Diamond \mathsf{E}(\mathsf{INT}(\neg\phi))$ and
    3.2. $\Diamond \mathsf{E}(\forall \phi[g] \in F_I : \neg\mathsf{BEL}(ctx(\phi)) \vee \exists \psi[g'] \in body(\phi) \dashv \psi)$
4. $\Delta \mathrel{\rsim\!|} \phi$ iff
    4.1. $\Delta \dashv \phi$ and
    4.2. $\Delta \vdash \neg\phi$ or
        4.2.1. $\Box \mathsf{A}\neg(\mathsf{INT}(\phi) \ \mathsf{U} \ \neg\mathsf{BEL}(ctx(\phi)))$ and
        4.2.2. $\Box \mathsf{A}(\forall \phi[g^c] \in I : \neg\mathsf{BEL}(ctx(\phi)) \vee \exists \psi[g'] \in body(\phi) \mathrel{\rsim\!|} \psi[g'])$ or
            4.2.2.1. $\exists \gamma[g^c] \in I$ s.t. $\gamma[g^c]$ succeds at Δ and
            4.2.2.2. $\psi[g'] \not\succ \gamma[g^c]$

3.5   Consistency

The next statements are quite straightforward.

Proposition 1 *(Subalterns$_1$) If $\vdash \phi$ then $\mathrel{|\!\sim} \phi$.*

Proof. Let us assume that $\vdash \phi$ but not $\mathrel{|\!\sim} \phi$, i.e., $\mathrel{\rightsquigarrow\mid} \phi$. Then, given $\vdash \phi$ we have two general cases. Case 1: given the initial assumption that $\vdash \phi$, by Definition 6 item 1.1, we have that $\Box \mathsf{A}(\mathsf{INT}(\phi))$. Now, given the second assumption, i.e., that $\mathrel{\rightsquigarrow\mid} \phi$, by Definition 6 item 4.1, we have $\dashv \phi$. And so, $\Diamond \mathsf{E}(\mathsf{INT}(\neg\phi))$, and thus, by the temporal semantics, we get $\neg\phi$; however, given the initial assumption, we also obtain ϕ, which is a contradiction.

Case 2: given the assumption that $\vdash \phi$, by Definition 6 item 1.2, we have that $\exists \phi[g] \in F_I : \mathsf{BEL}(ctx(\phi)) \wedge \forall \psi[g'] \in body(\phi) \vdash \psi[g']$. Now, given the second assumption, that $\mathrel{\rightsquigarrow\mid} \phi$, we also have $\dashv \phi$ and so we obtain $\Diamond \mathsf{E}(\forall \phi[g] \in F_I : \neg\mathsf{BEL}(ctx(\phi)) \vee \exists \psi[g'] \in body(\phi) \dashv \psi)$, and thus we can obtain $\forall \phi[g] \in F_I : \neg\mathsf{BEL}(ctx(\phi)) \vee \exists \psi[g'] \in body(\phi) \dashv \psi)$ which is $\neg(\exists \phi[g] \in F_I : \mathsf{BEL}(ctx(\phi)) \wedge \forall \psi[g'] \in body(\phi) \vdash \psi[g'])$. ∎

Corollary 1 *(Subalterns$_2$) If $\mathrel{\rightsquigarrow\mid} \phi$ then $\dashv \phi$.*

Proposition 2 *(Contradictories$_1$) There is no ϕ s.t. $\vdash \phi$ and $\dashv \phi$.*

Proof. Assume that there is a ϕ s.t. $\vdash \phi$ and $\dashv \phi$. If $\dashv \phi$ then, by Definition 6 item 3.1, $\Diamond \mathsf{E}(\mathsf{INT}(\neg\phi))$. Thus, by proper semantics, we can obtain $\neg\phi$. However, given that $\vdash \phi$ it also follows that ϕ, which is a contradiction. ∎

Corollary 2 *(Contradictories$_2$) There is no ϕ s.t. $\mathrel{|\!\sim} \phi$ and $\mathrel{\rightsquigarrow\mid} \phi$.*

Proposition 3 *(Contraries) There is no ϕ s.t. $\vdash \phi$ and $\mathrel{\rightsquigarrow\mid} \phi$.*

Proof. Assume there is a ϕ such that $\vdash \phi$ and $\mathrel{\rightsquigarrow\mid} \phi$. By Proposition 1, it follows that $\mathrel{|\!\sim} \phi$, but that contradicts the assumption that $\mathrel{\rightsquigarrow\mid} \phi$ by Corollary 2. ∎

Proposition 4 *(Subcontraries) For all ϕ either $\mathrel{|\!\sim} \phi$ or $\dashv \phi$.*

Proof. Assume it is not the case that for all ϕ either $\mathrel{|\!\sim} \phi$ or $\dashv \phi$. Then there is ϕ s.t. $\mathrel{\rightsquigarrow\mid} \phi$ and $\vdash \phi$. Taking $\mathrel{\rightsquigarrow\mid} \phi$ it follows from Corollary 1 that $\dashv \phi$. By Proposition 2 we get a contradiction with $\vdash \phi$. ∎

Considering these results, we get the next square of opposition where c denotes contradictories, s subalterns, k contraries and r subcontraries.
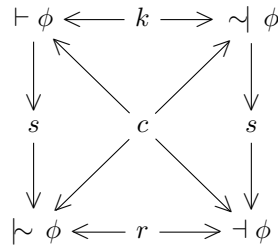
These results represent the following properties: Proposition 1 and Corollary 1 represent supraclassicality; Proposition 2 and Corollary 2 stand for consistency while the remaining statements specify the coherence of the square, and thus, the overall coherence of the system.

If we recover our working example, the scenario in which an agent intends to acquire its PhD, and we set the next configuration Δ of beliefs and intentions: $F_B = \{\top\}$, $B = \{scolarship\}$, $F_I = \{research : \top \leftarrow \top\}$, $I = \{phd : \top \leftarrow thesis, exam; thesis : scolarship \leftarrow research; exam : \top \leftarrow research\}$. And suppose we send the query: *phd?* The search of intentions with head *phd* in F_I fails, thus the alternative $\vdash \phi[phd]$ does not hold. Thus, we can infer, by contradiction rule (Proposition 2), that it is not strongly provable that *phd*, i.e., that eventually in some state the intention *phd* does not hold. Thus, the result of the query should be that the agent will get its PhD defeasibly under the Δ configuration. On the contrary, the query *research?* will succedd as $\vdash \phi[research]$, and thus, we would say *research* is both strongly and weakly provable (Proposition 1).

3.6 Soundness

The idea is to show the framework is sound with respect to its semantics. Thus, as usual, we will need some notions of satisfaction and validity.

Definition 7 *(Satisfaction) A formula ϕ is true in K iff ϕ is true in all configurations σ in K. This is to say, $K \models \phi \Leftrightarrow K, \sigma \models \phi$ for all $\sigma \in S$.*

Definition 8 *(Run of an agent in a model) Given an initial configuration β, a transition system Γ and a valuation V, $K_\Gamma^\beta = \left\langle S_\Gamma^\beta, R_\Gamma^\beta, V \right\rangle$ denotes a run of an agent in a model.*

Definition 9 *(Validity) A formula $\phi \in BDI_{AS(L)}^{CTL}$ is true for any agent run in Γ iff $\forall K_\Gamma^\beta \models \phi$*

Further, we will denote $(\exists K_\Gamma^\beta \models \phi \; \mathsf{U} \; \neg\mathsf{BEL}(ctx(\phi))) \vee \models \phi$ by $\approx \phi$. We can observe, moreover, that $\models \phi \geq \approx \phi$ and $\not\approx \phi \geq \not\models \phi$. With these remarks we should find a series of *translations* s.t.: $\vdash \phi \longrightarrow \forall K_\Gamma^\beta \models \phi \longrightarrow \models \phi$ and $\models \phi \longrightarrow \approx \phi$.

Proposition 5 *If $\vdash \phi$ then $\models \phi$.*

Proof. Base case. Taking Δ_i as a sequence with $i = 1$. If we assume $\vdash \phi$, we have two subcases. First subcase is given by Definition 6 item 1.1. Thus we have $\Box\mathsf{A}(\mathsf{INT}(\phi))$. This means, by Definition 5 items P4 and S5 and Definition 4, that for all paths and all states $\phi \in C_I \vee C_E$. We can represent this expression, by way of a translation, in terms of runs. Since paths and states are sequences of agent configurations we have that $\forall K_\Gamma^\beta \models \phi$, which implies $\models \phi$. Second subcase is given by Definition 6 item 1.2, which in terms of runs means that for all runs $\exists \phi[g] \in F_I : \mathsf{BEL}(ctx(\phi)) \wedge \forall \psi[g'] \in body(\phi) \vdash \psi[g']$. Since Δ_1 is a single step,

$body(\phi) = \top$ and for all runs $\mathsf{BEL}(ctx(\phi)))$, $ctx(\phi) \in F_B$. Then $\forall K_\Gamma^\beta \models \phi$ which, same as above, implies $\models \phi$.

Inductive case. Let us assume that for $n \leq k$, if $\Delta_n \vdash \phi$ then $\Delta \models \phi$. And suppose Δ_{n+1}. Further, suppose $\Delta_n \vdash \phi$, then we have two alternatives. First one being, by Definition 6 item 1.1, that we have an intention ϕ s.t. $ctx(\phi) = body(\phi) = \top$. Since $body(\phi)$ is empty, it trivially holds at n, and by the induction hypothesis, $body(\phi) \subseteq \Delta_{n+1}$, and thus $\models \phi$. Secondly, by Definition 6 item 1.2, for all runs $\exists \phi[g] \in I : \mathsf{BEL}(ctx(\phi)) \wedge \forall \psi[g'] \in body(\phi) \vdash \psi[g']$. Thus, for all runs $n, \forall \psi[g'] \in body(\phi) \vdash \psi[g']$, and so by the induction hypothesis, $body(\phi) \subseteq \Delta_{n+1}$, i.e., $\Delta \vdash \psi[g']$. Therefore, $\models \phi$. ∎

Proposition 6 *If $\vdash\!\!\!\sim \phi$ then $\approx\!\!\!\models \phi$.*

Base case. Taking Δ_i as a sequence with $i = 1$. Let us suppose $\vdash\!\!\!\sim \phi$. Then we have two subcases. The first one is given by Definition 6 item 2.1. So, we have that $\vdash \phi$ which, as we showed above, already implies $\models \phi$. On the other hand, by item 2.2, we have $\dashv \neg\phi$ and two alternatives. The first alternative, item 2.2.1, is $\lozenge\mathsf{E}(\mathsf{INT}(\phi) \ \mathsf{U} \ \neg\mathsf{BEL}(ctx(\phi)))$. Thus, we can reduce this expression by way of Definition 5 items P3 and S4, to a translation in terms of runs: $\exists K_\Gamma^\beta \models \phi \ \mathsf{U} \ \neg\mathsf{BEL}(ctx(\phi))$, which implies $\approx\!\!\!\models \phi$. The second alternative comes from item 2.2.2, $\lozenge\mathsf{E}(\exists\phi[g] \in I : \mathsf{BEL}(ctx(\phi)) \wedge \forall\psi[g'] \in body(\phi) \ \vdash\!\!\!\sim \psi[g'])$ which in terms of runs means that for some run $\exists\phi[g] \in I : \mathsf{BEL}(ctx(\phi)) \wedge \forall\psi[g'] \in body(\phi) \ \vdash\!\!\!\sim \psi[g']$, but Δ_1 is a single step, and thus $body(\phi) = \top$. Thus, there is a run in which $\exists\phi[g] \in I : \mathsf{BEL}(ctx(\phi))$, i.e., $(\exists K_\Gamma^\beta \models (\phi \ \mathsf{U} \ \neg\mathsf{BEL}(ctx(\phi)))$ by using the weak case of Definition 6 P5. Thus, by addition, $(\exists K_\Gamma^\beta \models (\phi \ \mathsf{U} \ \neg\mathsf{BEL}(ctx(\phi)))\vee \models \phi$, and therefore, $\approx\!\!\!\models \phi$.

Inductive case. Let us assume that for $n \leq k$, if $\Delta_n \ \vdash\!\!\!\sim \phi$ then $\Delta \approx\!\!\!\models \phi$. And suppose Δ_{n+1}. Assume $\Delta_n \ \vdash\!\!\!\sim \phi$. We have two alternatives. The first one is given by Definition 6 item 2.1, i.e., $\vdash \phi$, which already implies $\models \phi$. The second alternative is given by item 2.2, $\Delta \dashv \neg\phi$ and two subcases: $\lozenge\mathsf{E}(\mathsf{INT}(\phi) \ \mathsf{U} \ \neg\mathsf{BEL}(ctx(\phi)))$ or $\lozenge\mathsf{E}(\exists\phi[g] \in I : \mathsf{BEL}(ctx(\phi)) \wedge \forall\psi[g'] \in body(\phi) \ \vdash\!\!\!\sim \psi[g'])$. If we consider the first subcase there are runs n which comply with the definition of $\approx\!\!\!\models \phi$. In the remaining subcase we have $\forall\psi[g'] \in body(\phi) \ \vdash\!\!\!\sim \psi[g']$, since $body(\phi) \subseteq \Delta_n$, by the induction hypothesis $\Delta \ \vdash\!\!\!\sim \psi[g']$, and thus, $\Delta_{n+1} \ \vdash\!\!\!\sim \phi$, i.e., $\approx\!\!\!\models \phi$. ∎

Also, we can find a series of translations for the remaining fragments:

Corollary 3 *If $\dashv \phi$ then $\models\!\!\!\mid \phi$; and if $\sim\!\!\!\dashv \phi$ then $\approx\!\!\!\mid \phi$*

4   Conclusion

The formal model described above attempts to represent temporal and non-monotonic features of intentional reasoning. We observed the model preserves supraclassicality, consistency and soundness.

Currently we are trying to find relations between the notion of inference of this system and a notion of intention revision [5]. For example, is it the case

that intentions strongly proved cannot be contracted? And is it the case that intentions weakly proved can be revised? Conversely, revised intentions are defeasible? And so on. Plus, since the model of revision is related to AgentSpeak(L), we foresee implementations that may follow organically.

References

1. Alchourrón, C. E., Gärdenfors, P., Makinson, D.: On the logic of theory change: Partial meet contraction and revision functions. Journal of Symbolic Logic, 50, 510–530 (1985)
2. Bordini, R.H., Wooldridge, M., Hübner, J.F.: Programming Multi-Agent Systems in AgentSpeak using Jason (Wiley Series in Agent Technology). John Wiley & Sons (2007)
3. Bordini, R.H., Moreira, Á.F.: Proving BDI Properties of Agent-Oriented Programming Languages. Annals of Mathematics and Artificial Intelligence, 42, 197–226 (2004)
4. Bratman, M.E.: Intention, Plans, and Practical Reason. Cambridge University Press (1999)
5. Castro-Manzano, J.M., Barceló-Aspeitia, A.A., Guerra-Hernández, A.: Intentional learning procedures as intention revision mechanisms. Mexican International Conference on Artificial Intelligence, 51–56 (2010)
6. Cohen, P., Levesque, H.: Intention is choice with commitment. Artificial Intelligence, 42(3), 213–261 (1990)
7. Clarke, E.M. Jr., Grumberg, O.,Peled. D.A.: Model Checking. MIT Press (1999)
8. Dastani, M., van Riemsdijk, M.B., Meyer, J.C.: A grounded specification language for agent programs. Proceedings of the 6th international joint conference on Autonomous agents and multiagent systems '07 AAMAS '07, 1–8 (2007)
9. Emerson, A.: Temporal and modal logic. Handbook of Theoretical Computer Science, Elsevier Science Publishers, 995–1072 (1995)
10. Governatori, G., Padmanabhan, V. and Sattar, A.: A Defeasible Logic of Policy-based Intentions. Proceedings of the 15th Australian Joint Conference on Artificial Intelligence: Advances in Artificial Intelligence. LNAI-2557, Springer Verlag (2002)
11. Governatori, G., Terenziani, P.: Temporal Extensions to Defeasible Logic. Proceedings of the 20th Australian joint conference on Advances in artificial intelligence, 476–485 (2007)
12. Guerra-Hernández, A., Castro-Manzano, J.M., El-Fallah-Seghrouchni, A.: Toward an AgentSpeak(L) Theory of Commitment and Intentional Learning. Proceedings of the 7th Mexican International Conference on Artificial Intelligence: Advances in Artificial Intelligence MICAI 2008, LNCS, vol. 5317, 848–858, Springer-Verlag, Berlin Heidelberg, (2008)
13. Guerra-Hernández, A., Castro-Manzano, J.M., El-Fallah-Seghrouchni, A.: CTL AgentSpeak(L): a Specification Language for Agent Programs. J. Algorithms, 64(1), 31–40 (2009)

14. Konolige, K., Pollack, M. E.: A representationalist theory of intentions. Proceedings of International Joint Conference on Artificial Intelligence (IJCAI-93), 390–395 (1993)
15. K. M. Sim: Epistemic Logic and Logical Omniscience: A Survey. International Journal of Intelligent Systems, vol. 12, 57–81, John Wiley and Sons Inc. (1997)
16. Linder, B. Van: Modal Logic for Rational Agents. PhD thesis, Department of Computer Science, Utrecht University, 19th June (1996)
17. Nute, D.: Defeasible logic. INAP 2001, LNAI 2543M, Springer-Verlag, 151–169 (2003)
18. Icard, Th., Pacuit. E., Shoham, Y.: Joint revision of belief and intention. Proceedings of the Twelfth International Conference on the Principles of Knowledge Representation and Reasoning, (2010)
19. Prakken, H., Vreeswijk, G.: Logics for defeasible argumentation. In D. Gabbay and F. Guenthner (eds.), Handbook of Philosophical Logic, second edition, Vol 4, Kluwer Academic Publishers, 219–318 (2002)
20. Rao, A.S., Georgeff, M.P.: Modelling Rational Agents within a BDI Architecture. In: Huhns, M.N., Singh, M.P., (eds.) Readings in Agents, Morgan Kaufmann, 42–55 (1998)
21. Rao, A.S.: AgentSpeak(L): BDI agents speak out in a logical computable language. In: de Velde, W.V., Perram, J.W. (eds.) MAAMAW. LNCS, vol. 1038, Springer, Heidelberg, 42–55 (1996)
22. Reiter, R.: A logic for default reasoning. Artificial Intelligence, 13, 81–132, (1980)
23. Singh, M.P., Rao, A.S., Georgeff, M.P.: Formal Methods in DAI: Logic-Based Representation and Reasoning. In: Multiagent Systems: A Modern Approach to Distributed Artificial Intelligence, MIT Press, Cambridge, 331–376 (1999)
24. van der Hoek, W., Jamroga, W., Wooldridge, M.: Towards a theory of intention revision. Synthese, 155(2), 265–290 (2007)
25. Wooldridge, M.: Reasoning about Rational Agents. MIT Press (2000).

Modeling an Agent for Intelligent Tutoring in 3D CSCL based on Nonverbal Communication

Adriana Peña Pérez Negrón[1], Raúl A. Aguilar Vera[2], and Elsa Estrada Guzmán[1]

[1] CUCEI - Universidad de Guadalajara,
Blvd. Marcelino García Barragán #1421,
44430 Guadalajara, Mexico
adriana@sicenet.com.mx; elsa.estrada@red.cucei.udg.mx
[2] Mathematics School - Universidad Autónoma de Yucatán,
Periférico Norte Tablaje 13615, 97110, Mérida, Mexico
avera@tunku.uady.mx

Abstract. During collaboration, people's nonverbal involvement mainly intention is the achievement of the task at hand. While in 3D Collaborative Virtual Environments (CVE) the users' graphical representation −their avatars, are usually able to display some nonverbal communication (NVC) like gazing or pointing, in such a way that their NVC cues could be the means to understand their collaborative interaction; its automatic interpretation in turn may provide a virtual tutor with the tools to support collaboration within a learning scenario. In order to model a virtual tutor for 3D collaborative learning environments, based on literature review, the NVC cues to be collected; how to relate them to indicators of collaborative learning as participation or involvement; and to task stages (i.e. planning, implementing an evaluating) are here discussed. On this context, results from collecting NVC cues in an experimental application during the accomplishment of a task are then analyzed.

Keywords: CSCL, collaborative virtual environments, collaborative interaction, nonverbal communication, intelligent tutoring.

1 Introduction

There seems to be a general agreement on the motivational impact of virtual reality (VR) in the students, but there are other important reasons to use it for learning purposes. VR is a powerful context, in which time, scale, and physics can be controlled; where participants can have entirely new capabilities, such as the ability to have any object as a virtual body or to observe the environment from different perspectives; in virtual environments (VE) materials do not break, are dangerous or wear out. Also, VR allows safe experiences of distant or dangerous locations and processes [2, 18, 20].

Socio-constructivism is the fundamental theory that motivates educational uses for Collaborative Virtual Environments (CVE) [4]. Because group work improves cognitive development as well as social and management skills, CVE have the potentials to enable

innovative and effective education, involving debate, simulation, role-play, discussion groups, problem solving and decision-making in a group content.

In the joint effort to solve a problem or to take care of a task, the students will interact with each other; interaction takes place when an action or its effects are perceived by at least one member of the group other than the one who carried out the action [12]. The analysis of collaboration thus can be conducted through the observation of the interaction that affects the collaborative process. However, its automatic analysis is not trivial; a main challenge consists on computationally understanding and assessing it [11]. By addition, even that computers can record every student intervention, the completely understanding of unstructured dialogue has not being accomplished in Computer Supported Collaborative Learning (CSCL) yet [17].

A number of approaches have been proposed to monitor collaboration [17] mainly applicable to conventional interfaces less naturals than expected for a CVE and not easy to adapt. For example, with menus that in a VE will cover part of the view and may be difficult to operate considering that the user has to operate his graphical representation and very probably some objects too. Or based on text communication analysis, while oral communication is substituting text in VR applications, plus VEs allow other communication channels. As a result, these approaches may not appropriately fit CVEs.

CVEs bring remote people and remote objects together into a spatial and social proximity [21], providing a technology that supports interaction through auditory and visual allowing. In such a way that, this VEs visual characteristic, guided us to explore the users' avatar nonverbal communication (NVC). There are three different approaches to transmit NVC to a VE:

1) Directly controlled –with sensors attached to the user;
2) User-guided –when the user guides the avatar by defining its tasks and movements, and;
3) Autonomous –where the avatar has an internal state that depends on its goals and its environment, the state is directly or indirectly modified by the user and the NVC is automatically generated according to the new state [3].

As far as NVC features are automatically digitized from the user, they should be more revealing and spontaneous; but, succinct metaphors to display nonverbal cues also support the users' communication.

Now then effective collaborative learning includes both learning to collaborate and collaborating to learn, the students may require guidance in both collaboration and task oriented issues [10], while facilitating only collaboration is not particularly attached to the task at hand.

The modeled virtual agent intends is to guide collaboration for effective collaborative learning; its modeling assumes a CVE for learning in which the users' avatars interact to take care of a spatial task. The agent will not comprehend the students' dialogue; in doing so, generic analysis can be conducted and it can be mixed with other tutoring approaches like task oriented or dialogue analysis.

2   Nonverbal Communication in Collaborative Interaction

Broadly defined, nonverbal behavior might include most of what we do with our bodies; it includes also certain characteristics of verbal behavior by distinguishing the content, or meaning, of speech from paralinguistic cues such as loudness, tempo, pitch or intonation [13]. The use of certain objects like our decided outfit, or the physical environment when used to communicate something, without saying it, has also traditionally being considered as NVC.

Although NVC changes from person to person and from one culture to other, it is also functional, which means that different functional uses will lead to different arousal, cognitive and behavioral patterns of interchange [13]. Therefore, for its analysis it is particularly important taking into account its purpose.

Following Miles L. Patterson [13], the nonverbal involvement which purpose is to facilitate service or a task goal is essentially impersonal and usually constrained by the norms of the setting. NVC during collaborative interaction is more likely to have a routinely nature for interactants; gazes, pointing gestures or proximity to others will be mainly aimed to the achievement of the task.

2.1 Collaborative Learning

In the accomplishment of a task, a desired situation for an effective learning session should be a starting planning period that will help to create a shared ground or common ground [5] and to define how thinks are going to be done; followed by the implementation, that is, the task accomplishment on itself; and from time to time an evaluation episode where the students re-analyze their plans or the implementation, and change what is not appropriately working; whereas all the students have a significant participation in the three stages: i.e. planning, implementing and evaluating.

Group learning possibilities grow with its members' participation [16]. While the students participation in dialogue allows them to create a shared ground, which implies that they share knowledge, beliefs and assumptions of the task at hand in order to be able to work on it together [5]; an active student's participation corroborates that she/he is interested and understands the group activity. For collaborative learning students' participation is expected to have symmetry in both decisions making and implementing.

Jermann [10] suggested that by contrasting the students' participation in dialogue and implementation different types of division of labor can be inferred as follows:

− In sessions with *symmetric* in both *dialogue* and *implementation*: the absence of division of labor.
− The students' *symmetric* participation in *dialogue* and their *asymmetric* participation in *implementation*: a role based on division of labor without status differences, where subjects discuss plans for action together but only part of them does the implementation.
− The asymmetric participation in both dialogue and implementation: a hierarchic role

organization where some give orders and others execute them.
And the problem-solving strategies:

−   Dialogue and implementation alternation could reflect a systematic problem solving approach which follows the plan-implement-evaluate phases.
−   While almost null participation in dialogue and continuous implementation could reflect a brute force trial and error strategy.

Since the final purpose for the analysis of NVC cues is to model a virtual agent, the NVC cues retrieved from the environment have to be totally recognizable by a computer system.

In [14] has been argued that the collaborative interaction analysis based on NVC can be conducted with the cues available at the environment. On the other hand in a study conducted in a real life situation results showed that group member' participation rates in two NVC cues: i.e. amount of talking time and time of manipulation in the workspace, corresponded to their contribution to the accomplishment of the task; and that certain NVC cues: frequency of vocalizations, object manipulation, pointing gestures and gazes to peers can be the means to differentiate when the participants were planning, implementing or evaluating [15]. The rationalizations for the automation of these NVC cues during a collaborative learning session are next discussed:

Discussion period. During discussion episodes, planes, evaluation and agreements are settled. Then they should be distinguished from situations like a simple question-answer interchange, or the statements people working in a group produce alongside their action directed to no one in particular [8]; for that, a number of talk-turns involving most of the group members might be an appropriate method.

A talking turn, as defined by Jaffe and Feldstein [9]: begins when the student starts to speak alone and is kept while nobody else interrupts him/her. For practical effects, in a computer environment with written text communication, the talking turn can be understand as a posted message, and in oral communication to a vocalization placed by the user. Based only in talking turns, discussion periods could be inferred as in (1).

Discussion period $\Rightarrow$ (number of talking turns > threshold A) $\wedge$ (number of   **(1)**
group members involved > threshold B)

Artifact manipulation. When the task at hand involves objects, their manipulation is necessarily part of the interaction; e.g. it can be the answer to an expression. The artifacts or objects related to the learning session also represent the students' shared workspace.

During the planning and reviewing phases scarce implementation should be expected, the objects will be probably more just touched than moved, while in the implementation phase there has to be significant activity in the shared workspace. The initiation of the implementation phase can be established, like with discussion periods and based only in the workspace activity, through a degree of manipulation and a number of students involved (2).

Implementation phase $\Rightarrow$ (number of objects manipulated > threshold C) $\land$ (**2**)
(number of group members involved > threshold D)

When implementation is made by division of labor, this activity will probably appear in different locations at the same time. Considering, for example a group of five people, if at least two students are working in different area(s) than the other three, then division of labor could be assumed as in (3).

Division of labor $\Rightarrow$ number of students working in different areas of the (**3**)
workspace > threshold E

As mentioned, a combination of amount of talk and amount of manipulation can be used to understand division of labor and the followed problem solving strategy [10].

Deictic gestures. Deictic gestures are used for pointing, they can be performed in a VE through the user's avatar body movements such as a gaze or a hand movement, but they can also be the mouse pointing.

When a group is working with objects, the communication by reference serves to get a common focus in a quick and secure form [5], [7]. Thus, the directed deictic gestures to the workspace are useful to determine whether students are talking about the task. An isolated deictic gesture could be just an instruction given or a gesture to make clear a statement about an entity, while turns of deictic gestures can be related to creating shared ground, which in turn could be related to the planning phase. In such a way that during the planning stage the students' alternation of deictic gestures and talking turn can be expected as in (4).

Planning phase $\Rightarrow$ (**1**) $\land$ (alternated deictic gestures to the workspace > (**4**)
threshold F)

Gazes. Gazes usually have a target; this target indicates the students' focus of attention. By observing the students' gazes it can be overseen if the group maintains focus on the task, and they could also be helpful to measure the students' involvement degree on it.

In order to establish if a student is involved in the task, his/her gazes should be congruent with what is going on in the environment, that is, usually gazing to the speaker or to what he/she is pointing at during a discussion period then (5), and usually to the workspace during implementation as showed in (6).

A range from 70 to 75 per cent of the time for the student to maintain this congruence is suggested as an acceptable rate in gaze behavior [1]. In that same way, it can be overseen if the group as a whole maintains focus on the task.

Gaze target congruence in (**1**) $\Rightarrow$ % of the gazes directed to the speaker $\lor$ to (**5**)
the object pointed by the speaker

Gaze target congruence in (**2**) $\Rightarrow$ % of gazing directed to the workspace (**6**)

Including gazes to the analysis may provide accuracy to the distinction of a discussion period, the implementation phase and when division of labor. Where the gazing behavior expected in discussion periods could be the student's field of view directed to the peers with short shifts to the workspace and going back to peers, then (7); during the implementation stage, the student's field of view directed to the workspace with shifts to peers then (8); and in division of labor, the students working in different areas and gazing most of the time only to what they are doing as in (9).

$$\text{Discussion period} \Rightarrow \text{(number of talking turns > threshold A)} \land \text{(number of} \quad \textbf{(7)}$$
$$\text{group members involved > threshold B)} \land \textbf{(5)}$$

$$\text{Implementation phase} \Longrightarrow \text{(number of objects manipulated > threshold C)} \quad \textbf{(8)}$$
$$\land \text{(number of group members involved > threshold D)} \land \textbf{(6)}$$

$$\text{Division of labor} \Rightarrow \text{number of students working in different areas of the} \quad \textbf{(9)}$$
$$\text{workspace > threshold E} \land \textbf{(6)}$$

Now then the reviewing phases are expected to interrupt or to appear at the end of an implementation phase, the end or interruption of the implementation phase in the environment will be manifested as in (10). The end of the implementation phase can represent also the end of the accomplishment of the task. The reviewing phase should convey discussion periods and in some cases some workspace activity as a result of that review.

$$\text{Implementation phase pause} \Longrightarrow \exists \text{ (2)} \land \text{(number of objects manipulated <} \quad \textbf{(10)}$$
$$\text{threshold C)} \land \text{(number of group members involved < threshold D)}$$

$$\text{Reviewing phase} \Longrightarrow \exists \textbf{(10)} \land \textbf{(7)} \quad \textbf{(11)}$$

Adding gazes to the analysis should provide accuracy to the distinction of the reviewing phase, where the task results have to be observed in a more extended area than just an object as when implementing, the gazes will be spread in the area under review.

The statistical dispersion formula can be applied to identify the spread of gazes. Data of the gaze targets of the students collected during the implementation phase will provide their standard deviation. To quantify "nearly all" and "close to", it can be used the Chebyshev's inequality that states that no more than $1/k^2$ of the values are more than k standard deviations away from the mean to understand the spread of gazes (12). For example, for 2 standard deviations it is $1/4 = .25$, then if more than 25% of the gazes are out of the range of 2 standard deviation then gazes have been spread over the workspace.

$$\text{Gaze target spread in the workspace} \Rightarrow \text{threshold F } \sigma \text{ of gaze targets during} \quad \textbf{(12)}$$
$$\text{an implementation} \geq 1/\text{(threshold F) 2}$$

$$\text{Reviewing phase} \Longrightarrow \exists \text{ (10)} \land \text{(7)} \quad \textbf{(13)}$$

Some of these assumptions were observed in an experimental application, which results are showed in the next section.

3 Preliminary Study

A preliminary study was conducted with the purpose to understand the group process phases: planning, implementation, and evaluation, identifying patterns derived from certain NVC cues extracted from the group behavior during the session.
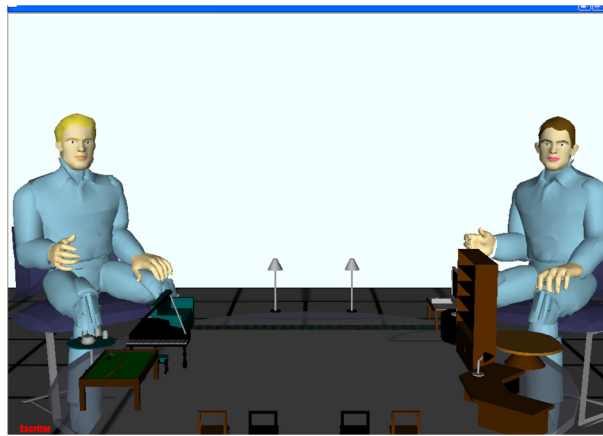
Fig. 1. Experimental application.
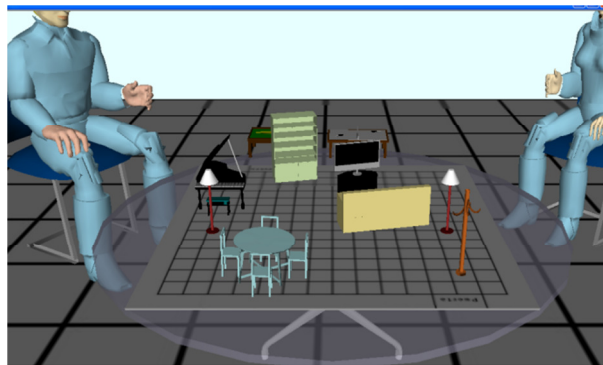
Fig. 2. Seeing down to the workspace.

The experimental application allows three users net-connected people to work in a collaborative task; the three users' avatars are placed around a table, the workspace.

The NVC cues in the environment and the students' actions available in the CVE are narrowed to those wanted to be observed and measured, avoiding other possibilities like navigation. These NVC cues are: talking turns, objects manipulation, gazes to the workspace and to peers, and pointing to objects. The avatars do not have a 'natural behavior'; they are just seated representations of the user that need a metaphorical representation of their actions in the environment. The user does not see his/her own avatar (see Figure 1).

The NVC cues are user-guided transmitted to the CVE through the keyboard and the mouse. The significant entities associated to the avatars actions are:

- Colored arrows coupled to their hair color (yellow, red, or brown) that take the place of their hands, and can be used to point the objects and/or grab them to move them;
- The avatars' head is another entity that can take four positions to change the user field of view –the change of view is controlled with the four keyboard arrows. To the front where the other two peers can be seen, to the right or left to see directly one of the peers, or down to see the workspace (see Figure 2); and,
- When the user is speaking a dialogue globe appears near his/her right hand –the user has to press the spacebar for the others to hear his/her voice.

3.1 Method

Subjects. Fifteen undergraduate students, 14 males and 1 female from the Informatics School at the Universidad of Guadalajara were invited to participate. Five groups were voluntarily formed of triads.

Materials and Task. The task consisted on the re-arrange of furniture on an apartment sketch to make room for a billiard or a ping-pong table; they decided which one of them. Sessions were audio recorder.

Procedure. A number of rules with punctuation were given regarding on how to place furniture such as the required space for the playing table, spaces between furniture and restriction on the number of times they could move furniture. Participants were allowed to try the application for a while before starting the task in order to get comfortable with its functionality. The time to accomplish the task was restricted to 15 minutes.

Data. Every student intervention within the environment was recorded in a logs file. The logs content is the user identification; the type of contribution he/she makes: i.e. move furniture, point furniture, a change in the point of view of the environment, when speaking to others; and the time the contribution was made with minutes and seconds.

3.2 Results

At a first glance to the data it could be overseen that the pointing mechanism was barely used; the speech content revealed that the users' had to make oral references to areas where there were no furniture because they could not point them.

Other identified problem related to gazes was that when the user was viewing the workspace area, he/she did not receive enough awareness about other users' gazes (see Figure 2); users had to verbally specify who they were addressing to if not to both members. We were particularly interested in observing if this unnatural gaze behavior was going to be accepted and used by the students.

Unfortunately, due to these misconceptions in the design of the environment gazes and pointing gestures had to be left out.

Discussion periods were defined as when the three group members had at least one talking turn. In order to determine the end of a discussion period, pauses of silences were considered in the range of three seconds; for automatic speech recognition, the end of an utterance is usually measured when a silence pause occurs in the range of 500 and 2000 ms [6], also the answer to a question usually goes in a smaller range, around 500 ms [19].
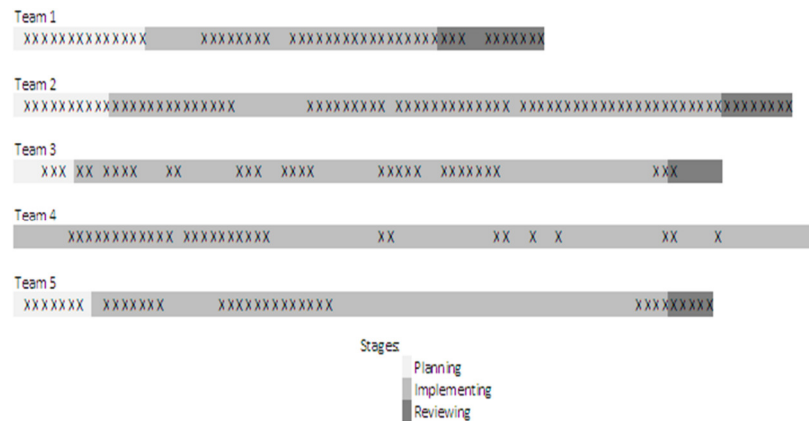
Fig. 3. The team stages during the sessions.

An external person was asked to determine through audio recorders, for each talking turn interchange whether the students were having an episode in which they were taking decisions, making plans or reviewing those; only two interchanges involving two of the three members had one of these characteristics, therefore most of the talking turn interchanges with the three members involved were discussion periods.

The stages were established as follows:

1. Planning stage – when discussion periods occur at the beginning of the session.
2. Implementation period – when at least one piece of furniture was moved.

3. Reviewing phase – discussion periods within the implementation period or at the end of it.

In Figure 3, graphics for each team session stages are presented, discussion periods are marked with an 'X'. A number of analyses can be derived from the distinction of these stages in the collaborative session such as stages times versus task effectiveness, of other related to group personality like cohesiveness.

Regarding a collaborative intelligent tutor, a clear opportunity to intervene is the fourth team which started with the implementation and then they had a discussion period while they kept the implementing, and continue working it seems that almost in silence. In the audio tape at some point they commented – "remember that we are not supposed to talk" with apparently no reason, and work to the end of the task in silence. However they fake talking, that is, they press the talking turn key probably to bring the others attention.

4   Discussion and Future Work

Nonverbal communication in a CVE could be the means to understand to a certain point what takes place during a learning session, its automatic analysis is proposed here as a tool for a virtual tutor to guide students to enhanced collaboration, as when the students are expected to start with a planning stage in which they create a common ground, and with an implementation that includes reviewing periods.

In order to understand these assumptions an experimental application was used to conduct a preliminary study. Unfortunately two misconceptions on its design invalidate the gazes and pointing mechanisms. Although, results showed that planning, implementing and reviewing stages can be distinguished through the retrieval from the logs of the talking turns and the manipulation of objects, also discussion periods can be determine.

There is no doubt of the importance of awareness; the lack of awareness for the other users invalidates the visual advantages in CVEs. An obvious next step is to adapt the application to give feedback for gazes when users have the view towards the workspace; along with a more free pointing facilitation to the entire workspace.

In this paper assessment rules for the automatic analysis of NVC cues were presented, using these methods a virtual tutor to facilitate collaborative interaction in a learning scenario can be modeled.

References

1. Argyle, M., & Cook, M.: Gaze and mutual gaze. Cambridge University Press, Cambridge (1976)

2. Bricken, M.: Virtual Reality Learning Environments: Potentials and Challenges. Computer Graphics, 25, 178–184 (1991)
3. Capin, T. K., Pandzic, I. S., Thalmann, N. M. et al.: Realistic Avatars and Autonomous Virtual Humans in VLNET Networked Virtual Environments (1997)
4. Chittaro, L., & Ranon, R.: Web3D Technologies in Learning, Education and Training: Motivations, Issues, Opportunities. Computers & Education Journal, 49, 3-18 (2007)
5. Clark, H. H., & Brennan, S. E.: Grounding in communication. In: Resnick, L.B., Levine, J.M. and Teasley, S.D. (eds.) Perspectives on socially shared cognition, pp. 127–149. American Psychological Association, Hyattsville, MD (1991)
6. Edlund, J., Heldner, M., Gustafson, J.: Utterance Segmentation and Turn-Taking in Spoken Dialogue Systems. Computer Studies in Language and Speech, 8, 576–587 (2005)
7. Gergle, D., Kraut, R. E., Fussell, S. R.: Language Efficiency and Visual Technology: Minimizing Collaborative Effort with Visual Information. Journal of Language and Social Psychology, 491–517 (2004)
8. Heath, C., Jirotka, M., Luff, P. et al.: Unpacking Collaboration: The Interactional Organisation of Trading in a City Dealing Room. Computer Supported Cooperative Work, 3, 147–165 (1995)
9. Jaffe, J., & Feldstein, S.: Rhythms of dialogue. Academic, New York, NY (1970)
10. Jermann, P.: Computer Support for Interaction Regulation in Collaborative Problem-Solving (2004)
11. Jermann, P., Soller, A., Lesgold, A.: Computer Software Support for Collaborative Learning. In: Anonymous What We Know About CSCL in Higher Education, Kluwer, Amsterdam pp. 141–166 (2004)
12. Martínez, A., Dimitriadis, Y., de la Fuente, P.: An XML-Based Model for the Representation of Collaborative Action (2002)
13. Patterson, M. L.: Nonverbal Behavior: A Functional Perspective. Springer-Verlag, New York (1983)
14. Peña, A., & de Antonio, A.: Inferring Interaction to Support Collaborative Learning in 3D Virtual Environments through the User's Avatar Nonverbal Communication. IJTEL, 2, 75–90 (2010)
15. Peña, A., & de Antonio, A.: Nonverbal Communication as a means to support collaborative interaction assessment in 3D Virtual Environments for learning. In: Juan, A.A., Daradoumis, T., Xhafa, F., et al (eds.) Monitoring and Assessment in Online Collaborative Environments: Emergent Computational Technologies for E-learning Support,IGI-Global, Hershey, PA, pp. 172–197 (2009)
16. Scrimshaw, P.: Cooperative writing with computers. In: Scrimshaw, P. (ed.) Language, classrooms & computers, pp. 100-110. Routledge, London-UK (1993)
17. Soller, A., Jermann, P., Muehlenbrock, M. et al.: Designing Computational Models of Collaborative Learning Interaction: Introduction to the Workshop Proceeding (2004)
18. Sonnet, H., Carpendale, S., Strothotte, T.: Integrating Expanding Annotations with a 3D Explosion Probe, 63–70 (2004)
19. Stivers, T., Enfield, N. J., Brown, P. et al.: Universals and Cultural Variation in Turn-Taking in Conversation. PNAS, 106, 10587–10592 (2009)
20. Winn, W. D.: Current Trends in Educational Technology Research: The Study of Learning Environments. Educational Psychology Review, 14, 331–351 (2002)
21. Wolff, R., Roberts, D., Steed, A. et al.: A Review of Tele-Collaboration Technologies with Respect to Closely Coupled Collaboration. IJCAT (2005)

Natural Language Processing

New Textual Representation
using Structure and Contents

Damny Magdaleno[1], Juan M. Fernández[2], Juan Huete[2], Leticia Arco[1],
Ivett E. Fuentes[1], Michel Artiles[1], and Rafael Bello[1]

[1] Computer Science Department, Central University "Marta Abreu" from Las Villas,
Camajuaní Road km 5½, Santa Clara, Villa Clara, Cuba
[2] Computer Science and Artificial Intelligence Department
University of Granada, Granada, Spain
{dmg, leticiaa, ifuentes, mae}@uclv.edu.cu
{jmfluna, jhg}@decsai.ugr.es

Abstract. The effectiveness of documents representation is directly related with how well can be compared their contents with another. When representing XML documents it is important not only its content, the structure can be exploited in tasks of text mining. Unfortunately, most XML documents representations do not consider both components. In this paper is presented a new form of textual XML documents representation using their structure and contents. The main results are: the new form of textual representation, following the criterion that depending on the location in which is presented a term within a document will have more or less importance in deciding how relevant this is in the document; it was joined to GARLucene software, increasing its potential for handling XML documents; the clustering, based on differential Betweenness of 25 textual collections represented with the new proposal, yielded better results than when they were represented with classic VSM.

Keywords: Textual representation, XML, clustering and document management.

1 Introduction

The increase of information in digital format, facilitated by storage technologies, poses new challenges to information processing tasks, among which may include: information retrieval, clustering and classification [1].

In performing these tasks, one of the steps is the Textual Representation (TR), which aims to transform textual document into a format that is suitable for input to algorithms application (e.g. machine learning, clustering and classification) in order to do Text Mining (TM) [2].

The effectiveness of a document representation is directly related to the accuracy with which the selected set of terms represents the document's contents and how well can be

compared that document's contents with another, that is, given two documents d1 and d2 and its representations r1 and r2, respectively, if r1 equals r2, this means that the content of d1 is equal to the contents of d2 with a level of abstraction [1]. So the TR have a key role in manipulating text documents, then a textual representation leads to good results in tasks such as clustering.

Among the different techniques of TR in the literature may be mentioned the Vector Space Model (VSM) [3], which is widely recognized as an effective representation for documents in the TM community, especially in the areas of information retrieval, clustering and classification. This representation sees the documents as a set of vectors where each dimension represents the weight of a term in the contents, which can be calculated, rather easily based on the number of term occurrences in the document, for example using inverse document frequency, or if exits information on the categories of documents using the Shannon entropy on all documents class set, for which is used the classification information [4]. In [5] the representation used is based on phrases rather than words to form the vector representation, using such phrases as input units for the functions of traditional weighting: Binary, TF and TF-IDF. In [6] are proposed the CONSOM model using two vectors instead of one to represent both the input documents with the aim of combining the vector space with what they call a conceptual space. The use of self-organizing maps with fuzzy logic for the RT content of Web pages was proposed in [4].

Some authors state that the documents are indivisible and independent units. Reflecting briefly on the concept of a document, can be found multiple types where it is more natural to treat them as a set of parts, these include scientific papers, which usually consist of title, abstract, keywords, a series of sections (can be divided into several subsections and so on), conclusions, among others. Therefore, given a set of documents $D = \{d_1, \ldots, d_m\}$, these correspond to a set of structural units $U = \{u_1, \ldots, u_n\}$. In this way the concept of document as indivisible unit disappears. Such is the case of XML format documents (Extensible Markup Language), which is a meta-language developed by the W3C[1] that arose from the need that the company had to store large amounts of information. An XML document is a self-descriptive hierarchical structure of information, which consists of a set of atoms, compound elements and attributes [7]. Added to this XML documents contain information on a semi-structured form [8], incorporating data and structure in the same entity. XML are extensible, with easy analysis and processing structure. The labels in XML documents allowing semantic content description of the elements. Thus, the structure of documents can be exploited for retrieval of relevant documents [9]. For all the above, XML documents are undoubtedly the standard data exchange format between Web applications and everyday more electronic data are presented on the web in this format [7]. For efficient organization and retrieval of relevant documents, a possible solution is to clustering XML documents based on their structure and / or its content [10]. A clustering algorithm attempts to find natural clusters of data based mainly on the similarity and relationships of objects, so as to obtain the internal distribution of the data set by its

---

[1] http://www.w3c.org.

partitioning into clusters. When the clustering is based on the similarity of the objects, it is intended that objects belonging to the same cluster are as similar as possible and the objects belonging to different clusters are as different as possible [11].

Therefore a proposal for TR for XML documents is presented in this paper, using the existing structure and contents therein, specifically dealing with the content in terms of the document's structure, following the criterion that depending on the location (Structural Unit, SU) in that a term (word) is present inside a document, it will have more or less importance in deciding how relevant this is in the paper. This representation will be used in a document clustering algorithm. The clustering algorithm applied in this paper is based on Differential Betweenness (DB) [12], which has shown good performance in textual domains. The organization of the paper is as follows: Section 2 shall treat forms of XML documents representation and related work; section 3 presents a new form of representation that weighs textual content based on the structure; in 4, application of the technique implemented in a system for managing documents is shown; section 5 will discuss the experimental results and finally; Section 6 presents conclusions.

2   XML Document Representation Forms

When the XML semi-structured documents, there are three ways to make textual representation: (1) representation that considers only the contents of the documents, (2) representation which considers only the structure, and (3) representation that considers these two dimensions of XML documents (structure and content).

2.1   Only Content Representation

This type of representation is often presented in the literature, but in the case of XML documents it ignores the advantage they offer, its structure. Thus, this approach focuses on treating the documents only by their content, either by performing a lexical analysis only, or including syntactic or semantic elements in the study. Those algorithms that perform lexical analysis, generally considered the documents as a bag of words, therefore, removed all the labels and lose the structural information provided by the documents [13]. Following this approach several authors rely on the traditional VSM representation.

2.2   Only Structure Representation

Making a TR of XML documents considering only its hierarchical structure is vitally important in tasks such as clustering, information extraction and integration of heterogeneous data, among others [9]. Several works represent XML documents in tree using its hierarchical structure, an example of this is made by [7, 14] using the tree view

to calculate the tree-edit distance or some variant to compare documents, this is just the number of operations (insertion, remove and replacement of nodes) to perform in a tree so that its structure is equal to the other tree with which it is compared. The smaller the number of operations is, the greater the similarity between the trees for XML documents. In [7] is proposed the Structural Summaries calculation for reducing trees to compare, given their nests and repetitions that may exist. Thus, representations are obtained as low as possible to maintain the relationships between elements of the tree and facilitate later comparisons. Other forms of document representation considering structure are based on the use of Edit Graph [15].

2.3   Representation using Structure and Content

Most existing approaches do not use these two dimensions (structure and content) because of its complexity. However, for best results in the later stages of the TR (e.g. clustering, classification), it is essential to use both [16]. Here are some works in the literature. A first and easy option is to mix in a VSM representation [17] the content and document tags. In [16] are used Close Frequent Sub-trees in charge of processing the document structure and then perform a preprocessing to the contents of documents. Other work carried out extensions to the VSM representation, called C-VSM and SLVM [17, 18]. In both forms for each document a matrix M_{ext} where e is the number of labels and t the number of terms is implemented, each cell will contain the frequency of each term t_i in the label e_j. C-VSM presented the "low contribution" problem to ignore the semantic relationship between different elements and SLVM not taking into account the relationship between common elements can present the "over contribution" problem. In order to eliminate these difficulties [13] proposed the Proportional Transportation Similarity, working with weighted comparisons according to the similarity of the items to compare in two documents.

3   New Textual Representation Weighting Content as related to Structure Position

Information in XML documents are in semi-structured format, so that the textual representation is essential for further processing. In this work we have selected the VSM representation [3], which will change the way of calculating the frequency of terms in each document. The modification proposed in this paper follow the criterion that a term has more or less important for comparing two documents, depending on the place it occupies within them.

That is, given three documents d_1, d_2, d_3 and the words w_1, w_2, ..., w_n, where w_1, ..., w_k, $k<n$, are common to d_1 and d_2 and are present in important parts of documents (e.g. abstract, keywords), and w_{k+1}, ..., w_n are common to d_1 and d_3, but are present in less

important sections of these, the relationship between the documents d_1 and d_2 is stronger than there between d_1 and d_3, because since their common words belong to key parts of the document, the information from these two documents is common significantly compared to the documents d_1 and d_3.

The Textual Representation referred to in this paper has four main modules: documents corpus transformation, term extraction, dimensionality reduction, matrix normalization and weighting, the next subsections will describe these.

3.1   Corpus Transformation

To do the TR, the input is a set of tokens of words obtained in a process of Information Retrieval, these tokens will be used to generate significant features (index terms). The first step in the corpus transformation can process XML documents, identifying in which SU is present a given content. Second, the resulting sequence of tokens is transformed converting all letters to capital letter, removing punctuation marks at the end of tokens, ignoring tokens containing alphanumeric characters, and substituting contractions by their full expressions [19].

3.2   Term Extraction

This submodule starts from a tokens sequence and produce an index terms sequence based on these tokens. This paper performs a lexical analysis of texts, identifying simple words like features. Thus, the statistical plane of the texts is basically exploited and the sequence of appearance of words in a document is not considered (bag-of-words model) [20], but take into account in which SU is present the word.

In the original VSM representation each document d_j is a vector of term frequencies d_{tf} = $(tf_d(t_1), ..., tf_d(t_m))^T$, where $tf_d(t)$ denotes the term t appearing frequency in the document d. In this proposal, as mentioned above, is takes into account documents' structure, so that the frequency ($tf_d(t)$) will be weighted, depending on what SU the analyzed token occupies, being defined for a token t_i in a document d_j as shown in Equation 1, where n is the number of SU present in d, tf_{tk} is the frequency of t in the SU k, and w_{kd} is the weight the SU k in document d

$$tf_d(t) = \sum_{k=1}^{n} (w_{kd} * tf_{tk})$$

(1)

In Equation 2 in shown how to perform the calculation of the each SU k in each document d; here Lk is the length of k, Ld is the length of the document d and p is a parameter that gives a degree of freedom to estimate weight.

$$w_{kd} = \left(e^{(-L_k/L_d)}\right)^p \qquad (2)$$

3.3 Dimensionality Reduction

This submodule reduced the representation dimensionality, eliminating stop-words, selecting all features whose score is above or below of a threshold, or the *m* best features, considering mainly I and II quality terms expressions [21] to calculate the term quality. In addition, the spelling is homogenized and words are reduced to root form [22].

3.4 Normalization and Weighting Matrix

At this TR stage a weighted vector is generated for any document, term frequencies vector based. In the proposed implementation scheme is used TF-IDF [21] to weigh the matrix values and is normalized by dividing the terms frequency by the documents length, see equations 3 and 4.

$$tfidf(t) = tf(t) * idf(t) \qquad (3)$$

$$idf(t) = \log\frac{n}{n(t)} \qquad (4)$$

Finally, Figure 1 shows the schematic representation of the text corpus.
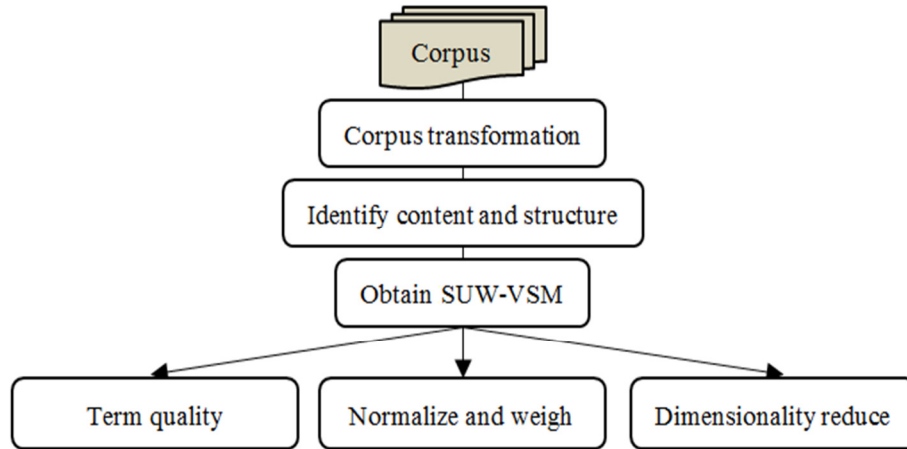
Fig. 1. Textual corpus representation scheme

4   Application of the Technique Implemented in a Management System for Scientific Papers

In [12], the System for Retrieved Research Papers Management using Lucene (GARLucene) is introduced following a general scheme that has four general modules: information retrieval or textual corpora specification process, textual corpus obtained representation, documents clustering and textual cluster obtained validation. This system uses the advantages of Lius[2] and Lucene[3] for indexing and retrieving textual information.

GARLucene in its original version manipulates XML documents but does not exploit their structure. In this paper, it is reported how it was added to GARLucene a textual representation form described in Section 3. This addition increases the GARLucene potential, since the better documents are represented, better cluster results.

4.1   Main Action to Incorporate New Textual Representation to GARLucene

For implementing this variant of XML document TR in GARLucene the following major actions were performed. Documents were indexed with Lucene library that allows incremental index creation, search and information retrieval indexing. To create the index is firstly used JDOM Java API, designed to work with XML documents to identify each SU in the documents, that was later provided as the Lucene fields and facilitate the creation of indexes. GARLucene reused largely Lucene facilities for TR. The first phase of the transformation is done in the indexing and retrieval.

Lucene allows the retrieved collection VSM representation, primarily through the *StandardAnalyzer* class that implements *StandardFilter* to normalize extracted tokens, *LowerCaseFilter* to lowercase tokens and *StopFilter*[4] to remove stop-words. Additionally, *Analyzer* allows obtaining words roots through heuristics, and treats the synonymy and polysemy. TR in GARLucene was enriched by adding the filtering methods for the feature selection calculating Quality Terms I and II [21] expressions. GARLucene implemented three variants of divisive hierarchical clustering algorithm using the edges betweenness

4.2   Clustering Algorithm based on Differential Betweenness

The clustering algorithm based on Differential Betweenness [12], parts from the proposal defined by [23] to use with the differential intermediation, achieving better results than those Newman obtained, since the good properties of the measurement are inherited.

---

[2] http://sourceforge.net/projects/lius
[3] http://lucene.apache.org
[4] Use a small stop-words list, enriched in this research.

Differential Betweenness and Cosine Similarity

When applying DB to textual domains a graph representation can be used where the interaction between two documents (edges' weight) is expressed in terms of how similar they are. Areas of high similarity values involve highly interconnected nodes. Generally, documents in the same cluster are more similar than documents in different cluster.

In [12] is illustrated the utility of the DB in the bridges detection between clusters, to cluster documents where Cosine similarity expresses the interrelationships between them. This way of calculating the edges centralities discover the bridges between clusters because, unlike the cosine similarity, it is able to exploit the graph topological properties.

Clustering Algorithm Based on the Similarity Matrix

This section show the clustering algorithm based on the concept of DB proposed by [12], see Figure 2. In [12] is described step by step this algorithm.

```
1. Obtaiment of the similarity graph.
2. Calculation    of    the    weighted    differential
   betweenness matrix.
3. Estimation of the edges to be eliminated.
4. Determination of the kernels of clustering by means
   of the extraction of the connected components.
5. Classification  of  the  nodes  not  belonging  to  the
   kernels.
```

Fig. 2. Clustering algorithm based in Differential Betweenness.

5   Experimental Results

This section aims to illustrate how much are improved the results of clustering based on DB when using the textual representation proposed, with respect to the results obtained when using the classical VSM representation.

5.1   Definition of Case Studies and Tools used

For achieve the experiments two case studies were defined, the first consists of 15 corpora formed as subsets of documents in the Biomed[5] collection, the second case study has 10 corpora of XML documents from papers recovered from the ICT[6] site of the Centro de Estudios de Informática (Centre of Studies of Informatics), in the Universidad Central

---

[5] Bioinformatics and Medical papers http://www.biomedcentral.com/info/about/datamining/
[6] http://ict.cei.uclv.edu.cu

"Marta Abreu" de Las Villas (Central University of Las Villas). Table 1 describes these corpora (case study 1, corpus 1 to corpus 15; case study 2, corpus 16 to corpus 25).

5.2   Experiments Design and Implementation

Since we had the reference classification of textual collections considered in the experiment, we selected Overall F-measure (OFM) measurement for the comparative study of the clustering results with both TR. Equation 5 shows the general expression of OFM; equation 6 shows the F-measure calculation, that combines both expressions Precision (Pr) and Recall (Re) (see Equation 7), considering the real threshold $\alpha \in [0.1]$. Here n_{ij} is the number of objects that are in both class i and cluster j, n_j is number of objects in the cluster j, n_i is the number of objects in the class i, n is the count of clustered objects and k is the count of reference classes.

Table 1. The description of case studies.

Corpus	Document count	Class count	Reference classification
1	54	2	Cystic Fibrosis, Diabetes Mellitus
2	31	2	Cystic Fibrosis, Lung Cancer
3	26	2	Cystic Fibrosis, Microarray
4	28	2	Cystic Fibrosis, Genetic Therapy
5	42	2	Cystic Fibrosis, HIV
6	53	2	Diabetes Mellitus, Lung Cancer
7	48	2	Diabetes Mellitus, Microarray
8	50	2	Diabetes Mellitus, Genetic Therapy
9	64	2	Diabetes Mellitus, HIV
10	25	2	Lung Cancer, Microarray
11	27	2	Lung Cancer, Genetic Therapy
12	41	2	Lung Cancer, HIV
13	22	2	Microarray, Genetic Therapy
14	36	2	Microarray, HIV
15	38	2	Genetic Therapy, HIV
16	37	2	Clustering, Fuzzy Logic
17	37	2	Clustering, Association Rules
18	37	2	Clustering, Rough Set
19	41	2	Clustering, SVM
20	30	2	Fuzzy Logic, Association Rules
21	30	2	Fuzzy Logic, Rough Set
22	34	2	Fuzzy Logic, SVM
23	30	2	Association Rules, Rough Set
24	34	2	Association Rules, SVM
25	34	2	Rough Set, SVM

$$Overall\ F - Measure = \sum_{i=1}^{k} \frac{n_i}{n} max\{F - Measure(i,j)\} \tag{5}$$

$$F - Measure(i,j) = \frac{1}{\alpha(1/\Pr(i,j)) + (1-\alpha)(1/Re(i,j))} \tag{6}$$

$$\Pr(i,j) = n_{ij}/n_j \qquad Re(i,j) = n_{ij}/n_i \tag{7}$$

Table 2 shows the results of applying OFM to the results of clustering based on the DB when the selected collections were represented with classic VSM and the variant propose in this paper.

Table 2. The comparison of the new and original TR by OFM applied to clustering.

Corpus	OFM, classic representation	OFM, new representation
1	0,710	0,710
2	0,660	0,659
3	0,670	0,670
4	0,681	0,629
5	0,676	0,676
6	0,716	0,716
7	0,762	0,851
8	0,757	0,741
9	0,675	0,675
10	0,660	0,668
11	0,678	0,660
12	0,663	0,680
13	0,675	0,754
14	0,715	0,715
15	0,606	0,688
16	0,684	0,870
17	0,674	0,946
18	0,674	0,973
19	0,959	0,976
20	0,674	0,967
21	0,665	0,659
22	0,736	1,000
23	0,864	1,000
24	0,703	0,971
25	0,858	1,000

After obtaining the results of the OFM for the algorithm applied to each collection, statistical tests were performed to compare and analyze the significance level and behavior of the two variants of TR analyzed. In this sense, were performed to compare the algorithms non parametric tests for two related samples, using the Wilcoxon test, see Table 3 and Table 4.

For interpreting the results was considered:

- − Highly significant, a significance less than 0.01,
- − Significant, a result of significance less than 0.05 and greater than 0.01,
- − Moderately significant, a result less than 0.1 and greater than 0.05,
- − Not significant, a result greater than 0.1.

Table 3. Ranks of results.

		N	Mean Rank	Sum of Ranks
Classic-New	Negative Ranks	14[a]	12,00	168,00
	Positive Ranks	5[b]	4,40	22,00
	Ties	6[c]		
	Total	25		

[a]Classic < New   [b]Classic > New   [c]Classic = New

Table 4. Wilcoxon test statistics of results.

	Classic-New
Z	2.938[a]
Aymp. Sig (2-tailed)	**0,003**

[a]Base on positive ranks.

In analyzing the results of the statistical test can be seen that there are highly significant differences between the two variants of textual representation, with the textual representation proposal presented in this paper that yielded the best results of clustering, considering the OFM validation measure

6 Conclusions

This paper presented a new form of textual representation of XML documents, using their structure and content. The new form of textual representation is the content based on the structure of the document, following the criterion that depending on the location (structural unit) in the presence of a term (word) within a document, you will have greater or lesser importance to decide how relevant this is in the document. The incorporation of the new form of textual representation in GARLucene has increased significantly the potential of the software for handling XML documents and extracting knowledge from

them. This new form of textual representation yields better clustering results considering the algorithm based on the Differential Betweenness, than using classical VSM representation.

References

1. Carrillo, R.M., A.L.L.: Una Representación Vectorial para Contenido de Textos en Tratamiento de Información, In: CCC-08-004. Coordinación de Ciencias Computacionales INAOE (2008)
2. Lewis, D.D.: Representation and Learning in Information Retrieval, in Department of Computer and Information Science. University of Massachusetts (1992)
3. Salton, G., Wong, A., and Yang C.S.: A Vector Space Model for Information Retrieval. Journal of the ASIS, 18(11): pp. 613-620 (1975)
4. García-Plaza A.P., Víctor Fresno, R.M.: Una Representación Basada en Lógica Borrosa para el Clustering de páginas web con Mapas Auto-Organizativos, In: Procesamiento del Lenguaje Natural. 79-86 (2009)
5. Bakus, J.H., M.F.; Kamel, M.: A SOM-based document clustering using phrases, In: 9th International Conference on Neural Information Processing ICONIP 2002. pp. 2212-2216 (2002)
6. Liu, Y., Wang, X., Wu, C.: ConSOM: A conceptional self-organizing map model for text clustering. Neurocomputing. 71(4-6): pp. 857-862. (2008)
7. Theodore Dalamagas, T.C., Klaas-Jan Winkel, Timos Sellis: A Methodology for Clustering XML Documents by Structure. Information Systems (2006)
8. Abiteboul, S., Querying semi-structured data. Proceedings of the ICDT Conference, Delphi, Greece (1997)
9. Guerrini, G.M.M., Sanz, I.: An Overview of Similarity Measures for Clustering XML Documents. (2006)
10. Tien T., R.N.: Evaluating the Performance of XML Document Clustering by Structure only.
11. Kruse, R., Döring C., Lesor M.J.: Fundamentals of Fuzzy Clustering, in Advances in Fuzzy Clustering and its Applications. Oliveira, J.V.D., Pedrycz, W. Editors. John Wiley and Sons: East Sussex, England. pp. 3-27 (2007)
12. Arco, L.: Agrupamiento basado en la intermediación diferencial y su valoración utilizando la teoría de los conjuntos aproximados, In: Ciencias de la Computación. Universidad Central "Marta Abreu" de Las Villas: Santa Clara, Villa Clara. pp. 187. (2009)
13. Wan, X., Yang, J.: Using Proportional Transportation Similarity with Learned Element Semantics for XML Document Clustering. International World Wide Web Conference Committee (2006).
14. Flesca, S., et al.: Fast detection of XML structural similarities. IEEE Trans. Knowl. Data Engin. 7(2): pp. 160-175 (2005)
15. Chawathe, S.S.: Comparing Hierarchical Data in External Memory. In: In Proceedings of International Conference on Very Large Databases (1999)
16. Kutty, S., et al.: Combining the structure and content of XML documents for clustering using frequent subtrees. INEX, pp. 391-401 (2008)
17. Doucet, A., AhonenMyka, H.: Naive clustering of a large XML document collection. INEX. pp. 84-89 (2002)
18. Yang, W., Chen, X.O.: A semi-structured document model for text mining. Journal of Computer Science and Technology, 17(5): pp. 603-610 (2002)

19. Lanquillon, C.: Enhancing Text Classification to Improve Information Filtering, in Research Group Neural Networks and Fuzzy Systems. 2001, University of Magdeburg "Otto von Guericke": Magdeburg. pp. 231. (2001)

20. Lewis, D.D., Ringuette M.:. A comparison of two learning algorithms for text classification. In: Third Annual Symposium on Document Analysis and Information Retrieval. University of Nevada, Las Vegas. (1994)

21. Berry, M.W.: Survey of Text mining: Clustering, Classification, and Retrieval. New York, NY, USA: Springer Verlag. (2004)

22. Frakes, W.B., Baeza-Yates, R.: Information Retrieval. Data Structure & Algorithms. New York: Prentice Hall. (1992)

23. Newman, M.E.J.: Analysis of weighted networks. Physical Review E. 70(52): pp. 056131. (2004)

Native Speaker Dependent System for the Development of a Multi-User ASR-Training System for the Mixtec Language

Santiago Omar Caballero Morales and Edgar De Los Santos Ramírez

Technological University of the Mixtec Region, Postgraduate Division, Highway to Acatlima K.m.
2.5, Huajuapan de Leon, Oaxaca, 69000, Mexico
scaballero@mixteco.utm.mx, edgarinteractivo@hotmail.com

Abstract. The Mixtec Language is one of the main native languages in Mexico, and is present mainly in the regions of Oaxaca and Guerrero. Due to urbanization, discrimination, and limited attempts to promote the culture, the native languages are disappearing. Most of the information available about these languages (and their variations) is in written form, and while there is speech data available for listening and pronunciation practicing, a multimedia tool that incorporates both, speech and written representation, could improve the learning of the languages for non-native speakers, thus contributing to their preservation. In this paper we present some advances towards the development of a Multi-User Automatic Speech Recognition (ASR) Training system for one variation of the Mixtec Language that could be used for the design of speech communication, translation, and learning interfaces for both, native and non-native speakers. The methodology and proposed implementation, which consisted of a native Speaker - Dependent (SD) ASR system integrated with an adaptation technique, showed recognition accuracies over 90% and 85% when tested by a male and a female non-native speakers respectively.

Keywords: Speech recognition, native languages, learning interfaces.

1 Introduction

Research on spoken language technology has led to the development of Automatic Speech Recognition (ASR), Text-To-Speech (TTS) synthesis, and dialogue systems. These systems are now used for different applications such as in mobile telephones for voice dialing, GPS navigation, information retrieval, dictation [1, 2, 3], translation [4, 5], and assistance for handicapped people [6, 7].

ASR technology has been used also for language learning, and examples of these can be found in [8, 9, 10] for English, [11] for Spanish and French among others, and [12] for "sign" languages. These interfaces allow the user to practice their pronunciation at home or work without the limitations of a schedule. They also have the advantage of mobility as

some of them can be installed in different computer platforms, or even mobile telephones for basic practicing. However, although there are applications for the most common foreign languages, there are limited (if any) applications for native or ancient languages.

In Mexico there are around 89 native languages still spoken by 6.6 millions of native speakers. Although the number of speakers may be significant (considering the total number of inhabitants in Mexico) this number is decreasing, especially in the Mixtec region.

The population of native speakers of the Mixtec language is decreasing given urban migration and development, culture rejection and limited attempts to preserve the language. This has been expressed by people living in communities in the Mixtec region of Mexico, and this can be corroborated by national statistics that show that the number of people who spoke any native language, 6.3 millions in 2000 (7.1% of the total population) decreased to 6.0 millions in 2005 (6.6% of the total population), and this amount was even higher in 1990 (7.5% of the total population) [13]. This increases the possibility of native languages being lost, as some dialects or variations had less than 10 known speakers (i.e., Ayapaneco, 4 speakers; Chinanteco of Sochiapan, 2 speakers; Mixtec of the Mazateca Region, 6 speakers [13]). In this case, historic antecedents or information about the language is not recorded, making very difficult to recover or save some part of the language. This may happen to other languages with more speakers. The Mixtec Language, with approximately 480,000 speakers, has been reported to lose annually 200 speakers.

To preserve a language is not an easy task, because all characteristics such as grammar rules, written expression, speech articulation, and phonetics must be documented and recorded. Although there are books and dictionaries that among the word definitions include examples about how to pronounce them, this is not as complete as listening the correct pronunciation from a native speaker

We consider that this goal can be accomplished by the use of modern technology such as that used for foreign language learning [10, 11] to promote the language among non-native speakers and thus, to contribute to its preservation. In this work we focus on the development of an ASR-Training system to allow a speaker to practice his or her pronunciation. The methodology and proposed implementation, which consisted of a native Speaker - Dependent (SD) ASR system integrated with a speaker adapting technique, achieved accuracies over 90% and 85% for a male and a female non-native users respectively.

The development of the native ASR-Training system is presented as follows: in Section 2 the details about the phonetics of the reference Mixtec language variation, and the speech corpus developed to build the native ASR system, are shown; in Section 3 the design of the SD native ASR system, which includes the supervised training of the system's acoustic models, and the adaptation technique for its use by non-native users, are shown; in Section 4 the details of the testing methodology by two non-native speakers and the performance of the system in real time are presented and analyzed; finally in Section 5 we discuss about our findings and future work.

2 The Mixtec Language

2.1 Phonetics

The Mixtec Language, or "Tu'un Savi" (Tongue/Language of the Rain) [14], is present mainly in the states of Sinaloa, Jalisco, Guerrero, Puebla, Oaxaca, and Yucatán. With a number of speakers of approximately 480,000, this is one of the main native languages in Mexico. The Mixtec is a tonal language [14], where the meaning of a word relies on its tone, and because of the geographic dispersion of the Mixtec population, there are differences in tones and pronunciations between communities, which in some cases restricts the communication between them [15]. Because of this, each variation of the Mixtec language is identified by the name of a community, for example, Mixtec from Tezoatlán [16], Mixtec from Yosondúa [17], or Mixtec of Xochapa [18], existing significant differences between vocabularies and their meanings: "cat" and "mouse" are respectively referenced as "chító" and "tíín" by the Mixtec of Silacayoapan, and as "vilo" and "choto" by the Mixtec of the South East of Nochixtlán. Hence, the Mixtec cannot be considered as a single and homogeneous language, and there is still a debate about its number of variations, which is within the range of 30 [19] to 81[20].

Table 1. Examples of Mixtec words with tones.

Word	Meaning	Word	Meaning
ñoó	*night*	yukú	*who*
ñoo	*town*	yuku	*mountain*
ñoo	*Palm*	yuku	*leaf*

Table 2. Repertoire of Mixtec phonemes.

No.	Phoneme	No.	Phoneme	No.	Phoneme
1	/á/	11	/o/	21	/m/
2	/à/	12	/ú/	22	/n/
3	/a/	13	/ù/	23	/nd/
4	/é/	14	/u/	24	/ñ/
5	/e/	15	/ch/	25	/s/
6	/í/	16	/d/	26	/sh/
7	/ì/	17	/dj/	27	/t/
8	/i/	18	/j/	28	/v/
9	/ó/	19	/k/	29	/y/
10	/ò/	20	/l/	30	/sil/

In general, the Mixtec language has three characteristic tones: high, medium, and low [14, 16, 17, 18, 21, 22, 23, 24]. In Table 1 some examples of words that change their meanings based on the tone applied on their vowels are shown, where (_) is used to identify the low tone, (´) the high tone, and the medium tone is left unmarked [14].

Although there are other tone representations, where the low tone also is represented with a horizontal line over the vowel [24], usually the high tone is represented with the diacritical (´).

Based on the phonemes identified in [14, 21-24] and by integrating the different tones in the vowels, the repertoire shown in Table 2 was defined. The low tone is represented by the diacritical (`) while the high tone is represented by (´), the medium tone is unmarked to keep consistency.

The phonetics of the Mixtec has some differences when compared with the Mexican Spanish language. For example, from Table 2:

– The Mixtec phoneme /dj/ represents a sound similar to the Spaniard Spanish **z** (phoneme /z/), which is stronger than **s** (/s/) in both languages. In the phonetics of the Mexican Spanish from the center region both sounds, **z** and **s**, are represented by the phoneme /s/ [25];
– The Mixtec phonemes /sh/ and /ch/ are pronounced in Mexican Spanish as the consonant **X** in the word "**X**icoténcatl" and **CH** in the word "**ch**icle" respectively;
– There are short pauses, uttered as a glottal closure between vowels within a word, which are represented by (') such as in "tu'un" or "ndá'a" ;
– The Mixtec phoneme /n/ sounds as **n** in the Mexican Spanish (associated with the consonant **N**) if it is placed before a vowel, but is mute if placed after the vowel.

2.2 Vocabulary

Because the purpose of the system is to be used for speech training and practicing of the Mixtec language, a vocabulary used for learning was chosen. For this, we established contact with a native speaker who teaches the Mixtec language at the local Cultural Center. The place of origin of this speaker is the community of San Juan Dikiyú in Oaxaca. Since this variation shares similarities with other variations in Oaxaca, we were confident about using it as the reference variation.

With support from the Mixtec teacher we selected 7 traditional Mixtec narratives from a total of 15 that he uses in his lessons for teaching, where the first were used for beginners and the last for more advanced students. The 7 narratives were read twice by the teacher in a recording studio, where the speech samples were recorded in WAV format with a sampling rate of 44,100 Hz and one audio channel (monaural). These recordings were transcribed at the phonetic and word levels (TIMIT standard) using the list of phonemes defined in Table 2 using the software WaveSurfer. All this material formed the **Training Speech Corpus** for the native ASR system which had a total of 192 different words.

Based on the frequency of phonemes of the corpus, which is shown in Figure 1, it was considered that the Training Corpus was phonetically balanced as there were enough samples from each phoneme for the supervised training of the acoustic models of the ASR system.
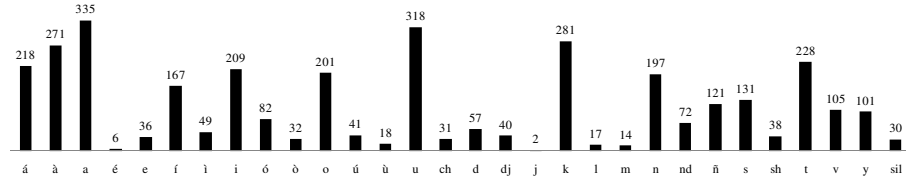
Fig. 1. Frequency distribution of the Mixtec phonemes in the Training Speech Corpus.

3 Mixtec Speaker-Dependent ASR System

The elements of the native ASR that were built with the Training Speech Corpus are shown in Figure 2.
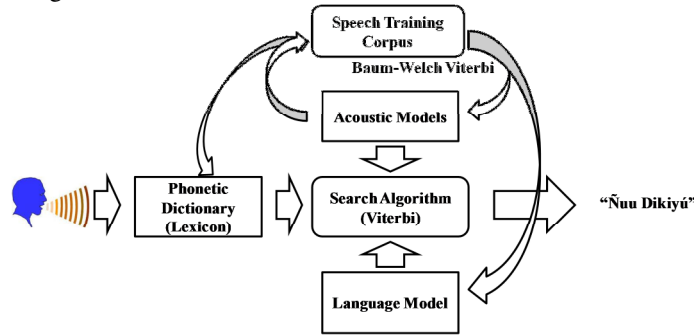
Fig. 2. Structure of the native ASR system.

These were implemented with the software HTK Toolkit [26], and each one was built as follows:

−   **Acoustic Models**: Hidden Markov Models (HMMs) [27, 28] were used for the acoustic modeling of each phoneme in the Training Corpus. These were standard three-state left-to-right HMMs with 10 Gaussian components per state. The front-end used 12 MFCCs plus energy, delta, and acceleration coefficients [26]. The supervised training of the HMMs with the Training Corpus (labeled at the phonetic level) was performed with the Baum-Welch and Viterbi algorithms.
−   **Lexicon**: the phonetic dictionary was made at the same time as the phonetic labeling of the Training Corpus. The phoneme sequences that formed each word in the vocabulary were defined by perceptual analysis considering the pronouncing rules presented in Section 2.1.

- **Language Model**: Word-bigram language models were estimated from the word transcriptions of the corpus. Speech recognition was performed with a scale grammar factor of 10.
- **Search Algorithm**: Speech recognition was performed with the Viterbi algorithm implemented with the module HVite of the HTK Toolkit.

3.1   Adaptation for Non-native Speakers

As presented in Section 2.2 the Speech Training Corpus of the native ASR was built with the speech samples from a single native speaker. Thus, the system described above is Speaker Dependent (SD) and it will show good performance only when used by the same speaker. For practicing and learning purposes this is a disadvantage.

Commercial ASR systems are trained with hundreds or thousands of speech samples from different speakers, which leads to Speaker-Independent (SI) systems. When a new user wants to use such system, it is common to ask the user to read some words or narratives to provide speech samples that will be used by the system to adapt the SI acoustic models to the patterns of the user's voice. SI ASR systems are robust enough to get benefits by the implementation of adaptation techniques such as MAP or MLLR [26, 28].

In the case of the development of a SI ASR system for the Mixtec language there are challenges given by the wide range of variations in tones and pronunciations, and the limited availability of native speakers to obtain training corpora. Because of this situation, the use of a speaker adaptation technique on this SD system was studied.

Maximum Likelihood Linear Regression (MLLR) was the adaptation technique used for the native SD ASR system in order to make it usable for non-native speakers. MLLR is based on the assumption that a set of linear transformations can be used to reduce the mismatch between an initial HMM model set and the adaptation data. In this work, these transformations were applied to the mean and variance parameters of the Gaussian mixtures of the SD HMMs, and it was performed in two steps:

- **Global Adaptation**. A global base class was used to specify the set of HMM components that share the same transform. Then a *global transform* was generated and applied to every Gaussian component of the SD HMMs.
- **Dynamic Adaptation**. The global transformation was used as an input transformation to adapt the model set, producing better frame/state alignments which were then used to estimate a set of more specific transforms by using a *regression class tree*. For this work, the regression class tree had 32 terminal nodes, and was constructed to cluster together components that were close in acoustic space, and thus could be transformed in similar way. These transforms become more specific to certain groupings of Gaussian components, and are estimated according to the "amount" and "type" of available adaptation data (see Table 3). Because each Gaussian component of an HMM belongs to one particular base class, the tying of

each transformation across a number of mixture components can be used to adapt distributions for which there are no observations at all (hence, all models can be adapted). The adaptation process is dynamically refined when more adaptation data becomes available [26].
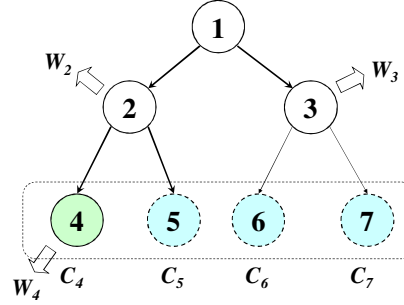
Fig.3. Binary regression class tree with four terminal nodes.

Table 3. Selection of words for supervised non-native speaker adaptation.

No.	Selected Word	Phonemes	No.	Selected Word	Phonemes
1	ÀNE'ECHOOS	à n e e ch o o s	14	KOÚNI	k o ú n i
2	ÁTOKÓ	á t o k ó	15	KUALÍ	k u a l í
3	DIKIYÚ	d i k i y ú	16	KÙTAKU	k ù t a k u
4	DJAMA	d j a m a	17	KUTÓ	k u t ó
5	DJÀVÌ	z à v ì	18	LAA	l a a
6	CHÁNÍ	ch á n í	19	LULI	l u l i
7	CHI	ch i	20	NDAKONÓ	nd a k o n ó
8	ÍDJONA	í z o n a	21	NDEEYÉ	nd e y é
9	ÍÑÒ	í ñ ò	22	NÍKÉE	n í k é e
10	KAMA	k a m a	23	ÑA	ñ a
11	KÌVÌ	k ì v ì	24	ÑUU	ñ u u
12	KOKUMI	k o k u m i	25	SÁXI	s á sh i
13	KÒÒÍÚN	k ò í ú	26	ÙXÌ	ù sh ì

As an example of how MLLR works, in Figure 3 a regression class tree is presented with four terminal nodes (or base classes) denoted as C_4, C_5, C_6 and C_7. Solid nodes and arrows indicate that there is enough data in that class to generate a transformation matrix, and dotted lines and circles indicate that there is insufficient data. During the "dynamic" adaptation, the mixture components of the models that belong to the nodes **2**, **3** and **4** are

used to construct a set of transforms denoted by W_2, W_3 and W_4. When the transformed model set is required, the transformation matrices (mean and variance) are applied in the following fashion to the Gaussian components in each base class: $W_2 \rightarrow C_5$; $W_3 \rightarrow \{C_6, C_7\}$; and $W_4 \rightarrow C_4$, thus adapting the distributions of the classes with insufficient data (nodes **5**, **6**, and **7**) as well as the classes with enough data.

For the native SD system, a selection of words from the Training Corpus was defined to allow the user to provide enough speech samples (adaptation data) from each phoneme listed in Table 2. These words are shown in Table 3 and have the frequency distribution of phonemes shown in Figure 4, which has a correlation coefficient of 0.69 with the distribution of the Training Corpus (Figure 1). Hence it was considered that the adaptation samples were representative of the Training Corpus and sufficient for MLLR adaptation.
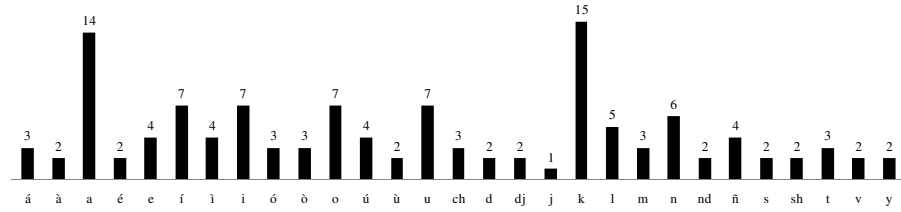
Fig. 4. Frequency distribution of the phonemes in the selection of words for non-native speaker adaptation.

3.2   Non-native Speakers

Two non-native speakers, a female and a male, were recruited to test the performance of the native SD ASR with the adaptation technique. Their background details are shown in Figure 5.

Name: GCV
Age: 28
Background: Computer Engineer

Name: SCB
Age: 35
Background: Business Manager

Fig. 5. Non-native speakers for evaluation of the native SD ASR system.

Prior to use the system, both received 6 hours of informative sessions which were distributed over three days. In these sessions, information about the pronunciation of the Mixtec words from the ASR system's vocabulary and the 7 narratives, which included the audios from the native speaker, were reviewed.
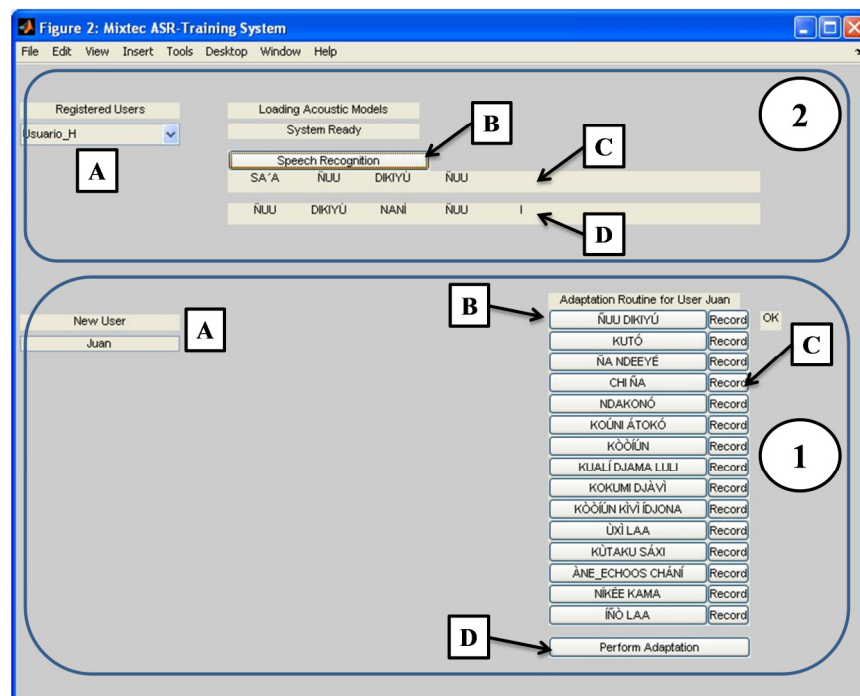
Fig. 6. Graphical User Interface for the native SD ASR-Training system.

3.3 Graphical User Interface

As shown in Figure 6, the native SD ASR system was integrated with a Graphical User Interface (GUI) for the adaptation and recognition tasks which were conducted as follows:

- **Adaptation (1).** As shown in Figure 6, there is a "New User" field (1A) where the user can write his/her name, for example, "Juan". When the user does this, the interface builds the respective directories and files to perform adaptation. On the right side there are buttons with the names of the adaptation words from Table 3 (1B), and with the label "Record" (1C). When the 1B buttons are pressed the audio file corresponding to that word (from the native speaker) is played, so the user can hear the correct pronunciation of that word before providing any speech sample for adaptation. When pressed the respective 1C button (the one next to that word) the interface records the user's pronunciation of that word. When the recording task is finished an "OK" is shown next to 1C. After all adaptation words are recorded the user can press the "Perform Adaptation" button (1D), which starts the MLLR adaptation with the audio samples from the user.

– **Recognition (2).** Once that the user got registered and performed adaptation, his/her data (i.e., MLLR transformations) is stored in directories identified by his/her name. After re-starting the interface, the new user's name is shown in the list of "Registered Users" (2A). At this point the user selects his/her name and the interface automatically loads the corresponding MLLR transformations and acoustic models, enabling the button "Speech Recognition" (2B) to perform ASR in real time when pressed. The user pronounces any phrase from the narratives (when pressing 2B) and the interface displays two outputs: in the field 2C the non-adapted response of the SD ASR is shown, while in 2D the MLLR adapted response is shown.

4   Performance of the Mixtec SD ASR-Training System

The measure of performance for the Mixtec ASR-Training system was the Word Recognition Accuracy (WAcc), which is analogous to the Word Error Rate (WER) [26]. For convenience we used both measures, which are defined as:

$$WAcc = (N-D-S-I)/N . \tag{1}$$

$$WER = 1 - WAcc . \tag{2}$$

where N is the total number of elements (words) in the reference (correct) transcription of the spoken words, D and I are the number of elements deleted and inserted in the decoded sequence of words (word output from the ASR system), and S the number of elements from the correct transcription substituted by a different word in the decoded sequence.

The Mixtec ASR was tested initially with the Training Corpus, and the performance results are shown in Table 4.

Table 4. Performance of the Mixtec ASR system when tested with the Training Corpus.

N	D	S	I	%WAcc	%WER
911	0	18	29	94.84	5.16

By replacing the word-bigram language model with a phoneme-based language model, a response at the phonetic level was obtained from the recognizer. A phoneme confusion-matrix, shown in Figure 7, was estimated from this response in order to identify patterns of errors at the low level of the baseline ASR.

As it can be observed, there were a few confusions between phonemes, for example: between vowels /á/, /à/, /a/, and /í/, /ì/, /i/; and a significant confusion between /nd/ and /d/. Analogous to Table 4, and as presented in Figure 7, the performance of the Mixtec ASR at the phonetic level is shown in Table 5.

As shown in Figure 7 and Table 5, the deletions and substitutions rates were approximately 10% of N (most of the deleted phonemes were vowels), while insertions represented approximately 5%. A %WAcc of 78% is normal based on the fact that there

was no restriction from the phonetic dictionary (Lexicon) to form valid sequences of phonemes (which lead to a %WAcc of 94.84%). These results show that the acoustic modeling of the tonal phonemes of the SD ASR system with the Training Corpus was performed satisfactorily. This is normal in most cases unless there were many variations or inconsistencies in the training speech.

Table 5. Performance of the phoneme-based Mixtec ASR system when tested with the Training Corpus.

N	D	S	I	%WAcc	%WER
3846	340	338	144	78.63	21.37
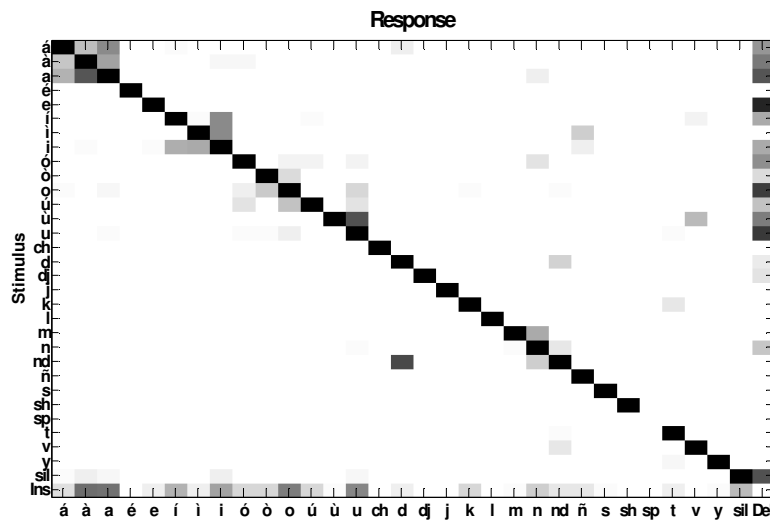
Fig. 7. Pattern of errors at the phonetic level of the Mixtec ASR system when tested with the Training Corpus.

The system was tested by the non-native speakers using three narratives (NTVs) with different levels of difficulty: 1 (easy level), 3 (medium level), and 6 (hard level). Each user was allowed to try up to 10 times the system in case that his/her uttered phrase wasn't recognized. If after those trials the phrase was not recognized, then the last result was recorded as the final response of the ASR system.

The performance results for the non-native speakers are shown in Table 6. The accuracy for the male user was -4.46% when no adaptation was performed. After the adaptation session, the performance increased to 92.57%. With the female user the non-adapted system performed with an accuracy of 9.90%, however after the adaptation session this increased to 88.12%.

Table 6. Performance of the Non-adapted and Adapted Mixtec ASR system
when tested by two non-native speakers.

User GCV							User SCB						
Non-adapted SD ASR-Training System							Non-adapted SD ASR-Training System						
NTV	N	D	S	I	%WAcc	%WER	NTV	N	D	S	I	%WAcc	%WER
1	53	4	32	13	7.55	92.45	1	53	8	30	7	15.09	84.91
3	53	2	32	20	-1.89	101.89	3	53	6	25	18	7.55	92.45
6	96	1	59	48	-12.50	112.50	6	96	4	66	18	8.33	91.67
Total	202	7	123	81	-4.46	104.46	Total	202	18	121	43	9.90	90.10
MLLR-adapted SD ASR-Training System							MLLR-adapted SD ASR-Training System						
NTV	N	D	S	I	%WAcc	%WER	NTV	N	D	S	I	%WAcc	%WER
1	53	0	1	0	98.11	1.89	1	53	0	2	0	96.23	3.77
3	53	0	3	2	90.57	9.43	3	53	0	5	3	84.91	15.09
6	96	0	8	1	90.63	9.38	6	96	0	10	4	85.42	14.58
Total	202	0	12	3	92.57	7.43	Total	202	0	17	7	88.12	11.88

While performing the testing sessions there were recorded the number of trials before the adapted system could recognize correctly the test phrase. For the male user (GCV), in 7 out of 49 phrases after the 10 trials the exact phrase was not obtained. A mean of 2.97 with a standard deviation of 3.17 was obtained for the number of trials before the recognizer could decode the correct phrase. In contrast, for the female user, in 17 phrases the correct phrase was not obtained after the 10 trials. This was reflected in a mean of 5.10 trials with a standard deviation of 4.08 for this user.

These differences in performances could be caused by the acoustic differences between the female's voice and the male's voice. Also, variations in the level of knowledge or ability to utter the Mixtec phonemes, which are user dependent, can be attributable factors. A matched pairs test [29] was used to test for statistical significant differences between both performances, obtaining a *p*-value of 0.21 (< 0.10) for the results presented in Table 6. Because of this, it was concluded that there was no statistical difference between both performances.

5   Conclusions and Future Work

In this paper we presented our advances towards the development of a Multi-user Mixtec ASR system for language learning purposes. The Mixtec language is a complex language given the diversity of tones and vocabulary, and so there are challenges to accomplish such system, especially with limited availability of native speakers for speech corpora. Nevertheless a native SD ASR system was developed for purposes of pronunciation training of a tonal language. This system, when integrated with a speaker adaptation technique, performed with levels of recognition accuracy of 92.57% (male user) and 88.12% (female user) for two non-native speakers, thus making it a multi-user system.

As presented in Table 6, MLLR is a very reliable adaptation technique when applied on a tonal SD ASR system, being able to accomplish with few speech samples (in this case, 26 words) improvements in recognition accuracy of around 90%. For non-native users, most of the word recognition errors were substitutions (12 for male user, 17 for female user) and insertions (3 and 7 respectively). As starting point, the results presented in this paper are encouraging, however we do realize that much more research is needed, and here we present our future work:

− Develop a technique to increase the performance of the native ASR system.
− Increase the Training Speech Corpus: add more vocabulary words and increase the complexity of the narratives; recruit more native speakers (both genders) in order to develop a native SI ASR system. Currently we are in talks to recruit three additional native speakers.
− Test the system with more users with different levels of expertise in the Mixtec language (group tests are being planned).
− Improve the GUI to increase usability: incorporate learning methodologies to extend the use of the ASR system for users that don't have previous knowledge of the language (with no informative sessions); integrate a measure of performance for the level of knowledge or practicing that the user gets by using the ASR system.

References

1. Philips: SpeechExec Pro Transcribe. http://www.dictation.philips.com/index.php?id=1440&CC=VV
2. Nuance: Dragon Speech Recognition Software. http://www.nuance.com/dragon/index.htm
3. IBM: Embedded ViaVoice.http://www-01.ibm.com/software/pervasive/embedded_viavoice/
4. Carnegie Mellon University (The Interactive Systems Laboratories): JANUS Speech Translation System. http://www.is.cs.cmu.edu/mie/janus.html
5. The German Research Center for Artificial Intelligence: Verbmobil - Translation of Spontaneous Speech. http://www.dfki.de/lt/project.php?id=Project_382&l=en
6. Green, P.D., Hawley, M.S., Enderby, P., Cunningham, S.P., Parker,M.: Automatic speech recognition and training for severely dysarthric users of assistive technology: The STARDUST project. Clinical Linguistics and Phonetics, 20:149–156 (2006)
7. Hawley, M., Cunningham, S., Cardinaux, F., Coy, A., O'Neill, P., Seghal, S., Enderby, P.: Challenges in developing a voice input voice output communication aid for people with severe dysarthria. In: Proc. European Conference for the Advancement of Assistive Technology in Europe (2007)
8. English Computerized Learning Inc.: Pronunciation Power Speech Test. http://www.englishlearning.com/products/pronunciation-power-speech-test/
9. Dalby, J., Kewley-Port, D.: Explicit Pronunciation Training Using Automatic Speech Recognition Technology. Computer-Assisted Language Instruction Consortium (CALICO) Journal, vol. 16 (1999)
10. Lesson Nine GmbH: Babbel. http://es.babbel.com/#Reconocimiento-de-voz

1. Rosetta Stone: Rosetta Stone Version 4 TOTALe. http://www.rosettastone.com/content/rosettastonecom/en.html
2. Cox, S., Lincoln, M., Tryggvason, J., Nakisa, M., Wells, M., Tutt, M., Abbott, S.: The Development and Evaluation of a Speech-to-Sign Translation System to Assist Transactions. Int. J. Hum. Comput. Interaction, 16(2):141–161 (2003)
3. Instituto Nacional de Estadística y Geografía (INEGI): Hablantes de Lengua Indígena en México. http://cuentame.inegi.org.mx/poblacion/lindigena.aspx?tema=P
4. Academia de la Lengua Mixteca: Bases para la Escritura de tu'un savi. Colección Diálogos: Pueblos Originarios de Oaxaca, México (2007)
5. Mindek, D.: Mixtecos: Pueblos Indígenas del México Contemporáneo. Comisión Nacional para el Desarrollo de los Pueblos Indígenas (2003)
6. Ferguson de Williams, J.: Gramática Popular del Mixteco del Municipio de Tezoatlán, San Andrés Yutatío, Oaxaca. Instituto Lingüístico de Verano, A.C. , México D.F. (2007)
7. Beaty de Farris, K., García, P., García, R., Ojeda, J., García, A., Santiago, A.: Diccionario Básico del Mixteco de Yosondúa, Oaxaca. Instituto Lingüístico de Verano, A.C., México, D.F. (2004)
8. Stark, S., Johnson, A., González de Guzmán, B.: Diccionario Básico del Mixteco de Xochapa, Guerrero. Instituto Lingüístico de Verano, A.C., México, D.F. (2003)
9. Instituto Lingüístico de Verano en México: Familia Mixteca. http://www.sil.org/mexico/mixteca/00e-mixteca.htm.
10. Instituto Nacional de Lenguas Indígenas: Catálogo de las Lenguas Indígenas Nacionales: Variantes Lingüísticas de México con sus autodenominaciones y referencias geoestadísticas. http://www.inali.gob.mx/pdf/CLIN_completo.pdf (2008)
11. Anderson, L. Alejandro, R.: Vocabulario de los verbos de movimiento y de carga: Mixteco de Alacatlatzala, Guerrero. Instituto Lingüístico de Verano, A.C. http://www.sil.org/americas/mexico/mixteca/alacatlatzala/P001-Vocab-MIM.pdf (1999)
12. García, A., Miguel, R.: Nadakua'a Ndo Tee Ndo Tu'un Ndo: Aprendamos a escribir nuestro idioma. Instituto Lingüístico de Verano, A.C., México, D.F. (1998)
13. Morales, M. North, J.: Ná Cahví Tuhun Ndáhv Ta Ná Cahyí Ña: Vamos a leer y escribir en mixteco (Mixteco de Silacayoapan, Oaxaca). Instituto Lingüístico de Verano, A.C., México, D.F. (2000).
14. Alexander, R.M.: Mixteco de Atatlahuca. Instituto Lingüístico de Verano. México, D.F. (1980)
15. Pineda, L.A., Castellanos, H., Cuétara, J., Galescu, L., Juárez, J., Llisterri, J., Pérez, P., Villaseñor, L.: The Corpus DIMEx100: Transcription and Evaluation. Language Resources and Evaluation. 44: 4, 347-370 (2010)
16. Young, S., Woodland, P.: The HTK Book (for HTK Version 3.4). Cambridge University Engineering Department, Great Britain (2006)
17. Rabiner, L.: A tutorial on hidden markov models and selected applications in speech recognition. Proc. of IEEE, 37, 257-286 (1989)
18. Jurafsky, D., Martin, J.H.: Speech and Language Processing. Pearson: Prentice Hall (2009)
19. Gillick, L., Cox, S.J.: Some statistical issues in the comparison of speech recognition algorithms. In Proc. IEEE Conf. on Acoustics, Speech and Signal Processing, 532-535 (1989)

Comparison of State-of-the-Art Methods
and Commercial Tools
for Multi-Document Text Summarization

Yulia Ledeneva[1], René García Hernández[1], Grigori Sidorov[2],
Griselda Mathias Mendoza[1], Selene Vargas Flores[1], and Abraham García Aguilar[1]

[1] Universidad Autónoma del Estado de México,
Unidad Académica Profesional Tianguistenco,
Paraje el Tejocote San Pedro Tlantizapan, 52600, Estado de México, Mexico
[2] Natural Language and Text Processing Laboratory,
Center for Computing Research (CIC),
National Polytechnic Institute (IPN),
Av. Juan Dios Batiz, s/n, Zacatenco, 07738,
Mexico City, Mexico
yledeneva@yahoo.com, renearnulfo@hotmail.com, www.g-sidorov.org

Abstract. The final goal of Automatic Text Summarization (ATS) is to obtain tools that produce the most human-similar summary. Almost all the papers on ATS research area present a review of the state-of-the-art of one side of the issue, since only is reviewed the-state-of-the-art of the tools reported in papers. However, we found a great number of developed commercial tools which are not reported in papers (which is understandable by competitive reasons), but also have not been evaluated. The question is what commercial tools are good in comparison to paper-published tools. This paper gives a survey for 18 commercial tools and state-of-the-art methods for multi-document summarization task testing on a standard collection of documents which contains 59 collections of documents.

Keywords: Automatic multi-document summarization, Copernic summarizer, Microsoft office word summarizer, Svhoong summarizer, pertinence summarizer, Tool4noobs summarizer.

1 Introduction

According to recent researches the volume of information on the public Web are estimated at 167 terabytes, while the deep web to be 400 to 450 times larger, thus between 66,800 and 91,850 terabytes [1]. Such amount of information cannot be revised by a normal human, only with the help of computer by means of intelligent algorithms and tools. Such types of algorithms and methods have a big necessity and urgency to be

developed, for example, automatic generation of text summaries for multi-document collection.

Humans tend to create summaries by generating and fusion of ideas, changing words and rephrasing long sentences. This manner of composing summaries is called abstractive summarization, contrary to the extracted summarization, where different text units (words, phrases, sentences, etc.) are extracted from the original collection of documents. The generation of extractive summaries does not require the understanding of the text.

Test summary is a short text transmitting the main ideas of the collections of documents without redundancy describing these ideas. In this paper, we take into account some important parameters to compare tools, which some of the tools permit to be changed depending of the resulted summary. These parameters are the size and format of the summary. The size of the summary depends on the user needs and can depend from the size of the original document. Therefore, the size of the summary must be the most flexible parameter. Another parameter is the format in which the summary is presented to the user, the most important key phrases or sentences can be highlighted within the summary or original document, without deleting the context in which such phrases occur. It is also desirable that the tools can work independently of domain and language of a given document, indeed it is not necessary that the original document is grammatically well written. We consider that to achieve a good summary, the tool should work mostly with text content and to a less degree with the document format. Also, a good tool to generate summaries should have a friendly interface. We consider that a good summary also must have coherence.

We consider two types of methods for generating multi-document summaries. There are commercial tools and the state-of-art methods. The differences are the prices for the commercial tools and lack of their description. For commercial tools, we consider two groups: installed and online tools (see the section 3).

Currently, there are commercial tools that automatically generate summaries compressing main ideas of a collection of documents. The first objective of the paper is to know which of the commercial tools produces summaries most similar to a human. The second objective is to compare the commercial tools to the state-of-the-art methods.

The paper is organized as follows. Section 2 summarizes the state-of-the-art of multi-document summarization methods. In Section 3, commercial tools are introduced. Section 4 presents the experimental settings and results. Sections 5 discuss obtained experimental results and give some conclusions of the paper.

2   State-of-the-Art Methods for Multi-Document Summarization

The following state-of-the-art methods are obtained promising results but not yet commercialized.

Maximal Frequent Sequences (MFSs):   This work presents a method to generate extractive summaries from a multi-document based on statistics, which is independent of

the domain and language. Ledeneva *et al.* [2, 3] experimentally shows that the words which are parts of bigrams (2-word sequences) which are repeated more than once in the text are good terms to describe the content of that text, so also called the maximal frequent sequences (sequences of words that are repeated a number of times and also are not contained in other frequent sequences). This work also shows that the frequency of the term as ranking of terms gives good results (while only count the occurrences of a term in repeated bigrams). Ledeneva *et al.* applies a method which has 4 stages for generating the summary. These steps are term selection, term weighting, sentence weighting and sentence selection. In term selection step, SFMs, repetitive bigrams (must appear at least twice in the text), and unigrams (simply words) are extracted. In term weighting step, the frequency of the term is used, which is the number of times the term occurs in the text. In sentence weighting, only the weight of all the terms contained in that sentence is calculated. Finally, sentence selection that composes the summary is performed by two criteria. First, the k sentences with bigger weight are selected. Second, k sentences with bigger weight are selected and completed with the first sentences (similar to baseline heuristic) that appear in the document (combined version). The best result is obtained with combined version when k=1, reaching 47% of similarity with the summaries made by a human.

MFS 1st method: In [4] are shown that MFSs are good descriptors if the lengths of the descriptors are considered, and words that derived from MFSs are good descriptors if the frequency is considered. For term selection option W, the term weighting option f showed best performance in all experiments.

MFS 2nd method: MFSs with higher threshold generate better summaries than MFSs with lower threshold [5]. It can be explained on reason that there exist in the language multiword expressions that can express the same content in the more compact way which can be detected more precisely using higher.

Then, we observed that, in contrast to MFSs, FSs is important if are extracted with lower threshold. It can be explained because there exist in the language a lot of single word or at least an abbreviation to express an important meaning.

Such single words or abbreviations should be considered as bearing the more important meaning with lower threshold because we need to extract more single words or abbreviations for knowing if they can be used for composing a summary.

The third hypotheses we explore in this work, is that MFSs represent in a better way the summarized content of collection of documents than FSs because their (MFSs) probability to bear important meaning is higher. It can happen because there are too many non-maximal FSs in comparison to MFSs.

MFSs using clustering sentence algorithms: In the previous method, sentences which have bigger weight are selected for composing the summary. However, if the sentences that are chosen in that order may include very similar sentences and do not provide new information in the summary. The work [6] uses a clustering algorithm based on MFSs to

make some groups of sentences, from which the most representative sentence from each group are selected to compose the summary.

TextRank graph based algorithm: Mihalcea [7, 8] constructs the graph to represent the text, so the nodes are words or other text sequences interconnected by vertices with meaningful relationships and the vertices are added to the graph for each sentence in the text. A relation of similarity is defined to establish the connections between sentences, where the relationship between two sentences can be seen as a process of "recommendation".

For the sentences extraction task, the goal is to qualify whole sentences and order them from most to least importance. A sentence that points to a certain concept in the text gives to the reader a "recommendation" to refer to other sentences in the text that point to the same concepts, and then a link can be established between any two sentences that share a common content. Since this method can determine the importance of each of the sentences, it was used to generate multi-documents summaries.

Baseline configuration: The baseline configuration consists of taken the first *n* sentences of the document to complete the summary to required size. This configuration supposes that the most important information of a collection of documents is in the first sections of the document. This simple heuristic has been shown to generate very good summaries in the field of news documents [9].

Baseline random configuration: This heuristic far from seeking to obtain best summaries attempts to determine the quality of the summaries when only a set of sentences are taken randomly as a summary. The idea is to determine if obtained results are significant comparing to other "intelligent" methods [3].

Best DUC systems: The best top 5 systems from 17 systems in DUC 2002 for multi-document summarization task are described in [9], see Figure 6 for more details.

3   Commercial Tools for Multi-Document Summarization

Currently, there are several commercial tools that help us in generating automatic summaries, among the most popular are the following tools. In this paper, the tools considered to analyze and compare are: Svhoong Summarizer, Pertinence Summarizer, Tool4noobs Summarizer, Copernic Summarizer, Microsoft Office Word Summarizer 2003 and Microsoft Office Word Summarizer 2007, and Microsoft Office Word Summarizer 7.

Svhoong Summarizer: This summarizer is available online. The text should be copied to the web page [11]. The final summary are the text underlined in the same page. The usage of this summarizer it is very tedious because the final summary should be saved sentence by sentence. It offers some options to generate summaries of different size, with the

following percentages 10, 20, 30, 40, 50, 60, 70, 80, 90 of the original text. In this work, the percentages were calculated and approximated according to available option of the tool. This step was made manually and took long time. It is available for 21 languages.

Pertinence Summarizer: This summarizer is available online [12]. With each document, Pertinence calculated percentages automatically depending on the number of word in the document. For example, 1% (34 words), 5% (171 words), 10% (342 words), etc. There are 3 forms to introduce text: copy to the web page, examine the document (this option was utilized in this work), or introduce the address of the web page. The tool does not have an option for 100 words, thus the percentage were automatically calculated for the given collection. It is available for 12 languages.

Tool4noobs Summarizer: This summarizer is available online [13]. It all integer percentages from 1 to 100 of the original text can be introduced. The original text should be copied to the web page. A least one sentence should be introduced. It permits to introduce 50 lines of text. The percentages were re-calculated, because the difference to 100 should be calculated.

This tool uses three steps to generate summaries: extraction of text; identification of the key-words in the text and its relevance; identification of sentences with key-words and generation of summary.

Copernic Summarizer. This software was developed exclusively for the generation of automatic summaries. It is a flexible and suitable tool. In this paper, we use version 2.1 which was installed on the Microsoft Windows operating system. It offers different options to generate summaries from multiples documents:

–   5%, 10%, 25% and 50% of words of the original collection of documents;
–   100, 250 and 1000 words.

According to [10], Copernic Summarizer uses the following methods:

1. Statistical model (S-Model). This model is used in order to find the vocabulary of the text.
2. Knowledge Intensive Processes (K-Process). Consider the way in which human make summary texts by taking into account the following steps:
3. Language detection. It detects the language (English, German, French or Spanish) of the document for applying specific processes.
4. The limits of sentence recognition.
5. Concept extraction. Copernic Summarizer uses machine learning techniques to extract keywords.
6. Document Segmentation. Copernic Summarizer organizes the information that it can be divided into larger related segments.
7. Sentence Selection. Sentences are selected according to their importance (weight) discarding those that decrease readability and coherence.

Table 1. Parameters of Commercial Tools.

Tool	Language	Price	Characteristic
Copernic Summarizer	Franch, English, Dutch, Spanish	$59 US	Installed
Microsoft Word 2003	Multilingual	$830.78	Installed
Microsoft Word 2007	Multilingual	$1400.00	Installed
OTS	Multilingual	Free software	Installed
Pertinence	Multilingual	Free software	Online
Tool4noobs	Multilingual	Free software	Online
Shvoong	Multilingual	Free software	Online

Microsoft Office Word Summarizer. This tool can be found in versions of Microsoft Office Word 2003 and Microsoft Office Word 2007. This tool can generate summaries of 10 or 20 sentences, 100 or 500 words (or less) or in percentages of 10%, 25%, 50% and 75% of words of the original document. If some of the percentages are not appropriate, the user can change as needed. This tool offers various ways of visualizing summaries. One is highlighting the color of important sentences in the original document.

The summary created by this tool is the result of an analysis of key words; the selection of these is done by assigning a score to each word. The most frequent words in the document will have highest scores which will be considered as important. The sentences containing these words will be included in the summary.

4   Experimental Results

For comparing the above mentioned applications the collection Document Understanding Conference (DUC) 2002 [9] was used, which was created by the National Institute of Standards and Technology (NIST) for the usage by researchers in the area of automatic text summarization. This collection has the data set of 60 document collections which consist of 567 news articles of different length about technology, food, politics, finance, etc. For each document in the collection was created two summaries by two human experts with a minimum length of 100 words.

ROUGE 1.5.5 evaluation toolkit, proposed by Lin [14, 15], is the tool used for the automatic comparison of summaries. In particular, we use n-gram statistics (where $n = 1$), which has the ability to measure similarity and determine the quality of an automatic summary compared to the both summaries created by a human. We use this tool, to compare quality of the generated summaries by commercial tools and the state-of-the-state methods.

4.1 Configuration of Experiments

Commercial tools were evaluated in the operating system Windows XP Professional Service Pack 2 (SP2). Each file was manually selected and applied to generated summary of 100 words. In the case of Microsoft Office Word 2003, 2007 and version 7 is not possible to use the option of 100 word summaries because sometimes produces summaries less than 100 word, which decrease the quality of summaries. For such problem was necessary to calculate the adequate percentage to produce a summary with minimum 100 words, calculated as follows: $(Number\_of\_diserable\_wrods / Number\_of\_total\_words)*100$.

4.2 Quality of Online Commercial Tools

The evaluation results of commercial tools are realized using ROUGE. The best obtained result was for online commercial tools Shvoong Summarizer.

4.3 Quality of Installed Commercial Tools (case Microsoft Office Word)
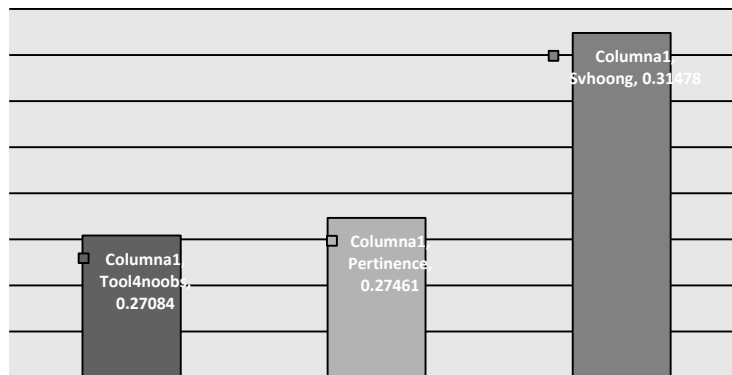
Figure 1. The evaluation results of online commercial tools testing using the operating system Windows XP, Vista,and 7.

Microsoft Office Word 2007 using the operating system Windows XP was the best obtained result than using the operating system Windows Vista or Windows 7 (see Figure 2). Microsoft Office Word 2007 using the operating system Windows 7 obtained less result than using Microsoft Word 2003 using different operating systems (see Figure 2).
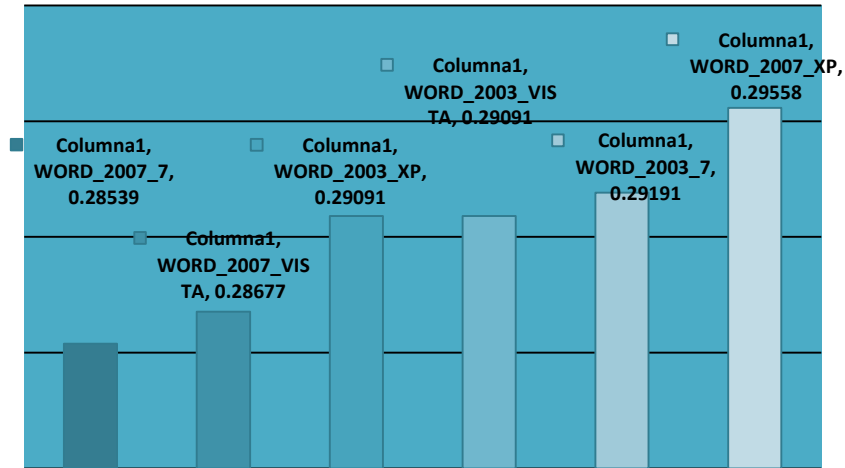
Figure 2. The evaluation results of different versions of installed commercial tool Microsoft Office Word tesitng in the operating system Windows XP, Vista, and 7.
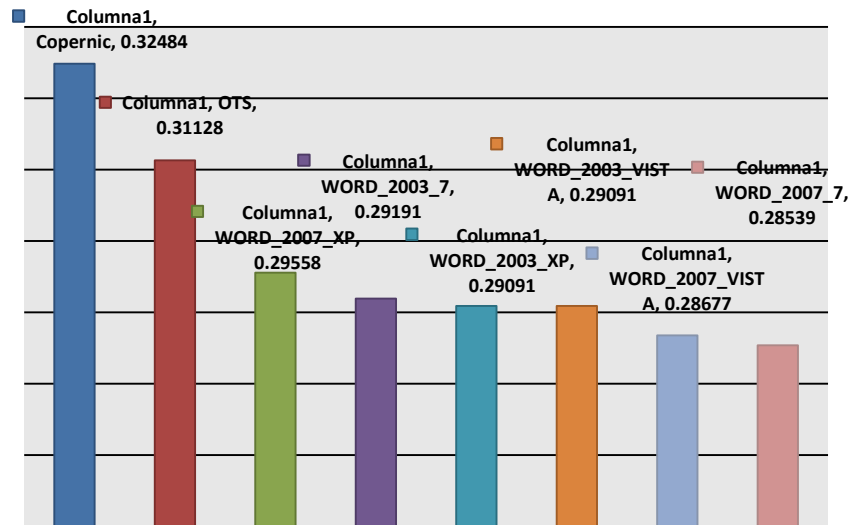
Figure 3. The evaluation results of all installed commercial tools testing using the operating system Windows XP, Vista, and 7.
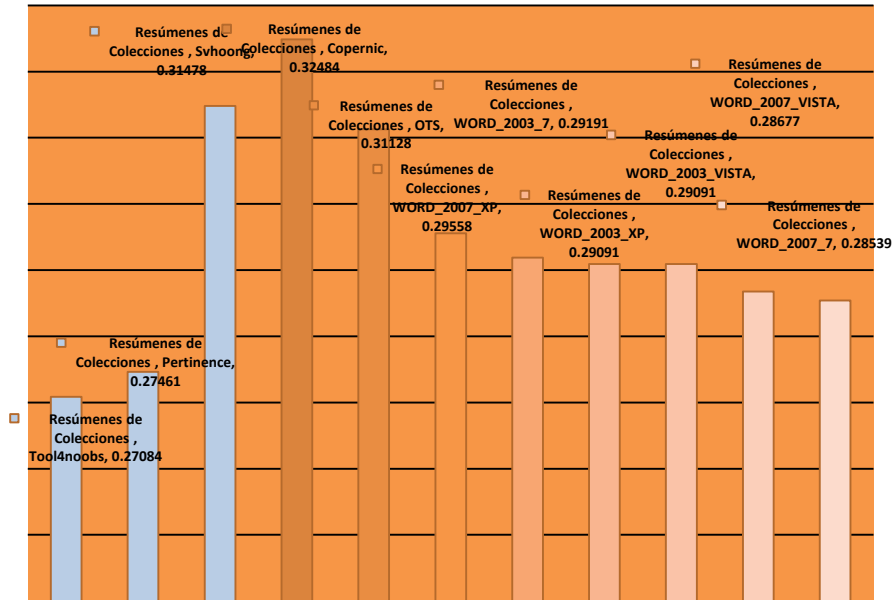
Figure 4. The evaluation results of all installed and online commercial tools testing using the operating system Windows XP, Vista, and 7.

4.4 Quality of all commercial tools

Copernic Summarizer obtained the best results of all installed commercial tools (see Figure 3).

Microsoft Office Word 2007 y Microsoft Office Word 2003 obtained less quality then online tools Copernic, OTS y a Shvoong. The installed commercial tools are marked with orange color (see Figure 4).

4.5 Quality of Commercial Tools and State-of-the-Art Methods

In order to see the quality of previous results compared to those obtained with the state-of-the-art methods, in Figure 5 are shown the best results obtained by commercial tools and the results reported by the state-of-the-art methods.

Figure 5 shows clearly that the results of Copernic Summarizer is the highest score, just below the proposed method MFSs (1Best+First) and below of Sentence Clustering with MFSs, which confirms this software is one of the best of its kind.
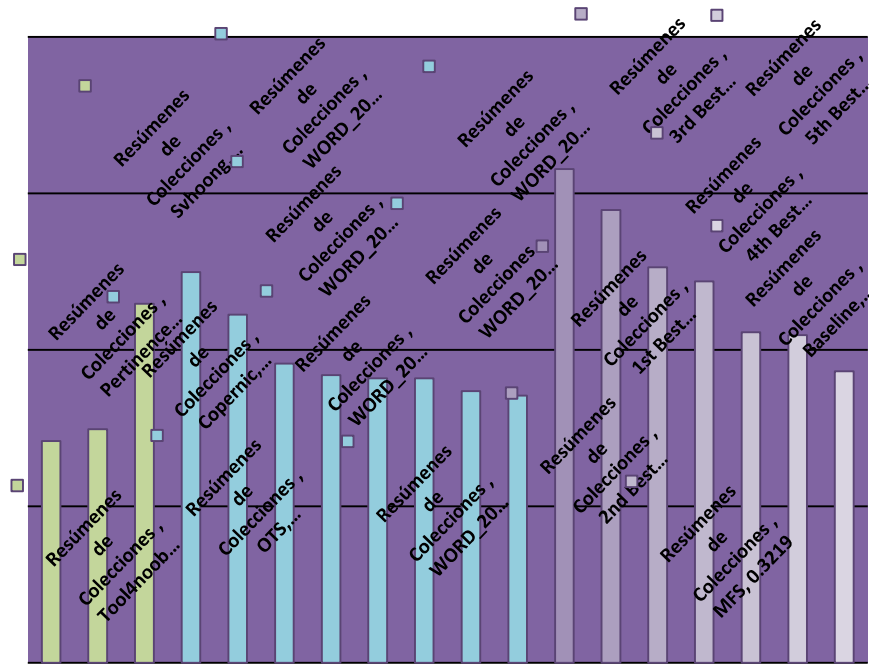
Figure 5. Results for the collection of documents obtained for commercial tools and the state-of-the-art methods.

Table 2. The results of Commercial Tools are ordered by the quality of Text Summaries.

Commercial Tools	F-measure	Characteristic
Copernic	0.32484	Installed
Svhoong	0.31478	Online
OTS	0.31128	Installed
WORD_2007_XP	0.29558	Installed
WORD_2003_7	0.29191	Installed
WORD_2003_XP	0.29091	Installed
WORD_2003_VISTA	0.29091	Installed
WORD_2007_VISTA	0.28677	Installed
WORD_2007_7	0.28539	Installed
Pertinence	0.27461	Online
Tool4noobs	0.27084	Online

According to Figure 1 Copernic Summarizer outperforms the two versions of Microsoft OfficeWord, although Microsoft Office Word 2003 was slightly better than its 2007 version. However, during the experimentation an inconsistency in Microsoft Office Word was observed because the generated summaries change depending on the operating system. In order to verify this fact the same setup package of Microsoft Office Word 2003 was installed on Windows XP Professional SP2, which also was done with Microsoft Office Word 2007. The resulting abstracts were assessed with the same version of ROUGE and obtained the results shown in Figure 2.

In Figure 2, we can observe the slight difference between the tools of auto summary of Microsoft Office Word. In contrast, Copernic Summarizer tool show the same results in both operating systems. We can conclude that Copernic Summarizer is independent of the operating system).

Table 3. The results of the State-of-the-Art Methods (SAMs) and Commercial Tools are ordered by the quality of Text Summaries.

Commercial Tools and State-of-the-Art Methods	F-measure	*Characteristic*
1st Best Method	0.3578	*SAMs*
2nd Best Method	0.3447	*SAMs*
3rd Best Method	0.3264	*SAMs*
Copernic	0.32484	*Installed*
MFS	0.3219	*SAMs*
Svhoong	0.31478	*Online*
OTS	0.31128	*Installed*
4th Best Method	0.3056	*SAMs*
5th Best Method	0.3047	*SAMs*
WORD_2007_XP	0.29558	*Installed*
Baseline	0.2932	*SAMs*
WORD_2003_7	0.29191	*Installed*
WORD_2003_XP	0.29091	*Installed*
WORD_2003_VISTA	0.29091	*Installed*
WORD_2007_VISTA	0.28677	*Installed*
WORD_2007_7	0.28539	*Installed*
Pertinence	0.27461	*Online*
Tool4noobs	0.27084	*Online*

Also, it is important to mention that Microsoft Office Word 2007 with Windows XP Professional SP2 obtained the worst result, among the versions of Microsoft Office Word.

Nevertheless, the best result, among the versions of Microsoft Office Word, was obtained with Microsoft Word 2003 with Windows Vista Home Premium SP1. This shows the dependence of these tools with respect to the operating system they are using.

5   Discussion and Conclusions

Only four commercial tools are better than baseline configuration: Svhoong, Copernic, OTS, WORD_2007_XP. Other six evaluated commercial tools are worst than the baseline configuration. All the state-of-the-art methods overcome the baseline configuration and quality of the commercial tools (see Figure 6).
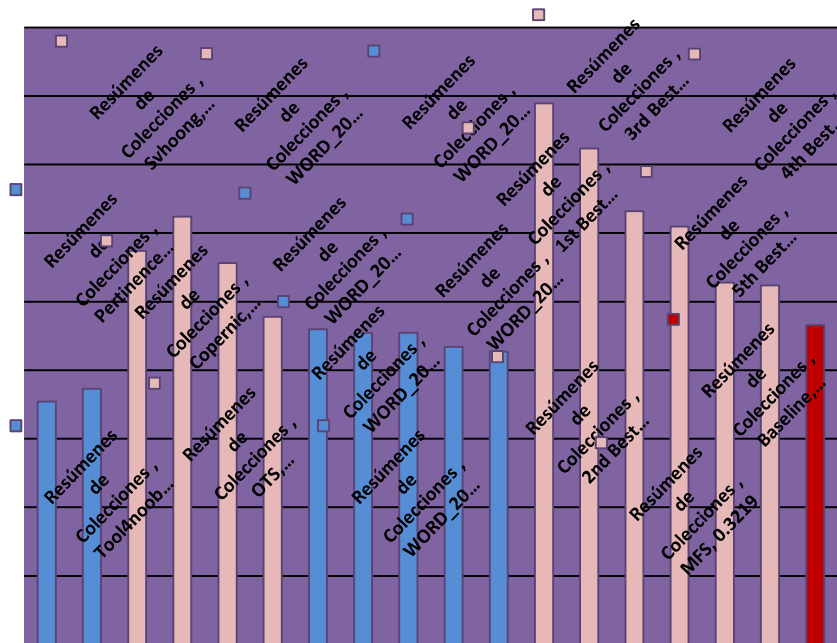
Figure 6. Results for the collection of documents obtained for commercial tools and the state-of-the-art methods.

In this paper, the evaluation of the automatic summaries generated by commercial tools (Copernic Summarizer, Microsoft Office Word Summarizer 2003 and Microsoft Office Word Summarizer 2007) was realized. The summaries were evaluated using the ROUGE system. The following conclusions can be given based on obtained results:

– 18 different automatic multi-document summarization state-of-the art methods and commercial tools were compared

– In most cases, the state-of-the-art methods are better that commercial tools
– Copernic Summarizer gets the best results of commercial tools.
– Copernic Summarizer is the best commercial tool
– Shvoong is the best online tool
– Microsoft Office Word is inconsistent because it generates different summaries depending on the operating system.
– The results obtained with Microsoft Office Word 2003 and Microsoft Office Word 2007 with Windows Vista were better than with Windows XP.
– Microsoft Office Word 2003 gets a better result than Microsoft Office Word 2007 with Windows Vista operating system.

We consider that computer methods can perform better and quicker than human the task of multi-document text summarization, in particular, reducing the contents of a big collection of documents to a single short text, so that the user can judge about the contents of the whole collection upon reading only this short text. However, it is still a challenge for computer methods to improve the quality for multi-document text summarization and even bigger challenge coherence. Good news is that the state-of the-art methods perform better than commercial tools.

References

1. Lyman, Peter and Hal R. Varian. How Much Information. Retrieved from http://www.sims.berkeley.edu/how-much-info-2003 (2003)
2. Yulia Ledeneva, Alexander Gelbukh, René A. García-Hernández. Terms Derived from Frequent Sequences for Extractive Text Summarization, 9th Conference on Intelligent Text Processing and Computational Linguistics (CICLing 2008), Lecture Notes in Computer Science, Springer-Verlag, Vol. 4919. pp. 593-604 (2008)
3. Yulia Ledeneva. Automatic Language-Independent Detection of Multiword Descriptions for Text Summarization, National Polytechnic Institute, PhD. Thesis, Mexico (2009)
4. Yulia Ledeneva, René García Hernández, Alexander Gelbukh. Multi-document Summarization using Maximal Frequent Sequences. Research in Computer Science, pp.15-24, vol. 47, ISSN 1870-4069 (2010)
5. Yulia Ledeneva, René García Hernández, Anabel Vazquez Ferreyra, Nayely Osorio de Jesus. Experimenting with Maximal Frequent Sequences for Multi-Document Summarization. Research in Computing Science, pp.233-244, vol. 45, ISSN 1870-4069 (2010)
6. René Arnulfo García-Hernández, Romyna Montiel, Yulia Ledeneva, Eréndira Rendón, Alexander Gelbukh, Rafael Cruz. Text Summarization by Sentence Extraction Using Unsupervised Learning, 7th Mexican International Conference on Artificial Intelligence

(MICAI08), Lecture Notes in Artificial Intelligence, Springer-Verlag, Vol. 5317 pp. 133-143 (2008)

7. Rada Mihalcea; Graph-based Ranking Algorithms for Sentence Extraction, Applied to Text Summarization; Department of Computer Science; University of North Texas; Texas; EUA (2004)

8. Rada Mihalcea, Paul Tarau. A language independent algorithm for single and multiple document summarization. In Proceedings of IJCNLP'2005 (2005)

9. DUC. Document Understanding Conference, www-nlpir.nist.gov/projects/duc.

10. Copernic Summarizer, Technologies White Paper (2003)
    http://www.copernic.com/data/pdf/summarization-whitepaper-eng.pdf

11. Online Tool Noobs Summarizer. http://www.tools4noobs.com/summarize/

12. Pertinence Summarizer. http://www.pertinence.net/index_en.html

13. Shvoong Summarizer. http://www.shvoong.com/summarizer/

14. Lin, C., y E. Hovy: Automatic evaluation of summaries using N-gram co-occurrence statistics. Proceedings of the 2003 Conference of the North American Chapter of the Association for Computational Linguistics on Human Language Technology. Vol. 1, pp. 71-78 (2003)

15. Lin, C.: ROUGE: A package for automatic evaluation of summaries. Proceedings of the Association for Computational Linguistics 2004 Workshop, pp. 74-81. Spain (2004)

16. Garcia, R., F. Martinez, A. Carrasco, Finding maximal sequential patterns in text document collections and single documents, Informatica, International Journal of Computing and Informatics, ISSN: 1854-3871, No. 34, pp. 93-101 (2010)

17. Sidorov, G. Lemmatization in automatized system for compilation of personal style dictionaries of literary writers. In: "Word of Dostoyevsky", Russian Academy of Sciences, pp. 266-300 (1996)

18. Gelbukh, A. and Sidorov, G. Approach to construction of automatic morphological analysis systems for inflective languages with little effort. Lecture Notes in Computer Science, N 2588, Springer-Verlag, pp. 215–220 (2003)

19. Sidorov, G., Barrón-Cedeño, A., and Rosso, P. English-Spanish Large Statistical Dictionary of Inflectional Forms. In: Proceedings of the Seventh International Conference on Language Resources and Evaluation (LREC'10), Valletta, Malta. European Language Resources Association (ELRA), pp. 277-281 (2010)

20. Esaú Villatoro-Tello, Luis Villaseñor-Pineda, Manuel Montes-y-Gómez, and David Pinto-Avendaño. Multi-Document Summarization Based on Locally Relevant Sentences. Mexican International Conference on Artificial Intelligence MICAI 2009. Guanajuato, Mexico, November 09-13, pp. 87-91, IEEE Computer Society (2009)

Evolutionary Algorithms and Process Optimization

The Application of the Genetic Algorithm based on Abstract Data Type (GAADT) Model for the Adaptation of Scenarios of MMORPGs

Leonardo F. B. S. Carvalho, Helio C. Silva Neto,
Roberta V. V. Lopes, and Fábio Paraguaçu

Federal University of Alagoas (UFAL - *Universidade Federal de Alagoas*),
Institute of Computing (IC - *Instituto de Computação*),
Campus A. C. Simões, 57072-970 Maceió, Alagoas, Brazil
{lfilipebsc,helio.hx,fabioparagua2000}@gmail.com,
rv2l@hotmail.com

Abstract. The importance of using Artificial Intelligence in video games has grow in response to a need in showing behaviors and other game elements in a closer accuracy to what is seen at the real world. In order to assist this need, this paper takes advantage of the context of MMORPGs (game worlds with rich and interactive environments where important events occur simultaneously) to demonstrate the application of the artificial intelligence technique of the Genetic Algorithm based on Abstract Data Type (GAADT) in changing the features of game maps of MMORPGs due to the passage of time, in an attempt to reproduce what is seen in the real world.

Keywords: Artificial Intelligence, genetic algorithms, GAADT, games, MMORPG.

1 Introduction

The Genetic Algorithms (GA) [6] are Artificial Intelligence (AI) algorithms that employ the evolutionary principle of the survival of the fittest to solve algorithmic problems using an heuristic search based on metaphors combining principles of search algorithms and biology.

In videogames, GAs are often used when the implementation of AI involves must deal with problems that have many possible outcomes or lots of variables that ought to be accounted to achieve proper results [4]. In this respect, this paper presents an instantiation of a GA known as GAADT (Genetic Algorithm based on Abstract Data Type) to solve a problem that fits both these characteristics, which is: "to change the features of pre-existing MMORPG (Massively Online Role-Playing Game) game maps in order to create new maps".

The problem above has a great level of abstraction. Thus, it must be stated that the aim of this research is not to create new maps from scratch. In fact, the instance of GAADT that will be presented by this paper uses existing game

maps as input and manipulates them to create new maps. Game maps may house various types of objects; however, only the type capable of representing the different geographical images that make up its scenario (known as tile) will be referred here.

After a game map is given as input to GAADT, the algorithm will start to create game maps that have some geographical features that are different from the ones of the input map, meaning that they have one or more group of cells whose tiles do not match the ones that are found in the input map for those specific locations. These differences occur in respect to the beginning of a season (spring, summer, autumn or winter) and to the unique geography originally depicted by each cell. However, it is not mandatory for a game map or its regions to have four properly defined seasons. Moreover, it is also unlikely that the transitional period from one season to another will ever repeat itself, which is a response to the fact that the values defining the extent of a season, its rainfall and even the time taken for switch between seasons are randomly chosen for each execution of GAADT.

The use of GAADT to change the topology/geographical features of scenarios of game maps - which was first shown in [3] - contrasts with other algorithms employed for this purpose due the fact that GAADT is an AI algorithm, while other identified approaches have a common link to computer graphics. Some of these approaches are listed in Table 1.

Paper	Technique	Limitations
[1]	Visualizations of dynamic terrains using a multiresolution algorithm with structural changes.	The algorithm is restrict to create a single kind of alteration in the game map (craters).
[7]	Multiresolution algorithm coupled with real-time optimally adapting meshes [5].	The model seems to apply only to real-time car driving in game maps simulating an off-road type of environment.
[10]	Use of multiresolution meshes to represent geometric objects. Each set of meshes corresponds to a different representation of a same object.	Unfit to systems requiring online updates.

Table 1: Different approaches for changing the geography of game maps

Now, this paper will be divided into different sections that better clarify the use of GAADT as solution to the problem of changing the geographical features of a game map. Following this section, Sec. 2 will detail the concepts of the adopted game maps. Next, Sec. 3 will present the concepts of GAADT and the instantiation used here. Last, Sec. 4 will show the results and conclusions drawn from this research.

2   Map Concepts

The game maps of this paper were created using an open-source third-part application known as Tiled [8]. Additional modules were created for this application in order to accomplish the objectives of the research. The relevant game map concepts are depicted in Figure 1 and described next.

- **Map**: a game world scenario consisting of a set of rectangular overlapping grids (known as layers) that have identical width (w_{map}) and height (h_{map}) values and are so that $\{w_{map}, h_{map} \in \mathbb{N} | (w_{map} > 0) \wedge (h_{map} > 0)\}$.
- **Layer**: a map grid that houses elements for building the map. A layer is located at a specific depth that is inferior to the l_{map} amount of layers of the map, hence $\{l_{map} \in \mathbb{N} | l_{map} > 0\}$. The width ($w_{map}$) and height ($h_{map}$) values of a layer indicates the number of cells it has in that direction. Each cell has the same width (w_{cel}) and height (h_{cel}) that are given as $\{w_{cel}, h_{cel} \in \mathbb{N} | (0 < w_{cel} \leq w_{map}) \wedge (0 < h_{cel} \leq h_{map})\}$. Thus, the game map is a cube whose elements are placed regarding their distance (x and y axis) and depth (z axis) from the map origin at $[0, 0, 0]$.
- **Tile**: a map object that occupies a single layer cell and has an image assigned to it that represents a geographical element. A tile has w_{cel} width and a h_{tl} height so that $\{h_{tl} \in \mathbb{N} | (h_{tl} = j \times h_{cel}) \wedge (1 \leq j < h_{map})\}$.
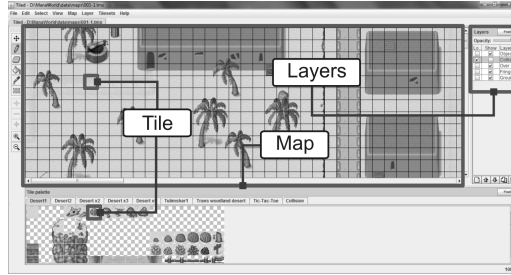

Fig. 1: Visual illustration of the game map concepts

3   GAADT's Instantiation to the Problem

As a detailed presentation of GAADT would be too long for the scope of this paper, this section will instead present the concepts of GAADT while simultaneously demonstrating its instantiation to the intended problem of the paper. Additional details of GAADT are available in [9].

3.1   Basic Types

Def. 1. Basis: the elementary genetic unit of chromosomes. Here, a basis is a $b = (x, y, z, tl, tp, in, fl)$ element that corresponds to a map cell at the x, y, z location that has the tl tile assigned to it, which is additionally identified by the tp description of its type of geography, by the unique index in of this description and by the fl flag that indicates if the tile of this cell requires a collision.

The bases of GAADT are part of a B set that is defined here according to a $DC = \{(x, y, z, tl, tp, in, fl) | (0 \leq x < w_{map}) \wedge (0 \leq y < h_{map}) \wedge (0 \leq z < \tilde{l}_{map}) \wedge (tl \in Tile) \wedge (in \in \mathbb{N}) \wedge (fl \in Boolean)\}$ set that has the $\tilde{l}_{map}$ value of the domain of the z coordinate as the amount of map layers intended exclusively for the allocation of tiles. The $Tile$ set of DC defines the domain of the tl tile objects and is so that $Tile = \{(w_{cel}, h_{tl}, gId, Img) | (Img \in Image) \wedge ((w_{cel}, h_{tl}, gId) \in \mathbb{N})\}$. The gId value is the unique index that identifies a tile.

Hence, the set of bases for this instance of GAADT is $B = DC \cup B_\lambda$. The B_λ set accords to GAADT's assumption that exists a b_λ innocuous basis whose data does not influence the identity of the gene that contains it. In turn, as this paper assumes that bases at different x, y, z coordinates are in fact different bases, the algorithm requires a $B_\lambda = \{b = (x, y, z, tl, tp, in, fl) | (tp = tp_\lambda)\}$ set of innocuous bases, whose elements have the same tp value that marks them as cell with no information.

The bases are arranged in groups in order to create genes. Each gene is a particular characteristic and thus, requires that its bases are connected in some way. For this reason, the creation of genes accords to a set of "formation rules" called Axioms for Formation of Genes (AFG).

Def. 2. Gene: a $g = \langle b_1, \ldots, b_n \rangle$ "micro region" of the game map that meets the requirements of the AFG set of rules.

$$AFG_1 = \{ \ \forall g = \langle b_1, \ldots, b_n \rangle \in G \ \forall (b_\alpha = (x_\alpha, y_\alpha, z_\alpha, tl_\alpha, tp_\alpha, in_\alpha, fl_\alpha), \\ b_\beta = (x_\beta, y_\beta, z_\beta, tl_\beta, tp_\beta, in_\beta, fl_\beta)) \in \{b_1, \ldots, b_n\} \,|\, z_\alpha = z_\beta\} \quad (1)$$

$$AFG_2 = \{ \ \forall g = \langle b_1, \ldots, b_n \rangle \in G \ \forall (b_\alpha = (x_\alpha, y_\alpha, z_\alpha, tl_\alpha, tp_\alpha, in_\alpha, fl_\alpha), \\ b_\beta = (x_\beta, y_\beta, z_\beta, tl_\beta, tp_\beta, in_\beta, fl_\beta)) \in \{b_1, \ldots, b_n\} \,| \\ (tp_\alpha = tp_\beta) \wedge (in_\alpha = in_\beta)\} \quad (2)$$

$$AFG_3 = \{ \ \forall g = \langle b_1, \ldots, b_n \rangle \in G \\ \exists_1 (b_{x+} = (x_{x+}, y_{x+}, z_{x+}, tl_{x+}, tp_{x+}, in_{x+}, fl_{x+}), \\ b_{x-} = (x_{x-}, y_{x-}, z_{x-}, tl_{x-}, tp_{x-}, in_{x-}, fl_{x-})) \in \{b_1, \ldots, b_n\} \\ \forall b = (x, y, z, tl, tp, in, fl) \in \{b_1, \ldots, b_n\} \,|\, ((x \leq x_{x+}) \wedge \\ (x_{x-} \leq x)) \wedge (0 < (x_{x+} - x_{x-} + 1) < (2 \times w_{mapa}/3))\} \quad (3)$$

$$AFG_4 = \{ \ \forall g = \langle b_1, \ldots, b_n \rangle \in G$$
$$\exists_1 \left(b_{y^+} = (x_{y^+}, y_{y^+}, z_{y^+}, tl_{y^+}, tp_{y^+}, in_{y^+}, fl_{y^+}), \right.$$
$$b_{y^-} = (x_{y^-}, y_{y^-}, z_{y^-}, tl_{y^-}, tp_{y^-}, in_{y^-}, fl_{y^-})) \in \{b_1, \ldots, b_n\} \qquad (4)$$
$$\forall b = (x, y, z, tl, tp, in, fl) \in \{b_1, \ldots, b_n\} \,|\, \left((y \leq y_{y^+}) \wedge \right.$$
$$(y_{y^-} \leq y)) \wedge (0 < (y_{y^+} - y_{y^-} + 1) < (2 \times h_{mapa}/3)) \}$$

The genes are arranged in groups in order to create chromosomes. Thus, each chromosome is an aggregation of characteristics and is a unique element that does not repeat itself within any present or future population of GAADT. The creation of chromosomes obeys its own set of "formation rules" known as Axioms for Formation of Chromosomes (AFC) that validates their sequences of genes. Figure 2 shows some examples of bases, genes and chromosomes that were obtained according to the defined B set and the stated AFG and AFC rules.

Def. 3. Chromosome: a $c = \{g_1, \ldots, g_n\}$ "macro region" of the game map that obeys the AFC set of rules.

$$AFC_1 = \{ \ \forall \, c = \{g_1, g_2, \ldots, g_m\} \in C$$
$$\forall \left(g_\alpha = \langle b_1^\alpha, \ldots, b_{n_1}^\alpha \rangle, g_\beta = \langle b_1^\beta, \ldots, b_{n_2}^\beta \rangle \right) \in \{g_1, g_2, \ldots, g_m\}$$
$$\forall b_i = (x_i, y_i, z_i, tl_i, tp_i, in_i, fl_i) \in \{b_1^\alpha, \ldots, b_{n_1}^\alpha\} \qquad (5)$$
$$\forall b_j = (x_j, y_j, z_j, tl_j, tp_j, in_j, fl_j) \in \{b_1^\beta, \ldots, b_{n_2}^\beta\} \,|$$
$$(x_i \neq x_j) \vee (y_i \neq y_j) \vee (z_i \neq z_j) \}$$

$$AFC_2 = \{ \ \forall c = \{g_1, g_2, \ldots, g_m\} \in C \ \forall (g = \langle b_1, \ldots, b_n \rangle) \in \{g_1, g_2, \ldots,$$
$$g_m\} \ \exists b = (x, y, z, tl, tp, in, fl) \in \{b_1, \ldots, b_n\} \,|\, z = 0 \} \qquad (6)$$

$$AFC_3 = \{ \ \forall \, c = \{g_1, g_2, \ldots, g_m\} \in C \ \forall \left(g_\alpha = \langle b_1^\alpha, \ldots, b_{n_1}^\alpha \rangle, \right.$$
$$g_\beta = \langle b_1^\beta, \ldots, b_{n_2}^\beta \rangle \right) \in \{g_1, g_2, \ldots, g_m\} \ \forall b_i = (x_i, y_i, z_i, tl_i,$$
$$tp_i, in_i, fl_i) \in \{b_1^\alpha, \ldots, b_{n_1}^\alpha\} \ \forall b_j = (x_j, y_j, z_j, tl_j, tp_j, in_j, fl_j)$$
$$\in \{b_1^\beta, \ldots, b_{n_2}^\beta\} \,|\, (z_i \geq z_j) \wedge (\forall z \in \{0, 1, \ldots, z_i\} \qquad (7)$$
$$\exists \left(g_\gamma = \langle b_1^\gamma, \ldots, b_{n_\gamma}^\gamma \rangle \right) \in (\{g_1, g_2, \ldots, g_m\} - \{g_\beta\})) \wedge$$
$$(\forall b = (x_b, y_b, z_b, tl_b, tp_b, in_b, fl_b) \in \{b_1^\gamma, \ldots, b_{n_\gamma}^\gamma\} (z_b = z)) \}$$

GAADT performs its operations according to cycle of evolutionary and stagnant periods that assumes that environmental changes mark the beginning of new evolutionary periods and arranges its chromosomes in groups known as populations. Every chromosome is a potential result for the problem that the algorithm is aiming to solve and, as a consequence, it assumes that the creation of an empty population reflects an incorrect assumption of the problem, as it would mean that the intended problem does not have a solution.

(a) Chromosome

(b) Gene at the $z = 0$ layer and its x, y locations

(c) Genes at the $z = 1$ layer and their x, y locations

(d) Gene at the $z = 2$ layer and its x, y locations

(e) Gene at the $z = 3$ layer and its x, y locations

(f) A chromosome of a single gene (at $z = 0$) and a single basis
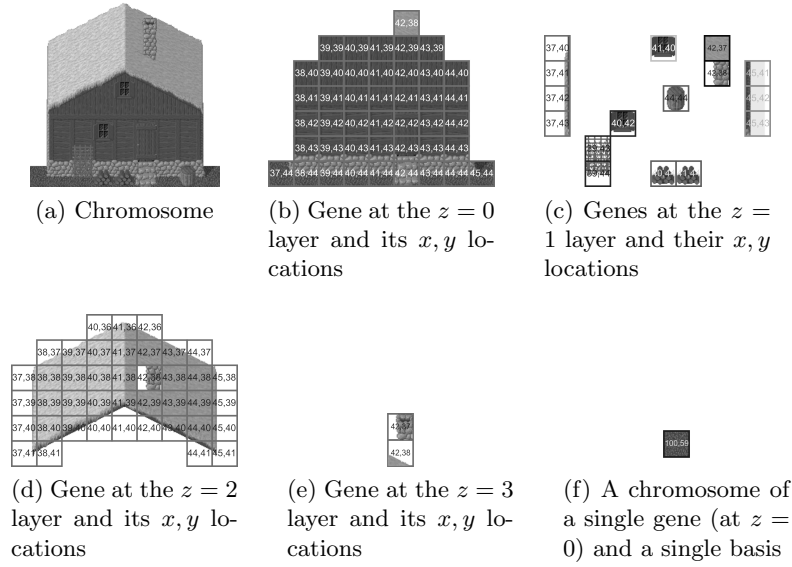
Fig. 2: Example of chromosomes with their genes along the x, y and z axes and with the bases standing as the genes' individual cells

Each loop of the cycle is known as a generation and spawns new chromosomes to GAADT's current population at the same time that removes from it the chromosomes it considers "unfit". In time, GAADT will start to converge and create populations that are increasingly similar to the one of the previous generation, until they become indistinguishable. This indicates that GAADT has reached a stagnant period, which will come to an end whenever a new environmental change occurs, forcing the evolutionary-stagnant process to repeat itself.

3.2 Genetic Operators

The genetic operators are responsible for creating new chromosomes for GAADT's populations. There are two operators that perform this task: the reproduction operator and the mutation operator.

The reproduction operator used here is a crossover operation that combines genes of two different chromosomes (parent-chromosomes) in order to create new chromosomes (child-chromosomes), while the mutation operator receives an input chromosome and switch some of its genes by new ones, thus, creating new chromosomes (mutant-chromosomes). The value that indicates the suitability of a chromosome to its environment is known as adaptation value (or fitness), which depends of the *degree* value of its genes that indicates the suitability of a gene to its environment.

Def. 4. Degree: the degree of a gene is a $degree : G \to \mathbb{Q}_+$ function mapping a gene to a k value known as $degree(g)$ that is so that $k \in \mathbb{Q}_+$. The $degree(g)$

function reflects a comparative stratification of the g gene suitability to its environment in respect to GAADT's intended problem.

Due the level of abstraction of the problem intended here, the *degree* function shown in (8) uses the $distri(g)$ function to exam how the micro-region of the game map corresponding to the g input gene match its surroundings. Equation (9) shows the $distri(g)$ function.

The $distri(g)$ function uses the $whiteInGene(g)$ function that combines all images within the tiles of the bases of its input gene into a single image and subject it to Canny's edge detection algorithm [2], creating a black and white image that outlines its geography (black background and white contours) and returning its amount of white pixels, which is used by (9) as an indicator of the correct placement of its geographic elements.

$$degree(g = \langle b_1, \ldots, b_n \rangle) = \begin{cases} \frac{distri(g)}{\#g} & \text{if } (pass > 1) \wedge (\exists_1 tp_{pass} \in INT \; \forall b = \\ & (x, y, z, tl, tp, in, fl) \in \{b_1, \ldots, b_n\} \,| \\ & tp = tp_{pass}) \\ 1 - \frac{distri(g)}{\#g} & \text{if } (pass = 1) \wedge (\exists_1 tp_{pass} \in INT \; \forall b = \\ & (x, y, z, tl, tp, in, fl) \in \{b_1, \ldots, b_n\} \,| \\ & tp = tp_{pass}) \\ 0 & \text{if } g \in G_\lambda \\ 1 \times 10^{-10} & \text{otherwise} \end{cases}$$

$$(8)$$

$$distri\,(g) = \begin{cases} 1 - \left(\frac{1}{\#g \times w_{cel} \times h_{cel}} \right) & \text{if } whiteInGene(g) = 0 \\ 1 - \left(\frac{whiteInGene(g)}{\#g \times w_{cel} \times h_{cel}} \right) & \text{otherwise} \end{cases} \qquad (9)$$

In addition to $distri(g)$, (8) uses the $INT = \langle tp_1, \ldots, tp_n \rangle$ sequence whose tp types of geography are mapped accordingly to the predominant type of environment of GAADT's input map and to its randomly chosen season. The tp values of INT are the same elements presented in Def. 1 and their position within INT denotes their level of importance to the geography that GAADT expects to achieve for the game map. Therefore, tp_1 is the most important type of geography for the intended game map while tp_n is the least important one. Each call to $distri(g)$ will randomly choose a *pass* value, $\{pass \in \mathbb{N}^* \,|\, pass \leq \#INT\}$, that will indicate the type of geography that will be taken into account (tp_{pass}). The G_λ set is the set of innocuous-genes, a subset of GAADT's G set of genes whose elements have no influence for the identity of a chromosome and that, for this instance of GAADT, corresponds to (10).

$$G_\lambda = \{g_\lambda = \langle b_1^{g_\lambda}, \ldots, b_n^{g_\lambda} \rangle \,|\, \forall \; i \in \{1, 2, \ldots, n\} \, (b_i^{g_\lambda} \in B_\lambda)\} \qquad (10)$$

Def. 5. Adaptation: the adaptation of a chromosome (or fitness) is a function $adapt : C \to \mathbb{Q}_+$ that sums the degree of its genes and is defined here as $adapt(c = \{g_1, \ldots, g_n\}) = \sum_{i=1}^{n} (\Theta\,(c, g_i) \times degree(g_i))$.

The Θ function above is a weight function that maps a gene into a rational value by identifying how much of a gene's *degree* contributes to the chromosome's adaptation. Here, the weight function merely accounts if the tp value within the bases of a gene is also an element of the INT sequence, resulting in 1 if $tp \in INT$ and 0 otherwise. The *adapt* function also makes possible to calculate the average adaptation of a population of chromosomes, which is so that $adapt_m(P = \{c_1, \ldots, c_n\}) = (\sum_{i=1}^{n} adapt(c_i))/\#P$.

The value of adaptation of a chromosome makes possible to select chromosomes for specific purposes from any of GAADT's populations. One such case is the selection of chromosomes better fitted to create new chromosomes by subjection to genetic operators. The first of these operators that will be shown here is the reproduction operator by crossover of chromosomes, which heavily relays on the selection operator.

Def. 6. Selection: an operator that chooses from a population the chromosomes better satisfying an r predicate from GAADT's Rq set of requirements. Hence, $sel(P_1, r) = P_1 \cap r$.

The r predicate used here is shown in (11), which has P_2 as the population of parents-chromosomes that suit r and INT_r as a subsequence of INT set at running time so that $INT_r = \{\langle tp_1^r, \ldots, tp_n^r \rangle \,|\, \forall i \in \{1, 2, \ldots, n\} \; \forall j \in \{1, 2, \ldots, m\} \; \exists tp_j \in INT (i \leq j) \wedge (j = i + (m - n)) \wedge (tp_i^r = tp_j)\}$.

$$r = \{P_2|\ (P_2 \subseteq C) \wedge (c = \{g_1, \ldots, g_n\} \in P_2) \leftrightarrow (\forall b = \atop (x, y, z, tl, tp, in, fl) \in \{g_1, \ldots, g_n\}\ \exists tp^r \in INT_r(tp = tp^r))\ \} \tag{11}$$

The P_2 resulting set of chromosomes of (11) may be further split into distinct $MALE$ and $FEMALE$ by applying their equivalent predicates over P_2. Therefore, assuming the predicates $M, F \in Rq$, follows that $MALE = sel(P_2; M)$ and $FEMALE = sel(P_2; F)$. These two new sets of chromosomes are used by the fecundation operation of (12).

$$fec(c^M, c^F) = \{\{g_1, \ldots, g_m\} \,|\ (c^M = \{g_1^M, \ldots, g_l^M\} \in MALE) \wedge \atop (c^F = \{g_1^F, \ldots, g_n^F\} \in FEMALE) \wedge \atop (g \subseteq \{g_1^M, \ldots, g_l^M\} \cup \{g_1^F, \ldots, g_n^F\}) \leftrightarrow \atop (\forall g^M \in \{g_1^M, \ldots, g_l^M\} \; \forall g^F \in \{g_1^F, \ldots, g_n^F\} \atop (domi(g^M, g^F) = g))\ \}$$

$$\tag{12}$$

The *domi* function of (12) receives two input genes and returns their dominant one. A g_1 gene is dominant over a g_2 gene if both express the same characteristic and $degree(g_1) \geq degree(g_2)$. Therefore, if $degree(g_2) > degree(g_1)$ the *domi* function returns g_2. Additionally, if g_1 and g_2 do not express the same characteristic *domi* returns a g_λ innocuous-gene. Here, g_1 and g_2 express the same characteristic if $\{\exists_1 tp \in INT |\ \forall g_1, g_2 \in G \; \forall i, j \in \mathbb{N}^* \; \forall b_i = (x_i, y_i, z_i, tl_i, tp_i, in_i, fl_i) \in g_1 \; \forall b_j = (x_j, y_j, z_j, tl_j, tp_j, in_j, fl_j) \in g_2((i \leq \#g_1) \wedge (j \leq \#g_2) \wedge (tp_i = tp_j = tp))\}$.

Def. 7. Crossover: the crossover is a reproduction operation defined by a $cross : MALE \times FEMALE \to P$ function, which is so that $cross(c_1, c_2) = \{c = \{g_1, \ldots, g_n\} | \ c \subseteq fec(c_1, c_2)\}$.

The other genetic operator for creating new chromosomes is the mutation operator. It acts as a safeguard that prevents the removal of chromosomes having some characteristics suitable to GAADT's current environment, but that do not meet the minimal adaptation value required to be kept in the current population. Once a chromosome is mutated its adaptation value is calculated again.

Def. 8. Mutation: an operator that replaces some of the genes of its input chromosome. It is defined by a $mut \subseteq \wp(P)$ predicate corresponding to the function $mut(c) = \{c' | (\exists G_1, G_2 \subset G) \to (c' = change(c, G_1, G_2)) \wedge (c' \in cut(P))\}$.

The *change* function of the definition above is of type $change : C \times \wp(G) \times \wp(G) \to C$ and is defined here as (13). Additionally, the *cut* function of *mut* is an acceptance criterion of the Rq set of requirements, $cut \in Rq$, that is imposed to every chromosome subject to mutation and that is defined here as $cut(P) = \{C_\Delta | \ \forall c \in C((c \in C_\Delta) \leftrightarrow (adapt(c) \geq adapt_m(P)))\}$.

$$change(c, G_1, G_2) = \begin{cases} (c \cup G_1) - G_2 \text{ if } (c \cup G_1 \in AFC) \wedge (c - G_2 \in AFC) \\ c \cup G_1 \qquad \text{if } (c \cup G_1 \in AFC) \wedge (c - G_2 \notin AFC) \\ c - G_2 \qquad \text{if } (c \cup G_1 \notin AFC) \wedge (c - G_2 \in AFC) \\ c \qquad\qquad \text{if } (c \cup G_1 \notin AFC) \wedge (c - G_2 \notin AFC) \end{cases} \quad (13)$$

3.3 The Algorithm

The populations of GAADT are part of an environment defined by the 8-tuple $E = \langle P, \wp(P), Rq, AFG, AFC, Tx, \Sigma, P_0 \rangle$. The P value is the current population of GAADT and $\#P \in \mathbb{N}^*$. Simultaneously, $\wp(P)$ is the power set of P; Rq is the set of environmental requirements guiding the evolution of chromosomes; AFG and AFC are, respectively, the sets of Axioms for Formation of Genes and of Chromosomes; Tx is the taxonomic classification of the chromosomes of P, which prevents them from occurring multiple times within a population and of resurging on any future population; Σ is the set of genetic operator; and P_0 is the initial population.

GAADT itself is established as the function $GAADT : E \to E$ shown at (14) and that assumes $P_t \subseteq C$ as its input population and $P_{t+1} \subseteq C$ as the next population of the algorithm, which contains the chromosomes that were produced from P_t as result of the environmental requirements imposed by the Rq set and the genetic operators of Σ. Consequently, $P_{t+1} = cross(a, b) \cup mut(c) \cup p_{cut}(P_t)$ and $a, b, c \in P_t$.

$$GAADT(P_t) = \begin{cases} P_{optm} & \text{if } P_{optm} = \{c | \ \forall c \in P_t(adapt(c) \geq k)\} \neq \varnothing; \\ P_{t+1} & \text{if } t + 2 = T; \\ GAADT(P_{t+1}) & \text{otherwise} \end{cases}$$

$$(14)$$

The Rq set of requirements of GAADT also contains two stopping criteria to halt its execution. The first of these criteria is defined in respect to what the instantiation of GAADT is considering as an optimal solution to its intended problem and is presented in (14) as definition of the minimal adaptation value k that must be met by the chromosomes of the P_{optm} optimal population. The last criterion establishes a maximum number of interactions (generations) that GAADT can perform before returning a result. In (14) this corresponds to the defined T value that is so that $T \in \mathbb{N}$. This last criterion ensures that GAADT's evolutionary process will eventually stop and therefore, is computable.

4   Results and Conclusions

Figure 3 shows a map provided as input to GAADT (Fig. 3a) and the map that results of its evolutionary process (Fig. 3b). The map area of Fig. 3b that diverges from Fig. 3a corresponds to the chromosome of greatest adaptation value that exists within the last population created by GAADT before the halt of its process. In this particular example, a forest input map (Fig. 3a) was subject to a period of drought that was caused by an extend summer and began to acquire geographic features commonly seen in deserts (Fig. 3b).

(a) Input map (forest)   (b) Output map (desert)
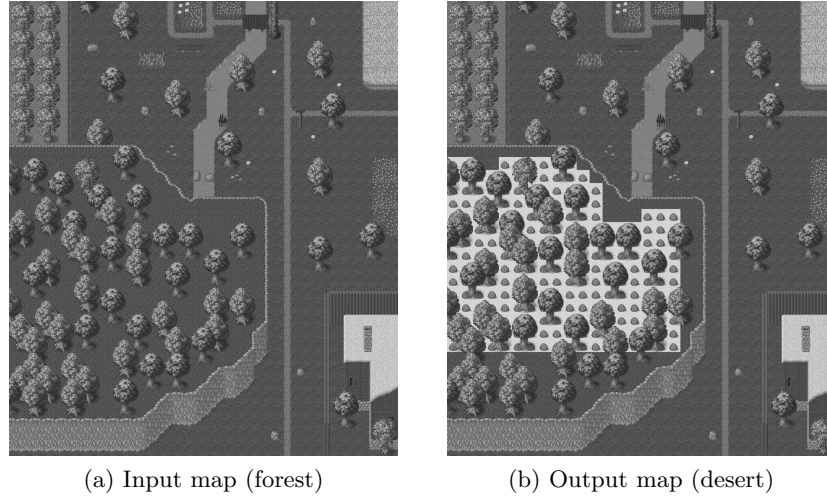
Fig. 3: An input map and the output map created from it by GAADT

The number of interactions performed by GAADT to create the map of Fig. 3b is shown in Table 2, along with the chromosomes of greater and lower adaptation value and the average adaptation of the population of each generation. Table 2 also makes possible to identify stagnant periods of GAADT's evolutionary process, which correspond to the generations presenting identical values for

the greatest, lowest and average adaptation of its chromosomes (generations 3 to 5 and 6 to 7). After seven generations with no changes in any of these three values, the evolutionary process of this instance of GAADT is halted.

Results			
generation	greatest adaptation	lowest adaptation	average adaptation
1	0,924541016	0,00302477	0,572786602
2	0,946289063	0,00302477	0,611779318
3	0,9921875	0,00302477	0,63175816
4	0,9921875	0,00302477	0,63175816
5	0,9921875	0,00302477	0,63175816
6	0,993339978	0,00302477	0,672413871
7	0,993339978	0,00302477	0,672413871
8	0,996235983	0,01467041	0,713797671
9	0,996235983	0,01467041	0,713797671
10	0,996235983	0,01467041	0,713797671
11	0,996235983	0,01467041	0,713797671
12	0,996235983	0,01467041	0,713797671
13	0,996235983	0,01467041	0,713797671
14	0,996235983	0,01467041	0,713797671

Table 2: Adaptation values for the chromosomes of GAADT in creating the map of Fig. 3b

The result seen in Fig.3b and achieved by the process detailed in Table 2 shows that even thought the use of GAADT contrasts with the traditional use of computer graphics to modify the geography of game maps, it is a valid approach that provides resulting maps suitable to MMORPGs and that add an extra element of dynamic that players can explore.

However, it is the authors' believe that such results can be further improved by refining the parameters of the instance of the algorithm in order to achieve an even better distribution of the geographic elements of the resulting maps.

An identified drawback is the time required by the algorithm to obtain a resulting map. In this respect, the map shown in Fig. 3b took roughly 10 hours to be created from the map of Fig. 3a. This is a consequence of GAADT using its Σ set of genetic operators to create all possible variations of the input map that obey the restrictions imposed by the Rq set of requirements.

To solve this drawback, future approaches to this problem will focus on either implementing the GAADT instance seen here in hardware in order to reduce the processing time by taking advantage of its higher processing speeds; or, refactoring the instance of GAADT as to improve its execution in addition to generalize it so it become applicable for game maps whose structure is different from that of the game maps used here.

References

1. Cai, X., Li, F., Sun, H., Zhan, S.: Research of Dynamic Terrain in Complex Battlefield Environments. In: Technologies for E-Learning and Digital Entertainment, Lecture Notes in Computer Science, vol. 3942. Springer Berlin / Heidelberg (2006)
2. Canny, J.: A Computational Approach to Edge Detection. IEEE Transactions on Pattern Analysis and Machine Intelligence PAMI-8(6) (1986)
3. Carvalho, L.F.B.S., Neto, H.C.S., Lopes, R.V.V., Paraguau, F.: Application of a genetic algorithm based on abstract data type in electronic games. In: Proceedings of the 9th Mexican International Conference on Artificial Intelligence - Special Session - (MICAI 2010). pp. 28–33. IEEE Computer Society Press (2010)
4. Carvalho, L.F.B.S.: An Evolutive game of Checkers. End of course work, Institute of Computation, Federal University of Alagoas, Brazil (2008)
5. Duchaineau, M., Wolinsky, M., Sigeti, D., Miller, M., Aldrich, C., Mineev-Weinstein, M.: Roaming terrain: Real-time optimally adapting meshes. In: Proceedings of the conference on Visualization '97 (1997)
6. GOLDBERG, D.E., HOLLAND, J.H.: Genetic algorithms and machine learning. Machine Learning 3(2-3), 95–99 (1988)
7. He, Y., Cremer, J., Papelis, Y.: Real-time extendible-resolution display of on-line dynamic terrain. In: Proceedings of The 2002 Conference on Graphics Interface (2002)
8. Lindeijer, T., Turk, A.: Tiled Map Editor. Available at: `http://www.mapeditor.org/` (2006-2011), last accessed on December 19 2010
9. Lopes, R.V.V.: A Genetic Algorithm Based on Abstract Data Type and its Specification in Z. Ph.D. thesis, Computer Center, Federal University of Pernambuco (2003)
10. Shamir, A., Pascucci, V., Bajaj, C.L.: Multiresolution dynamic meshes with arbitrary deformations. In: Proceedings of IEEE Visualization 2000 (2000)

Increasing the Performance of Differential Evolution by Random Number Generation with the Feasibility Region Shape

Felix Calderon, Juan Flores, and Erick De la Vega

Universidad Michoacana de San Nicolás de Hidalgo,
División de Estudios de Posgrado, Facultad de Ingeniería Eléctrica,
Santiago Tapia 403 Centro, Morelia, Michoacán, CP 58000, Mexico
`calderon@umich.mx, juanf@umich.mx, edelavega@faraday.fie.umich.mx`

Abstract. Global optimization based on evolutionary algorithms can be used for many engineering optimization problems and these algorithms have yielded promising results for solving nonlinear, non-differentiable, and multi-modal optimization problems. In general, evolutionary algorithms require a set of random initial values; in the case of constrained optimization problems, the challenge is to generate random values inside the feasible region. Differential evolution (DE) is a simple and efficient evolutionary algorithm for function optimization over continuous spaces. It outperforms search heuristics when tested over both benchmark and real world problems. DE with Penalty Cost Functions is the most used technique to deal with constraints, but the solution is moved by the penalty factor, losing accuracy. Additionally, the probability to reach the optimal value is near zero for some constrained optimization problems, because the optima of the objective function are located out of the feasible region, therefore the optimal solutions of the problem lie at the border of the feasible region. In this paper we propose an improved DE algorithm for linearly constrained optimization problem. This approach changes the restricted problem to a non-restricted one, since all individuals are generated inside the feasible region. The proposed modification to DE increases the accuracy of the results, compared to DE with penalty Functions; this is accomplished by the generation of random numbers whose convex hull is shaped by the feasible region. We tested our approach with several benchmark and real problems, in particular with problems of economic dispatch of electrical energy.

Keywords: Differential evolution, feasible region, optimization.

1 Introduction

For a differentiable function $f(x) : \mathbb{R}^D \to \mathbb{R}$, computing the minimum $x^* = [x_0^*, x_1^*, \cdots, x_{D-1}^*,]$, can be done using gradient-based methods [1]. Nevertheless, these techniques fail for non-differentiable and discontinuous functions. An alternative is to solve the problem using evolutionary computation; these meta-heuristics compute an initial set of prospect solutions, called initial population.

The most common way to generate a random initial population within a feasible reagion $\mathcal{R}$, is computing a random number with uniform distribution using Equation (1). The population generated this way is uniformly distributed inside a hyper-cube, therefore, when minimizing the function $f(x)$ restricted by constraints of the form $x_j^{min} <= x <= x_j^{max}$ it is very easy to compute the solution using Genetic Algorithms.

$$x_j = x_j^{min} + \alpha * (x_j^{max} - x_j^{min}) \quad \forall j \in [0, D] \qquad (1)$$

Nevertheless, the problem contains a set of linear constraints that limit the region, turning it into a line, a plane, or a hyper-plane (depending on the number of dimensions of the problem). In general, the problem we are to solve using Differential Evolution has the form given by Equation (2)

$$f(x) \qquad s.a \qquad \begin{aligned} a_i^T x + b_i &>= 0 \quad \forall i \in [0, M_1 - 1] \\ a_k^T x + b_k &= 0 \quad \forall k \in [0, M_2 - 1] \end{aligned} \qquad (2)$$

An example of this kind of constrained problem is Economic Dispatch (ED) [2]; ED consists of supplying electrical energy to a load using a set of generation units. Electrical generators have constraints that limit the amount of energy it can provide, and a linear constraint associated with energy conservation. Santos [3] proposes a solution to this problem using Differential Evolution with penalty functions. The problem includes linear constraints and forbidden generation zones.

In this paper, we propose to model the feasible region by a set of points forming the convex hull of the feasible area. Calderon *et al.* [4] presents a GA-based solution using a set of vectors delimiting the feasibility region. Lara *et al* [5] propose an algorithm to compute the convex hull corresponding to an ED problem with a set of inequalities limiting the generation hyper-cube, and one linear constraint – a hyper-plane – where feasible solutions dwell. Based on that set of points, an initial population living inside the feasible region can be computed via linear combinations of points in that convex hull. Nevertheless, Differential Evolution has proven to be more precise than GA [6]. An algorithm for computing a convex hull has exponential time nevertheless given the characteristics for this problem Lara *et al* present an linear algorithm with respect to the intersection points between the hyper plane and the hyper cube (for details see [5]).

To solve a problem like the one pose in Equation (2) using Differential Evolution, we need to guarantee an initial population within the feasible area. Additionally, when the DE operators are applied there is no guarantee for the population to remain within the feasibility region. Our proposal does guarantee both, that the initial population is generated inside and fills uniformly the feasibility region, and that the DE evolution operators keep the population inside that region.

It is very common for evolutionary algorithms to use penalty functions to maintain the population within the feasibility space. The penalty function is

charged a cost λ each time a constraint is violated. A problem with penalty functions is that their associated cost moves the solution; besides, if the probability to generate a solution is near zero, the accuracy of the result, in general, is very poor. The basic form of Equation (2) using a penalty function, can be written as in Equation (3).

$$F(x) = f(x) + \lambda \sum_{i=0}^{M-1} C(-a_i^T x - b_i)$$ (3)

where $C(y) = 1$ if $y > \tau$ and 0 otherwise; τ is a threshold.

Figure 1(a) shows a rectangle described by the limits $[x_0^{min}, x_0^{max}]$ and $[x_1^{min}, x_1^{max}]$ in two dimensions. That rectangle will contain the initial population if their individuals are generated from Equations (1). Nevertheless, where linear constraints like those in Equation (2) are included in the problem formulation, the feasibility space does not fill that rectangle. Figure 1(b) shows how the area of Figure 1(a) divides in two regions. Let us call $\mathcal{R}_1$ to the unfeasible region and $\mathcal{R}_2$ the feasible region (marked in the figure by numbers 1 and 2, respectively). If we generate a random individual using (1), the probability to generate it within the feasible region is $P(X) = Area(\mathcal{R}_2)/Area(\mathcal{R})$. The probability to generate an individual in the feasible region can decrease for a certain set of constraints; in that case, it is more likely to generate individuals outside the feasible region, or even worse, the probability to generate individuals in the feasible region may be null. A case where the feasible region has zero probability is when we minimize $f(x)$ subject to $x_0^{min} \leq x_0 \leq x_0^{max}$, $x_1^{min} \leq x_1 \leq x_1^{max}$, and $ax_0 + bx_1 = c$.

The rest of the paper is organized as follows. Section 2 describes how to generate a population with the same shape as the feasible region, and proves that the population is indeed inside it. This scheme allows us to change a constrained optimization problem to an unconstrained one. Section 3 presents the details of the DE algorithm and proposes a modification for it to generate all individuals within the feasible region. Section 4 compares solutions obtained by DE with penalty functions with Differential Evolution with Number Generation based on the Feasible Region Shape (DE-NGFRS), as well as the solutions using Mathematica (in some cases), and solutions to problems of economic dispatch. Finally, Section 5 presents the conclusions.

2 Generation of a Random Population with the Shape of the Feasible Region

Number Generation with Feasible Region Shape (NGFRS) is described in this section; NGFRS produces a random population with the shape of the feasible region. We will assume we have a set of vertices $q = \{q_0, q_1, \cdots, q_i, \cdots, q_{N-1}\}$, located on a hyper-plane on D dimensions, which define the convex hull of the feasible region. One way to generate an individual x inside the feasible region is by a linear combination of the vertices, given by Equation (4), as proposed in Calderon *et al.* [4].
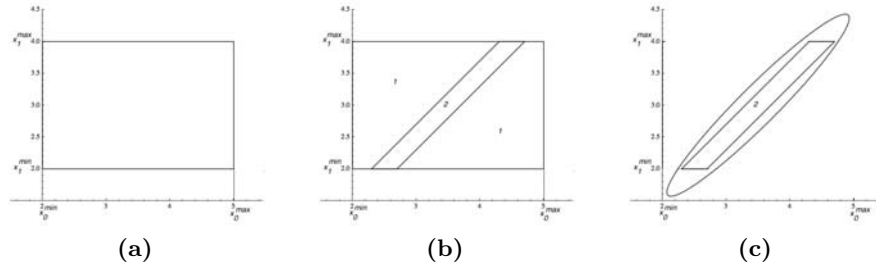
Fig. 1. Feasible Regions generated by a) eq. (1) , b) eq. (2) and c) algorithm 1

$$x = \sum_{i=0}^{N-1} q_i \alpha_i \quad s.t. \quad \sum_{i=0}^{N-1} \alpha_i = 1 \tag{4}$$

where α_i is a random weight, such that $\alpha_i \sim U(0,1)$.

This constraint on the weights generates individuals distributed around the center of the feasible area, reducing the probabilities to generate a random individual at the vertices of the feasible region. This is due to the fact that the sum of random numbers follows a Gaussian distribution, according the central limit theorem [7]. Our proposal consists basically on the generation of random individuals with a normal distribution, covering the feasible area (described by its set of vertices). The mean of the generated population, μ, lies at the center of the feasible region, and the covariance matrix Σ is shaped as an ellipsoid around the feasible region (see Figure 1(c)). The sample mean and covariance of the that distribution is computed from the set of vertices q, using Equations (5), and (6).

$$\mu = \frac{1}{N} \sum_{i=0}^{N-1} q_i \tag{5}$$

$$\Sigma = \frac{1}{N} \sum_{i=0}^{N-1} (q_i - \mu)(q_i - \mu)^T \tag{6}$$

Generating random numbers with zero mean and unity variance such that $z \sim N(0,1)$ is an easy task. The problem is to generate random numbers with nonzero mean and a covariance different to 1. The expected value of numbers z is $E[z] = 0$ and $E[zz^T] = I$ (I is the identity matrix), given that their mean is zero and their variance is unity. A property of the expected value that will be used to modify the mean and covariance of the randomly generated numbers is given by Equations (7) and (8). To modify the mean of the distribution, we simply add a value μ to numbers z, according to (7). The procedure to modify the covariance is not as straightforward, though.

$$E[z + \mu] = E[z] + \mu = \mu \tag{7}$$
$$E[z\Sigma z^T] = \Sigma E[zz^T] = \Sigma \tag{8}$$

If we represent the covariance matrix in Equation (8) by a singular values decomposition given by $\Sigma = R\Lambda R^T$, where R is a rotation matrix and $\Lambda = diag[\lambda_0, \lambda_1, \cdots, \lambda_{D-1}]$, we can generate numbers that follow a normal distribution $x \sim N(\mu, \Sigma)$, from a random number $z \sim N(0, 1)$, those numbers can be generated by making

$$E[z\Sigma z^T] = E[zRLL^T R^T z^T] = E[xx^T] = \Sigma$$
$$x = RLz + \mu \tag{9}$$

where $L = diag[\sqrt{\lambda_0}, \sqrt{\lambda_1}, \cdots, \sqrt{\lambda_{D-1}}]$.

This Equation guarantees to produce a random number inside an ellipsoid from the normal distribution. This number is not necessarily within the feasible region, though. To verify that the number is inside the polygon, we take Equations (4) and take them to a matrix form (see Equation 10). The solution by minimum squared can be computed using Equation 11.

$$\begin{bmatrix} x \\ 1 \end{bmatrix} = \begin{bmatrix} q_0 & q_1 & q_2 & \cdots & q_{N-1} \\ 1 & 1 & 1 & \cdots & 1 \end{bmatrix} \begin{bmatrix} \alpha_0 \\ \alpha_1 \\ \alpha_2 \\ \vdots \\ \alpha_{N-1} \end{bmatrix} \tag{10}$$

$$X = Q\alpha$$
$$\alpha = [Q^T * Q]^{-1} Q^T X \tag{11}$$

So, point x is inside the polygon iff the values of α follow $0 \le \alpha_i \le 1$. This procedure is known as computation of the varicentric coordinates [8]. Algorithm 1 summarizes all step described above for Generating Random Numbers inside the Feasible Region. In our test we take advantages of generating the random number with Gaussian distribution instead of uniform distribution because the firsts generate a elliptical shape over the feasible region and the uniform produce a shaped region quite different to the feasible region and in some cases do not cover all the feasible region.

3 Differential Evolution

Differential Evolution (DE) was developed by Storn and Price [9, 6] around 1995 as an efficient and robust meta-heuristic to optimize functions of arbitrary complexity. Like most algorithms in Evolutionary Computation, DE is a population–based optimizer. Most of these methods produce new individuals, by different

---

Algorithm 1 Algorithm NGFRS

Input: $q = \{q_0, q_1, \cdots, q_{N-1}\}$
Output: A set of random numbers x

Compute mean μ and an covariance matrix Σ by eq (5) and (6)
Compute eigenvalue decomposition $\Sigma = R\Lambda R^T$
Compute $L = diag[\sqrt{\lambda_0}, \sqrt{\lambda_1}, \cdots, \sqrt{\lambda_{N-1}}]$
For $i = 0, 1, 2, \cdots$
    Generate $z \sim N(0, 1)$
    Compute $x = RLz + \mu$
    Compute the α values solving eq (11)
    If $\alpha_i < 0$ and $\alpha_i > 1$ for one value, reject the number and generate a new value

---

heuristic techniques, as perturbations of old ones (e.g. crossover, mutation, etc.). DE produces new individuals adding the scaled difference of two randomly selected individuals to a third one.

DE maintains two vector populations, containing $N_{pop} \times N_{par}$ real-valued parameters. Population $x^{(g)}$ contains N_{pop} vectors for each generation g, where the kth individual in $x^{(g,k)}$ has N_{par} parameters. Population $v^{(g)}$ are mutant vectors produced from $x^{(g)}$. Each vector in the current population is recombined with a mutant to produce a trial population, $u^{(g)}$. The trial population is stored in the same array as the mutant population, so only two arrays are needed.

The initial population is generated on a searching space $\mathcal{R}$ by random numbers following a uniform probability distribution, with a (possibly) different range for each dimension. Discrete and integral variables are represented by real numbers and then interpreted in the right way. In order to have a Initial population inside the feasible region, instead of the initial population generated by Equation (1), we propose to use Algorithm 1.

Differential mutation adds a scaled randomly chosen, vector difference to a third vector, as you can see in Equation (12)

$$v^{(g,k)} = x^{(g,r_0)} + F(x^{(g,r_1)} - x^{(g,r_2)}) \tag{12}$$
$$\forall k \in [1, N_{pop}]$$

where F is a positive real number that control the rate at which the population evolves. The difference vector indices, r_1 and r_2, and the index r_0 are chosen randomly from $[1, N_{pop}]$.

To complement the differential mutation strategy, DE uses uniform crossover, also known as discrete recombination. Crossover takes place according to Equation (13)

$$u_j^{(g,k)} = \begin{cases} v_j^{(g,k)} & \text{if } rand(0,1) \leq Cr \text{ or } j = j_{rand} \\ x_j^{(g,k)} & \text{otherwise} \end{cases} \tag{13}$$
$$\forall <j, k> \in [1, N_{par}] \times [1, N_{pop}]$$

where $Cr \in [0, 1]$ is a user defined parameter that controls the proportion of components copied from the mutant onto the trial vector. $v_j^{(g,k)}$ is the jth component of the ith individual of the gth generation of population $v^{(g)}$.

If the trial vector $u^{(g,k)}$ has an equal or lower fitness value than its target vector $x_j^{(g,k)}$, it replaces the target vector in the next generation (Equation 14).

$$x^{(g+1,k)} = \begin{cases} u^{(g,k)} \text{ if } f(u^{(g,k)}) \leq f(x^{(g,k)}) \\ x^{(g,k)} \text{ otherwise} \end{cases} \qquad (14)$$
$$k \in [1, N_{pop}]$$

Differential Evolution may create a new vector outside of the feasibility region. If so, then reject it and set $x^{(g+1,i)} = x^{(g,i)}$. The complete algorithm for minimizing $f(x)$ inside a feasible region, given by q, is presented in Algorithm 2, which additionally to the DE operation, randomly generates a new random number if a probability $\gamma \leq 0.5$. With this condition it is more likely for the population to reach the global minimum inside the feasible region.

Algorithm 2 DE-NGFRS

Input: q, N_{pop}, N_{gen}, F, C_r and $f(x)$
Output: $x^{(*,*)}$

Compute a initial population $x^{(g)}$ by algorithm 1, with mean $\overline{q}$ and compute
the fitness fuction $f(x)$ with out restriction, for each population member
For $g = 0, 1, 2, \cdots, N_{gen}$ {
    For $k = 0, 1, 2, \cdots, N_{pop}$ {
        Generate $\gamma \sim U(0, 1)$
        if $\gamma < 0.5$ {
          Compute $v^{(g,k)}$ by Equation (12)
          Compute the crossover $u^{(g,k)}$ by Equation (13)
          Select $x^{(g+1,k)}$ by (14)
          If $x^{(g+1,k)}$ is out of the feasible region set $x^{(g+1,k)} = x^{(g,k)}$
        }
        else compute $x^{(g+1,k)}$ by algorithm 1 with mean $x^{(g,k)}$
    }
}

---

4 Results

To show our algorithm's performance, we test it with five functions. The first one is a sixth degree two-dimensional function; the second one is the Rosenbrock function, and the remaining three functions are the objective functions belonging to the Economic Dispatch problems known as IEEE14 [10], Wong [12] and Wood [11]. The following subsections present the details of these experiments.

4.1   Sixth Degree Function

This first experiment aims to solve the function $f_1(x)$ (15). The convex hull of the feasible region was determined computing the intersection of the search space with the linear constraint of the optimization problem. The set of vertices of the convex hull is $q = \{[-23, -95], [-24, -94], [-20, -50], [19, 1], [20, -2], [10, -40]\}$. To solve this problem using DE with a penalty function (3) the cost associated to violating a constraint was $\lambda = 1 \times 10^{10}$. Table 1 presents the best, mean, and worst case of 100 independent runs of Algorithm DE-NGFRS. The same problem was presented to Mathematica, which failed to compute a solution. DE with a penalty function converges in some cases and it does not in others.

$$f_1(x) = -3x^6 + 2x^5 - x + 2y^3 + 45y + 23 \qquad (15)$$

$$s.a$$

$$x + y + 118 \geq 0, 11x - y + 170 \geq 0, 17x - 13y - 310 \geq 0$$

$$-3x - y + 58 \geq 0, -19x + 5y + 39 \geq 0, -5x + 170 + 3y \geq 0$$

Table 1. Sixth Degree Function results for one hundred independent runs

Algorithm	values	time (sec)	x	$f_1(x)$
DE-NGFRS	Min	0.0203	[-24.0000,-94.0000]	-5.90900×10^8
	Mean	0.0203	[-24.0000,-94.0000]	-5.90900×10^8
	Max	0.0203	[-23.9983,-93.9818]	-5.90900×10^8
Mathematica	Always	10.73650	[1.5250, 0.0000]	0.234956
Pelnalty Function	Min	0.046	[-24.0000,-94.0000]	-5.9090×10^8
	Mean	0.049	$[-1.58 \times 10^{22}, -1.12 \times 10^{47}]$	-2.8228×10^{145}
	Max	0.048,	$[-1.48 \times 10^{24}, -1.11 \times 10^{49}]$	-2.82282×10^{147}

4.2   Rosenbrock Function

This experiment solves a problem using the Rosenbrock function constrained to a thin band described by Equation $f_2(x)$ (16). The vertices of the convex hull of the feasible region are $q = \{[2, 4], [-39, 101], [-40, 100], [1, 3]\}$ and the cost for the penalty function was $\lambda = 100$ (3). Table 2 shows the results; our proposal outperforms the other schemes in every case. DE with a penalty function converges only in some cases, and Mathematica presents similar results with executions times greater than those taken by Algorithm DE-NGFRS.

$$f_2(x) = (1 - x_0)^2 + 100(x_0 - x_1^2)^2 \qquad (16)$$

$$s.a$$

$$-97.0x_0 - 41.0x_1 + 358 \geq 0, x_0 - x_1 + 140.0 \geq 0$$
$$97.0x_0 + 41.0x_1 - 220 \geq 0, -x_0 + x_1 - 2.0 \geq 0$$

Table 2. Results for Rosenbrock Funcion, for one hundred independent runs

Algorithm	values	time (sec)	x	$f_2(x)$
	min	0.484	[1.99889, 3.99889]	0.998889
DE-NGFRS	mean	0.484	[1.99889, 3.99889]	0.998889
	max	0.484	[1.99880, 3.99889]	0.998889
Mathematica	Always	8.07094	[1.99888, 3.99888]	0.998889
	min	2.089	[1.99889, 3.99889]	0.998889
Penalty	mean	2.151	[-3.76033, 17.30290]	48.9379
	Max	2.156	[-7.58911, 57.60030]	173.776

4.3 Economic Dispatch

This subsection presents the results obtained by solving the economic dispatch problem with three electrical networks corresponding to IEEE14 (see [10]), Wood (see [11]), and Wong (see [12]). The cost (objective) functions for each of the networks are given by Equations (17), (18), and (19), respectively. The sets of vertices of the convex hulls of the corresponding feasible regions were computed using the algorithm proposed by Lara *et al.* [5]; those vectores are shown on Table 3. The set of convex hull vectors is computed and then we proceed to solve the unconstrained version of the optimization problem using Algorihm 2. The average time to compute those vectors was 20 ms.

Table 4 shows the comparative results for these networks. The table shows that we solve the economic dispatch in a time much lower than those reported in [4] producing results with better accuracy. See the results for the Wong problem using Algorithm DE-NGFRS.

$$f_{IEEE14}(x) = 2 \times 10^{-5} + 0.003x_0 + 0.01x_0^2 + 2 \times 10^{-5} + 0.003x_1 + 0.01x_1^2 \quad (17)$$
$$+ 2 \times 10^{-5} + 0.003x_2 + 0.01x_2^2 + 2 \times 10^{-5} + 0.003x_3 + 0.01x_3^2$$
$$+ 2 \times 10^{-5} + 0.003x_4 + 0.01x_4^2$$
$$s.a.$$
$$10 \leq x_0 \leq 80, \quad 10 \leq x_1 \leq 60, \quad 10 \leq x_2 \leq 60, \quad 10 \leq x_3 \leq 60,$$
$$10 \leq x_4 \leq 80, \quad and \quad x_0 + x_1 + x_2 + x_3 + x_4 = 300.5576$$

$$f_{Wood}(x) = 749.55 + 6.950x_0 + 9.680 \times 10^{-4}x_0^2 + 1.270 \times 10^{-7}x_0^3 \quad (18)$$

$$+1285.00 + 7.051x_1 + 7.375 \times 10^{-4}x_1^2 + 6.453 \times 10^{-8}x_1^3$$
$$+1531.00 + 6.531x_2 + 1.040 \times 10^{-3}x_2^2 + 9.980 \times 10^{-8}x_2^3$$
$$s.a$$
$$320 \le x_0 \le 800, \quad 300 \le x_1 \le 1200, \quad 275 \le x_2 \le 1100$$
$$and \quad x_0 + x_1 + x_2 = 2500$$

$$f_{Wong}(x) = 11.20 + 5.10238x_0 - 2.64290 \times 10^{-3}x_0^2 + 3.3333 \times 10^{-6}x_0^3 \quad (19)$$
$$-632.00 + 13.01x_1 - 3.05714 \times 10^{-2}x_1^2 + 3.3333 \times 10^{-5}x_1^3$$
$$+147.144 + 4.28997x_2 + 3.08450 \times 10^{-4}x_2^2 - 1.7677 \times 10^{-7}x_2^3$$
$$s.a$$
$$100 \le x_0 \le 500, \quad 100 \le x_1 \le 500, \quad 200 \le x_2 \le 1000$$
$$and \quad x_0 + x_1 + x_2 = 1443.4$$

Table 5 shows the parameters used to perform these tests, the average and standard deviation of the error function of 100 independent runs for the five test problems. Table 5 includes the name, population size N_{pop}, the number of generations N_{gen}, the mutation parameter F, the crossover parameter C_r, and the mean $\overline{f(x)}$ and standard deviation $EstDev(f(x))$ of the error function $f(x)$. Note that the mean of the error function is consistent in all experiments, with a very low standard deviation. The population size and generation number depend of the number of variables and this parameter is hand picked for the best results in general we can use the biggest for this parameters with the same results, obviously the execution time will be quite different.

5   Conclusions

Evolutionary computation has proven to be a good tool to solve non-linear optimization problems, exhibiting an advantage over traditional gradient-based methods, specially for discontinuous and non-differentiable objective functions. These difficult problems become even harder when constraints are added to the problem. Those constraints often represent relations that have to be preserved among the problem variables, energy or flow conservation, etc. One way of dealing with constrained optimization problems is to add penalties to the objective function when an individual lies outside the feasible region. Unfortunately, this approach leads to time wasted in generating and discarding individuals outside the feasible regions. There are situations where the proportion of the size of the feasible region, with respect to the search space is zero. This fact affects an evolutionary search from the moment of generating the initial population, and later on the individuals produced by evolutionary operations; in those cases most time is wasted in discarding individuals violating the constraints, and the population gets to an impasse.

Table 3. Convex Hull Vectors computed by Lara *et al.* [5]

Network	Active Power Vectors in KW
IEEE 14	$v_1 = [40.5576, 60.0000, 60.0000, 60.0000, 80.0000]^T$ $v_2 = [80.0000, 20.5576, 60.0000, 60.0000, 80.0000]^T$ $v_3 = [80.0000, 60.0000, 20.5576, 60.0000, 80.0000]^T$ $v_4 = [80.0000, 60.0000, 60.0000, 20.5576, 80.0000]^T$ $v_5 = [80.0000, 60.0000, 60.0000, 60.0000, 40.5576]^T$
Wood	$v_1 = [320.0, 1080.0, 1100.0]^T$ $v_2 = [800.0, 600.0, 1100.0]^T$ $v_3 = [320.0, 1200.0, 980.0]^T$ $v_4 = [800.0, 1200.0, 500.0]^T$
Wong	$v_1 = [343.40, 100.00, 1000.00]^T$ $v_2 = [100.00, 343.40, 1000.00]^T$ $v_3 = [100.00, 500.00, 843.40]^T$ $v_4 = [500.00, 500.00, 443.40]^T$ $v_5 = [500.00, 100.00, 843.40]^T$

Table 4. Comparative Results for Economic Dispatch problems.

Network	Algorithm	Demand	Generation Cost	Time (seg.)	Active Power Vector Solution
IEEE 14	[10]	300.5576	181.5724	-	[60.2788 60.0000 ... 60.0000 60.0000 60.2788]
	[4]	300.5576	181.5724	4.276	[60.2789 59.9999 ... 59.9999 59.9997 60.2789]
	DE-NGFRS	300.5576	181.5724	0.811	[60.2788 60.0000 ... 60.0000 60.0000 60.2788
Wood	[11]	2500.1000	22730.21669	-	[726.9000 912.8000 860.4000]
	[4]	2500.0000	22729.32458	2.814	[725.0078 910.1251 864.8670]
	DE-NGFRS	2500.0000	22729.32458	0.027	[724.9915 910.1534 864.8551]
Wong	[12]	1462.4480	6639.50400	-	[376.1226 100.0521 986.2728]
	[4]	1443.4000	6552.23790	2.842	[343.3980 100.0415 999.9604]
	DE-NGFRS	1443.4000	6552.09315	0.260	[343.4000 100.0000 1000.0000]

Table 5. Parameters, Average and Standard Deviation for all the examples

Example	N_{pop}	N_{gen}	F	C_r	$\overline{f(x)}$	$EstDev(f(x))$
G6	50	500	0.95	0.90	-5.9090×10^8	0.01118
Rosenbrock	1500	500	1.2	0.90	0.9988	1.8058×10^{-15}
IEEE14	1000	1000	0.95	0.90	181.5724	3.8849×10^{-12}
Wood	50	700	0.95	0.90	22729.3246	2.9451×10^{-11}
Wong	500	700	0.95	0.90	6552.0931	1.6024×10^{-11}

In this paper we present an algorithm called NGFRS, which allows us to generate a population of individuals that fills a convex area delimited by linear constraints. The same ideas of NGFRS have been applied to solve non-linear, linearly constrained optimization problems; the resulting algorithm is called DE-NGFRS. It has been empirically shown that NGFRS exhibits a performance way superior to DE with a penalty function. The results obtained in the solution of economic dispatch problems using DE-NGFRS was compared with the results presented for those problems in previous work; DE-NGFRS proved to improve those results. Additionally, DE-NGFRS proves to be better than Algorithm GA-V, which is based on Genetic Algorithms.

References

1. Jorge, N., Wright, S.J.: Numerical Optimization. Springer (2000)
2. Stevenson, W.D.: Elements of Power System Analysis. Mc Graw Hill (1982)
3. dos Santos Coelhoa, L., Marianib, V.C.: Improved differential evolution algorithms for handling economic dispatch optimization with generator constraints. Energy Conversion and Management, **48**, 1631–1639 (2007)
4. Calderon Felix, Fuerte-Esquivel Claudio R, S.J., J., F.J.: A constraint-handling genetic algorithm to power economic dispatch. MICAI 2008: Advances in Artificial Intelligence Lecture Notes in Computer Science, 371–381 (2008)
5. Lara, C., Flores, J.J., Calderon, F.: On the hyperbox hyperplane intersection problem. Infocomp Computer Journal Computer Science, **8**, 21–27 (2009)
6. Storn, R., Price, K., Lampinen, J.: Differential Evolution. A Practical Approach to Global Optimization. Springer–Verlag, Berlin, Germany (2005)
7. Fischer, H.: A History of the Central Limit Theorem: From Classical to Modern Probability Theory. Springer (2010)
8. Lawson, C.L.: Properties of n-dimensional triangulations. Computer-Aided Geometric Design, **3**, 231–246 (1986)
9. Storn, R., Price, K.: Differential evolution – a simple and efficient adaptive scheme for global optimization over continuous spaces. Technical Report 95-012, ICSI (1995)
10. Ongsakul, W., Ruangpayoongsak, N.: Constrained dynamic economic dispatch by simulatedannealing/genetic algorithms. In: Power Industry Computer Applications, 2001. PICA 2001. Innovative Computing for Power - Electric Energy Meets the Market. 22nd IEEE Power Engineering Society International Conference, 207–212 (2001)
11. Wood, A., Wollenberg, B.: Power Generation, Operation, and Control. John Wiley and Sons Inc (1984)
12. Wong, K., Fung, C.: Simulated annealing based economic dispatch algorithm. In: Generation, Transmission and Distribution, IEE Proceedings C. Volume 140, 509–515 (1993)

Determination of Optimal Cutting Condition for Desired Surface Finish in Face Milling Process Using Non-Conventional Computational Methods

Muthumari Chandrasekaran and Amit Kumar Singh

North Eastern Regional Institute of Science and Technology (NERIST), India
se1@yahoo.com

Abstract. CNC (Computer Numerical Control) milling process is one of the common metal removal operation used in industries because of its ability to remove material faster with reasonably good surface quality. Surface roughness is the most important attributes of the manufactured component in finish machining process. To obtain required surface finish the selection of optimal cutting condition so as to minimize the total production time is aimed in this work. In contrast to structured conventional/traditional algorithm, this paper discusses the use of three non-conventional optimization methods viz., Particle Swarm Optimization (PSO), Teaching Learning Based Optimization (TLBO), and Fuzzy set based optimization to solve optimization problem. To demonstrate the procedure and performance of the approach illustrative examples are discussed. The algorithms are coded in Matlab$^{®}$ and computational efforts, accuracy of result, effectiveness of algorithm are compared.

Keywords: Finish milling, fuzzy set, optimization, PSO, TLBO.

1 Introduction

Optimization of machining parameters is an important step for the selection of cutting conditions in CNC machining being used in today's automated manufacturing system. Among several CNC machining process, face milling is one of the commonly used metal removal operations for machining casted components due to its ability to remove material faster with reasonable good surface quality. For optimizing the process, number of researchers used various conventional and non-conventional optimization techniques both for single or multi pass machining problems. The conventional methods of optimization such as graphical techniques, constrained optimization strategy, dynamic programming, branch and bound algorithm, etc., have been used for the optimization of cutting parameters [1,2]. These techniques are found to be ineffective since they either result in local minima, or take long time to converge on a reasonable result. Mukherjee and Ray [3] mentioned that the determination of optimal cutting conditions through cost–effective

mathematical models is a complex research for long time and the techniques for process modeling and optimization have undergone substantial development and expansion. In recent past, the researchers have used soft computing techniques as they are being preferred to physics-based models for predicting the performance of machining processes. Chandrasekaran et al. [4] have reviewed nearly 20 years of research work in the area of metal cutting processes with the application of soft computing methods. The use of major soft computing tools such as neural networks, fuzzy sets, genetic algorithms, simulated annealing, ant colony optimization, and particle swarm optimization in performance prediction and optimization of four common machining process viz., turning, milling, drilling, and grinding is aimed in their work.

Wang [5] employed an optimization strategy for single pass end milling on CNC machine tools considering many practical constraints for optimization of minimum production time per component. Shunmugam et al. [6] used GA for optimization of multi pass face milling process to minimize minimum production cost. The machining parameters such as cutting speed, feed per tooth, depth of cut, and number of passes are optimized. Baek et al. [7] developed a method for optimization of a face milling process using a surface roughness model. Rao et al. [8] carried out the optimization of multi pass milling using three non-conventional optimization algorithms namely artificial bee colony (ABC), particle swarm optimization (PSO) and simulated annealing (SA). From the review of literatures, most of the researchers used soft computing based optimization methods and found good results over conventional optimization approach. The literature related to milling optimization is mainly concerned with single objective only, mostly of minimization of production time or cost. Also the fuzzy set based optimization, teaching learning based optimization is not attempted earlier in optimizing milling process.

In the present work, the determination of optimal cutting condition to achieve desired surface finish in a face milling process for minimizing the total production time is attempted. Three non-conventional optimization methods, viz., PSO, TLBO and Fuzzy set based optimization are employed to solve the problem. The accuracy of the results, computational effort, and efficiency of algorithm are found advantageous in comparison with conventional optimization techniques.

2   Mathematical Formulation

In CNC milling, the desired surface roughness is aimed in finish pass during which the depth of cut remains constant. The surface roughness mainly depends on selected cutting conditions viz., cutting velocity and feed per tooth. In this work, an optimization model proposed by Singh et al. [9] to minimize the total production time is used. The total production time composed of: (i) Actual machining time (Tm), (ii) Work piece loading and unloading time (Tl/u), (iii) Cutter change time (Ttc) and (iv) Machine preparation time (Tp) to produce batch of components. Thus the total production time being sum of all above is expressed as:

$$P_t = T_m + T_{l/u} + T_{tc} + T_p \tag{1}$$

$$P_t = \frac{\pi DL}{1000Vf_z z} + T_{1/u} + t_c \frac{\pi DL}{1000Vf_z z} \times \left[\frac{Vd^{x_v} f_z^{y_z} W^{t_v} z^{p_v}}{C_v K_v D^{q_v}} \right]^{1/m} + \frac{t_s}{B_s} \tag{2}$$

The objective is to minimize P_t.

Machining Constraints.

The practical constraints imposed during the process are mainly due to: (i) parameter bounds and (ii) operating constraints. The parameter bounds are expressed as:

$$V_{min} \leq V \leq V_{max} \quad \text{and} \quad (f_z)_{min} \leq f_z \leq (f_z)_{max} \tag{3}$$

Operating constraints namely cutting force, and cutting power constraints are considered in this modeling. The cutting force constraint aims to prevent chatter as well as to limit deflection of cutter which would otherwise lead to produce poor surface finish and dimensional deviation. The peripheral cutting force during face milling is given by [10].

$$P_z = \frac{C_F K_F W^{t_F} z^{p_F} d^{x_F} f_z^{y_F}}{D^{q_F}} = C_1 d^{x_F} f_z^{y_F} \tag{4}$$

where C_F and K_F are constants, t_F, p_F, x_F, y_F and qF are exponents and

$C_1 = \dfrac{C_F K_F W^{t_F} z^{p_F}}{D^{q_F}}$ hence, $P_z \leq P_{z_{(max)}}$.

Surface finish is affected by various parameters such as cutting speed, feed, depth of cut, tool geometry, etc. The empirical relation based on dominating parameters is expressed as [10]

$$R_a = 0.0321 \frac{f_z^2}{r} \tag{5}$$

where, r is the cutter tooth nose-radius. Hence the surface finish constraint satisfies if $R_a \leq R_{(max)}$. Combining cutting force and surface finish constraints, the variable bounds for feed are obtained as:

$$f_{z_{(min)}} \leq f_z \leq \min \left\{ f_{z_{(max)}}, \sqrt{\frac{R_{max} r}{0.0321}}, \left[\frac{Pz}{C_1 d^{x_F}} \right]^{1/y_F} \right\} \tag{6}$$

The cutting power during machining process should not exceed the maximum power (P_{max}) available at the machine tool spindle. It is given by

$$P = \frac{C_P K_P W^{t_P} z^{p_P} V d^{x_P} f_z^{y_P}}{D^{q_P}} = C_2 V d^{x_P} f_z^{y_P} \tag{7}$$

where C_P and K_P are constants, t_P, p_P, x_P, y_P and q_P are exponents and $C_2 = \dfrac{C_P K_P W^{t_P} z^{p_P}}{D^{q_P}}$.

Hence, $P \leq P_{(max)}$. This imposes the variable bounds for cutting speed as:

$$V_{min} \leq V \leq \min\left\{ V_{max}, \frac{P}{C_2 d^{x_P} f_z^{y_P}}, \right\} \tag{8}$$

3   Solving by Non-Conventional Optimization Methods

A. Particle Swarm Optimization Method

PSO is a population based stochastic optimization technique inspired by social behavior of bird or fish schooling, developed by Eberhart and Kenedy [11] in 1995. Similar to the behavior of birds a group of random particles (solutions) is initialized and searches for global optimum solution by updating generations. For n-dimensional space the position and velocity of ith particle in the search space is initialized as   and   respectively. The objective function value is considered as fitness value of each particle. The best solution of each particle (pbest) and the current global best (gbest) are stored. The new coordinates of the particle are updated in every generation according to the following relation:

$$v_{ij}(t+1) = w.v_{ij}(t) + c_1 r_1 (pbest_{ij}(t) - x_{ij}(t)) + c_2 r_2 (gbest_{ij}(t) - x_{ij}(t)) \tag{9}$$

$$x_{ij}(t+1) = x_{ij}(t) + v_{ij}(t+1) \tag{10}$$

$$j = 1, 2, 3, \ldots\ldots.n$$

where c_1 and c_2 are learning factors and r is a random number between (0,1) and w is the inertia weight for the present velocity.

Number of particles, particle co-ordinate range, learning factors, inertia weights and termination criteria are important PSO parameters. The algorithm effectiveness is mainly depends on proper selection of these values.

An Example.

Consider a finish pass milling process at a constant depth of cut of 1.5 mm to obtain desired surface finish of 2.0 μm. The length (l) and width (w) of the work piece is 300 mm and 150 mm respectively. The cutter size (D) is 160 mm. The length of travel by the cutter (L) is considered as (L + D) and is 460 mm. A work material of grey cast iron is machined with cutter made of cemented carbide. The other parameters remain constant as shown in Table 1.

Table 1. Numerical data of the example problem.

Process : Face Milling	
Cutting speed range (V)	50 – 300 m/min
Table feed range (f_z)	0.1 – 0.6 mm/tooth
Number of teeth (z)	16 Nos
Tool change time (t_c)	5 min
M/c preparation time (t_s)	15 min
Loading and unloading time ($T_{l/u}$)	1.5 min
Batch size (Bs)	150 Nos.

Constants and exponents
Tool life: C_v = 445, K_v = 1.0, m = 0.32, x_v =0.15, y_v = 0.35, p_v = 0, q_v = 0.2, t_v = 0.2
Cutting Force: C_F =534.6, K_F = 1.0, t_F = 1, p_F = 1.0, x_F =0.9, y_F = 0.74, q_F = 1.0
Cutting Power: C_P = 0.5346, K_P = 1.0, t_P = 1.0, p_P = 0, x_P =0.9, y_P = 0.74, q_P = 1.0

PSO was performed for desired surface roughness value of 2.0 μm. Ten particles are considered as initial population and the particle's co-ordinates are randomized in the solution space. In subsequent iterations all swarms move towards optimum and it is reached in 8th iterations. The optimum parameters are 180.9 m/min and 0.137 mm/tooth for V and f_z respectively. The total production time obtained is 2.2061 min. The algorithm was coded in Matlab® and run on a Pentium 4 PC.

B. Teaching-Learning-Based Optimization (TLBO) Method

In solving machining optimization problems 'nature-inspired' heuristic optimization techniques are becoming popular and proven to be better than conventional optimization methods. However, the applications of these algorithms are effective for specific kind of problem and the selection of optimal controlling parameters found to be difficult. Rao et al. [12] proposed a new optimization technique known as "Teaching-Learning-Based-Optimization (TLBO)" based on philosophy of the teaching-learning process. TLBO being population based method has a 'group of learners' learns both from the teacher in 'Teacher phase' as well as through interaction between them in 'Learner phase'. They have applied this technique for different benchmark design optimization problems and

shows better performance with less computational effort. This technique is applied here for obtaining optimal cutting parameters for finish milling process in which 'initial randomized solution' considered as 'number of learners', 'best solution of the iteration' as 'teacher of the iteration' and 'decision variables' as 'courses or subjects offered' by them in the process of learning.

Steps in the TLBO.

The optimization methodology based on TLBO [12] consists of following steps:

Step 1: Randomize initial population (n=number of learners) and the termination criteria (i.e., number of generation).

Step 2: In teacher phase, first calculate mean of each decision variables (V & f_z) of the optimization problem and identify mean row vector (i.e., MD = [V, f_z]). The new mean (M_new,D) is the best solution of the iteration and will act as a teacher.

Step 3: Now update the current solution by adding the 'difference of the means' to it. The difference between the means is given by Eq. 11.

$$Diff_D = r(M\_new_D - t_f \times M_D) \tag{11}$$

where r is a random number in the range [0,1] and t_f is teacher factor which is either 1 or 2. The new solution is accepted if it gives better function value otherwise not.

Step 4: In learner phase, select any two learners (data sets) and evaluate its function

values. Based on their function values the new data set (X_{new}) is calculated. If P_{t_1} and P_{t_2} are the two function values,

$$X_{new} = X_{old} + r(X_1 - X_2) \ \ if \ \ P_{t_1} < P_{t_2}$$
$$and \ \ X_{new} = X_{old} + r(X_2 - X_1) \ \ if \ \ P_{t_2} < P_{t_1} \tag{12}$$

Accept X_{new} if it gives better function value otherwise not.

Step 5: Continue from Step 2 till the termination criteria is met.

An Example.

   For the illustrated problem stated in previous section the optimum cutting condition obtained by TLBO is (180.9, 0.137) and the total production time at optimal cutting condition is 2.2061 min and the solution is converged in three iterations. Table 2 shows iteration wise result of the problem. Number of problems having depth of cut from 1.5 mm to 2.5 mm for different values of surface roughness are tested and results are better than PSO.

Table 2. Iteration wise result.

Iteration No.	Optimum cutting parameters (V (m/min) and f_z (mm/tooth))	P_t (min)
Input data (d,Ra): 1.5 mm, 2.0 μm		
1	177.9, 0.137	2.2172
2	180.7, 0.137	2.2073
3	180.9, 0.137	2.2061

C. Fuzzy Set Based Optimization Method

Prof. Zadeh introduced fuzzy set theory in 1965 and it has been applied to a number of engineering problems. Its applications include: (i) use of fuzzy set operations in decision making, (ii) use of fuzzy arithmetic wherein physical variables are considered as fuzzy numbers and (iii) use of fuzzy logic in modeling and control problems. Recently, Chandrasekaran et al. [13] have developed a fuzzy rule based optimization procedure for solving general optimization problems, which can provide an approximate and multiple solutions. They used fuzzy set theory as a general optimization tool for optimizing multi pass turning process and the method is applied here to obtain optimum cutting condition.

Steps in the Fuzzy Set Optimization.
The proposed optimization strategy using fuzzy logic consists of the following steps:

Step 1: The search domain is divided into a number of cells with the decision variables fuzzified into a number of fuzzy sub-sets. Membership grade 1 is allotted to centroids of the cell and 0 to the boundaries of the cell. A linear membership function is considered for the fuzzy subset.

Step 2: Machining is performed at each cell centroids and evaluate the function values at cell centroids. Now, decide the minimum ($P_{t_{min}}$) and maximum ($P_{t_{max}}$) values.

Fuzzyify them into n number of overlapping fuzzy sets as shown in Figure 5. If $P_{t_{min}}$ and $P_{t_{max}}$ are the variable bounds then for i-th fuzzy subset of the fuzzified variable, the value at the vertex corresponding to the membership grade 1 is given by:

$$\text{value at the vertex} = P_{t_{min}} + \frac{P_{t_{min}} - P_{t_{min}}}{n-1}(i-1) \tag{13}$$

The right and left limits of the fuzzy subset (vertices corresponding to 0 membership grades) are given by

$$right\,\lim it = P_{t_{\min}} + \frac{P_{t_{\max}} - P_{t_{\min}}}{n-1} i \quad and$$

$$left\,\lim it = P_{t_{\min}} + \frac{P_{t_{\max}} - P_{t_{\min}}}{n-1}(i-2) \tag{14}$$

The first fuzzy subset does not have a left vertex (0 membership grade) and last fuzzy subset does not have a right vertex (0 membership grade). Now, for each cell, the consequent part of the rule is the output of fuzzy subset at cell centroids and the strength of the rule is the membership grade of the fuzzy subset. A typical rule has the following form: "**If V is high and f_z is high, then P_t is very low**"

Step 3: Based on the rule base, desired objective and constraints the cell having the highest strength of the rule is selected and the search refined (starts with Step 1) in it. This identifies the optimum zone in which there is no significant variation in function value but provides number of optimal cutting conditions.

An Example.

Consider a finish pass milling process having depth of cut of 1.5 mm to obtain maximum desired surface roughness value of 2.0 μm. The linguistic sub division of search domain satisfying the constraints for this problem is as shown in Figure 1. The size of the search domain varies with problem in order to satisfy required constraints. Machining is performed at each of cell centroids and results are shown in Table 3.
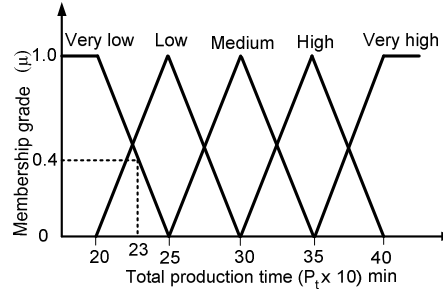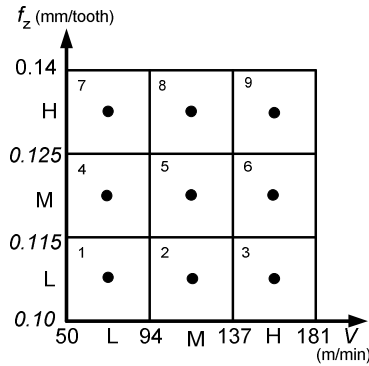

Fig. 1. Linguistic division of search domain   **Fig. 2**. Fuzzification of output variable.

Choosing $P_{t_{\min}} = 2.0$ and $P_{t_{\max}} = 4.0$ the output variable is fuzzified into 5 fuzzy subsets as shown in Figure 2. Table 4 depicts the rule base along with strength of the rules. As the problem objective is to minimize the function value, the rule 9 corresponds to cell 9 with the cutting condition of cell centroid (159.1, 0.132) having higher strength (membership grade) at low function value of 2.312, is fired. Thus, the search domain is reduced to $137 \le V \le 181$ and $0.125 \le f_z \le 0.14$.

Table 3. Function values at centroids of each cell.

Cell No.	Cell centroids V (m/min), f_z (mm/tooth)		Total Production time (P_t) (min)
1	(71.8,0.106)	(low-low)	3.498
2	(115.5,0.106)	(medium-low)	2.788
3	(159.1,0.106)	(high-low)	2.473
4	(71.8,0.119)	(low-medium)	3.301
5	(115.5, 0.119)	(medium-medium)	2.670
6	(159.1,0.119)	(high-medium)	2.384
7	(71.8, 0.132)	(low-high)	3.141
8	(115.5,0.132)	(medium-high)	2.570
9	(159.1,0.132)	(high-high)	2.312

Input data (d,R_a): 1.5 mm, 2.0 μm

Table 4. Fuzzy rule base with membership strength.

Cell No	Cutting speed (V)	Feed (f_z)	Total production time (P_t)	Membership grade
1	Low	Low	High	1.0
2	Medium	Low	Low	0.4
3	High	Low	Low	1.0
4	Low	Medium	Medium	0.4
5	Medium	Medium	Low	0.6
6	High	Medium	Very Low	0.2
7	Low	High	Medium	0.8
8	Medium	High	Low	0.8
9	**High**	**High**	**Very Low**	**0.4**

The new search is now initiated in the identified search domain, dividing it into 4 cells with the fuzzy sub-set being 'low' and 'high'. This provides new domain: $159.1 \leq V \leq 180.9$ and $0.13 \leq f_z \leq 0.14$. The function value has no significant variation which is in the range between 2.2 and 2.3. Thus, with the given range of cutting speed and feed rate, the fuzzy set based optimization provides the following solution.

$$159.1 \leq V \leq 180.9, \quad 0.13 \leq f_z \leq 0.14 \tag{15}$$

With small variation in time the fuzzy set based optimization provides multiple numbers of solutions.

A number of other problems having depth of cut varying from 1.5 mm to 2.5 mm for different values of desired surface roughness are tested. The optimum zone provides multiple solutions to the problem. The function value and surface roughness produced in optimum fuzzy domain do not vary significantly.

4   Results and Discussion

Table 5 shows the comparison of the results obtained by three optimization methods. Based on computational results presented herein, it may be concluded that the proposed non-conventional optimization methods are advantageous and can be applied to machining optimization problem. PSO algorithm being a random search obtains optimal or near optimal global solution with 10 or less number of iterations. It requires proper selection of controlling parameters and algorithm effectiveness mainly depends on it. TLBO takes less number of iterations in reaching global optimum solution. Though the result obtained by both techniques is very close. Of the two, TLBO provides marginally better result than PSO. Fuzzy set based optimization technique provides multiple numbers of solutions having feasibility for alternative selection of optimum cutting condition. It may be noted that the optimal solution obtained by PSO and TLBO for different problems are within the optimum fuzzy domain. The linguistic subdivision of the domain provides an optimum zone in the solution space range, in which the objective function value does not change drastically. The feasibility of incorporating an expert knowledge is one of the main advantages of this method.

Table 5. Comparison of results.

Desirable surface finish $R_a(\mu m)$	For 1.5 mm depth of cut		
	Optimum cutting parameters (V, f_z), Minimum production time (P_t)and Number of iterations (i)		
	PSO $(V,f_z):P_t:i$	TLBO $(V,f_z):P_t:i$	Fuzzy set $(V; f_z; P_t)$
2.0	(180.9,0.137):2.2061:8	(180.9,0.137):2.2061:3	$159.1 \leq V \leq 180.9; 0.13 \leq f_z \leq 0$ $2.2 \leq P_t \leq 2.3$
2.5	(166.7,0.150):2.1894:8	(166.7,0.150):2.1893:3	$157 \leq V \leq 167; 0.14 \leq f_z \leq 0.15$ $P_t = 2.2$
3.0	(156.3,0.167):2.1743:7	(156.3,0.167):2.1742:2	$147.4 \leq V \leq 156.8; 0.16 \leq f_z \leq 0$ $P_t = 2.2$
4.5	(134.3,0.205):2.1401:9	(134.3,0.205):2.1400:4	$127.2 \leq V \leq 134.5; 0.19 \leq f_z \leq 0$ $2.1 \leq P_t \leq 2.2$
5.0	(129.2,0.216):2.1313:7	(129.2,0.216):2.1310:3	$122.6 \leq V \leq 129.2; 0.21 \leq f_z \leq 0$ $2.1 \leq P_t \leq 2.2$

   In general the result shows that the total production time per component reduces as the maximum allowable surface finish increases. Figure 3 shows the result of total production time Vs desired surface roughness for different values depth of cut. From the graph it is evident that the production time decreases as depth of cut decreases. However in finish machining process depth of cut remains constant. Among the other two influencing parameters i.e., feed and cutting velocity, feed is constrained mainly due to desired surface roughness value while cutting velocity by cutting power. Since the cutting power is the function feed, depth of cut and cutting velocity, the increased depth of cut proportionately decreases optimum cutting velocity while feed remains fixed due to surface roughness criterion.
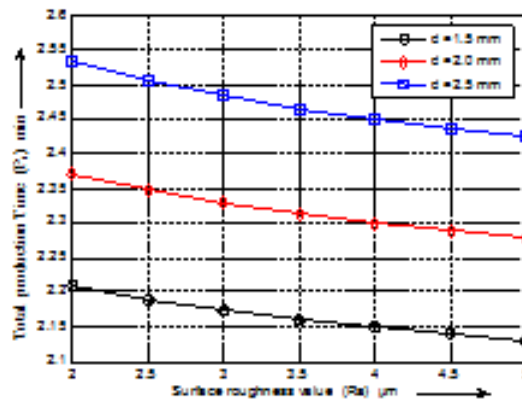

Fig. 3. Variation of 'Ra' Vs 'P_t'.

5   Conclusions

In this work, CNC milling process is optimized to minimize total production time and so as to obtain desired surface finish value of the components produced. Cutting speed and feed per tooth as decision variables and practical constraints such as cutting force, cutting power, surface roughness, and variable bounds of the decision variables are considered in model formulation. Three non-conventional optimization methods viz., PSO, TLBO, and Fuzzy set based optimization are employed to solve the problem. The solution methodology is presented with an illustrated example and numbers of problems are solved.

   Both PSO and TLBO provide better solution accuracy with less computational effort compared with conventional optimization techniques. Of the two, TLBO provides marginally better result than PSO with less number of iterations. PSO need proper

selection of controlling parameters and effectiveness of algorithm is mainly depends on it. While TLBO is free from such algorithm parameters and found easy to implement it. Fuzzy set optimization is based on linguistic subdivision of the domain providing a 'range of optimal solution' in which the objective function value does not change drastically. Thus the procedure provides multiple numbers of optimal solutions having feasibility for alternative selection. Source codes for all three methods are written in MATLAB 7.2 and computational time takes less than a second in Pentium-IV with RAM 512. The code can be used for other finish machining process as well as for multi pass machining with necessary modification

References

1. Armarego, E.J.A., Smith, A.J.R., Wang, J.: Constrained optimization strategies and CAM software for single-pass peripheral milling. Int. J. Prod. Res. vol. 31, no. 9, pp. 2139–2160 (1993)
2. Wang, J., Armarego, J.A.: Computer-aided optimization of multiple constraint single pass face milling operations. Mach. Sci. Technol., vol. 5, no. 1, pp. 77–99 (2001)
3. Mukherjee, I., Ray, P.K.: A review of optimization techniques in metal cutting processes. Computers & Industrial Engineering, vol. 50, no. 1–2, pp. 15–34 (2006)
4. M. Chandrasekaran, M., Muralidhar, C., Krishna, M., Dixit, U.S.: Application of soft computing techniques in machining performance prediction and optimization: a literature review. Int. J. of Adv. Manuf. Technol, vol. 46, no. 5–8, pp. 445–464 (2010)
5. Wang, J.: Computer aided economic optimisation of end milling operations. Int. J. Prod. Econ., vol. 54, pp. 307–320 (1998)
6. Shunmugam, M.S., Bhaskara Reddy, S.V., Narendran, T.T., Selection of optimal conditions in multi-pass face-milling using a genetic algorithm. Int. J. Mach. Tools Manuf., vol. 40, pp. 401–414 (2000)
7. Baek, D.K., Ko, T.J., Kim, H.S.: Optimization of feed rate in a face milling operation using a surface roughness model. Int. J. of Mach. Tools & Manuf., vol. 41, pp. 451–462 (2001)
8. Rao, P.V., Pawar, P.J.: Parameter optimization of a multi-pass milling process using non-traditional optimization algorithms. Applied soft computing, Vol. 10, 2010, pp. 445–456 (2010)
9. Singh, A.K., Chandrasekaran, M., Murali Krishna, C.: Optimization of finish-pass milling process with practical constraints using particle swarm intelligence. Proc. 3rd Intl. & 24th AIMTDR conference, Visakhapatnam, India. pp. 519–524 (2010)
10. Nefedov, N., Osipov, K.: Typical examples and problems in metal cutting and tool design. MIR Publishers, Moscow (1987)
11. Kennedy, J., Eberhart, R.: Particle swarm optimization. In: Proc. IEEE Intl. Conf. on Neural Networks (ICNN'95) Perth, Australia (1995)

12. Rao, P.V., Sasani, V.J., Vakharia, D.P.: Teaching-learning-based optimization: A novel method for constrained mechanical design optimization problems. Computer-Aided Design, vol. 34, pp. 303-315 (2011)

13. Chandrasekaran, M., Muralidhar, M., Dixit, U.S.: Optimization of engineering problems by Fuzzy set theory: An Application to Multipass Turning process. In: Proc. IISN-2010 Conf. ISTK, Yamuna Nagar, Haryana, INDIA. pp. 539–542 (2010)

Dynamic Quadratic Assignment to Model Task Assignment Problem to Processors in a 2D Mesh

A. Velarde M.[1], E. Ponce de Leon S.[2], E. Díaz D.[2] and A. Padilla D.[2]

[1] NSS Softtek, Unix Developer
[2] Universidad Autónoma de Aguascalientes, Mexico

Abstract. Mesh multicomputers systems are a viable option for parallel computing. The process of executing a task in such systems is to assign a set of *n+1* mesh-free processors to the task at the head of the queue consisting of n subtasks. We assume that a task has a parent process and child processes that are called subtasks. These allocations are based on methods that seek to maintain the execution of the task in adjacent processors, and methods that avoid maintaining free sub-meshes in the mesh caused by tasks that have completed their execution. Assign N facilities to a number N of sites or locations where it is considered a cost associated with each of the assignments can be seen as a quadratic assignment problem whose solution combinations grow exponentially, an NP-complete problem. This paper describes a method for modelling dynamic quadratic assignment problem of assigning tasks to processors in 2D mesh multicomputers system, using the simplest class of the Estimation of Distribution Algorithm (EDA), the Univariate Marginal Distribution Algorithm (UMDA) which aims to enable calculation of a distribution joint probability from the selected tasks in the queue that are susceptible to initiate enforcement in the mesh. Experiments are based on a comparison the proposed method with two more methods of allocation of tasks to processors: Hilbert curves and linear assignment. The results show better time allocation, and better utilization of free processors but more times during the process of full recognition of the mesh. The denser workload down to 256 with 256 subtasks tasks each, 16×16 mesh size, that correspond to 256 processors.

Keywords: Parallel computing, mesh multicomputer, estimation of distribution algorithm, univariate marginal distribution algorithm.

1 Introduction

Distributed computing has been considered as the future of high performance computing [1]. The study of partitioning of different distributed computing systems such as multiprocessor systems shared memory multicomputers systems with transfer messages and wide-area distributed systems have been extensively studied in order to get more computing power, and thus permit tasks that are inherently parallel [2], run on shorter time. Examples of these tasks that require more computing power than a single node can provide are: access to distributed

data in different groups of computers [3], the graphics processing tasks [2] and in fields of science and engineering.

Parallel computing consists of a set of processors which cooperate with each other to find a solution to a given problem [4]. The processor communication can be based on shared memory or distributed memory model. In shared memory architectures also known as multiprocessor systems, processors communicate via shared memory. However, in parallel computers with distributed memory also known as multicomputers the processors communicate is by exchanging messages through interconnection network [5].

To solve a problem using parallel computing should break down problem into smaller subproblems that can be solved in parallel. The results should be efficiently combined to obtain the end result of the main problem, but is not easy to break a problem due to data dependency that exists in it and then. Due to data dependency that exists in a problem, it is not easy to divide it into subproblems because the load of communication when the problem is running in parallel is very high. The important point here is the time taken for communication between two processors compared to the processing time. Due to this factor communication scheme should be well planned to get a good parallel algorithm [4].

There are several approaches to implement parallel computing: through meshes [6], squares (grids) [3], and heterogeneous platforms [2], using certain performance metrics, heuristics such as simulated annealing [1] or the greedy algorithm [3], and alternative methods such as measuring the workload, where the workload is generated not by discovery but dynamically by user models that interact with the system and whose behaviour in simulation is similar to the behaviour of users in reality [8].

The vast majority of research converge on the approach that two structures are to be developed in software for coexistence of multiple processors executing tasks in parallel: the allocation Processor and Task Scheduler [9].

Some of the objective functions that is desirable to minimizing or maximizing in the research work are: reduce the starvation of jobs, decrease internal fragmentation, reduce external fragmentation, reduce costs communication within local networks to reduce communication costs in wide area networks, reduce the number of jobs in the queue, maximize the number of jobs running in parallel, maximizing the time response to users to maintain their satisfaction and motivate them to bring more jobs to the system [8].

The optimization problems that model a physical system which involves one objective function perform the task of finding an optimal solution is called a single objective optimization, and when the problem optimization involves more than one objective function, the task of finding one or more optimal solutions is known as multi-objective optimization, also known as Multiple Criterion Decision-Making (MCDM) [10].

In evolutionary computation have emerged parallel multi-objective evolutionary algorithms their application to solve problems with long performance, excessive memory requirements to solve complex problems, decrease the like-

lihood of falling into local optima, find solutions domains simultaneously and work with multi-objective [11].

The objective of this paper is to describe a method for modelling dynamic quadratic assignment problem of assigning tasks to processors in 2D mesh multicomputers system, using the simplest class of the estimation of distribution algorithm (EDA), the univariate marginal distribution algorithm (UMDA)which aims to enable calculation of a distribution joint probability from the selected tasks in the queue that are susceptible to initiate enforcement in the mesh, considering two structures that are necessary to execute tasks in parallel: the Allocation Processor and Task Scheduler.

2   Allocation Algorithms

Efficient allocation of processors and scheduling tasks are two critical processes if the computational power of large-scale multicomputers want to effectively use [12]. Allocation Processor is responsible for finding, selecting and assigning all processors on which a parallel job will run, while the Task Scheduler is responsible for determining the order in which the jobs are selected for execution using a scheduling policy [13].

If a job arrives and can not be immediately executed within the system due to lack of free processors, or the existence of other jobs running, it is sent to the queue. Once the processors are assigned to a task, they remain allocated exclusively to it until the task ends. When the task ends and leaves the system, processors are released and made available to Allocation Processor. One of the main goals of parallel execution is to minimize the time that a job waits a set of free processors in the mesh are assigned to it, so it is important to develop algorithms with efficient allocation strategies processors, that minimize waiting time of tasks within the mesh.

Is necessary to consider the following definitions:

Definition 1. *An n-dimensional mesh has $k_0 \times k_1 \times ... \times k_{n-2} \times k_{n-1}$ nodes, where k_i is the number of nodes along the ith dimension and $k_i \geq 2$.Each node is identified by n coordinates, $\rho_0(a)$, $\rho_1(a)$, ... , $\rho_{n-2}(a)$, $\rho_{n-1}(a)$, where $0 \leq \rho_i(a) < k_i$ for $0 \leq i < n$. Two nodes a and b are neighbours if and only if $\rho_i(a) = \rho_i(b)$ for all dimensions except for one dimension j, where $\rho_j(b) = \rho_j(a) \pm 1$. Each node in a mesh refers to a processor and two neighbours are connected by a direct communication link.*

Definition 2. *A 2D mesh, which is referenced as $M(W, L)$ consists of $W \times L$ processors, where W is the width of the mesh and L is the length. Each processor is denoted by a pair of coordinates (x, y), where $0 \leq x < W$ y $0 \leq y < L$. A processor is connected by a bidirectional communication link to each of its neighbours.*

Definition 3. *In a 2D mesh, $M(W, L)$, a sub-mesh $S(w, l)$ is a sub-two-dimensional mesh nodes belonging to $M(W, L)$ with width w and length l, where $0 < w \leq W$ y $0 < l \leq L$. $S(w, l)$ is represented by the coordinates (x, y, x', y'), where (x, y) is the lower left corner of the sub-mesh and (x', y') is the upper right corner. The node of the lower left corner is called the base node of the sub-mesh node and the upper right corner is the end node. In this case $w = x' - x + 1$ and $l = y' - y + 1$. The size of $S(w, l)$ is $w \times l$ processors.*

Definition 4. *In a 2D mesh $M(W, L)$, an available sub-mesh $S(w, l)$ is a free sub-mesh that satisfies the conditions: $w \geq \alpha$ y $w \geq \beta$ assuming that the assignment of $S(\alpha, \beta)$ requested, where the assignment refers to selecting a set of processors for a task arrival.*

2.1   Processor Allocation Strategies

Two strategies have been developed for the allocation of processors [12], and their classification reflects the type of recognition is performed on the mesh of processors: *contiguous processor allocation strategies* and *non contiguous processor allocation strategies*. In this section we briefly summarize processor allocation research, paying special attention to request partitioning based strategies used in our study.

Strategies contiguous processor allocation, appears when you have a partial recognition of the system and can be assigned for the execution of work, only contiguous sub-mesh of processors to jobs that request. The figure 1 shows a contiguous allocation strategy of 4 processors in a mesh of size 4×4.
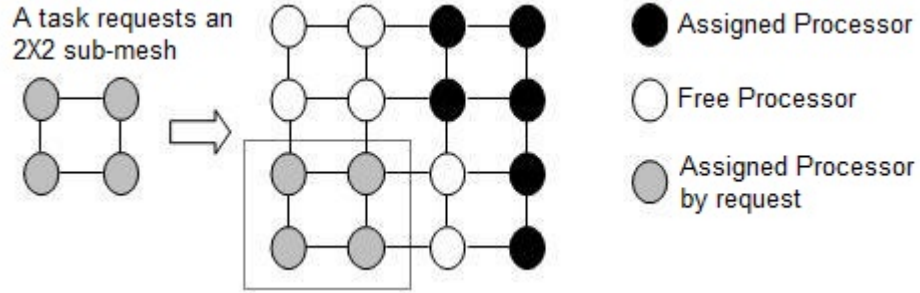
Fig. 1. Contiguous allocation of 4 processors in a mesh of size 4×4.

Such a strategy implies that even with the number of free processors in the system, it is not possible to assign if the sub-meshes are not contiguous. Suppose a task T that requests a sub-mesh 2×2 as shown in figure 1, there is still a number of free processors containing the sub-meshes that are not contiguous, so the task should be put into the queue system where it remains until a sub-mesh size requested is available. This causes a 4-processor external fragmentation.

The fragmentation of processors can be of two types: internal and external [14]. Internal fragmentation occurs when more processors are assigned to a job that really requires, while external fragmentation occurs when there are enough free processors to satisfy outstanding allocation requests but can not be assigned because it is not contiguous, figure 1 exemplifies this kind of fragmentation.

Contiguous processor allocation strategies have been developed by different research for 2D mesh connected multicomputers, examples of these are the Two Dimensional Buddy System (2DBS) [15], Frame Sliding (FS) [16], Adaptive Scan [17] , First Fit (FF) and Best Fit (BF) [18]. 2DBS strategy only applies to square mesh systems by leading to external processor fragmentation. The FS strategy is applicable to a mesh of any size and shape but made âĂŃâĂŃno acknowledgement of all sub-nets free, so it produces external fragmentation. The FS technique applies an operation that allows a frame to slide across the screen. AS strategy improves system performance by applying an exchange procedure orientation of the application when it can not be accommodated in the original orientation, for example if a job requests a sub-grid is $\alpha \times \beta$ not available, can be assigned to a sub-mesh $\beta \times \alpha$ however, the allocation time is high compared with FS because the search of processors in the mesh is at a distance of a processor in a vertical direction. FF and BF strategies detected all free sub-mesh big enough, but lack the ability to complete detection of sub-nets because they do not exchange the orientation of the applications.

To reduce the fragmentation of contiguous processor allocation produced, *non-contiguous processor allocations strategies* have been proposed [19]. In the *non-contiguous allocation* techniques jobs can run on multiple disjoint sub-meshes, avoiding a wait of one sub-mesh size and shape required. Figure 1 when a job requests allocation of a sub-grid of size 2×2) contiguous allocation fails because a sub-mesh the number of processors available is not contiguous. However, the four free processors (drawn with white circles into the figure 1) can be assigned to work when we adopt a non-contiguous allocation. Although non-contiguous allocation can increase the transfer of messages on the network, improving the contiguity to reduce external processor fragmentation and increase usefulness.

The widespread adoption of wormhole routing [19], whose main characteristic is the latency of messages, less sensitive to the distance and have the ability to moderate heavy traffic conditions in practical systems, has consider non-contiguous allocation for multicomputers that use long distance communication. The method used to respond to requests for partitioned allocation has a significant impact on the performance of non-contiguous allocations, so you should go to maintain a high degree of contiguity among processors assigned to a parallel to the overhead of communication reduced without affecting overall system performance [19].

The non-contiguous allocation strategies have been developed are: Random [14], Paging [14], Multiple Buddy Strategy MBS [14], Adaptive Scan Multiple Buddy and ANCA [19], Adaptive Multiple Scan Buddy and AS & MB [21], and variants of page Recent [24]. At Random [14], internal and external fragmentation is eliminated but there is a high interference of communication between

jobs. In the Paging method [14], there is a degree of contiguity among processors assigned to a parallel, which increases if you use more pages size. However there may be internal fragmentation of the processor when pages are allocated to large jobs do not require complete. MBS [14], improves the performance compared to previous strategies but it presents problems when assigning a sub-mesh contiguous free processors, so you can increase the communication overhead. ANCA [19] divide the application in 2^i equal parts in the ith iteration and requires partitioning and assignment occur in the same iteration, which causes in a previous iteration are not allocated sub-meshes to a large part of the application, which can increase the communication overhead. The performance of AS & MB [21], the response time and service are identical the MBS [14], however AS & MB has high overhead allocation for large meshes. In the variants paging unit allocation is a single processor, which requires more time to make a decision allocation in large mesh, while in MBS [14] and ANCA [19], allocation unit increases so it takes a long time to make an assignment in large systems.

3   Task Assignment Problems in a Computer Environment Distributed

The problems of assignment, have evolved along with the architecture of distributed and parallel systems, this evolution has brought some problems with performance, on which is:

- All resources reside under a single domain.
- The resource set is invariant.
- Applications and data reside on the same site or the data collection is a highly predictable.

The scheduling in multicomputers Systems (Job Scheduling Task Scheduler) is the selection and assignment of a partition of processors to a parallel task, with the inherent objective of maximizing the performance of a running workflow [6].The task and its subtasks that are distributed among the processors to be executed communicate with each other to synchronize or to exchange any partial or final result [5].

In multicomputers system once a task or process has assigned to a multiple nodes, can be use any scheduling local algorithm. However, precisely because it has very little control when assigns a process to a node, it is important to the decision of which process should be in which node. Therefore worth considering how to allocate effectively processes to nodes. The algorithms and heuristics used to make such assignment is called processor allocation algorithms [7] performed the schedule Job [7]. There are processor allocation algorithms have been proposed over the years, considering the local assignment in which the task is assigned on one processor and those that allow assignment to a subset of multicomputers system processor, which will be explained in detail in the following sections. Both types of algorithms seek to maximize the clock cycles [7] to avoid and the waste of CPU due to the lack of local labour, minimize the total bandwidth of

communication and ensure equity for users and processes. The differences lie in what is known and what is to be achieved. Among the properties of a process that could be known are: the needs CPU time, memory consumption and the amount of communication with all other processes.

4 Metaheuristics Applied to the Problem of Scheduling Tasks

As defined above, the allocation of tasks is a scheduling problem of tasks that should be assigned to a set of machines. Considering the variation of the job shop (JS) applicable to this research project, then describe some metaheuristics applied to this particular planning problem, in the knowledge that for every aspect of the problem of planning there are different uses of heuristics.

In [25] used branch and bound techniques and present the known graph-directed search method, with which proceeds to traverse a tree, whose nodes are sequences of operations manufacturing in line. They do not consider lines with penalties for delays or for the steps of the tasks from one machine to another, hence the direct applicability of a method sweep of trees in the instrument selection process and trajectories.

In [26] is incorporated two new concepts in the development of an algorithm GRASP (Greedy Randomized Adaptive Search Procedures) for the JSP standard: a strategic escalation procedure (another form of probability distribution) to create candidates for technical solution and a POP (its acronym in English Proximate Optimality Principle) also in the construction phase. Both concepts have already been applied to solve quadratic assignment problem. Genetic algorithms are applied in [27]. In this paper, the representation of chromosomes is based on random charges of elitism, the authors seek to mimic the behaviour of a variable work environment in a flexible production line. On the other hand in [28], is the division of tasks in very small chromosomes so that the populations generated are as varied as possible. Tabu Search is used in [29], in this work are as neighbourhoods for the implementation of the tabu list to the movement of a candidate operation i-ésima task to program a machine to another machine, with the Tabu list that matrix of operations and machines which run, other interesting works can be found in [30] considers a flexible route, which is defined as one where there are machines that can run more than one type of operation, extending the definition of the JSP, in [31] apply the concepts of JSP on distributed computing techniques in programming tasks.

5 The Quadratic Assignment Problem

In Quadratic Assignment Problem (QAP), we have a set of n places and n tasks, and assign to each place a task, so there $n!$ possible assignments. To measure the cost of each possible allocation, multiply the flow between each pair of tasks by the distance between the assigned locations and all pairs are added. Our goal

is to find the allocation that minimizes the costs of this process. Considering the example of assigning the tasks of the input queue of figure 2,where you have 3 tasks with 4 different machines, then you have 12 possible assignments to perform 3 tasks, otherwise, if you have a list of tasks that must be assigned glued to a mesh of processors should consider the distances between processors which will be assigned tasks and subtasks, as well as costs of communication between them [29].
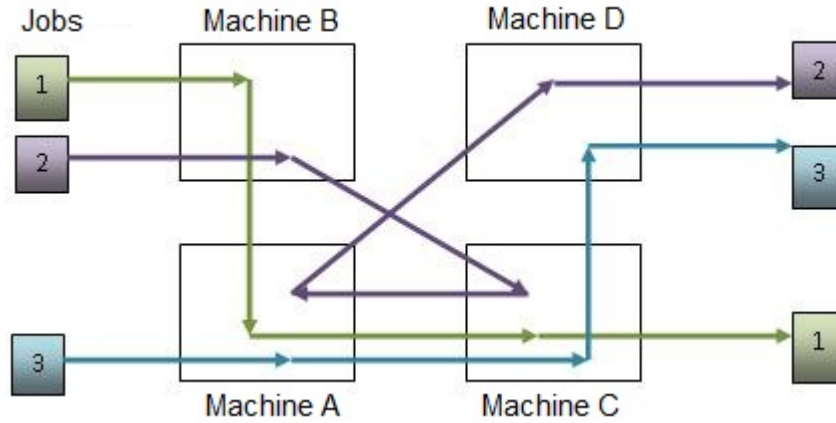
Fig. 2. Three tasks with four different machines

Mathematically we can formulate the problem by defining two matrices of size $n \times n$: a matrix flow F whose $(i,j)-ith$ elements represents the flows between tasks i and j and an array of distances D whose $(i,j)-ith$ elements represent the distance between sites i and j. An assignment is represented by the vector p, which is a permutation of the numbers $1, 2, \ldots, n$. $p(j)$ is the place where the task j is assigned. With this definition, the quadratic assignment problem can be written as:

$$min_{p\in} \ \sum_{i=1}^{n} \ \sum_{i=1}^{n} \ f_{ij}dp(i)p(j)$$

QAP is NP-complete. It is seen as the problem of NP-complete combinatorial optimization more difficult. Troubleshooting larger than 30 (eg over 900 0-1 variables) is computationally impractical. Among the algorithms used to solve the QAP the Branch and Bound has been the most successful. However, the loss of a lower limit is one of the greatest difficulties, because it is inaccurate or the time required to calculate it is computationally impractical.

6 Statement of Dynamic Quadratic Assignment Problem to model the assignment of tasks to processors in a 2D mesh multicomputers System

Given the gaps in the mesh, the chance to swap tasks at time t is given by the minimization function:

$$min\ e(\pi^t) = (d_{ij})(m_{ij}) + ... + (d_{ik,jk})(m_{ik,jk})$$

Looking for the smallest value found in the set of all possible assignments at time t whose domain is the possible permutations of tasks within a sub-grid.

6.1 Description of the Modelling Problem

The assumption that we have a priori in the Modelling Problem is the knowledge of the degree of communication between the main task and subtasks of all tasks that are in the queue, and the relationship between those subtasks, for example if you have a task *T1* with three subtasks *S11, S12 and S13* the interaction that can occur between them is illustrated in figure 3 through lines showing the message transfer.
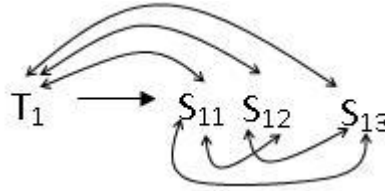
Fig. 3. Message passing between tasks, a task with 3 subtasks.

There is also a symmetric matrix of distances between processors that specifies the hops that a message must be made between a processor and another. Given this process of allocation of processors is based on carrying out a calculation of allocation of processors based on their availability in the Grid and Tasks in the queue.

6.2 Example

Consider the following example. At a time t we have a mesh processor array of size 4×4 whose status is shown in Table 6.2, where 1 represents a processor busy which was assigned to a task at time *t-1*, and 0 is not a free processor has been assigned to a task or subtask, the symmetrical distance between processors are given by a the distance matrix where every value is calculated for each pair of

processors and the distance between them is defined as the length of the shortest path that connects a processor with the other on the mesh. In the queue are 4 Tasks pending execution in the order presented in Table 6.2, these tasks are waiting for the mail run and a matrix of communication costs of each task with its subtasks and among subtasks in Table 6.2.

Table 1. State matrix of the mesh in time t.

1	1	1	1
1	1	1	1
0	0	0	1
0	0	0	0

Table 2. Input queue of tasks in a time t.

T_1	S_{11}	S_{12}	S_{13}	0
T_2	S_{21}	S_{22}	0	0
T_3	S_{31}	S_{32}	S_{33}	0
T_4	S_{41}	0	0	0

To generate the first assignment we take the state matrix of the mesh by a random assignment of tasks taken from the queue and will fit in the free sub-meshes. Each individual in the population represents an allocation of tasks and subtasks in the gaps as shown in Table 6.2 represents the matrix of assignments according to the state matrix at time t, in this way would generate an initial population random size 2, consisting of tasks T_1 and T_2.

To obtain the first value of the objective function, calculates the cost of the allocation for each task based on the communication costs between tasks and the distances between processors, given the passage of messages from one processor to another and vice versa . When considering message passing between processors must calculate the cost of their transfer, from source to destination and vice versa, i.e. for the case of the transfer rate exemplification of T_1 to S_{11} is different from S_{11} to T_1, but may be that both weights are equal, but the values âĂŃâĂŃof the distances remain the same. So to calculate the values is given in the operations shown in Table 6.2 for the task T_1, and Table 6.2 for the task T_2. The totals of the respective individuals are added to obtain the cost of the solution shown in Table 6.2, which is 35.

This is given by:

C_{ij} is the communication cost of i y j.

i is the task or subtask of the task.

j is the task or subtask of the task.

Table 3. Matrix communication costs between tasks.

	T_1	S_{11}	S_{12}	S_{13}	T_2	S_{21}	S_{22}	T_3	S_{31}	S_{32}	S_{33}	T_4	S_{41}
T_1	0	3	0	3	0	0	0	0	0	0	0	0	0
S_{11}	2	0	1	4	0	0	0	0	0	0	0	0	0
S_{12}	0	1	0	2	0	0	0	0	0	0	0	0	0
S_{13}	3	5	3	0	0	0	0	0	0	0	0	0	0
T_2	0	0	0	0	1	3	0	0	0	0	0	0	0
S_{21}	0	0	0	0	2	0	4	0	0	0	0	0	0
S_{22}	0	0	0	0	4	3	0	0	0	0	0	0	0
T_3	0	0	0	0	0	0	0	0	1	3	2	0	0
S_{31}	0	0	0	0	0	0	0	1	0	1	2	0	0
S_{32}	0	0	0	0	0	0	0	4	5	0	1	0	0
S_{33}	0	0	0	0	0	0	0	2	5	2	0	0	0
T_4	0	0	0	0	0	0	0	0	0	0	0	0	3
S_{41}	0	0	0	0	0	0	0	0	0	0	0	2	0

Table 4. Task allocation matrix according to state of the mesh at time t, which represents a first solution of the dynamic quadratic assignment problem.

1	1	1	1
1	1	1	1
S_{11}	S_{12}	S_{21}	1
T_1	S_{13}	T_2	S_{22}

Table 5. Calculating the cost of transferring messages to the task T_1.

$T_1 \to S_{11}$	$S_{11} \to T_1$	$(3+2)*1$	5
$T_1 \to S_{12}$	$S_{12} \to T_1$	$(0+0)*2$	0
$T_1 \to S_{13}$	$S_{13} \to T_1$	$(3+3)*1$	6
$S_{11} \to S_{12}$	$S_{12} \to S_{11}$	$(1+1)*1$	2
$S_{11} \to S_{13}$	$S_{13} \to S_{11}$	$(4+5)*2$	18
$S_{12} \to S_{13}$	$S_{13} \to S_{12}$	$(2+3)*1$	5
		Total	35

Table 6. Calculating the cost of transferring messages to the task T_2.

$T_2 \to S_{21}$	$S_{21} \to T_2$	$(1+2)*1$	3
$T_2 \to S_{22}$	$S_{22} \to T_2$	$(3+4)*1$	7
$S_{21} \to S_{21}$	$S_{22} \to S_{21}$	$(4+3)*1$	7
		Total	17

C_{ij} is the distance between processors which is assigned the task and subtask or subtasks.

The second assignment is generated by assigning tasks T_3 and T_4 to the mesh as shown in table 6.2.

Table 7. Task Allocation Matrix according to the State of the mesh in time t, which represents a second solution of the dynamic quadratic assignment problem.

1	1	1	1
1	1	1	1
S_{31}	S_{33}	0	1
T_3	S_{32}	T_4	S_{41}

It calculates the second value of the objective function in the same way as above, the values âĂŃâĂŃare given in Table 6.2 for Task T_3, and Table 6.2 for task T_4.

Table 8. Calculating the cost of transferring messages for task T_3.

$T_3 \rightarrow S_{31}$	$S_{31} \rightarrow T_3$	$(1+1)*1$	2
$T_3 \rightarrow S_{32}$	$S_{32} \rightarrow T_3$	$(3+4)*1$	7
$T_3 \rightarrow S_{33}$	$S_{33} \rightarrow T_3$	$(2+2)*2$	8
$S_{31} \rightarrow S_{32}$	$S_{32} \rightarrow S_{31}$	$(1+5)*2$	12
$S_{31} \rightarrow S_{33}$	$S_{33} \rightarrow S_{31}$	$(2+5)*1$	7
$S_{32} \rightarrow S_{33}$	$S_{33} \rightarrow S_{32}$	$(1+2)*1$	3
		Total	39

Table 9. Calculating the cost of transferring messages for task T_4.

$T_4 \rightarrow S_{41}$	$S_{41} \rightarrow T_4$	$(3+2)*1$	5
		Total	5

The generation of the third and fourth assignment shown in Table 6.2 occurs when assigning tasks to the mesh T_2 and T_4 with values âĂŃâĂŃobtained through the calculations in the first and second generation are applied in this, for the third value of the objective function.

In the fourth generation are assigned tasks T_2 and T_3 to the mesh to obtain a fourth value of the objective function. The assignment produced is shown in Table 6.2.

Table 10. Task Allocation Matrix according to the State of the mesh in time t, which represents a third solution to dynamic quadratic assignment problem.

1	1	1	1
1	1	1	1
0	0	T_{21}	1
T_4	S_{41}	T_2	S_{22}

Table 11. Task Allocation Matrix according to the State of the mesh in time t, which represents fourth solution of dynamic quadratic assignment problem.

1	1	1	1
1	1	1	1
S_{31}	S_{33}	T_{21}	1
T_3	S_{32}	T_2	S_{22}

7 UMDA for Dynamic Modeling Quadratic Assignment Problem to Model the Problem of Assigning Tasks to Processors in a 2D Mesh

The behaviour of the algorithms Evolutionary Computation most common (genetic algorithms and evolutionary strategies) depend on various parameters associated with them, crossover and mutation operators, crossover and mutation probabilities, population size, number of generations, replacement rate generation, etc. If you have no experience in the use of evolutionary algorithms in the optimization problem to be resolved, the determination of appropriate values âĂŃâĂŃfor the above parameters in itself becomes an optimization problem [54]. For this reason, together with the fact that predicting the movements of the population of individuals in the search space is extremely difficult, has led to the birth of a type of algorithms known as estimation algorithm distributions (EDAs).

In contrast to the genetic algorithms, EDA do not require operators crossover or mutation. The new population of individuals are obtained by simulating a probability distribution, which is estimated from a database containing selected individuals in generation above. For further reference the reader can consult [54].

In this type of algorithms used to estimate the model in each generation, the joint probability distribution from the selected individuals, $p_l(x)$ is as simple as possible. In fact, the joint probability distribution is factored as a product of independent univariate distributions. That is:

$$p_l(x) = p(x|D_{l-1}^{Se} = \prod_{i=1}^{n} p_l(x_i)$$

Each univariate probability distribution estimated from the frequencies marginal:

$$p_l(x_i) = \frac{\sum_{j=1}^{N} \delta_j(X_i = x_i | D_l - 1_e^S)}{N}$$

where:

$$\delta_j\left(X_i = x_i | D_{l-1}^{Se}\right) = \begin{cases} 1 \ if \ in \ the \ j - th \ event \ of \ D_{l-1}^{Se}, \ X_i = x_i \\ 0 \qquad\qquad\quad in \ another \ case. \end{cases}$$

The pseudo code for the UMDA, see Table 12.

Table 12. Pseudo code for the UMDA.

UMDA
$D_0 \leftarrow$ Generate M individuals (initial population) randomly

Repeat for $l = 1, 2, ...$ until the stopping criterion check

$\quad$ $D_{l-1}^{Se} \leftarrow$ Select $N \leq M$ individuals
$\quad$ of D_{l-1} according to a selection method

$\quad$ $p_l(x) = p(x|D_{l-1}^{Se} = \prod_{i=1}^{n} p_l(x_i) =$

$\quad$ $\prod_{i=1}^{n} \frac{\sum_{j=1}^{N} \delta_j(X_i = x_i | D_l - 1_e^S)}{N} \leftarrow$
$\quad$ To estimate the joint probability distribution

$\quad$ $D_l \leftarrow$ Sample M Sample m individuals, the new population from $p_l(x))$

Reading Parameters: Once you have completed the first assignment of tasks to the grid of processors, tasks start their execution so that at time t begin to vacate the sub-meshes. producing sets of processors that wait for tasks to be performed, as shown in Table 6.2. Based on the queue of tasks (see section), the planner performs a search of the tasks that can fit in such sub-meshes unoccupied. Once this selection is necessary to generate the initial population.

Initial population generation. Generating the initial population to generate each individual (allocation). The pseudo code for the generation of initial population is shown in Table 13.

Evaluate Population. As explained in Section 6.2, we obtain the total generated in Tables 6.2, 6.2, 6.2 y 6.2. The totals obtained are added to the assessment of an individual by the value obtained by the same objective function. The pseudo code for the evaluation of the population shown in Table 14.

Estimating the Probabilistic Model. In this part we will use the simplest probabilistic model, in which all the variables describing the problem are independent, so we calculate the frequency of apparition of a task in each empty cell of the mesh at time t of a part of the population who are the best individuals through a selection by truncation and the percentage of truncation. In this case the frequency of occurrence can be shown in Table 7, the pseudo code for estimating the probabilistic model shown in Table 16.

Generate the population from the Probabilistic Model. Pseudo code for generation the population from the probabilistic model is shown in Table 17, where

Table 13. Pseudo code for the generation of initial population.

Initial Population
Repeat for $Tasks = 1, 2, ...$ until the end of the queue of tasks
if TasksNumber in the position $Tasks =$
Number of free processors in the submeshes
Storage Allocation
if not
Consider the following sub-mesh empty
end if
Report the number of tasks and identification

Table 14. pseudo code for the evaluation of the population.

Evaluate Population
Repeat for $Tasks = 1, 2, ...$ until the end of the queue of tasks
that can be admitted to free submeshes.
Make the sum of the amounts obtained in each
calculation of the cost of transferring messages for tasks
Report the total value of the objective function

if you generate a random number between 0 and 4 and if it is between 0 and 1 the task T_1 is assigned.

Save the best individual. This process is accomplished by taking each population generated the best individual at the time of ordering the current population. The process of ordering from low to high is because the search is performed is minimized.

8   Experimental Design and Results

Experiments are based on a comparison the proposed method with two more methods of allocation of tasks to processors: *linear assignment* and *Hilbert curves*. *Linear assignment* is the most used method in the allocation of processors, the ease of implementation allows tasks to be quickly placed into the free mesh but presents difficulties when they begin to release sub-meshes and these are not contiguous. The nature of the method allows assignments of the bottom left of the mesh to the right. The recognition that the algorithm makes is based on a linear path of the mesh. The problems with this method are that we can not assign

Table 15. Frequencies of occurrence of each task in each cell.

	P(0,0)	P(0,1)	P(0,2)	P(0,3)	P(1,0)	P(1,1)	P(1,2)
T_1	1	0	0	0	0	0	0
S_{11}	0	0	0	0	1	0	0
S_{12}	0	0	0	0	0	1	0
S_{13}	0	1	0	0	0	0	0
T_2	0	0	3	0	0	0	0
S_{21}	0	0	0	0	0	0	3
S_{22}	0	0	0	3	0	0	0
T_3	2	0	0	0	0	0	0
S_{31}	0	0	0	0	2	0	0
S_{32}	0	2	0	0	0	0	0
S_{33}	0	0	0	0	0	2	0
T_4	1	0	1	0	0	0	0
S_{41}	0	1	0	1	0	0	0
$\sum$	4	4	4	4	3	3	3

Table 16. Pseudo code to Estimate the probabilistic model.

Estimating probabilistic model

Repeat for $AssignedTasks = 1, 2, ...$ until the end of the tables that
   contain the tasks that can be allocated to submeshes Free.

   Verify that the net position of each task is assigned, 1 posted on each
   assignment and stored in the matrix of the estimated
   probabilistic model
Report the values obtained in the frequency allocation

---

free sub-meshes in a different order, and presents difficulties when attempting to take free sub-meshes assignment by the linearity of procedure, this produces a high segmentation in the tasks and increasing the transfer of messages on the mesh.

Hilbert curves method is a very interesting method for assign tasks into the mesh. The Hilbert curve is a space filling curve that visits every point in a square grid with a size of 2×2, 4×4, 8×8, 16×16, or any other power of 2. It was first described by David Hilbert in 1892. Applications of the Hilbert curve are in image processing: especially image compression and dithering. It has advantages in those operations where the coherence between neighbouring pixels is important. The Hilbert curve is also a special version of a quad tree; any image processing function that benefits from the use of quad trees may also use a Hilbert curve.

The results obtained in tests arise in three important ways:

The waiting time processes in the input row. Both methods of assignment Gilbert curves and linear allocation establish a philosophy based on FIFO, both

Table 17. Pseudo code to generate the population from the probabilistic model.

Generation the population from the probabilistic model

if ($random \leq Dif[0]$) then P(0,0)=Sym[0]
else
    if ($random \leq Dif[1]$) then P(0,0)=Sym[1]
else
    if ($random \leq Dif[2]$) then P(0,0)=Sym[2]

---

do not compete for the assignment early into the mesh of processors so that a null starvation guaranteed, but the waiting times in the row are proportional to the times of the processes. Both methods ensure the allocation of tasks with subtasks in free submeshes close but as shown in the chart when the number of tasks, subtasks and their sizes increase, the waiting times are increased by the same proportionality.Gilbert curves during the process of free submeshes shows contiguous allocation, but due to allocation method used does not allow use them, but shows a tendency to use cluster of processors, which ensures that as the tasks increase also increases the processor usage across the grid, avoiding leaving idle processors.

The proposed method allows for competition on the waiting list. Every time a part of the mesh is indicated as free processor allocator is responsible to perform a search for tasks that can fit in the sub-grid. There is a greater tendency towards starvation of processes, when small submeshes are unoccupied small tasks are arranged, when small submeshes are unoccupied small tasks are arranged, when large tasks release large number of processors there are occupation by a small tasks too, tasks that require lots of processes waiting indefinitely until the requirements of small tasks are handled so that the waiting time for certain tasks tends to be higher.

The number of occupied meshes. In the two methods that use a FIFO allocation free submeshes processors can remain idle, even if there are jobs in the queue that require equal or lesser number of processors, these tasks wait until the shift assignment will be valid. In the proposed method dispatcher will search tasks that required number of processors is equal to or less than the number of processors in the sub-grid free. As shown in Figure 2, the proposed method allows greater utilization of processors in the allocation of tasks, reducing the idleness of processors.

9   Future Works

The works are planned to develop in the future are: Hardware implementation multicomputers system. Hardware implementation multicomputers system consisting of a number n of dedicated computers interconnected through a medium that allows message passing. Operate within the hardware structure with evolutionary algorithms to enable an evaluation of allocation of processors time,

processes starvations and percentage of idle processors vs percentage of processors used. Allow a real evaluation of evolutionary algorithms in a real scenario. Perform the evaluation with other evolutionary algorithms that include the three aspects that are being evaluated.

References

1. Jian Chen and Valerie E. Taylor: Mesh Partitioning for Efficient Use of Distributed Systems. IEEE Transactions on Parallel and Distributed Systems, Vol. 13, No. 1, January (2002)
2. Pierre-Francois Dutot, Tchimou N.Takpe, Frederic Suter: Scheduling Parallel Task Graphs on (Almost) Homogeneous Multicluster Platforms. IEEE Transactions on Parallel and Distributed Systems, Vol. 20, No. 7, July (2009)
3. Alessandro Amoroso, Keith Marzullo: Multiple Job Scheduling in a Connection-Limited Data Parallel System. IEEE Transactions on Parallel and Distributed Systems, Vol. 17, No. 2, February (2006)
4. C. Xavier and S. S. Iyengar: Introduction to Parallel Algorithms. Editorial: Wiley-Interscience, New York USA (1998)
5. A. Yassin Al-Dubai, M. Ould-Khaoua, L. M. Mackenzie: An Efficient Path-Based Multicast Algorithm for Mesh Networks, ipdps, pp.283, International Parallel and Distributed Processing Symposium (IPDPS'03) (2003)
6. Debendra Das Sharma and Dhiraj K. Pradhan: Job Scheduling in Mesh Multicomputers. IEEE Transactions on Parallel and Distributed Systems, Vol. 9, No. 1, January (1998)
7. T. Srinivasan, Jayesh Seshadri, Arvind Chandrasekhat and J. B. Siddharth Jonathana: Minimal Fragmentation Algorithm for Task Allocation in Mesh-Connected Multicomputers Proceedings. IEEE International Conference on Advances in Intelligent Systems Theory and Applications AISTA 2004 in conjunction with IEEE Computer Society, IEEE Press (2004)
8. Edi Shmueli and Dror G. Feitelson. On Simulation of Parallel-Systems Schedulers: Are We Doing the Right Thing? IEEE Transactions on Parallel and Distributed Systems, Vol. 20, No. 7, July (2009)
9. A. Velarde M., E. E. Ponce de Leon S., E. Diaz, A. Padilla: Planning and Allocation of processors in 2D meshes. Doctoral Consortium. Mexican Internacional Conference on Artificial Intelligence MICAI 2010 Pachuca Hidalgo, México (2010)
10. Kalyanmoy Deb: Multi-Objective Optimization using Evolutionary Algorithms. John Wiley & Sons, LTD. New York USA (2001)
11. Metaheuristics in Combinatorial Optimization: Overview and Conceptual Comparison CHRISTIAN BLUM Université Libre de Bruxelles AND ANDREA ROLI Universitá degli Studi di Bologna
12. Saad O. Bani Mohammad: Efficient Processor Allocation Strategies for Mesh-Connected Multicomputers. Tesis Doctoral. Faculty of Information and Mathematical Sciences University of Glasgow UK (2008)

13. B.S. Yoo and C.-R. Das: A Fast and Efficient Processor Allocation Scheme for Mesh-Connected Multicomputers, IEEE Transactions on Parallel & Distributed Systems, vol. 51, no. 1, pp. 46-60 (2002)
14. V. Lo, K. Windisch, W. Liu, and B. Nitzberg: Non-contiguous processor allocation algorithms for mesh-connected multicomputers, IEEE Transactions on Parallel and Distributed Systems, vol. 8, no. 7, pp. 712-726 (1997)
15. K. Li and K.H. Cheng: A Two-Dimensional Buddy System for Dynamic Resource Allocation in a Partitionable Mesh Connected System, Journal of Parallel and Distributed Computing, vol. 12, no. 1, pp. 79-83 (1991)
16. P.J. Chuang and N.F. Tzeng: Allocating precise submeshes in mesh connected systems, IEEE Transactions on Parallel and Distributed Systems, vol. 5, no. 2, pp. 211-217 (1994)
17. J. Ding and L.-N. Bhuyan: An Adaptive Submesh Allocation Strategy for Two-Dimensional Mesh Connected Systems, Proceedings of the 1993 International Conference on Parallel Processing, vol. 2, pp. 193-200 1(993)
18. Y. Zhu: Efficient processor allocation strategies for mesh-connected parallel computers, Journal of Parallel and Distributed Computing, vol. 16, no. 4, pp. 328-337 (1992)
19. C.Y. Chang and P. Mohapatra: Performance improvement of allocation schemes for mesh-connected computers, Journal of Parallel and Distributed Computing, vol. 52, no. 1, pp. 40-68 (1998)
20. J. Mache, V. Lo, and K. Windisch: Minimizing Message-Passing Contention in Fragmentation-Free Processor Allocation, Proceedings of the 10th International Conference on Parallel and Distributed Computing Systems, pp. 120-124 (1997)
21. K. Suzaki, H. Tanuma, S. Hirano, Y. Ichisugi, C. Connelly, and M. Tsukamoto: Multi-tasking Method on Parallel Computers which Combines a Contiguous and Non-contiguous Processor Partitioning Algorithm. Proceedings of the 3rd International Workshop on Applied Parallel Computing, Industrial Computation and Optimization, Lecture Notes in Computer Science, Springer, London, pp. 641- 650 (1996)
22. S. Bani-Mohammad, M. Ould-Khaoua, and I. Ababneh: A New Processor Allocation Strategy with a High Degree of Contiguity in Mesh-Connected Multicomputers, Journal of Simulation Modelling, Practice & Theory, vol. 15, no. 4, pp. 465-480 (2007)
23. P.Liu, Ch. Ch. Hsu and J. J. Wu: I/O Processor Allocation for Mesh Cluster Computers, IEEE Proceedings of the 2005 11th International Conference on Parallel and Distributed Systems ICPADS-05 (2005)
24. D. P. Bunde, V. J. Leung and J. Mache: Communication Patterns and Allocation Strategies, Sandia Technical Report SAND2003-4522 (2004)
25. P. Brucker, B. Jurisch, and B. Sievers: A branch and bound algorithm for the job-shop scheduling problem. Journal of Discrete Applied Mathematics. No. 49, pp.105-127 (1994)
26. S. Binato, W. Hery, D. Loewenstern, and M. Resende: A GRASP for Job Scheduling. Technical Report No. 00.6.1 AT& T Labs Research (2000)
27. J. Goncalves, J. Magalhaes, M. Resende: A Hibrid Genetic algorith for the Job Shop Scheduling. AT& T Labs Research Technical Report TD-5EAL6J (2002)
28. L. Davis: Job shop scheduling with genetic algorithms. First International Conference on Genetic Algorithms and their Applications, pp. 136-140 (1985)
29. E. Taillard: Parallel Taboo Search Technique for the Job shop Scheduling Problem. Journal on Computing Science, No. 6 pp. 108-117 (1994)

30. J. Chambers, W. Barnes: Taboo Search for the Flexible-Routing Job Shop Problem. Department of Computer Sciences, University of Texas-USA, Reporte Técnico (1997)
31. V. Subramani, R. Kettimuthu, S. Srinivasan, P. Sadayappan: Distributed Job Scheduling on Computational Grids using Multiple Simultaneous Requests. Department of Computer and Information Science of Ohio State University, USA. Disponible http://www.gridforum.org (2003)

Bioinformatics and Medical Applications

New Method for Comparing Somatotypes using Logical-Combinatorial Approach

Ignacio Acosta-Pineda[1] and Martha R. Ortiz-Posadas[2]

[1] Master in Biomedical Engineering
[2] Department of Electrical Engineering,
Universidad Autónoma Metropolitana Iztapalapa, Mexico
nss_33@hotmail.com, posa@xanum.uam.mx

Abstract. This paper proposes a new method for comparing somatotypes using the logical-combinatorial approach of pattern recognition theory, through the mathematical modeling of a function to evaluate the similarity between somatotypes, considering the 10 anthropometric dimensions defined in the Heath-Carter method. This similarity function was applied to a sample of different individual somatotypes and the results were compared with the ones obtained by the two methods most commonly used: the somatotype dispersion distance and the somatotype attitudinal distance. We obtained correct results with the method presented in this work and it offers a new perspective for comparison between somatotypes.

Keywords: Somatotype comparison, somatotype similarity, Heath-Carter method, logical-combinatorial approach, pattern recognition.

1 Introduction

The term somatotype corresponds in such a way with the biotype term, and is one of the most frequent tasks of Kineanthropometry, the discipline that studies the human body through the measures and assessments of their size, shape, proportionality, composition, biological maturation and body functions. The technique of somatotyping is used to appraise body shape and composition. Somatotype concept is very useful in different areas of healthcare, such as diet monitoring, effect of ergogenic aids, eating disorders and/or sport sciences, in order to compare an athlete somatotype with his/her team, or with a standard reference, or with a normal population, or itself at different stages of the training [1].

The somatotype is defined as the quantification of the present shape and composition of the human body. It is expressed in a three-number rating representing endomorphy, mesomorphy and ectomorphy components respectively, always in the same order. Endomorphy is the relative fatness, mesomorphy is the relative muscle-skeletal robustness, and ectomorphy is the relative linearity or slenderness of a physique. To

calculate these components it is used the anthropometric somatotype method of Heath-Carter [1], where 10 anthropometric dimensions (variables) are needed. Three variables (in millimeters) are required for the measurement of endomorphy: triceps skinfold, subscapular skinfold and supraspinale skinfold; these are introduced in equation (1) in order to obtain the endomorphy component.

$$Endomorphy = -0.72 + 0.15x - 0.0007x^2 + 0.0000014x^3 \qquad (1)$$

Where x = [(sum of the three folds)*170.8]/(height in cm).

For measuring mesomorphy, five measurements (in centimeters) are needed: U = humerus breadth, F = femur breadth, B = upper arm girth–triceps skinfold, P = calf girth–medial calf skinfold, H = height; and these are entered into equation (2).

$$Mesomorphy = 0.86U + 0.60F + 0.19B + 0.16P - 0.13H + 4.5 \qquad (2)$$

Ectomorphy calculation needs height in centimeters and weight in kilograms, and the calculation of HWR (height-weight ratio) by equation (3).

$$HWR = \frac{height}{\sqrt[3]{weight}} \qquad (3)$$

If HWR <= 38.28,   ectomorphy = 0.1
If 38.28<HWR<40.75,   ectomorphy = (HWR*0.463) –17.63
If HWR >= 40.75,   ectomorphy = (HWR*0.732)–28.58 [1]

Traditionally, the three-number somatotype rating is plotted on a two-dimensional somatochart (Fig. 1) using X, Y coordinates derived from the rating. The coordinates are calculated by equations (4) and (5) respectively.

$$X = ectomorphy - endomorphy \qquad (4)$$

$$Y = 2(mesomorphy) - (ectomorphy + endomorphy) \qquad (5)$$

Somatotypes with similar relationships between the dominance of the components are grouped into thirteen categories named to reflect these relationships. These categories are shown in the somartochart of Fig. 1.

Because the somatotype is a three-number expression, meaningful analyses can be conducted only with special techniques. Somatotype data has been analyzed by methods such as the somatotype dispersion distance (SDD), that is the difference between two individual somatotypes of interest [1] and it is defined by equation (6)

$$SDD = \sqrt{3(X_1 - X_2)^2 + (Y_1 - Y_2)^2} \qquad (6)$$

Where X_1 and Y_1 are the somatotype coordinates of the individual 1, and X_2 and Y_2 are the coordinates of the individual 2 Where X_1 and Y_1 are the somatotype coordinates of the individual 1, and X_2 and Y_2 are the coordinates of the individual 2.
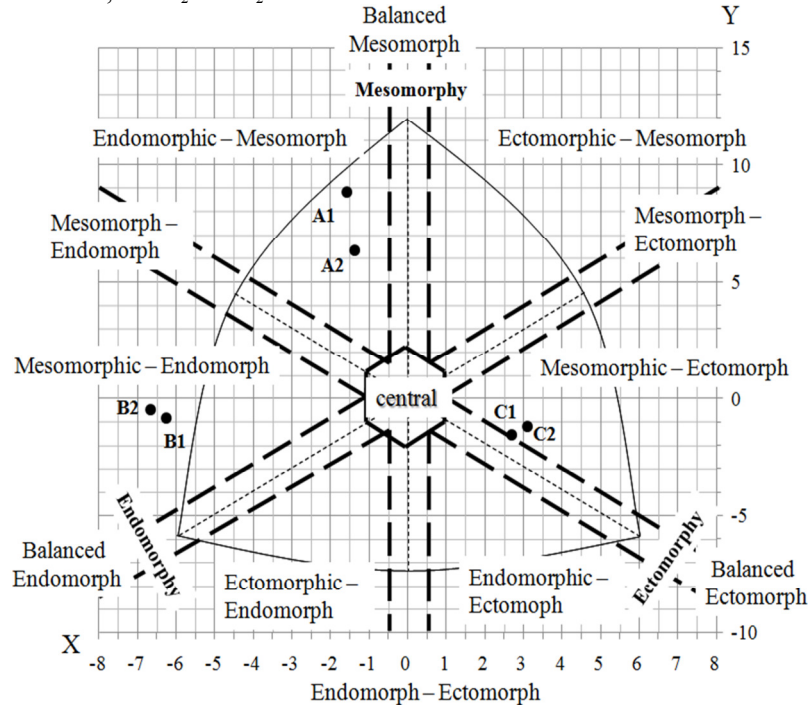
Fig. 1. Somatochart with the 13 somatotype categories [1] and location of the six somatotypes selected for this study.

Other method is the somatotype attitudinal distance (SAD) that is the difference in component units between two somatotypes and is defined by (7).

$$SAD = \sqrt{(I_A - I_B)^2 + (II_A - II_B)^2 + (III_A - III_B)^2} \qquad (7)$$

where A and B are two individual somatotypes and I, II and III are the endomorphy, mesomorphy and ectomorphy component respectively of the individual somatotype [1].

For many works attempting mathematical modeling, the likelihood between two objects may be represented using a function of distance (a norm) since closeness and likelihood have generally been treated as synonyms: two objects are more alike the closer they are found from each other and, given this, it is possible to agree if some details are specified, such as the space of representation of the objects, the kind of variables (qualitative or quantitative) which describe them, their domains, the comparison criteria for their values,

etc. Likewise, it is important to consider the way in which full object descriptions are attempted. In this sense, it is important to distinguish between likelihood and closeness in those cases where these terms are not synonyms.

This paper proposes a new method for comparing somatotypes, using the logical-combinatorial approach of pattern recognition theory [2], through the mathematical modeling of a function to evaluate the similarity between two somatotypes, considering the 10 anthropometric dimensions defined in the Heath-Carter method [1], and defining differential comparison criteria for each variable. The similarity function was applied to 6 different individual somatotypes, and these results were compared with the results obtained by both methods SDD and SAD.

2 Methodology

2.1 Mathematical Model [3]

Let O = {O_1, . . ., O_m} be a finite set of m objects, each object is described in terms of the finite set of variables X= {x_1, . . ., x_n}, where each variable x_i, i=1, . . ., n is defined on its domain M_i = {m_{i1}, m_{i2}, . . .}.

Definition 1. Let the initial space representation (ISR) be the object space representation defined by the Cartesian product of M_i sets

$$I(O) = (x_1(O), . . . , x_n(O)) \in (M_1 \times ... \times M_n)$$

Where I(O) is the object description of O in terms of the variables x_i, i=1, ..., n. $x_i(O)$ is the value taken by the variable x_i in the object O.

Definition 2. Let **C** = {C_1, ..., C_n} be a set of functions called comparison criteria for each variable $x_i \in X$ such as: C_i: $M_i \times M_i \rightarrow \Delta_i$; i=1, . . ., n where Δ_i can be of any nature, it is an ordered set and can be finite or infinite.

Definition 3. Let $\omega \subseteq X$ be a support set, where $\omega \neq \{\emptyset\}$. A system of support sets is defined as Ω = {ω_1, ..., ω_s}. By ωO we denote the ω-part of O formed by the variables $x_j \in \omega m$, m=1, ..., s.

The system of support sets Ω will allow analysis of the objects to be classified, done by paying attention to different parts or sub-descriptions of the objects, and not analyzing the complete descriptions. Examples of systems of support sets are combinations with a fixed cardinality, combinations with variable cardinality, the power set of features, etc.

The analogy between two objects is formalized by the concept of similarity function. This function is based on the comparison criterion C_i generated for each variable x_i. It is important to mention that the similarity function can evaluate the similarity or difference between two objects, i.e., between their descriptions.

Definition 4. Let $\beta:(M_i \times M_i)^2 \to \Delta$ be the similarity function, where Δ (as in the comparison criterion function) can be of any nature; it is an ordered set and can be finite or infinite. For $I(O_i)$ and $I(O)$ being two object descriptions in the domain $(M_1 \times \ldots \times M_n)$, $\beta(I(O_i), I(O))$ is defined by:

- $\beta((C_1(x_1(O_i), x_1(O)), \ldots, C_n(x_n(O_i), x_n(O))))$,   if C_i denotes similarity
- $1 - \beta((C_1(x_1(O_i), x_1(O)), \ldots, C_n(x_n(O_i), x_n(O))))$,   if C_i denotes difference

Definition 5. Let β_ω be a partial similarity function defined by:

$$\beta_\omega\left(I(O_i), I(O_j)\right) = 1 - \sum_{x_i \in \omega} C_i\left(x_i(O_i), x_i(O)\right) \tag{8}$$

where ω represents a support set.

2.2   Somatotype Mathematical Model

We used the 10 anthropometric dimensions (variables) proposed in the Heath-Carter method [1], described in the introduction. It was defined their domain by previously classifying 38 subjects [4], and the difference comparison criteria (*Definition 2*), shown in Table 1. The 0 means there is no difference and 1 represents the greatest difference between the two values compared.

Table 1. Somatotype variables, domain and comparison criteria.

Variable	Domain	Comparison criteria
x_1: Supraspinale skinfold	[6, 55]	$C_2\left(x_2(O_i), x_2(O_j)\right) = \begin{cases} 1 & if\ \frac{\|x_2(O_i) - x_2(O_j)\|}{49} \le 0.1 \\ 0 & in\ ot\ er\ case \end{cases}$
x_2: Subscapular skinfold	[8, 41]	$C_2\left(x_2(O_i), x_2(O_j)\right) = \begin{cases} 1 & if\ \frac{\|x_2(O_i) - x_2(O_j)\|}{33} \le 0.1 \\ 0 & in\ ot\ er\ case \end{cases}$
x_3: Triceps skinfold	[4, 25]	$C_2\left(x_2(O_i), x_2(O_j)\right) = \begin{cases} 1 & if\ \frac{\|x_2(O_i) - x_2(O_j)\|}{21} \le 0.1 \\ 0 & in\ ot\ er\ case \end{cases}$
x_4: Medial calf skinfold	[0.5, 3.0]	$C_2\left(x_2(O_i), x_2(O_j)\right) = \begin{cases} 1 & if\ \frac{\|x_2(O_i) - x_2(O_j)\|}{2.5} \le 0.1 \\ 0 & in\ other\ case \end{cases}$
x_5: Calf girth, right	[30.0, 43.0]	$C_2\left(x_2(O_i), x_2(O_j)\right) = \begin{cases} 1 & if\ \frac{\|x_2(O_i) - x_2(O_j)\|}{13} \le 0.5 \\ 0 & in\ other\ case \end{cases}$
x_6: Upper arm girth, elbow flexed and tensed	[29.0, 41.0]	$C_2\left(x_2(O_i), x_2(O_j)\right) = \begin{cases} 1 & if\ \frac{\|x_2(O_i) - x_2(O_j)\|}{12} \le 0.5 \\ 0 & in\ other\ case \end{cases}$

x_7: Biepicondylar breadth of the femur	[8.0, 12.0]	$C_2\big(x_2(O_i), x_2(O_j)\big) = \begin{cases} 1 & if \quad \dfrac{|x_2(O_i) - x_2(O_j)|}{4} \le 0.5 \\ 0 & in\ other\ case \end{cases}$
x_8: Biepicondylar breadth of the humerus	[5.0, 8.0]	$C_2\big(x_2(O_i), x_2(O_j)\big) = \begin{cases} 1 & if \quad \dfrac{|x_2(O_i) - x_2(O_j)|}{3} \le 0.5 \\ 0 & in\ other\ case \end{cases}$
x_9: Body mass (weight)	[51.0, 120.0]	$C_2\big(x_2(O_i), x_2(O_j)\big) = \begin{cases} 1 & if \quad \dfrac{|x_2(O_i) - x_2(O_j)|}{69} \le 0.1 \\ 0 & in\ ot\ er\ case \end{cases}$
x_{10}: Stature (height).	[157.0, 190.0]	$C_2\big(x_2(O_i), x_2(O_j)\big) = \begin{cases} 1 & if \quad \dfrac{|x_2(O_i) - x_2(O_j)|}{33} \le 0.1 \\ 0 & in\ ot\ er\ case \end{cases}$

We defined three support sets (*Definition 3*), one for each somatotype component: $\Omega_{endo} = \{x_1, x_2, x_3, x_{10}\}$; $\Omega_{meso} = \{x_3, x_4, x_5, x_6, x_7, x_8\}$; $\Omega_{ecto} = \{x_9, x_{10}\}$. Likewise using *Definition 5*, we defined three partial similarity functions described below:

$$\beta_{endo}\big(\Omega I(O_i), \Omega I(O_j)\big) = 1 - \sum_{t=1,2,3,10} \frac{C_t\big(x_t(O_i), x_t(O_j)\big)}{4} \tag{9}$$

$$\beta_{meso}\big(\Omega I(O_i), \Omega I(O_j)\big) = 1 - \sum_{t=3}^{8} \frac{C_t\big(x_t(O_i), x_t(O_j)\big)}{6} \tag{10}$$

$$\beta_{ecto}\big(\Omega I(O_i), \Omega I(O_j)\big) = 1 - \sum_{t=9}^{10} \frac{C_t\big(x_t(O_i), x_t(O_j)\big)}{2} \tag{11}$$

Finally, the total similarity function was composed by the three partial similarities as follows.

$$\beta_{total}(I(O_i), I(O_j)) = \frac{\beta_{endo} + \beta_{meso} + \beta_{ecto}}{3} \tag{12}$$

All similarity functions were bounded in the interval [0, 1], where 0 means there are no similarity (greatest difference) and 1 corresponds to identical somatotypes.

The procedure to calculate the similarity between two somatotypes using the similarity function is described as follows: First, calculate the partial similarity of the three components *(β_{endo}, β_{meso}, β_{ecto})* between of somatotypes using the equations (9), (10) and (11) respectively; second, calculate the overall similarity between somatotypes using the equation (12).

3   Results

From the sample of 38 subjects previously classified [4] we selected six: A_1, A_2 with a rating of endomorphic-mesomorph; B_1, B_2 with a rating of mesomorphic-endomorph and C_1, C_2 with a rating of mesomorphic-ectomorph. These somatotypes were placed in the somatochart (Fig. 1). We calculated the similarity between these six somatotypes described in terms of the 10 variables defined by Heath-Carter (Table 2); using three methods: 1) Similarity Function, proposed in this work; 2) Somatotype Dispersion Distance (SDD); and 3) Somatotype Attitudinal Distance (SAD).

First, we calculated the pairwise similarity between somatotypes belonged to the same class in order to show similarity between these somatotypes should be high, and then we calculated the similarity between somatotypes belonged to different classes, whose likeness should be low. As follows it is shown the application of each method in the calculation of the similarity between two different somatotypes.

Table 2. Description of 6 subjects with Heath-Carter 10 variables.

Variable	A_1	A_2	B_1	B_2	C_1	C_2
x_1	10	15	30	32	6	6
x_2	10	11	25	27	7	8
x_3	5	8	23	20	4	4
x_4	0.8	0.8	1.6	1.7	0.8	0.5
x_5	35.5	34.5	33	34	29	30
x_6	37.5	36	33	32	28	29.5
x_9	65	60	80	82	52	51
x_7	8.8	9.2	9	8.8	8.4	8.5
x_8	6	6.5	6.2	6	5.5	5.8
x_{10}	162	165	172	170	167	169

3.1   Similarity Function β (Proposed Method

To illustrate the application of partial and total similarity functions, we calculated the similarity between somatotypes A_1 and B_1. We calculated the partial similarity between endomorphy components of both somatotypes using (9):

$$\beta_{endo}\big(\Omega I(O_{A1}), \Omega I(O_{B1})\big) = 1 - \sum_{t=1,2,3,10} \frac{\left(\frac{|10-30|}{49} + \frac{|10-25|}{33} + \frac{|5-23|}{21} + \frac{|162-172|}{33}\right)}{4} = 0.49$$

Using (10) and (11), partial similarity between mesomorphy and ectomorphy components respectively was calculated.

$$\beta_{meso}\left(\Omega I(O_{A1}), \Omega I(O_{B1})\right) = 1 - \sum_{t=3}^{8} \frac{C_t\left(x_t(O_i), x_t(O_j)\right)}{6} = 0.73$$

$$\beta_{ecto}\left(\Omega I(O_{A1}), \Omega I(O_{B1})\right) = 1 - \sum_{t=9}^{10} \frac{C_t\left(x_t(O_i), x_t(O_j)\right)}{2} = 0.74$$

Using (12) the overall similarity between the two somatotypes was calculated:

$$\beta_{total}(I(O_{A1}), I(O_{B1})) = \frac{(0.49)+(0.73)+(0.74)}{3} = 0.65$$

3.2   Somatotype dispersion distance (SDD) and Somatotype attitudinal distance (SAD)

For calculating SDD between both somatotypes A_1 and B_1 it was necessary to calculate the three components (endomorphy, mesomorphy, ectomorphy) for each somatotype and then, the X, Y coordinates. This is illustrated following the next procedure:

1. Calculate parameter x:
$x_{A1} = [(10+10+5)170.18]/162 = 26.26, \qquad (x_{A1})^2 = 689.58, \qquad (x_{A1})^3 = 18108.57$

2. Calculate endomorphy component using (1):
Endomorphy$_{A1}$= -0.72 + 0.15(26.26) - 0.0007(689.57) + 0.0000014(18108.57)
Endomorphy$_{A1}$= 15.68
Endomorphy$_{B1}$= 7.32

3. For calculating mesomorphy component, we identify the equivalence among the parameters used in equation (2) and variables in Table 2. So the equivalence is: U=x_8, F=x_7, B=x_6-x_5, P=x_4 and H=x_{10}, then:
Mesomorphy$_{A1}$= 0.86(6) + 0.6(8.8) + 0.19(2) + 0.16(0.8) - 0.13(162) + 4.5
Mesomorphy$_{A1}$= -5.77
Mesomorphy$_{B1}$= -10.34

4. Ectomorphy component needs to calculate the HWR (height-weight ratio) by equation (3). For both somatotypes:
$$HWR_{A1} = \frac{162}{\sqrt[3]{65}} = 40.5, \qquad HWR_{B1} = \frac{172}{\sqrt[3]{80}} = 40$$

If 38.28<HWR<40.75, then ectomorphy = (HWR*0.463) –17.63,   then:
Ectomorphy$_{A1}$ = [40.5(0.463)] –17.63 = 1.12

Ectomorphy$_{B1}$ = 0.89

5. Calculate coordinates X and Y using equations (4) and (5) respectively:

X_{A1} = 1.12-2.77 = -1.65, X_{B1} = -6.43
Y_{A1} = 2(-5.77) – (2.77-1.12) = -15.43, Y_{B1} = -28.89

6. Calculate SDD using (6):

$$SDD_{A1-B1} = \sqrt{3(-1.65 - (-6.43))^2 + (-15.43 - (-28.89))^2} \simeq 15.7$$

7. Calculate SAD using equation (7):

$$SAD_{A1-B1} = \sqrt{\frac{(2.77_{A1} - 7.32_{B1})^2 + (-5.77_{A1} - (-10.34)_{B1})^2 +}{+(1.12_{A1} - 0.89_{B1})^2}} \simeq 6.8$$

The similarity result for all cases is shown in Table 3. Clearly it is showed that between somatotypes belong to the same class, the similarity is high ($\beta \geq 0.9$), and in the case of somatotypes belonging to different classes there is a low similarity ($\beta \leq 0.85$). However observe that somatotypes A_1-C_1 obtained a similarity β = 0.84, this is because even both somatotypes are different in their muscular proportions, both have a thin physique.

On the other hand, the distances *SDD* and *SAD* between somatotypes belonged to the same class are short and in the case of somatotypes belonged to different classes the distances are large. Observe that distance between subjects A_1-B_1 and subjects A_1-C_1 have almost the same value; this means that A_1 is far different from B_1 as from C_1, and this is why their distance is large in both cases. By the other hand, observe pair A_1-A_2 (belong to the same class): both SDD and SAD are shorter, but SAD is 40% shorter than SDD. Moreover, distances are also shorter for both pairs B_1-B_2 and C_1-C_2; but interpretation about these distances is not clear enough.

Related with function β, observe the similarity between these same pairs of somatotypes (A_1-B_1), A_1 is more different than B_1 because of their similarity (β = 0.654) is lower than similarity between A_1-C_1 (β = 0.84); meaning the pair (A_1-C_1) have a 20% higher similarity.

Table 3. Results of similarity and both distances SDD and SAD.

	A_1-A_2	*B_1-B_2*	*C_1-C_2*	*A_1-B_1*	*B_1-C_1*	*A_1-C_1*
Similarity β	0.91	0.94	0.96	0.65	0.62	0.84
SDD	2.68	0.87	0.96	15.7	15.2	12.7
SAD	1.58	0.38	0.82	6.80	6.55	5.30

5   Conclusion

Calculate the somatotype by the anthropometry method, needs to enter the 10 body measures into the three component rating (endo, meso and ecto-morphy). This rating is plotted on a two-dimensional somatochart, previously calculating coordinates X, Y by using the three components. These component ratings are used also in the equations for two and three-dimensional distances between somatotypes, called the somatotype dispersion distance (SDD) and somatotype attitudinal distance (SAD) respectively. Analysis of the three-number somatotype rating presents the problem of how should such a rating be analyzed. How far (near) most be the distance between somatotypes, in order to decide which class the somatotype belongs to.

In this sense, the similarity function proposed in this work, offers a new perspective for comparing somatotypes, it does not need the three component rating neither the somatochart. It just uses the 10 body measurements from the individual somatotype description and the similarity function, in order to compare somatotypes. Furthermore, sometimes in biotypological research or sport sciences, it is necessary to analyze one of the three components in a separately way. Our method allows comparing (analyzing) each component in an individual manner by defining the support sets and the partial similarity function. Finally we shown that our method is effective for comparing somatotypes and estimates the similarity between them, and all these characteristics make it simpler than the traditional methods.

5   References

1. Carter, J.E.L.: The Heath-Carter Anthropometric Somatotype Instruction Manual. Department of Exercise and Nutritional Sciences. San Diego State University. USA (2002)
2. Martínez-Trinidad, J.F., Guzmán-Arenas A.: The Logical Combinatorial Approach to Pattern Recognition, An Overview Through Selected Works. Pattern Recogn. 34(4), 741-751 (2001)
3. Ortiz-Posadas, M.R., Vega-Alvarado, L, Toni B,: A Mathematical Function to Evaluate Surgical Complexity of Cleft Lip and Palate. Comput. Meth. Prog. Bio. 94, 232-238 (2009)
4. Acosta-Pineda, I., Ortiz-Posadas, M.R.: Somatotype Classification Using the Logical-Combinatorial Approach (in Spanish). In: V Latin-American Biomedical Engineering Congress, vol. 3, pp.1-4. IFMBE Press, La Habana, Cuba (2011)

Modeling of 2D Protein Folding
using Genetic Algorithms and Distributed Computing

Andriy Sadovnychyy

DMAS, DCNI, UAM Cuajimalpa,
Artificios 40, col. Hidalgo, Delegación Álvaro Obregón,
México D. F., C.P. 01120, Mexico
`asadovnychyy@gmail.com`

Abstract. In this work, it is presented an application of parallel programming for studying of a scalable problem in the area of bioinformatics (Protein Folding) using a genetic algorithm. The properties of proteins depend on its configuration in space. Calculation of its configuration is a hard problem so we used some approximations models like 2D square lattice. For finding an optimal configuration of the protein in the space (configuration with minimal energy) genetic algorithm is used. It makes it possible to find an optimal configuration several times faster than a full calculation of interaction between atoms. Disadvantage of genetic algorithms is computation load. Therefore the parallel genetic algorithms are applied in this work. Parallel genetic algorithms operations (like mutation, crossover and fitness) are realized in parallel mode. For this the multi-agent system are useful. They make it possible to realize many independent functions in parallel mode.

Keywords: Protein folding, PH model of protein, genetic algorithm, parallel computing.

1   Introduction

There are many problems of bioinformatics, such as folding, docking and molecular design can be classified as "difficult problem of optimization". This family of problems is those for which not guaranteed to find the best solution in a reasonable time. Therefore the term NP-hard problem is used in the context of the complexity of algorithms. Recently, several studies have shown that hybrid algorithms, metaheuristics and parallel patterns have improved the search optimization methods, resulting in quite acceptable solutions, and even robust, which solved many increasingly large and complex problems with tolerable computing time [1, 2]. Examples of such problems are the problems which we deal with. This work proposes the development of a conceptual and computational infrastructure that allows integration through metaheuristics and hybrid algorithms, key models, heuristics and algorithms for the study of biologically interesting problems. In

this work we postulate that many of these problems can be effectively modeled through a conceptual and computational infrastructure based on multi-agent systems (MAS) that supports the work of algorithms based on metaheuristics.

Using techniques for developing parallel models allows solving large and complex problems in tolerable computing times. But to use all their advantages, parallel genetic algorithms must submit all data structures into a specific model. We have to develop computational algorithms using parallelization techniques. All tools can be heterogeneous and distributed. It means that the simulation system can use the advantages of each of its elements assigning the task to more suitable block. Using metaheuristic implemented through the interaction of agents in the computing infrastructure allows interrelate the properties of all molecules with the activity or function to be optimized, generating a functional mathematical approach to describe such relationship. The simulations of protein folding have the benefits of using heterogeneous systems. Applying this kind of processing power changes the whole dynamic of the simulation and could significantly reduce the time required to conduct research. In this work we develop the methods, algorithms and computational model structures that allow, through metaheuristics and hybrid algorithms, undertaking the study of biologically interesting problems mentioned above.

2   Methods

The modeling of physics and chemistry processes is very complex. This problem can be studied through alternative strategies, such as methods, techniques and models of intelligence artificial (IA), science and computer engineering, and sciences information, among other disciplines. It is noteworthy that such strategies have left aside those traditional approaches in physics and chemical commonly biological science researchers have used as study models [3]. Depending on empirical knowledge engaged in theoretical model, this relationship will be more successful to reproduce and predict the properties of a complex system of this nature. In this sense, we will mention some of the problems of biological interest that we intend to address in this work and specify why this complexity and strategies have been employed to get a solution.

The folding or folding of a protein is the physical process by which these biomolecules are rearranged in three-dimensional structure. The prediction of protein folding has been commonly addressed through combination of a model for the random generation of conformations proteins in a 2D or 3D space (hydrophobic-hydrophilic model), and an approximation algorithm for finding the closest conformation native state protein model. Both algorithms were used a criterion of minimizing some function of free energy. Genetic algorithm is one of the most commonly used techniques for approximation [4]. When this technique is used, the prediction of three-dimensional structure of a protein can be formulated as a search through its conformation space to find a global minimum of the energy state.

The multi-agent systems paradigm is very effective in designing a methodology for cover the entire spectrum of construction of a simulation, from design to development, implementation and control (dynamic) runtime [5, 6]. Critical points of biological systems - concerned with structures, activities and interactions - can be captured directly by abstractions that are "Kept alive" design at run time, supported by appropriate infrastructure. The simulation and modeling can then be framed as an experiment in online or in simulation system, where researchers can observe and interact dynamically with the system and its environment through changes in their structures, or directly modifying the global biological process.

Agent-based systems and multi-agent systems (MAS) are considered strategies to manage the correct level of abstraction modeling and building complex systems. In fact, biological systems exhibit all the characteristics of complex systems. However, as noted in [1], a biological system is much more than a complex system, it is a system consistent, as it implies levels of functionality, localization, individualization and therefore specialization, dimensionality (micro and macro levels) and other scenarios for these levels of operation.
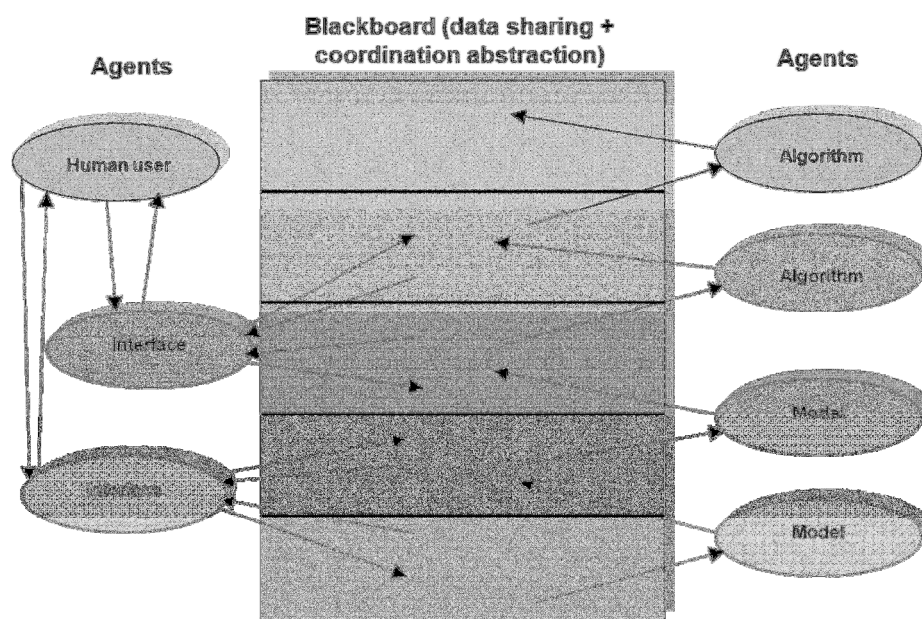
Fig. 1. Principal structure of simulation system.
Interaction among agents is realized indirectly through a blackboard,
which represents the communication coordination abstraction.

In this work we will use an infrastructure for modeling MAS biological systems strongly based on location, distribution and interaction (communication) of the components of the system and therefore provide for better solutions compared to generating strategies traditionally used. We will also make an analysis from a viewpoint theory to explain the reasons why the infrastructure is better and which of its properties can be used in other evolutionary systems.

3   Multi-agent System

The principal structure of simulation system can be seen in Figure 1. There its main components, the agents and the blackboard, are presented. As can be seen in this figure, the architecture provides three types of agents: model agents, algorithm agents and interface agents [8]. According to this Multi-Agent System architecture, the interaction among agents is realized by indirect communication, through a communication-coordination abstraction, represented in this figure by the blackboard.

Fig. 2. Semantics assigned to the different blackboard levels and types of agents.

Figure 2 shows the semantics assigned to the different blackboard levels and types of agents when protein folding is modeled. Evolution, the bioinformatics framework, allows inducing folding of molecular-chain representations with the aim to explore both the behavior and efficiency of EA by following the most relevant variables of chain folding. Regarding the software development, our work will progress by using the bioinformatics framework as a scaffold or mainframe devoted to the development and testing of

gradually more complex and robust EA and their associated parameters, with more realistic representations of the problem and with improved fitness functions. This framework would also allow adding functionalities for the user to tract results and algorithm efficiency, to interactively bias the conformational search with biological sense, or to perform graphical and numerical analysis.

4   Experimental Results

The goal of experiments is to compare the performance of our simulation system with similar simulations and others previously published. Also to see if our simulation system can shed some light in the study of how proteins tend to fold and if there is some phenomena that could be identified and explained.

The HP-48 problem. This problem is defined by the sequence

$HP\text{-}48 = P_2H(P_2H_2)_2P_5H_{10}P_6(H_2P_2)_2HP_2H_5 =$
$PPHPPHHPPHHPPPPPPHHHHHHHHHH$

In this problem the optimal sequences have a square shape in the H beads with several options for the P beads. This problem was reported in [9] as very difficult.

According to the results in previous sections, this problem is likely to be difficult simply because of this square shape. Any algorithm should have problems here.
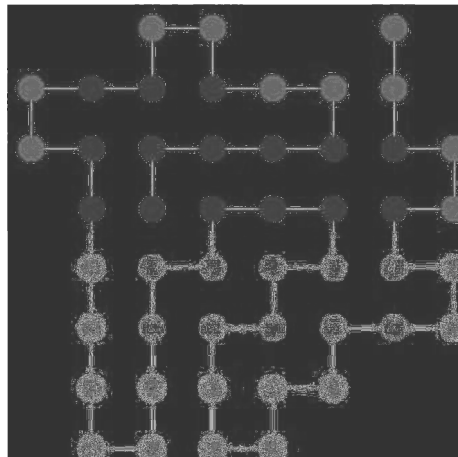
Fig. 3. A near optimal configuration for HP-48.

Figure 3 shows one nearly optimal configuration found. One can see that the shape of the H beads is more or less close to a rounded square. This is the kind of shapes that are more easily found by our algorithm and we think that this is also the one that is more likely to be present in nature. The 2D square model induces a bias that makes it difficult

to find square shaped optima. So we think that it is not good to try and solve this kind of problems. It should suffice with the use of more rounded shapes to be able to study the traits present in real life protein folding.

The genetic algorithm for find the optimal configuration was used. Each of gen presents the direction of connection in the protein structure. The gen shows three directions: straight, left and right. On basis of this information we construct the model protein. We start construct the model from the first amino acid and first direction to straight, then we continue construct in concordance with the chromosome.

Figure 4 shows the principal structure of genetic algorithm. On phases "Initial population", "Crossover and mutation", "Selection" and "Termination" the algorithm works with whole population. On these stages the processing of each chromosome is depended of others.

On phase "Fitness" the algorithm calculates the level (fitness function) of each chromosome. On this stage the processing of chromosome is independent. And we calc the fitness function for each chromosome simultaneously, en parallel.
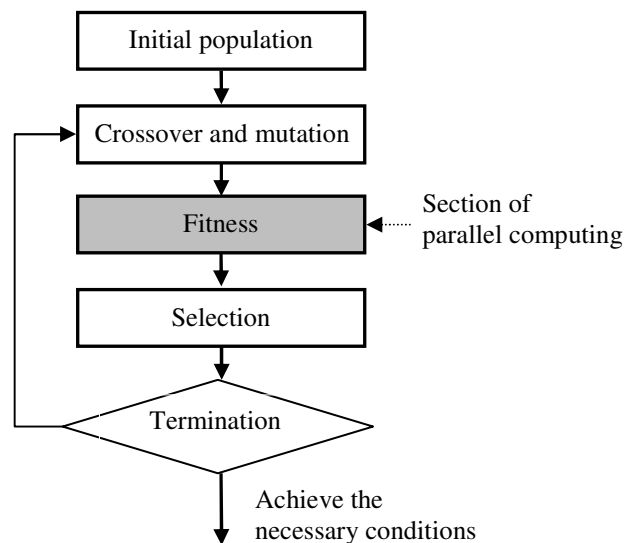
Fig. 4. Principal structure of genetic algorithm.

The main algorithm waits for termination of all parallel calculations, receives all results (values of each fitness functions) and makes "selection".

During the phase "selection", the algorithm assigns the rank for each genome and selects pairs for "Crossover" stage.

Figure 5 shows cluster's structure that we are used for realize computing. The cluster has Server, which controls and distributes tasks for nodes. Each node has 2 CPUs with 8

cores (16 cores for node) and work like SMP machine. We consider that each core like a separate CPU.

We use Open MPI [10, 11] library and Open MP API [11, 12] for computing parallelization.
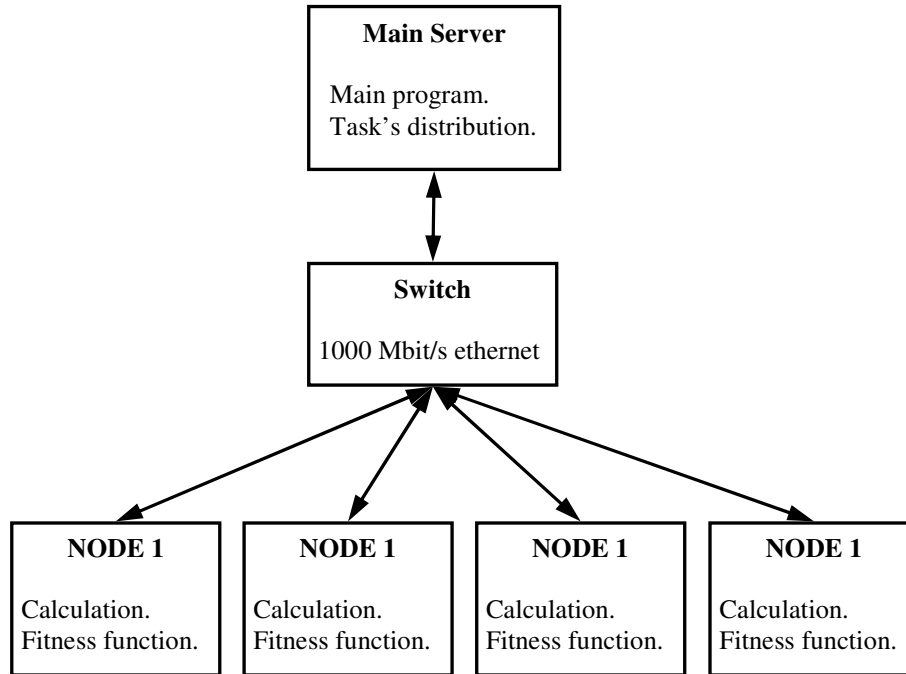
Fig. 5. The cluster's structure

The Open MPI library provides tools for communication between the nodes. It uses sockets for sends and receives data. Open MPI automatically analyses the topology of distributed system (cluster) and then chooses the best (fastest) way for send data, messages.

The open MPI model uses distribute memory, so all processes have own local memory and have not access to memory of others. They can communicates by the send/receive function (send/receive massages).

The main program (in the server) has whole generation of population. Divides one for parts and send them for each node. The nodes from 1 to P-1 receive N/P genomes, where: N – number of genome in the population and P – number of node. And node P receives the rest $N - \frac{N}{P} * (P - 1)$ of genome.

Then in the node we use Open MP API. Open MP realize shared memory paradigm. So each thread has access to global memory.
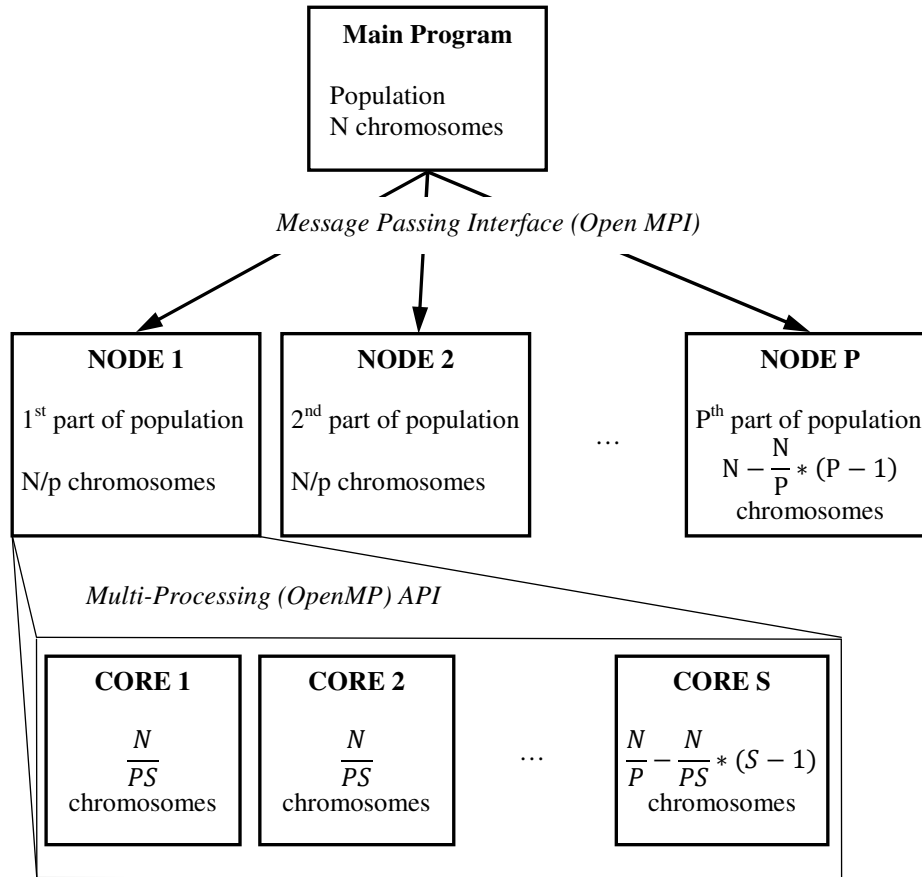
Fig. 6. Task distribution in the cluster.

MP starts one thread for each CPU (core) y divides task of node between S threads.

The threads from 1 to S-1 calculate $\frac{N}{PS}$ part and the last thread S calculate $\frac{N}{P} - \frac{N}{PS} * (S-1)$ part of task of node.

Table 1. Time of computing. Only MP API

CPUs	1	2	3	4	5	6	7	8
Seconds	94.2	66.9	57.7	53.2	50.4	48.6	47.3	46.3
CPUs	9	10	11	12	13	14	15	16
Seconds	45.5	45.0	44.4	44.0	43.7	43.4	43.1	42.9

The table 1 and figure 7 show the time of computing using only one node. In this case we use only Open MP API.
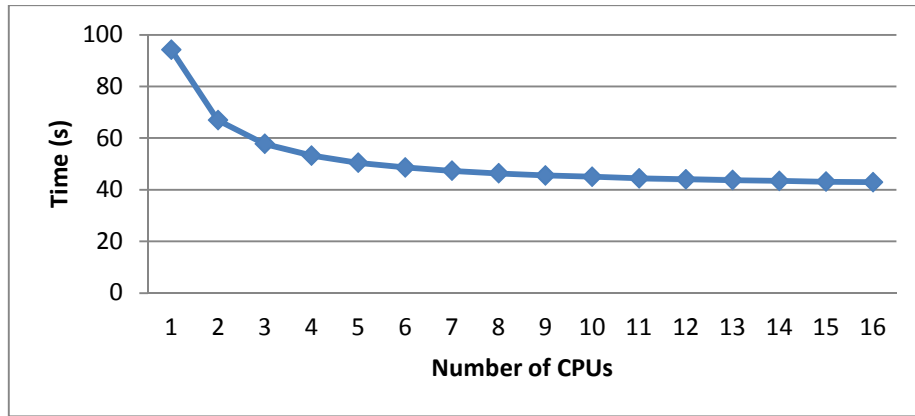
Fig. 7. Time of computing. Only MP API.
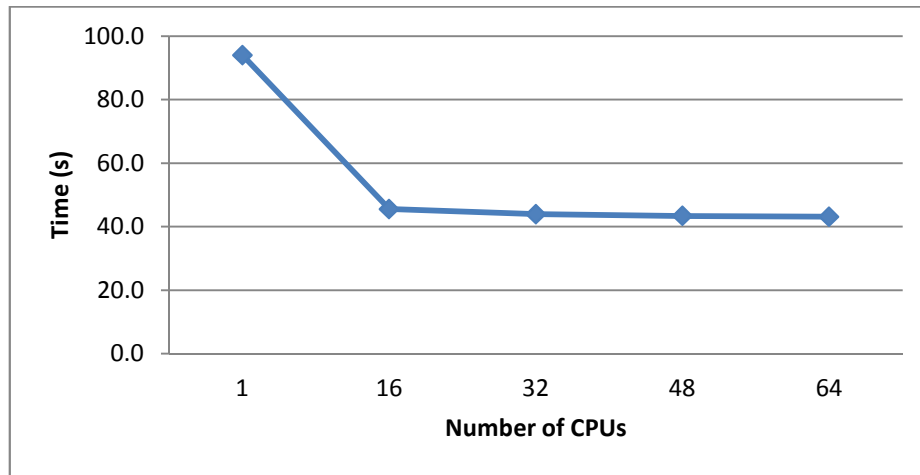
Fig. 8. Time of computing. MPI library with MP API.

Table 2. Time of computing. MPI library with MP API.

Nodes	1	1	2	3	4
CPUs	1	16	32	48	64
Seconds	95.3	45.5	43.9	43.4	43.1

The table 2 and figure 8 show the time of computing using Open MPI for distribute the tasks between the nodes, and Open MP API for calculate the part of task in parallel mode. In this case we use mixed mode Open MPI library+ Open MP API.

5   Conclusions

The methods of genetic algorithms allow finding optimal configurations of the proteins in space. That makes it possible to model proteins properties. Using parallel genetic algorithms, it is possible to analyze the whole of population in multiprocessors system. All of these methods together decrease, by several times, time of modeling.

In the experiment we used different techniques for parallelize computing. The experiment shows that than we incise number of CPU (processing units) the time of computing is decreased. But there is limit of number of processing unit in our experiment. According to Amdahl's law $\frac{1}{(1-P)+\frac{P}{S}}$ where S is a number of processing unit and P is a parallel part of the algorithm, this limit depends on the parallel part of algorithm.

The directions for future research are to change the algorithm for increasing the parallel part and to design methods and models for simulation of protein folding with parallel genetic algorithms in distributed system like clusters or grid.

References

1   Kitano, H.: Computational System Biology. Nature, Vol. 420, pp. 206-210 (2002)
2   Oliveto, P.S., Lehre P.K., Neumann, F.: Theoretical Analysis of Rank Based Mutation – Combining Exploration and Exploitation. Proceedings of the Eleventh Congress on Evolutionary Computation (2009)
3   C. Clementi: Coarse-grained models of protein folding: toy models or predictive tools?, Current Opinion in Structural Biology. 18, 10-15 (2008)
4   Cervantes, J., Stephens, C.R.: Rank Based Variation Operators for Genetic Algorithms. Proceedings of the 2008 international Genetic and Evolutionary Computation Conference (GECCO08) pp. 905-912 (2008)
5   Zambonelli, F. and A. Omicini: Challenges and research directions in agent-oriented software engineering. Autonomous Agents and Multi-Agent Systems, 9(3):253–283 (2004)
6   Parunak, V.D., R. Savit, and R. L. Riolo: Agent-based modelling vs. equation based modelling: A case study and users' guide. In J. S. Sichman, N. Gilbert, and Conte, R., editors, Multi-Agent Systems and Agent-Based Simulation, pages 10–26, Springer-Verlag (1998)
7   Omicini, A., A. Ricci, M. Viroli, C. Castelfranchi, and L. Tummolini. 2004. Coordination artifacts: Environment-based coordination for intelligent agents. In N. R. Jennings, C. Sierra, L. Sonenberg, and M. Tambe, editors, 3rd international Joint Conference on Autonomous Agents and Multiagent Systems (AAMAS 2004), volume 1, pages 286–293, New York, USA, 19–23 ACM (2004)

8   Cervantes, J., Sánchez, M., González, P.P.: Emerging traits in the application of an evolutionary algorithm to a scalable bioinformatics problem, Evolutionary Computation (CEC), 2010 IEEE Congress. Barcelona, pp 1–8 (2010)

9   Cox, G.A., Mortimer-Jones, T.V., Taylor, R.P. Johnston R.L.: Development and Optimization of a novel Genetic Algorithm for Studying Model Protein Folding. Theor Chem Acc (2004) 112: 163–178 DOI 10.1007/s00214-004-0601-4 (2004)

10 Open MPI v1.4.3 documentation, http://www.open-mpi.org/doc/v1.4/

11 Michael Jay Quinn: Parallel programming in C with MPI and OpenMP, McGraw-Hill Higher Education, 529 p. (2004)

12 Barbara Chapman, Gabriele Jost and Ruud van der Pas: Using OpenMP. Portable Shared Memory Parallel Programming. Massachusetts Institute of Technology, 353 p. (2008)

13 Andriy Sadovnychyy, Pedro Pablo Gonzales Pérez and Jorge Cervantes: Design parallel genetic algorithms for multi-agent systems. GESTS International Transactions on Computer Science and Engineering. Volume 64, Number 1, pp 67-72 (2011)

Neural Network Based Model
for Radioiodine (I-131) Dose Decision
in Patients with Well Differentiated Thyroid Cancer

Dušan Teodorović[1,2,*], Milica Šelmić[1], and Ljiljana Mijatović-Teodorović[3, 4]

[1] University of Belgrade, Faculty of Transport and Traffic Engineering, Serbia
`duteodor@gmail.com, m.selmic@sf.bg.ac.rs`
[2] Serbian Academy of Sciences and Arts, Belgrade, Serbia
[3] University of Kragujevac, Medical Faculty, Kragujevac, Serbia
[4] Clinical Center Kragujevac, Serbia
`mijatoviclj@gmail.com`

Abstract. A classifier system based on Artificial Neural Network is developed to suggest I-131 iodine dose in radioactive iodine therapy. The inputs to the system consist of patient's diagnosis based on histopathologic findings, patient's age, and TNM classification. The output of the neural network is proposed I-131 iodine dose that should be given to the patient. The training group was composed of 72 patients with well differentiated thyroid cancer. The test group consisted of 20 patients. An artificial neural network was trained using Levenberg-Marquardt back-propagation algorithm. By comparing the results obtained through the model with those resulting from the physician's decision, it has been found that the developed model is highly compatible with reality. The accuracy of the developed neural network has been exceptional. The developed classifier system could be used in educational purposes.

Keywords: Neural networks, radioactive iodine therapy, thyroid cancer.

1 Introduction

Although thyroid cancers represent less than 1% of all malignances, they are most common endocrine carcinomas, and ones of the ten most common cancers in women [6]. Between these, more than 95% are well differentiated thyroid cancers (WDTC) of follicular cell origin, papillary and follicular carcinomas. After the Chernobyl nuclear disaster the incidence of WDTC has increased in many European countries. Age, female sex, radiation exposure of neck region (particularly in children), and the positive familiar anamnesis of other malignances are the most important risk factors that increase the probability of WDTC.

Although WDTC have a very good prognosis in the vast majority of patients, there are still patients with high risk factors, who need, after total or near total thyroidectomy, the

---

*Corresponding author. Tel.: +381 -11-3091-210; fax: +381-11-2638-912.
E-mail address: <u>duteodor@gmail.com</u>

radioactive iodine therapy [7, 11]. Ability of the thyroid follicular cells to take up iodine via sodium iodide symporter at the basolateral cell membrane, enable the use of radioiodine for the therapy of WDTC.

Experienced physician relatively easily determines the dose of I-131 iodine in WDTC treatment. On the other hand, this task is very complex for beginners and/or computers. Choice of dose proposed by a physician cannot be easily described by precise rules and/or mathematical algorithms. Artificial Neural Networks (ANN) that are information-processing systems are able to learn from experience, and to apply to new cases generalizations derived from previous instances [3, 12]. They are also capable to abstract essential characteristics of input data that often contain irrelevant information. ANN have been applied to various biomedical problems during last few decades [4, 5, 8, 9, 10]. The most important ANN applications in medicine are in the areas of image analysis, diagnostic systems, and drug development.

In this paper, we developed simple neural network for prescription of the I-131 iodine dose in WDTC treatment. We used a great number of medical records. All medical records that we used contain information on patient's diagnosis, age, TNM classification (T - Tumor size, N - metastases in lymph nodes, M - distant metastases), as well as I-131 dose proposed by a physician. We trained artificial neural network by presenting to the network set of patient's characteristics (histopathologic diagnosis, age, TNM classification of tumor), and applied therapy (doses). In other words, we created many (patient, therapy) pairs and presented them to the network. Trained network has been capable to propose the best therapy for every new case.

The main objective of this paper is to research the possibility of developing a classifier system that could improve the quality of decisions of young physicians that treat WDTC. In other words, our intention is to use the classifier system mainly in educational purposes. Since neural networks are well known for being a black box, the medicine student won't learn how to reach an appropriate decision. On the other hand, our main attention is to help students in testing of their acquired knowledge.

To the best of our knowledge, this research represents first attempt to apply neural network concepts in WDTC therapy. The paper is organized as follows. Neural networks fundamentals are given in Section 2. Section 3 describes proposed neural network for prescription of the I-131 iodine dose in WDTC therapy. Results and discussion are given in Section 4. Section 5 contains conclusion.

2   Neural Networks Fundamentals

The Artificial Neural Network (ANN) is a mathematical model that is based on a simplified model of the brain, the processing task being distributed over numerous neurons (nodes, units, or processing elements). The power of a neural network is obtained as the result of the connectivity and collective behavior of these simple nodes. Artificial neural networks demonstrate a notable number of the brain's properties. For example,

they are able to learn from experience, to apply to new cases generalizations derived from previous instances, and to abstract essential characteristics of input data that often contain irrelevant information.

Neural networks have been applied in medicine during the last few decades. There are a lot of various clinical and laboratory data related to every patient. The basic idea of using ANN in medicine is to have better diagnoses, predictions, decision making, and medical image analysis based on clinical and laboratory data. The pioneers of using ANN in medicine were Anderson [1], and Specht [9]. Donald Specht [9] used neural network to detect heart abnormalities. The inputs were EKG data. The possible outputs were "normal", or "abnormal" [2, 9]. Anderson [1] developed "Instant Physician". The main idea was to develop neural network capable to make diagnosis and recommend patient's treatment based on a set of symptoms. The network developed performed well and was capable to give the same diagnosis and treatment as proposed by physician. We follow this idea in our paper.

3 Neural Network for Prescription of the I-131 Iodine Dose in WDTC Treatment

The problem considered in this paper belongs to the pattern classification problems. In pattern classification problems, every input vector belongs to a specific category. In our case, input vectors (patterns) are patient's characteristics (age, histopathologic diagnosis, TNM classification of tumor). Various doses of I-131 iodine given by a physician represent categories. In the numerical example that we consider we have three categories (doses of 1.85 GBq, 3.7 GBq, 5.5 GBq respectively).

We set a two-layered neural network (Figure 1). Between input and hidden layers there is a full connectivity. We use the proposed network to determine the dose of I-131 iodine. The dose is determined according to patient's histopathologic diagnosis, age, as well as TNM classification. The input layer has 5 nodes, as well as hidden layer. The output layer contains one node. The following are inputs to the network:

PD - patient's diagnosis
PA - patient's age
T - tumor size
N - metastases in lymph nodes
M - distant metastases
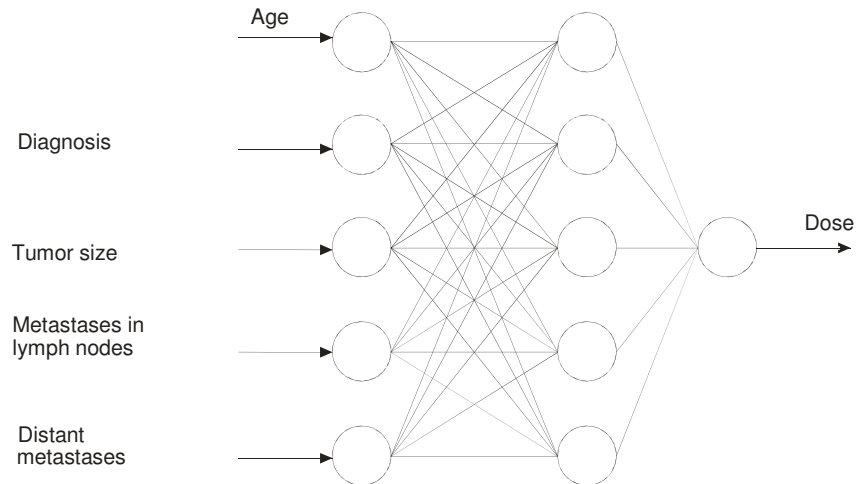
Fig. 1. Neural network for choice of the I-131 iodine dose.

The output of the network *D* represents the dose received by a patient. We described patients' diagnosis by the following integer numbers:

1 – Microcarcinoma papillare glandulae thyreoideae,
2 - Ca papillare glandulae thyreoideae multifocale,
3 - Ca papillare glandulae thyreoideae,
4 - Hurtle cell carcinoma glandulae thyreoideae,
5 - Ca folliculare gl. thyreoideae (multifocale),
6 - Ca folliculare gl. thyreoideae,
7 - Ca folliculare gl. thyreoideae (atypicum),
8 - Microcarcinoma papillare multicentricum.

The proposed neural network for choice of the I-131 iodine dose is shown in Fig. 1.

4   Results and Discussion

The proposed neural network is trained on 72 examples of physician's decisions, and after that tested on 20 examples. Patients used in this research were patients from the University Clinical Center in Kragujevac, Serbia. They had undergone I-131 iodine therapy between 2005 and 2011. The physician whose decisions were used to train the neural network has 23 years of experience in nuclear medicine.

During network preparation there were three kinds of sets. All of these sets were generated by random splitting. First set was presented to the network during training, and

network was adjusted according to its error. In our code, training set was 70% from whole set of patients characteristic (50 patents from 72). Second set was used for validation. These patients were used to measure network generalization, and to halt training when generalization stops improving. Finally, third set was used for testing. These patients' characteristics have no effects on training and so provide an independent measure of network performance during and after training. In our code these two sets included 15 % of whole data set (in total 11 patients).

The characteristics of the patients from the training and testing groups are given in the Table 1.

Table 1. Training and testing groups: Patients' age, diagnosis, tumor size, metastases in lymph nodes and distant metastases.

Patient Ordinary Number	Age	Diagnosis	T	N	M	Dose
1	33	1	2	0	0	2
2	21	1	2	0	0	1
3	65	2	2	0	0	2
4	77	4	4	1	0	2
5	81	5	4	0	1	2
....						...
91	63	5	3	0	0	2
92	56	3	1	1	0	3

Patient's age (*PA*) is expressed in integer numbers. Tumor size (*T*) is expressed in [cm]. The variable (*N*) that describes existence of the metastases in the lymph nodes has the following possible values: 0 (in the case when there are no metastases in the lymph nodes (*N0*)); 1 (in the case when there are metastases to level VI: pretracheal, paratracheal, and prelaryngeal (*N1a*)); 2 (in the case when there are metastases from to unilateral, bilateral, contralateral cervical or superior mediastinal node (*N1b*)). The variable *M* that describes existence of the distant metastases has the following possible values: 0 (in the case when there are no distant metastases); 1 (in the case when there are distant metastases).

The trained neural network made the same decision as a physician in 66 cases (91%) in the case of training group. In the case of test group network made the same decisions as a physician in all 20 cases (100%). The regression plot is shown in Fig. 2. On the abscissa are target values (doses given by physician), while on the ordinate output values (dosed recommended by trained neural network) are given. As it can be seen from this plot, in all cases target value of proposed dose was equal to output value.

5   Conclusion

The physician needs to be very knowledgeable, experienced and trained properly to adequately perform the studied task. In order to imitate physician's decisions we developed a simple neural network that has the ability to adapt and learn. Training of the proposed neural network involves use of a data base of collected physician's decisions that are values for the input and the output of the neural network. The neural network learns by adjusting the connection strengths to minimize the error of the outputs.
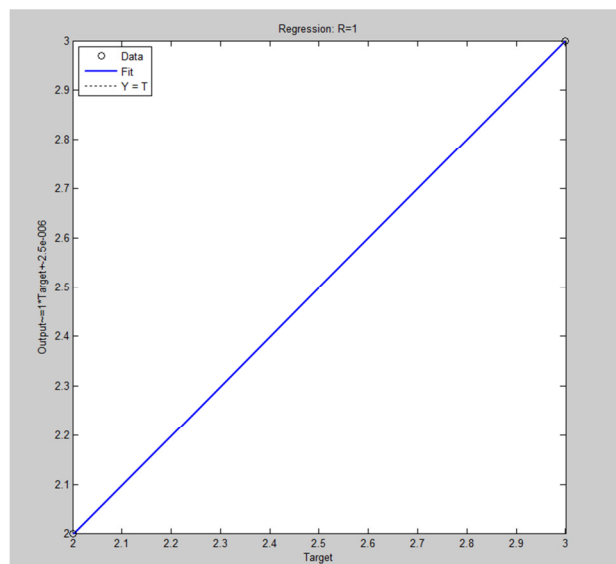
Fig. 2. Regression plot.

The experience gained during this research indicated the importance of getting enough representative training and testing data. However, due to the nature of the information and all the difficulties of obtaining them, the number of available data was limited.

The purpose of the study in this phase of work was to develop a simple judgment system. Our aim was to create artificial neural network that would assist medical students to test their knowledge. We proposed neural network, which in the simplest form, is able to describe the actual judgment process. In other words, we showed that the proposed feedforward neural network has capability to imitate the actual decisions of the experienced physician. The developed classifier system could be used in educational purposes. It could assist and guide young physicians. The system developed can make the appropriate decision without knowing the functional relationships between individual variables.

References

1. Anderson, J.A: A Memory Storage Model Utilizing Spatial Correlation Functions. Kybernetics 5, 113−119 (1968)
2. Caudill, M., Butler, C.: Naturally Intelligent Systems, MIT Press, Cambridge, MA.
3. Fausett, L., Fundamentals of Neural Networks, Prentice Hall, Saddle River, New Jersey (1990)
4. Holst, H, Åström, K., Järund, A.: Automated interpretation of ventilation-perfusion lung scintigrams for the diagnosis of pulmonary embolism using artificial neural networks. European Journal of Nuclear Medicine 27, 400−406 (2000)
5. Patil, S., Henry, J.W., Rubenfire, M., Stein, P.D.: Neural network in the clinical diagnosis of acute pulmonary embolism. Chest 104,1685−1689 (1993)
6. Riesco-Eizaguirre, G., Santisteban, P.: New insights in thyroid follicular cell biology and its impact in thyroid cancer therapy. Endocrine-Related Cancer 14, 957–77 (2007)
7. Savin, S., Cvejic, D., Mijatovic, Lj., Zivancevic Simonovic, S.: Measuring thyroglobulin concentrations in patients with differentiated thyroid carcinoma. Journal of Medical Biochemistry 29, 1−5 (2010)
8. Scott, J.A., Palmer, E.L.: Neural network analysis of ventilation perfusion lung scans. Radiology 186, 661−664 (1993)
9. Specht, D.F.: Vectorcardiographic Diagnosis Using the Polynomial Discriminant Method of Pattern Recognition, IEEE Transactions on Bio-Medical Engineering, BME-14, 90−95 (1967)
10. Tourassi, G.D., Floyd, C.E., Sostman, H.D., Coleman, R.E.: Acute pulmonary embolism: artificial neural network approach for diagnosis. Radiology 189, 555–558 (1993)
11. Vrndic, O.B., Savin, S.B., Mijatovic, Lj., Djukic, A., Jeftic, I.D., Zivancevic Simonovic S.T.: Concentration of thyroglobulin and thyroglobulin-specific autoantibodies in patients with differentiated thyroid cancer after treatment with radioactive Iodine 131. Labmedicine 42, 27−31 (2011)
12. Wasserrnan, P.D.: Neural Computing: Theory and Practice, Van Nostrand Reinhold, New York (1989)

Evaluation of Hydrocephalic Ventricular in Brain Images using Fuzzy Logic and Computer Vision Methods

Miguel Ángel López Ramírez[1], Erika Consuelo Ayala Leal[1], Arnulfo Alanis Garza[1], and Carlos Francisco Romero Gaitán[2]

[1] Division de Posgrado Instituto Tecnologico de Tijuana, Fraccionamiento Tomas Aquino S/N, Tijuana, Baja California, C.P. 22414, Mexico
[2] Facultad de Medicina Universidad Autonoma de Baja California, Calzada Tecnologico No. 14418, Mesa de Otay, Tijuana Baja California, C.P. 22390, Mexico

Abstract. The purpose of this paper is classify cases of hydrocephalic ventricular of human brain images using fuzzy logic, based on the size of the ventricles of the human brain, using intelligent techniques combined with computer vision, the analysis of the ventricles size was based databases using magnetic resonance cases of normal ventricles, the criterion based of the fuzzy logic inference system and vision using the height, and volume of the ventricles to classify the hydrocephalic cases. The height, area and volume of the ventricles of the left and right brain were measured in 13 individuals, 10 normal and 3 cases of hydrocephalus. We expect that the symptoms of hydrocephalus using the proposed method are classified by the size of the ventricles with a significantly higher percentage when considering a large number of cases of hydrocephalus.

Keywords: Computer vision and image processing, bioinformatics and medical applications, fuzzy logic.

1 Introduction

The Hydrocephalus can be defined as a disturbance of the formation of flow, or absorption of cerebrospinal fluid (CSF) that leads to an increase in the volume occupied by the fluid in the central nervous system.

This condition could be termed as a disorder of CSF hydrodynamics. Acute hydrocephalus occurs in days, sub acute hydrocephalus occurs within weeks, and chronic hydrocephalus occurs over months or years. Conditions such as brain atrophy and focal destructive lesions also lead to an abnormal increase of cerebrospinal fluid in the central nervous system. In these cases, brain tissue loss leaves a void that is filled passively with CSF. These are not the result of a hydrodynamic disorder and therefore are not classified as hydrocephalus. A major misnomer used to describe these conditions was hydrocephalus ex vacuo.

This review focuses on the problems related to defining hydrocephalus and on the development of a consensus on the classification of this common problem. Such a consensus is needed so that diverse research efforts and plans of treatment can be understood in the same context. The literature was searched to determine the definition of hydrocephalus and to identify previously proposed classification schemes. The historic perspective, purpose, and result of these classifications are reviewed and analyzed. The concept of the hydrodynamics of cerebrospinal fluid (CSF) as a hydraulic circuit is presented to serve as a template for a contemporary classification scheme. Finally, a definition and classification that include all clinical causes and forms of hydrocephalus are suggested. The currently accepted classification of hydrocephalus into "communicating" and "no communicating" varieties is almost 90 years old and has not been modified despite major advances in neuroimaging, neurosciences, and treatment outcomes. Despite a thorough search of the literature using computerized search engines and bibliographies from review articles and book chapters, we identified only 6 previous attempts to define and classify different forms of hydrocephalus [1].

2   Motivation

In research, the needs of specialists impact area of medicine of Neuroradiology generates a motivation for this research project to develop image analysis methods of the brain using computer vision and intelligent systems, namely that all is not resolved in this field of neuroimaging, the idea is to develop an automated system that can serve as a support for medical specialists and thus to have a better diagnostic criteria based on the analysis of brain images.

2.1   Fuzzy Logic

Fuzzy logic is a form of many-valued logic; it deals with reasoning that is fixed or approximate rather than fixed and exact. In contrast with traditional logic theory, where binary sets have two-valued logic: true or false, fuzzy logic variables may have a truth value that ranges in degree between 0 and 1. Fuzzy logic has been extended to handle the concept of partial truth, where the truth value may range between completely true and completely false. Furthermore, when linguistic variables are used, these degrees may be managed by specific functions [2].

Fuzzy logic starts in 1965 proposal of fuzzy set theory by Lotfi Zadeh [3, 4]. Though fuzzy logic has been applied to many fields, from control theory to artificial intelligence, it still remains controversial among most statisticians, who prefer Bayesian logic, and some control engineers, that prefer traditional two-valued logic [5].

In this paper we use fuzzy logic to determine if the person has hydrocephalus or not, using two fuzzy systems that use height, area and volume of the left and right ventricles, which were obtained from a database of CT images Excel Medical Center.

3   The Ventricles of the Brain Metric Height, Area and Volume

We utilized a database of 13 individuals with 45 scans each for a total of 585 sample images to obtain the necessary metrics and to test the fuzzy inference system, 10 are normal people with hydrocephalus and 3 if then shown as obtained measures of height, area and volume of right and left ventricles [6].
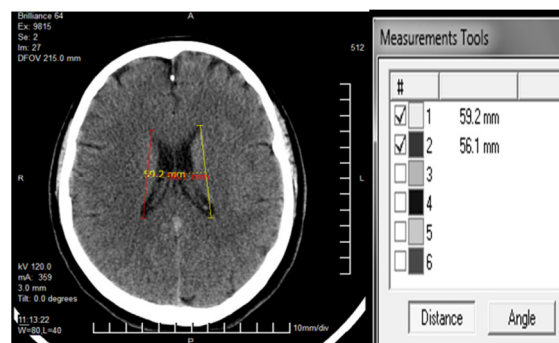
Fig. 1a) Computerized axial tomography, height of the ventricles, **1b)** Measurement Tools.
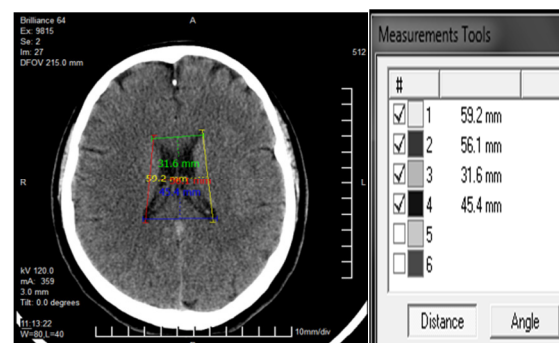
Fig. 2a) Computerized axial tomography, Area of the ventricles, **2b)** Measurement Tools.

It was used to support development of specialized software from Philips with which we read the CT images and look at different angles of the image. Figures 1a and 1b show an example of how to calculate the height of the right and left ventricles in the image by

drawing a line that covers each Ventricle, measures are in units of millimeters, the height within the brain image of the left ventricle are shown in red and yellow ventricle right.

The height is obtained by drawing a straight line from end to end for each left and right ventricle, for example, in this case we have the height:
Right ventricle size: 59.2mm, Left ventricular measures: 56.1mm

The calculation of the area of the ventricles using the height of each ventricle and its base, forming a rectangle, take the base and the height and divide by two to calculate the area for each of the ventricles multiplying the base times height, it is in figures 2a) and 2b).

The following shows how to calculate the area of each ventricle for example:

> Area = (base) x (Height
> Right ventricle height 59.2mm and 38.5mm base of the right ventricle.
> Area = (59.2mm) x (38.5mm) = 2279.2 mm^2

The following is an example of the calculation of the volume using the area and height of the ventricles:

> Volume = (Area) x (Height)
> Right ventricular volume: Area = 2279.2mm^2, Height = 59.2mm from the right ventricle to obtain the volume of the right ventricle. Volume = (2279.2mm^2) x (59.2mm), Volume = 134928.64 mm^3

The calculation of Left ventricular volume, area = 2159.85mm^2, height = 56.1mm, obtaining the right ventricular volume, Volume = (2159.85mm^2) x (56.1mm), Volume = 121167.58 mm^3

The following tables show the results of measurements of each of the test images which specify the measures normal and Hydrocephalus cases:

Table 1. Measurements (part 1).

Measures	Brain		Normal		Hydrocephalus	
Height(mm)	Ventricle	Right	50.7	68.0	70.0	90.0
		Left	48.9	72.1	73.0	90.0
Area(mm^2)	Ventricle	Right	870.94	1350.60	1270	2396
		Left	875.94	1355.57	1273	2386
Volume(mm^3)	Ventricle	Right	100	50	190	420
x million		Left	89	215	180	410

Table 2 shows measures of 10 normal individuals. VBH is the height of the ventricle of the brain, VBA is the area of the brain ventricle and VBV is the volume of the ventricle of the brain.

Table 2. Measurements (part 2).

Person		VBH		VBA		VBV	
		Right	**Left**	**Right**	**Left**	**Right**	**Left**
	1	60.0	54.8	1093.47	1093.47	131216.4	119844.312
	2	56.2	56.4	1187.93	1187.93	133760.918	133998.504
	3	66.2	70.9	1355.57	1355.57	179478.262	192220.676
	4	62.9	60.8	1237	1237	155614.6	150919.2
Normal	5	64.6	72.1	1467.81	1467.81	189641.859	211658.923
	6	50.7	51.9	875.94	875.94	88821.076	90923.35
	7	68.6	53.4	1242.87	1242.87	170522.45	132739.05
	8	50.7	48.9	991.02	991.02	100489.420	96921.756
	9	62.3	54.2	958.21	958.21	119393.277	103870.235
	10	66.3	65.3	1112.04	1112.04	147453.852	145229.812

Table 3 shows the measures of height, area and volume of the ventricles of the individual cases of hydrocephalus.

Table 3. Measurements (part 3).

Person		VBH		VBA		VBV	
		Right	Left	Right	Left	Right	Left
	1	75	73.7	1273.243	1273.243	190986.562	187676.091
Hydrocepha lus	2	86.5	84.6	2386.84	2386.84	412924.185	403854.174
	3	83.4	77	1888.71	1888.71	315036.828	290861.34

4 Evaluation of Fuzzy Inference System for Hydrocephalus

The proposed inference system uses three input variables, which are the height, area and volume of the ventricles, and one output variable, which is the staging evaluation hydrocephalus or normal membership functions are type triangular system is Mamdani type inference, the ranges established for the input variables and output based on the results tables 1, 2 and 3 is similar for right and left ventricle.

Figure 4 shows the inference system of evaluation cases of hydrocephalus to the right ventricle.

This fuzzy system is to the right ventricle of the brain has three input variables and output variable, and each input variable has three membership functions and the output variable has two membership functions. It is noted that the lowest height of the ventricles according to our tests was 48 mm and the highest was the 90 mm. as shown in Figure 5.

Figure 6 shows that the range area of the ventricles is a normal measure that would be 875.94 mm ^{2} and a case of hydrocephalus which would be 2386.84 mm^2.

Figure 7 shows that the lowest volume is 98 mm ^{3} and the highest volume was 420 mm^3 (it is necessary to multiply the range by one million).
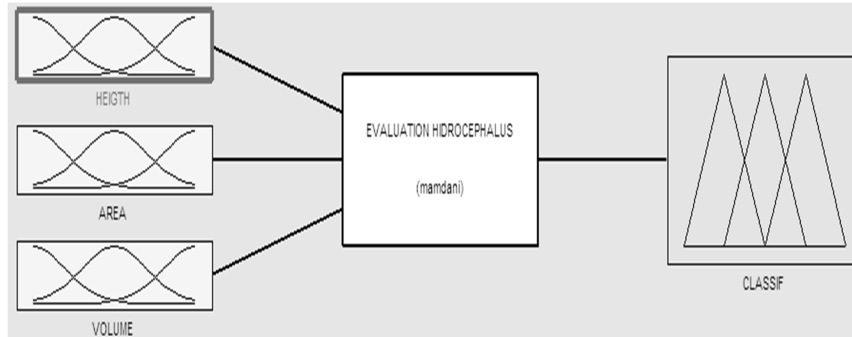
Fig. 4. Fuzzy system with three input variables and output.
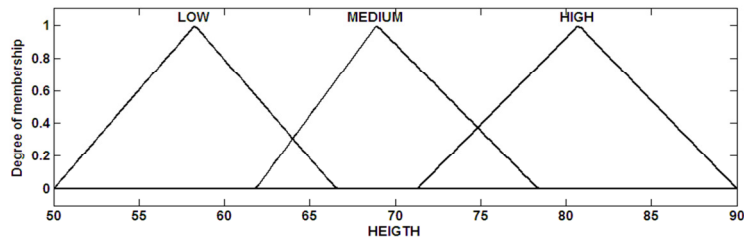
Fig. 5. Each variable has three membership functions are low, medium and high.
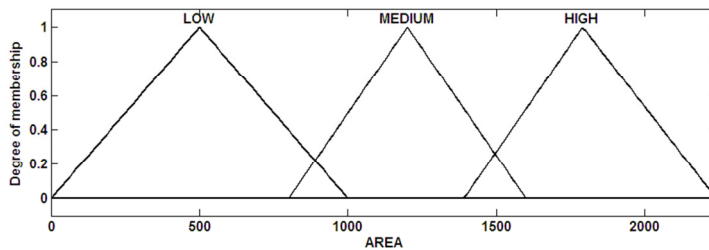
Fig. 6. Membership Functions of right ventricular Area.

Figure 8 shows the output of the fuzzy system that evaluates which cases of normal ventricles and those with a problem of hydrocephalus.

We can see that the output range consider the criterion of height. In the case of individuals who have longer ventricle of 90mm height are be considered cases of hydrocephalus, the criterion of the rules of fuzzy inference system considers its area and volume.

Figure 9 shows the rules of the two fuzzy systems as shown below, An example of the rules is if the ventricle is high, its area is high and the volume is high then classified as hydrocephalus
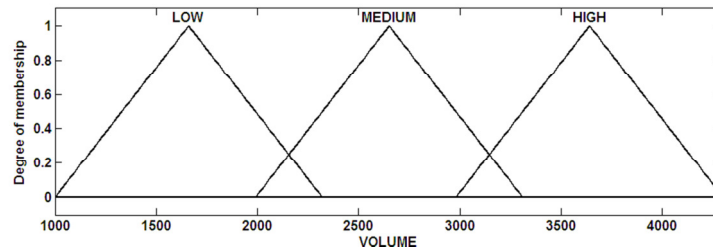
Fig. 7. Membership functions of right ventricular volume.
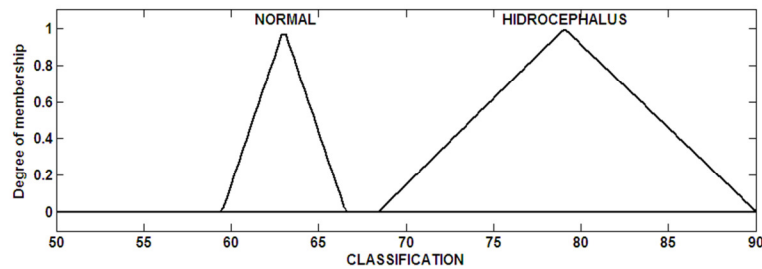
Fig. 8. Output membership functions to classify cases of hydrocephalus.

1. If (HEIGTH is LOW) and (AREA is LOW) and (VOLUME is LOW) then (CLASSIF is NORMAL)

2. If (HEIGTH is LOW) and (AREA is MEDIUM) and (VOLUME is LOW) then (CLASSIF is NORMAL)

3. If (HEIGTH is MEDIUM) and (AREA is HIGH) and (VOLUME is HIGH) then (CLASSIF is HIDRO)

4. If (HEIGTH is HIGH) and (AREA is HIGH) and (VOLUME is HIGH) then (CLASSIF is HIDRO)

5. If (HEIGTH is HIGH) and (AREA is MEDIUM) and (VOLUME is MEDIUM) then (CLASSIF is HIDRO)

6. If (HEIGTH is MEDIUM) and (AREA is MEDIUM) and (VOLUME is MEDIUM) then (CLASSIF is NORMAL)

7. If (HEIGTH is HIGH) and (AREA is HIGH) and (VOLUME is MEDIUM) then (CLASSIF is HIDRO)

8. If (HEIGTH is LOW) and (AREA is MEDIUM) and (VOLUME is MEDIUM) then (CLASSIF is NORMAL)

9. If (HEIGTH is MEDIUM) and (AREA is HIGH) and (VOLUME is MEDIUM) then (CLASSIF is HIDRO)

10. If (HEIGTH is MEDIUM) and (AREA is HIGH) and (VOLUME is HIGH) then (CLASSIF is HIDRO)

Fig. 9. The rules of the evaluation of fuzzy inference system.

5   Results and Conclusions

We utilized a database of 13 individuals with 45 scans each for a total of 585 sample images, To have a more diverse enough valid requires a larger database, and establishes contact with a neuroradiological center to get information, The results provide a criterion to classify cases of hydrocephalus based on the action of the ventricles height, area and volume, is one of the criteria that can be used to classify hydrocephalus and information required to relate the patient's clinical history. The tests were performed using a fuzzy inference system with a triangular membership function; it is necessary to experiment with other types of membership functions to see which provides better results and be able to use genetic algorithms for optimization of membership functions. Average measures were used the database, and statistical methods that allow us to validate the results.

We conclude that proposed method is a good approach, the proposed method is intended to be automated, and using methods of vision obtained measurements of the image and enter the evaluation system of fuzzy inference.

References

1.   Espay, A.J., Crystal, A., Howard:
     `http://emedicine.medscape.com/article/1135286-overview`, (2010)
2.   Novák, V., Perfilieva, I., Močkoř, J.: Mathematical principles of fuzzy logic Dodrecht: Kluwer Academic (1999)
3.   Fuzzy Logic. Stanford Encyclopedia of Philosophy. Stanford University (2006)
     `http://plato.stanford.edu/entries/logic-fuzzy/` Retrieved (2008)
4.   Zadeh, L.A.: Fuzzy sets, Information and Control 8 (3): 8–353 (1965)
5.   Zadeh, L.A. et al.: Fuzzy Sets, Fuzzy Logic, Fuzzy Systems, World Scientific Press (1996)
6.   Jung-Woo, N., Chi-Bong, C., Dong-Cheol, W., Kyung-Nam R., Eun-Hee, K., Hwa-Seok, C.: Evaluation of Hidrocephalic Ventricular Alterations in Maltese Dogs Using Low Field MRI. Vol.9, Num 1, International Journal Applications Veterinary Medical (2011)
7.   Merge Efilm Helathcare Workstation Version 3.4, Philips, Software.
8.   Francis, J.Y., Hahn, K.R.: Iowa City, Iowa: Frontal Ventricular Dimensions On Normal Computed Tomography. Vol. 126, No. 3.
9.   Jamous, M., Sood, S., Kumar, R., Ham, S.: Frontal and Occipital Horn Width Ratio for the Evaluation of Small and Asymmetrical Ventricles Pediatry Neurosurgery. 39, 17–21 (2003)
10. Sullivan, E.V., Pfefferbaum, A., Adalsteinsson, E., Swam, G.E., Carmelli, D.: Differenctial Rates of Regional Brain Change in Collosal and Ventricular Size 4 Year Longitudinal MRI Study of Elder Men. Cerebral Cortex, 12:438-445;1047-3211/02 (2002)

Robotics, Planning, and Scheduling

Ball Chasing Coordination in Robotic Soccer using a Response Threshold Model with Multiple Stimuli

Efren Carbajal and Leonardo Garrido

Intelligent Autonomous Agents Research Group,
Department of Computer Science, ITESM, Monterrey, Mexico
{A00937789,leonardo.garrido}@itesm.mx

Abstract. In any system made of several robots task allocation is an indispensable component in order to achieve coordination. We present two different approaches commonly found in literature to solve the dynamic assignment of the ball chasing task, i.e. multi robot task allocation and division of labour. In particular, we explore both approaches in a 3D simulation robotic soccer domain called Robotstadium. Moreover, we evaluate and compare four controllers representing different coordination implementations belonging to either of the two approaches. We show that by formulating the problem as one of division labour and then employing a response threshold model with multiple stimulus as arbitration mechanism, we provide an efficient algorithm with respect to a proven benchmark solution. We also present evidence indicating that this communication-less algorithm result in an emergent team behavior which *indirectly* also address the positioning problem of robots within the soccer field, keeping physical interference low.

Keywords: Task allocation, response threshold, division of labour, robotic soccer.

1 Introduction

In the last two decades, researchers have given more and more attention to Multi-Robot Systems (MRS). Besides an important reduction in hardware prices, there are some other advantages of MRS like performance benefits, and the accomplishment of inherently complex tasks, which explain its growing use by the scientific community. An example of this can be found in RoboCup, a robotic soccer competition which foster research in robotics and Artificial Intelligence (AI) [1].

Task allocation, the process of assigning individual robots to sub-tasks of a given system-level task, is a very important component of any MRS [13]. In robotic soccer a team of robots have to work together in order to win a match against other team of robots. This entails that robots have to cooperate and coordinate with each other. Where the global task of playing soccer require

different roles or sub-tasks like defense, goalkeeper, passing, and shooting be carried out in order to achieve a team behavior.

Robotic soccer researchers have labeled this problem also as dynamic assigning roles or role allocation [10, 14]. Solutions found in literature often involve the construction of a model of the environment and the use of explicit communication to assign roles. A intuitive idea to solve this problem it is to following a centralized approach, however, the environment is only partial observable to each robot, and no single individual has enough information to make correct decisions [14]. Another attempt is to follow a well known approach in Multi-Agent Systems (MAS): negotiation. But, there are some issues concerning to communication in real time environments which make this technique unsuitable [15].

To overcome those issues some researchers had combined local and global information about ball, using global information only when more reliable local information is not available [14].

Given the difficulties experienced and the importance of local information, it seems suitable the use of a Swarm Intelligence (SI) approach to this problem. SI gives special importance to self-organization, local information, implicit communication to achieve emergent coordination. According to Lerman *at al.* [13]:

> "Emergent coordination algorithms for task allocation that use only local sensing and no direct communication between robots are attractive because they are robust and scalable"

In this paper we propose the use of a response threshold model as a SI task allocation mechanism for the ball chasing task in Robotstadium, a robot soccer simulation based on the Standard Platform League (SPL) of RoboCup and its rules [2].

Section 2 introduce the response threshold model and how this is extended in order to cover some issues present in the domain.

Section 3 shows the arquitecture of the generic controller (i.e. the controller used as base for all the coordination strategies). Section 4 describes the coordination strategies. Section 5 describes the experimental setup. Section 6 shows the results and offers an interpretation. Section 7 concludes.

2   Response Threshold

There are different classes of mathematical models which try to explain division of labour in social insects. According to Beshers *et al.* [5] response threshold models is one them, and in their work they described this class of model. In this model every individual has its own internal response threshold for every task,and engaging in this when the level of the stimulus related to such task exceeds their threshold [6]. This kind of models have been successfully implemented by researchers in MAS and robotics. Examples of these applications are: artificial mail retrieval system [8] in MAS domain, and clustering objects [3] and foraging [11] in MRS.

2.1 Fixed Threshold Model with One Task and One Stimuli

Bonabeau *et al.* [7] have developed a simple model of division of labour in insect societies. This model is describe by the authors as following. Suppose X is the state of an individual (where $X = 0$ indicate that the task is not been performed, and $X = 1$ indicates the task is been performed), and θ_i the response threshold of individual i ($i = 1, 2... ... n$). Then the probability that an inactive individual i starts performing the task P_i per unit time is:

$$P_i(X = 0 \rightarrow X = 1) = \frac{s^2}{s^2 + \theta_i^2} \ . \tag{1}$$

From the eq. 1 we know that the probability that an individual will perform a task depends on s which is the magnitude of the stimulus related task. Similarity, an individual will become inactive with a probability p as describe in eq. 2. Where $\frac{1}{p}$ is the average time spend by an individual before stops performing the task, therefore, p can be found experimentally.

$$P_i(X = 1 \rightarrow X = 0) = p \ . \tag{2}$$

2.2 Fixed Threshold Model with One Task and Multiple Stimuli

In this paper, we propose a slightly different model a little less stochastic. In this model, the probability $P_i(X = 1 \rightarrow X = 0)$ is not independent of stimulus, so it is not a constant p. Instead, we model this probability as the inverse of $P_i(X = 0 \rightarrow X = 1)$ as it is describe in eq. 3. However, this can't be done without some sort of mechanism which allows to decrease the stimulus while performing the task independently of the execution's duration. Here is where the reference to multiple stimuli comes into play. Basically, we employ different types of stimuli that can be classify either as a excitatory or inhibitory, thus the intensity and direction of the stimulus can be calculated as the difference between the sum of excitatory and the sum of inhibitory stimulus as shown in eq. 4.

$$P_i(X = 1 \rightarrow X = 0) = 1 - \frac{s^2}{s^2 + \theta_i^2} \ . \tag{3}$$

$$s = \sum s_{excitatory} - \sum s_{inhibitory} \ . \tag{4}$$

2.3   Stimulus

Table 1. List of stimuli names and types

Stimulus	Type
Distance to the ball	Excitatory
Number of teammates closer to the ball	Inhibitory
Presence of obstacles (sonar)	Inhibitory

This model differs from the original in two aspects: the number of different stimuli related to the task, and how the probability to stop performing the task is computed. Generally in literature the stimulus is only one straightforward measurement of the environment. However, we believe there are several factors involved in the decision making of whether or not approaching to the ball could derive in a good output, specially when there is not direct communication among the individuals. Those factors and their nature are shown in table 1. Taking into account both type of stimulus: excitatory and inhibitory, make possible for the individual to engage in performing the task when excitatory stimulus predominates, or stop performing the task when inhibitory stimulus outweigh excitatory one. The result is a less stochastic response which adapts more quickly to dynamic environment, making the controller better suited for a real-time, coarse-grained MRS competition.

3   Controller

The control algorithm is based on a simple finite state machine (FSM) as it is depicted in figure 1. Different states represent the different phases of the soccer game, that is, the subtasks in which the overall game is decomposed. These sub-tasks are as follows:

Search The robot look for the ball just by moving its head. If ball has already been seen and there is no perception gained about a teammate robot, then the controller change Chase state. Otherwise, If ball is seen but a teammate perception is received then, it makes a transition to Wait state.

Chase Robot moves toward the ball and remains in this state until ball is close enough, that is when the Shoot state takes place. While going after the ball, this may gets outs of sight, in that case the controller returns to the Search state.

Wait In this state robot is stand up tracking the ball until no perception of other robot is received, alternatively switch to Chase state. Other possibility is to lose out the ball, in which case the controller is forced to return to search state.
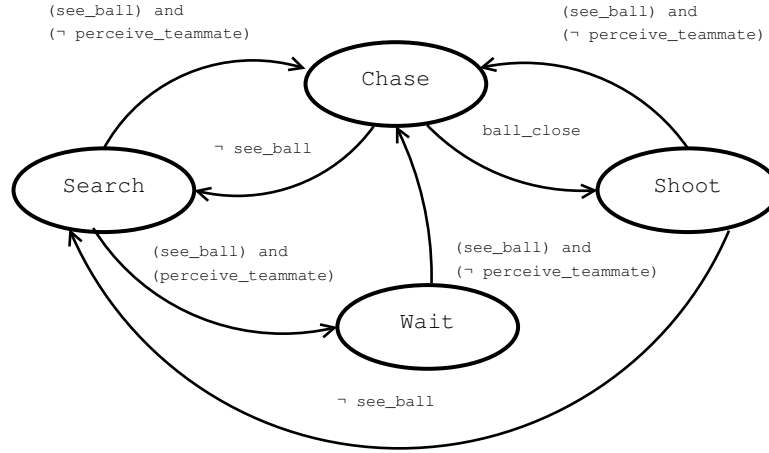
Fig. 1. Finite State Machine diagram.

Shoot Robot hit the ball in goal direction, then as ball moves along, robot either lose it and return to Search state, or start to chase it again, switching back to Chase state.

Transitions between states occur on the base of events that are external (e.g. Perception of another robot) to the robot. The edge labels between states (as shown in figure 1 represent the conditions (also called predicates) that must be true for the transition to occur. The complete list of the predicates, their meanings and how they are evaluated is given in table 2. Their truth values are evaluated from sensor readings at every control cycle.

Table 2. Definition of constants and predicates used by the control algorithm

B_D	Maximum distance between robot and ball to try to kick the ball
`see_ball`	Ball is detected using visual information obtained from the camera
`perceive_teammate`	A teammate is communicating that it is closer to the ball
`ball_close`	Distance to ball $< B\_D$

4 Coordinations Strategies and Evaluation Metrics

In order to coordinate robots, allocation strategies addressed in this work employ two types of communication mechanisms. The first refers as "public" emphasizes in the existence of an explicit collaborative information flow between teammates through a emitter/receiver device. Whereas in the latter, which we are call "private", there is no explicit information sharing but intead robot recognition algorithms are employed to communicate indirectly by *sensing* the presence of

others teammates. On the other hand, the keyword "utility" refers to the use of utility values for the purpose of allocate the chaser role. While the the keyword "reactive" indicate the existence of simple rules which rely solely in perceptions to determine the execution of the ball chasing task.

In threshold-based systems, the *propensity* of any agent to act is given by a response threshold. Basically, if the demand is above the agents threshold then that agent continues to perform the task, conversely, if the demand is below its threshold then the agent stops performing that particular task. In the algorithm presented in this paper the visual perception of the ball, teammates and opponents, represents the agent estimation of the demand or stimuli associated with the ball chasing task.

Thus, in what follows we present four different role allocation algorithms which can be described by some of the previous characteristics.

Public, Utility, Single Robot Allocation Algorithm (PuUS) In this strategy each robot consult the messages of the rest of the team, the message from each teammate consist in the estimation of distance (utility) from its own perspective to the ball. By comparing this messages to its own perception, the individual is able to determine whether or not is the closest robot to the ball, in which case, start chasing the ball. This approach ensures only one robot chase the ball at any given time and it is also the more frequent used among researchers in RoboCup. This path is suitable to formulate the assignation of tasks to robots as a task allocation problem.

Public, Utility, One or Less Robots Allocation Algorithm (PuUOoL) This strategy is based on the previous one, and supported on the fact that there are scenarios when reallocation of the chase task among robots could derive to collisions. One special case is when the closest robot to the ball isn't seeing it, giving rise to more collisions. Therefore this strategy is proposed as an alternative version of PuUS with the additional rule that no robot chase the ball until every robot is stand up and looking to the ball. This rule ensures that the average number of robots chasing the ball at any moment be of one or less.

Private, Reactive, Multiple Robot Allocation Algorithm (PrRM) In this implementation every robot has been programmed to chase the ball without previous communication; therefore, it will be times when more than one robot is in chasing mode. To avoid a grievous situation of undesired collisions, a reactive behavior that interrupt chasing activity is used. The reactive mechanism consist in the recognition of a teammate closer to the ball, in which case the robot stops and waits. This strategy is more in tune with the the division of labour approach follow by bio inspired researchers. Notice that this allocation strategy allows more than one chaser at the same time.

Private, Multiple-Stimulus-Threshold, Multiple Robot Allocation Algorithm (PrMSTM) This algorith is a modified version of PrRM but instead of reactive rules, robots have a threshold model to force action in a stochastic fashion. As explained in section 2, the intention of this mechanism

is to ponder several key aspects (i.e. multiple stimulus) of the environment in order to assess the *demand* to execute the ball chasing task.

In order to evaluate the performance of such implementations, we make use of the direct output of every soccer robotic controller: goals (i.e. goals scored as well as goal conceded). But we also propose the use of complementary metrics making emphasis in the intention we have in this work to produce results that are interesting to continue with and validate beyond simulation level. Additional metrics proposed in this work are physical interference and efficiency. Both of them been of much interest in MRS [12, 9].

Performance The main indicator of performance in soccer is the goal difference (i.e. goals scored minus goals conceded). Because depending the team you choose as reference team lose of win the match, this number can take negative values (when reference team lose). To avoid confusion we are going to use as reference the team running implementations of strategies to test. In addition, those results were normalized in order to ensure only zero or positive numbers. The reason behind applying normalization to the data is because positive numbers are required to estimate the efficiency as it is discussed further in efficiency description. To summarize, for performance we mean the output of a normalization process that employs the goal differenceas the only input to generate zero or positive numbers. The normalization consist in adding all numbers with the absolute of the most negative (minimum value of goal difference) such that the most negative one will become zero and all other number become positive.

Efficiency Lets start by defining efficiency, we refer to efficiency as the capability to convert some valuable resource into another new valuable resource. In the context of robotic soccer, we define as the input resource the energy spent by the robot moving around, and as output resource,the total number of goals scored and conceded. However, the energy spent by a robot depends on too many factors, known and unknown, and a precise measurement it is far beyond the reach of this work. Conveniently, we know that the displacement of a robot is proportional to the energy it uses. Thus, we decide to use the displacement as an approximation of the energy spent. This way we end up with equation 5.

$$\eta_i = \frac{\Delta_i}{\epsilon_i} \ . \tag{5}$$

Where:

η_i = Team's efficiency during match i
Δ_i = Normalized goal difference during match i
ϵ_i = Displacement in meters during match i

Interference Another important issue related to the performance of a generic MRS are collisions, also known as *physical interference* [4, 9]. According to Goldberg at al. [9] physical interference arises in competition for space. They

show with experiments that the measurement of it can be an effective tool for system design and evaluation. In Robotstadium's case, space competition are present mostly in a particular task: chasing the ball. The number of collisions by members of the tested team was tracked down with help of an emulated GPS device in the supervisor's code (i.e. referee code that along with code of controllers and world complete the simulation).

5   Experimental Setup

The main objetive of this study is to challenge two ideas widely established in practice. The first is related to the number of robots which should be chasing the ball at any given time during the match. So far this number has remained fix to one by roboCup researchers. As a consequence, two out of the four implementations evaluated in this section represent a division of labour approach which inherently allocate tasks without restrictions in the number of individuals that engage in them. The second idea is about the need of make use of a spatial model, autolocalization and explicit commmunication in order to distribute robots, improve performance and reduce collisions among robots. A way to challenge this idea is by contrasting it with bio inspired implementations, which produce an emergent team behavior that result in a self-organized distribution of robots in the field without direct communication or a concrete spatial model of the environment.
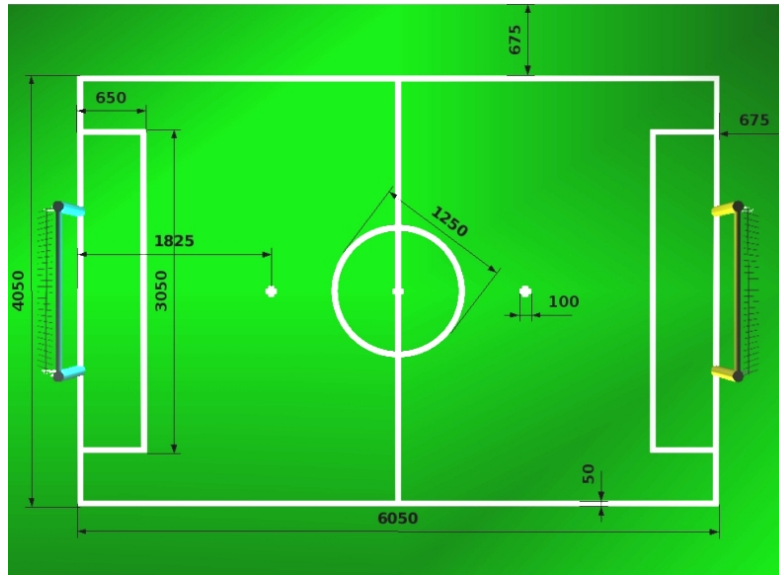
Fig. 2. Robotstadium field measures in millimeters taken from the top orthographic projection of the simulation in Webots
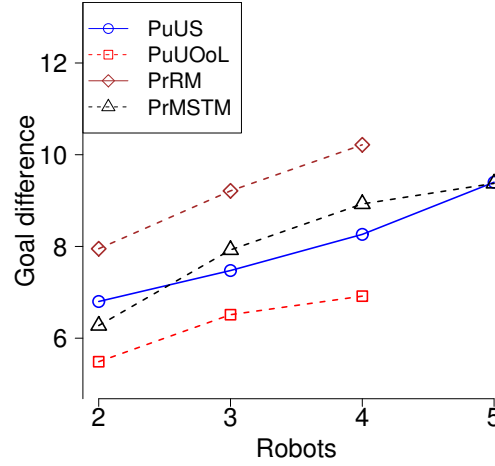
Fig. 3. Comparison of performance as group size increases

An experimental trial consist in running complete match divided in two half periods of 10 minutes, where in one side of the field there is a team representing one of the four strategies, while in the other side, there is a single robot. In this manner, experimental trials have been performed with each of the four strategies: PuUOoL, PuUS, PrRM and PrMSTM; and for each strategy forty trials were performed with two, three, and four robots. An extra run of experiments with five robots for the two better performed strategies were added as an attempt to shed light to further conclusions. As a result, a total of 560 experiments were carried out.

6 Results and Discussion

Data obtaining from all the experiments have been analyzed with a two-way ANOVA statistic test. Where performance, interference and efficiency were explained using coordination strategy as a categorical variable and team size (number of robots) as numerical variable. In all three tests both variables, strategy and team size, were found to be statistically significant with p-values < 0.05.

Beforehand we hypothesized that PrRM would produce the higher number of interferences among all strategies, thus, its performance would be outperformed by that of strategies PuUS and PuUOoL. Surprisingly, this was not the result as shown in fig. 3, despite the high level of interference. We believed this is due a higher chance to get first to the ball and to handicap the other team's robot. However, when looking to interference, as fig. 4 shows it, the performance gains of PrRM become overshadow by exponential growth in interferences.

On another hand, performance of PuUOoL was lower among all implementations. And performance of PuUS and PrMSTM was similar between them with no statistically significant difference observed. A slightly better performance was

presented in the threshold strategy when the team size is 4, but with virtually the same performance when the team size reach 5 robots. Besides the fact of both implementations achieved almost the exact performance when team size was fixed to five, it is worth to note as well that PrMSTM strategy tendency to improve along the team size increases, ends abruptly when arrives to the five robots per team, resulting in both strategies performance curves crossing each other.
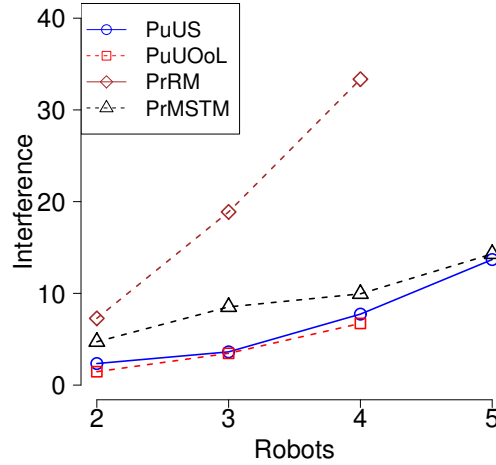
Fig. 4. Comparison of interference level as group size increases

Could these two seemingly independent issues be related?, we suspect they are indeed, we believe the performance of both strategies is bound by the field size, which may happens to be too small to allow an equal and active participation from all the robots. Outcome from efficiency, seems confirm this. Even when there was no apparent gain in performance in PrMSTM when passing from four to five robots, there was a gain in efficiency, and since efficiency is affected either by performance or energy spent, this gain must come mostly from a reduction in the latter. This reduction in energy spent is more pronounced than in others team size configurations, which can be explain by a good coverage of whole field by the five robots. Note that if this hypothesis were correct, may imply that PrMSTM strategy is also good at adapting or showing robustness to environmental changes. However, more evidence is needed to support this. So far we can only conclude that both controllers performed at a similar level.

As mentioned before, we hypothesize that the presence of interference of PrRM would be greater than found in PuUO, and the latter greater than found in PuUOoL. As figure 4 shows it, the guess was correct. However, we didn't know what to expect about the magnitude of those difference, neither of the level of interference in PrMSTM. The outcome is that the amount of collisions in strategy PrRM is, to a large extent, bigger than the rest of implementations.
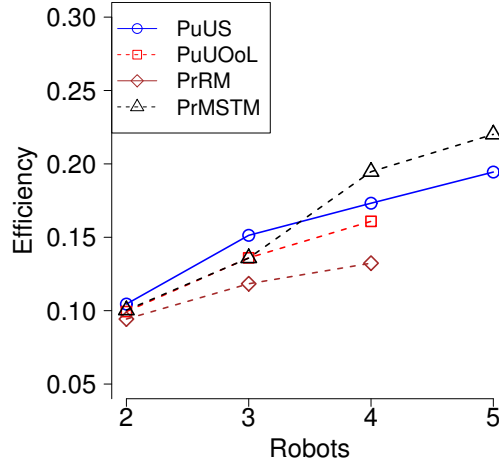
Fig. 5. Comparison of efficiency results as group size increases

Unlike PrRM, in PrMSTM the interference level is not a grievous problem, in fact, this is comparable to those in PuUOoL and PuUS when four or five robots are set per team.

Another hypothesis we were interested to proved is related to the efficiency. Due to the restriction of one at most, we were expecting a more efficient use of energy in PuUS and PuUOoL. But as shown in figure 5 this was not exactly the case. For three robots per controller PuUS is the most efficient, however, as the number of robots increase to four and up to five, PrMSTM takes the credit as the most efficient.

Is interesting how PrMSTM and PrRM both representing a division of labour approach are at the same time the most efficient and inefficient. This indicate the influence of the threshold model in regulating the number of active chasers. A exception of PrMSTM, what happened with the rest of implementations was that efficiency holds almost steadily from the start only gaining a little with every increase in team size. From the scalability perspective, we can observe in figure 5 that efficiency curves for all strategies, except for PrMSTM, resembled logarithmic functions, this fact indicate marginal returns while adding more robots.

7 Conclusions

In this paper, we have presented a comparative study of four distributed, multi robot allocation mechanisms that allow a team of autonomous, embodied agents to dynamically allocate the fittest individual(s) to a given task. These coordination algortihms can be classified in two approaches, task allocation with PuUS and PuUOoL as representatives, and division of labour with PrRM and

PrMSTM as representatives. We compared their performance and efficiency in a robotic soccer case study concerned with a ball chasing task.

We showed that framing the ball chasing task assignment as a division of labour problem and using a multiple stimulus threshold model to address it, the system performs as well as the benchmark solution (i.e.PuUS for been the most widely used among researchers) while at the same time arrive to additional benefits as a significant increment in efficiency when the team size is set to four or five robots without any sort of direct communication.

References

1. Robocup objective: Pushing the state of art. `http://www.robocup.org/about-robocup/objective/`
2. Robotstadium: online robot soccer competition. `http://robotstadium.org`
3. W Agassounon and A Martinoli. Efficiency and robustness of threshold-based distributed allocation algorithms in multi-agent systems. *Proceedings of the first international joint conference on Autonomous agents and multiagent systems part 3 AAMAS 02*, pp. 1090–1097 (2002)
4. R C Arkin and T Balch. Cooperative multiagent robotic systems. *Artificial Intelligence and Mobile Robots*, pp 277–296 (1998)
5. S N Beshers and J H Fewell. Models of division of labor in social insects. *Annual Review of Entomology*, 46(413-440):413–440 (2001)
6. E Bonabeau, M Dorigo, and G Theraulaz. *Swarm Intelligence: From Natural to Artificial Systems*, Oxford University Press (1999)
7. E Bonabeau, G Theraulaz, and J L Deneubourg. Quantitative study of the fixed threshold model for the regulation of division of labour in insect societies. *Proceedings Biological Sciences*, 263(1376):1565–1569 (1996)
8. Eric Bonabeau, Andrej Sobkowski, Guy Theraulaz, and J L Deneubourg. Adaptive task allocation inspired by a model of division of labor in social insects. *Bio Computation and Emergent Computing*, pp. 36–45 (1997)
9. D Goldberg and M J Matarić. Interference as a Tool for Designing and Evaluating Multi-Robot Controllers. *AAAIIAAI*, 8:637–642 (1997)
10. Eric Henry Work, Chown, Tucker Hermans, and Jesse Butterfield. Robust Team-Play in Highly Uncertain Environments (Short Paper). (Aamas) (2008)
11. M J B Krieger and J B Billeter. The call of duty: Self-organised task allocation in a population of up to twelve mobile robots. *Robotics and Autonomous Systems*, 30(1-2):65–84 (2000)
12. Thomas H. Labella, Marco Dorigo, and Jean-Louis Deneubourg. *Division of labor in a group of robots inspired by ants' foraging behavior*. PhD thesis (2006)
13. Kristina Lerman, Chris Jones, Aram Galstyan, and Maja J Mataric. Analysis of Dynamic Task Allocation in Multi-Robot Systems. *The International Journal of Robotics Research*, 25(3):225–241 (2006)
14. Michael J Quinlan, Steven P Nicklin, Stephen R Young, Timothy G Moore, Stephan K Chalup, and Richard H Middleton. The 2005 NUbots Team Report. *Electrical Engineering* (2006)
15. Thomas Rofer, Michael Weber, Hans dieter Burkhard, J Matthias, G Daniel, Jan Hoffmann, and Bastian Schmitz. German Team: RoboCup 2005 (2005)

IOCA: An Interaction-Oriented Cognitive Architecture

Luis A. Pineda, Ivan V. Meza, Héctor H. Avilés, Carlos Gershenson, Caleb Rascón,
Montserrat Alvarado, and Lisset Salinas

Instituto de Investigaciones en Matemáticas Aplicadas y en Sistemas (IIMAS),
Universidad Nacional Autónoma de México (UNAM), México D. F., Mexico
lpineda@unam.mx

Abstract. In this paper an interaction-oriented cognitive architecture for the specification and construction of situated systems and service robots is presented. The architecture is centered on an interaction model, called *dialogue model*, with its corresponding program interpreter or *Dialogue Manager*. A dialogue model represents the task structure of a specific application, and coordinates interpretations produced by the system's perceptual devices with the system's intentional actions. The architecture also supports reactive behavior, which relates context independent input information with the system's rendering devices directly. The present architecture has been used for the specification and implementation of fixed multimodal applications, and also of service robots with spoken language, vision and motor behavior, in a simple, integrated and modular fashion, where the cognitive architecture's modules and processes are generic, but each task is represented with a specific dialogue model and its associated knowledge structures.

Keywords: Dactylogical alphabet, contour chains, ALVOT algorithms, differentiated weighting diagram.

1 An Interaction-oriented Cognitive Architecture

Autonomous systems capable of interacting with the world through language, vision and motor behavior need to be able to perform reactive and representational behaviors. Reactive behavior involves responding to world's stimuli directly in a context independent manner, while representational or "intentional" behavior involves assigning interpretations to the world's stimuli, mostly in a context dependent manner, and acting upon those interpretations. Detecting and avoiding an obstacle and turning towards a source of sound are better thought of as reactive behaviors, while reasoning, planning and problem-solving are representational processes. Reactive and representational behaviors can also be distinguished in terms of the time elapsed from the stimulus to the response: while the reactive loop is performed instantaneously, the latter can take several seconds, minutes or even longer periods of time. Consequently, several reactive behaviors can be embedded within one representational loop. Another distinctive feature between these two

kinds of behaviors is that while the flow of attention, language and thought is mostly sequential, several reactive processes can be performed simultaneously, and the agent can be mostly unaware of performing these behaviors. Yet, despite all these differences, representational and reactive behavior need to be coordinated in order the agent interacts with the world in a coherent and robust fashion. The integration and coordination of these functionalities in autonomous agents requires the definition and construction of a congruent computational framework; for this, over the last few years we have been developing and testing the Interaction-oriented Cognitive Architecture (IOCA). A cognitive architecture is a system that integrates perception, thought and action, where the specific knowledge of the task and domain can vary but the computational structures and processes remain constant (e.g. [Chong et al., 2007]). IOCA is oriented towards the interaction between the computational agent and the world, including the interpretation of external representations (e.g. spoken language, text, diagrams, posters, etc.). The input-output representational loop involves the recognition and interpretation of the external stimuli, the selection of the appropriate action by the Dialogue Manager (DM), and its full specification and rendering.
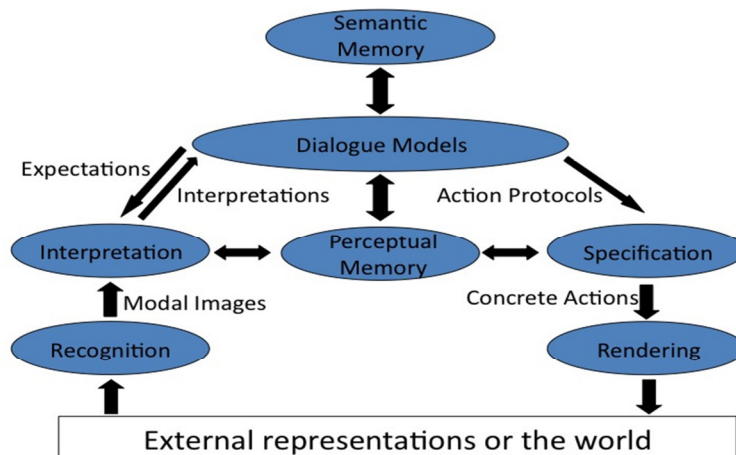
Fig. 1. Interaction-oriented Cognitive Architecture (IOCA).

IOCA incorporates a semantic and a perceptual memory; this distinction corresponds loosely to the traditional distinction between semantic and episodic memory that is widely used in cognitive psychology and neuropsychology [Tulving, 1972]. The semantic memory holds concepts, particular and general, used while carrying out the task and its domain. The knowledge stored in this structure has a propositional character and is modality independent. We are using a logical representation with Prolog clauses in our

current implementations, but alternative schemes, like semantic networks or description logics, could also be used.

The perceptual memory, in turn, stores associations between modality specific *internal images* or "percepts" and their corresponding interpretations or *meanings*. Internal images, on the one hand, represent the sensitive characteristics of the external stimuli and are associated to a perception modality. However, these images also capture the way the sensed information is structured (i.e. the external pattern). For instance, an object in the world, such as a diagram, a map, a text, etc., can all be perceived through the visual channel. The image, however, is "seen" differently in each case, and stored in a particular format or code, that corresponds to that particular "way of seeing". In the present framework each of these codes corresponds to a *modality*; thus, there is a modality for each "way of seeing", and each may involve one or more recognition devices (e.g. an Automatic Speech Recognition (ASR) System or a vision recognition machine). In addition, an internal image codifies the corresponding external pattern independently of its meaning. For instance, the product of an ASR system is an uninterpreted text; a SIFT vector is the product of codifying a visual image independent of its interpretation. Internal images are minimal information structures aimed to distinguish the particular concept in the input from the set of particular or general concepts in the interpretation context. Consequently, internal images do not have to be fully fleshed out representations of external objects (e.g., 2-D or 3-D geometric constructions with color or texture). The patterns represented through internal images can be dynamic and evolve in space and time. For instance, the visual pattern of a physical gesture, like "halt", that can be codified as a Hidden-Markov Model [Avilés *et al*., 2010a]. Regular expressions and specialized natural language grammars are also considered as internal images in the perceptual memory. In this view, particular or general concepts are associated to the regular expressions or grammars that "select" these concepts.

The meanings of internal images, on the other hand, are represented in a propositional format, which is modality-independent, and the expressions representing these meanings can be thought of as "tags" of the corresponding percepts. In this way, internal images can be interpreted as expressing particular or general concepts. This structure also permits to access concepts or interpretations via their percepts and vice versa. The associations between internal images and their interpretations can be established beforehand when the application is developed, or dynamically when the concept associated with the image is provided by the human user at the time the image is recognized by the system in the interactive task.

We turn now to the description of the main representational loop. The recognition modules translate external patterns sensed by the recognition devices into the corresponding internal images in the corresponding modal code, mainly in context independent way and in a bottom-up fashion.

The *interpretation module* is responsible of assigning interpretations or meanings to such internal images. This is a context dependent process that takes into account the expectations of the system that are present in the interpretation situation, as will be elaborated in Section 2. This process uses the perceptual memory and performs a

qualitative match between the images recovered by the recognition devices and the images in the perceptual memory, which are stored in the same modal code. The result of the interpretation process is the "meaning" (i.e. the interpretation) associated to the external image in the interpretation context. As the number of associations in the perceptual memory can be quite large, the *expectations* of the current situations are also used as the indexes of the associations to be considered in specific interpretation situation. By this account, the expectations not only set up the interpretation context but also select the relevant memories to be used for the particular interpretation act. The recognition and interpretation levels of the architecture correspond to the overall perceptual process whose purpose is to assign interpretations to the external patterns conveying linguistic messages or events in the world that are attended to and acted upon "intentionally" by the computational agent.

The central module in the interaction loop is the dialogue model with its associated program interpreter or D*ialogue Manager* (DM). This contains the specification of the task's structure and relates expectations and interpretations with the corresponding intentional actions. Interpretations and actions at this level are specified in a propositional format that is independent of the input and output modalities.

In the output side, *actions* are performed as a response to interpretations; these can be *external*, like displaying an image, synthesizing a text or moving a robot, but also *internal*, like performing a reasoning or a planning task, involving only the representational structures of the system. In this sense, we distinguish linguistic and interaction protocols, which are stated through the dialogue models, from the "thought" processes, which are internal actions that are called upon by the dialogue model when required. Actions can be composite and involve a number of basic actions, more than one output device, and an internal and external part. Dialogue models have also access to the interaction history, and expectations and actions can be stated dynamically in terms of the events that happened before in the current task. Dialogue models can also access the knowledge stored in the semantic and perceptual memory (e.g. for heterogeneous reasoning). Finally, the action protocols specified in dialogue models are fully specified before they are sent to the specific rendering devices of the system.

IOCA differs from other cognitive architecture in that it is focused on the communication channel, and on the inclusion of a perceptual memory for the explicit recollection of sensory information. IOCA also aims to distinguish the main communication loop involving interpretations from the cognitive processes proper, and also to understand the relation between representational and reactive behavior. In doing so, IOCA focuses on the questions related to the interaction between language, perception and thought.

2   Specification and Interpretation of Dialogue Models

The central component of the cognitive architecture is the dialogue model –or interaction model– through which the task structure and the communication protocols between the computational agent and the human user are specified. Dialogue models are defined in relation to a basic notion: the situation. A situation is an "intentional state" of the agent, which is defined in relation to the expectations of the agent in the situation (either possible messages with communicative intent produced by the human interlocutor or natural event in the world), the actions the agent should perform in case a specific expectation is met, and the situations into which the agent moves after performing such action. In this way, situations are contextualized in terms of generic interaction protocols. These protocols represent the structure of the task, and traveling from the initial to the final situation corresponds to performing the task successfully.

Expectations are the set of potential speech acts types (e.g. [Levinson, 1983]) that can be expressed by the interlocutor in the situation, in addition to the potential natural events that can occur in the world in the situation, that are also handled intentionally. Expectations are expressed through statements involving the system *S* and the human user *U* like, for instance, "*S* expects that *U* commands *S* to make *p*" or "*S* expects that *U* ask *S* to provide information *q*". However, as the expectations are embedded in the protocols and the corresponding actions assume this intentional interpretation (i.e., *S* makes *p* and *S* provides information *q*), the intentional statements are implicit in the interpretation process and only the conceptual content in the expectations is stated explicitly in the dialogue models (e.g. the propositions *p* and *q* in the examples above). The central component of the cognitive architecture is the *dialogue model* –or interaction model– through which the task structure and the communication protocols between the computational agent and the human user are specified. Dialogue models are defined in relation to a basic notion: the *situation*. A situation is an "intentional state" of the agent, which is defined in relation to the expectations of the agent in the situation (either possible messages with communicative intent produced by the human interlocutor or natural event in the world), the actions the agent should perform in case a specific expectation is met, and the situations into which the agent moves after performing such action. In this way, situations are contextualized in terms of generic interaction protocols. These protocols represent the structure of the task, and traveling from the initial to the final situation corresponds to performing the task successfully.

Expectations are the set of potential speech acts types (e.g. [Levinson, 1983]) that can be expressed by the interlocutor in the situation, in addition to the potential natural events that can occur in the world in the situation, that are also handled intentionally. Expectations are expressed through statements involving the system *S* and the human user *U* like, for instance, "*S* expects that *U* commands *S* to make *p*" or "*S* expects that *U* ask *S* to provide information *q*". However, as the expectations are embedded in the protocols and the corresponding actions assume this intentional interpretation (i.e., *S* makes *p* and *S* provides information *q*), the intentional statements are implicit in the interpretation

process and only the conceptual content in the expectations is stated explicitly in the dialogue models (e.g. the propositions p and q in the examples above).

Speech acts are normally direct, in the sense that declarative statements are used for communicating facts or beliefs, interrogative for making questions, and imperatives for commands, etc., where each of these modalities of expression has a characteristic intonation. However, the basic relation between the type of intention and the modality of expression is often changed, as when a command is expressed through a polite question (e.g., "Could you show me poster A?"), producing the so-called indirect speech acts, which pose great challenges to the interpretation process. In order to interpret speech acts, either direct or indirect, we take advantage of the context present at the interpretation situation, and the interpretation problem is seen as what is the most likely intention among the expectations of the situation that is intended by the interlocutor. In this sense, expectations are conceived as *a priori* knowledge, while the input information (the actual external stimuli) is taken as evidence (i.e. likelihood) in favor of a particular expectation. The actual interpretation of the input message is the "grounded" expectation that is best met by the input information in the interpretation situation. This makes the interpretation process as a whole have a strong Bayesian flavor. However, *a priori* knowledge and likelihoods need not be numerical probabilities, as the "product operator" between these two is the interpreter, that collects the output of the recognition devices, looks up the relevant percepts in the perceptual memory, and produces the actual interpretation, expressed as a grounded speech act in the dialogue model.

Natural states and events in the world that are expected by the computational agent are also treated intentionally, and are defined as expectations of the situations in which they are likely to occur. For instance, if a robot is standing in front of a door it may have the expectation that the door is open or that it is closed. In this case, the actual image recognized visually has no communicational intent, but nevertheless it is an expectation that has to be acted upon intentionally in the context (e.g. crossing the door if it is opened or asking for the door to be opened otherwise). In this case, although the stimulus is visual, it is subject to interpretation and the behavior has a representational character.

Speech acts can express propositional or conceptual content (e.g. "Please, explain me poster A."); can assert that the message has been understood as intended (e.g. "Do you want me to explain poster A?"); and can maintain the communication channel so the interlocutors can establish and preserve a "common ground" (e.g. "I didn't hear you, can you say it again?") [Clark and Schaefer, 1989]. The structure of practical dialogues [Allen *et al.*, 2001] oriented to solve specific tasks has been analyzed with tagging schemes that consider these three levels of speech acts (i.e. conceptual content, agreement, and communication) and the relations between a speech act and the preceding and following acts, which establishes a strong restriction in the structure of intentional transactions [Allen and Core, 1997; Pineda *et al.*, 2007]. These intuitions are also used in the specification of dialogue models: agreement and communications protocols can be stated to make sure the system and the user have a common ground. Also, whenever no expectation in a situation is satisfied, the system is out of context (i.e. the common ground has been lost) and invokes recovery protocols, stated also as dialogue models, with the

purpose to set itself in context again. These protocols can also be used to restore the context when an expected natural event does not occur when it should.

The actions performed by the system in response to an interpretation are also thought of as speech acts. For the specification of these actions we follow loosely Rhetorical Structure Theory (RST) [Mann and Thompson, 1988], where an action predicate stands for a "rhetorical structure" with one or more basic actions. Each basic predicate in the structure stands for a particular action, either internal or external. For instance, an explanation may involve a presentation, an elaboration, a generalization expressed through spoken language, and even an exemplification expressed through a picture or a video. Motor actions are also stated through rhetorical structures (e.g. *move*(*a*, *b*)). Action predicates have to be fully specified, possibly using information in the perceptual memory, before the corresponding actions are rendered in an output modality.

Dialogue models have a graphical representation where situations are represented through nodes and situation relations are represented through directed links. Every link has a label of the form $\alpha{:}\beta$, where α stands for an expectation and β stands for the action that is performed by the system when the expectation α is satisfied in the current situation s_i. As a result of performing such action, the system moves to the situation s_j at the end of the link, as illustrated in Figure 2. Situations can be basic, in the sense that a particular interpretation act takes place at the situation (e.g., through language or vision, or both). Situations are typed, and there is one type of situation for each modality defined in the perceptual memory, so the DM considers the situations type in order to select the appropriate recognition devices, with the particular modality code, to perform each basic interpretation act. There is also a special type of situation that we refer to as *recursive*, which embeds a full dialogue model. This expressive power permits to model complex applications in a simple and modular way, where composite tasks have a stack structure. The formalism corresponds to recursive transition networks (RTN), augmented with functions that permit the dynamic specification of expectations, actions and next situations. We refer to this formalism as Functional-RTN or F-RTN [Pineda, 2008; Pineda *et al*., 2010].
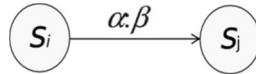
Fig. 2. Graphical Representation of Dialogue Models.

The conceptual content in expectations can be of three kinds, which are as follows:

(1) **Propositional:** These are concrete expectations represented with constants or saturated propositions (e.g. *a*, *p*(*a*, *b*)) in the dialogue models.

(2) **Predicative:** These are expectations involving a limited form of abstraction, represented as open predicates or predicative functions (e.g. *p*(*x*), *q*(a, *y*)) in the dialogue models. To meet expectations of this kind, one or more parameter needs to be extracted from the world, and these become the arguments in the

expression representing the interpretation. For instance, if the robot asks the users for his or her name, the expectation is represented as *name*(x), and the interpretation of the user's reply, in case the expectation is met. For instance, "I'm Peter", is represented as *name*(*peter*). These predicates are interpreted indexically in relation to the agents involved in the transaction and in relation to the local spatial and temporal context.

(3) **Functional:** These depend of the interaction history at the level of the interpretations, actions and situations, which is collected by the system along the interaction. In the present framework, this "working memory" structure is called the *anaphoric context*. Although the task protocols are specified in advance through the dialogue models, expectations and actions can change along the task, and need to be determined dynamically in relation to the context. These kinds of expectations are represented through explicit functions in the dialogue models. These functions have the anaphoric context as one of their argument, and their values are propositional or predicative expressions representing expectations. Functional expectations are evaluated first, and their values are passed top-down to the interpreter in the current interpretation act.

The next situation in a dialogue model's transition can also depend on the anaphoric context. In this case, the situation to which the agent has to move is represented through a function h whose argument is again the anaphoric context but its value is the actual next situation. In Figure 3, the function h is represented by a small dot, and its possible values by dashed-links.
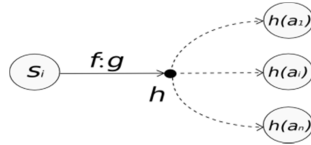
Fig. 3. Functional representation of expectations, actions and transitions.

Situations are also parametric objects, and their arguments can be bound with the interpretation and action predicates' arguments, allowing the establishment of co-reference relations between terms in the interaction structure.

The system's intentional actions can also be propositional, predicative and functional, and can be determined dynamically. Predicative actions can be defined through open predicates where the free variables are bound to the situation's or expectation's arguments in the corresponding transition. Functional actions can be defined through explicit functions, as it is with expectations and next situations.

Finally, the functions that define the described functional objects can access information stored in the semantic memory, which can be considered as an additional argument. Thus, functional expectations, actions, and next situations are dynamic objects

that depend not only of the anaphoric context, but also on the particular and general concepts of the application task and domain.

3 Coordination of Representational and Reactive Behavior

In the architecture discussed so far, speech acts produced by the system's interlocutor and natural events in the world need to be synchronized with the expectations of the current situation in order that the computational agent can interpret them. Otherwise, the external stimuli are left unattended by the agent, even if those stimuli are defined as expectations of other situations.
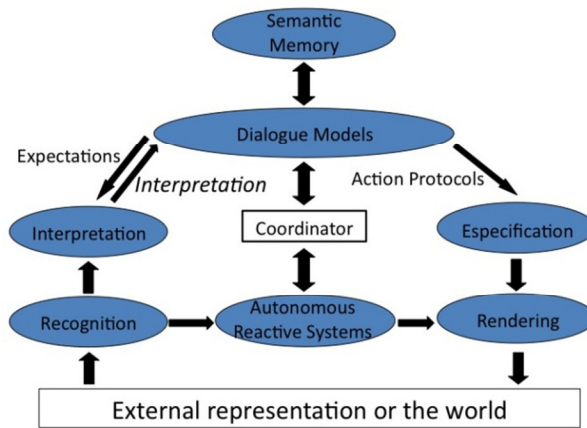
Fig. 4. IOCA with Reactive Capabilities.

Most traditional applications in static worlds with a fixed interaction initiative, such as when the robot is restricted to obey user commands or the human is guided passively by the robot, can be modeled through this expectations-based architecture. However, their model is too weak for robots that need to move or navigate flexibly and robustly in a dynamic environment; in circumstances where unexpected obstacles can appear or things can be moved; or when other dynamic agents are present, such as human interlocutors taking the interaction initiative spontaneously. In order to cope with dynamic environments, IOCA needs to be extended with a set of reactive modules, which relate the input information collected by the recognition devices with the rendering devices directly. In Figure 4 it is shown where an Autonomous Reactive System (ARS) has been added. At the moment, we are considering two main ARSs: the Autonomous Navigation System (ANS) and an Autonomous Position and Orientation Source of Sound Detection System (APOS) to allow the robot to face its interlocutor reactively. This extension requires, in addition, the inclusion of a control structure for coordinating the dialogue models with the

ARSs that we called *The Coordinator,* also shown in Figure 4. This figure illustrates that the main representational loop may embed a number, possible large, of reactive loops. In this respect, IOCA loosely resembles a subsumption architecture [Chong *et al*., 2007].

The coordination between representational and reactive behavior is not trivial, as reactive actions can change the spatial and temporal context expected by the dialogue models, and the system needs to relocate itself in the context dynamically. In order to address this problem, we are studying three basic coordination behaviors, which are as follows:

(1)   The interpretation process of the current dialogue model inside the DM and the ARSs can proceed concurrently without interfering with each other.
(2)   The DM can put on hold and reactivate the ARSs, and vice versa.
(3)   An ARS can load and execute a recovery dialogue model directly.

For the ARSs we are considering a basic navigation function such that given a metric map, the robot's position and orientation in this map, and a target position and orientation, the system produces and executes a plan (i.e., a sequence of moving commands) to reach the target. During this process, the system avoids obstacles reactively and adjusts its estimated position and orientation continuously in the metric map. In the present project we are focusing on the definition of the coordinator, and for the actual navigation we are exploring the use of available tools (e.g. [Vaughan *et al*., 2003]). This basic navigation functionality is called upon intentionally by an action directive stated and performed by a dialogue model; in this mode the reactive behavior is subsumed into the representational main loop in a natural way.

The APOS, in turn, monitors the acoustic environment continuously. Whenever a human voice is detected: it suspends the navigation system; turns to the interlocutor; executes a dialogue model to attend the interruption; and resumes the navigation task maintaining the original target, starting from the position and orientation that it was left after the interruption.

The coordination involves conditions in which the reactive behavior takes precedence over the representational one. For instance, imagine the robot is moving from position A to B as a result of an action request, and is carrying out a conversation with the user concurrently. In this scenario the robot has to notify the user that the navigation task has been completed when it reaches position B. To do this, the ANS has to put on hold the interpretation of the current dialogue model, make the notification, and resume the DM. Another instance in which reactive behavior takes precedence is when the APOS handles an spontaneous information request produced by the user in the middle of a moving action, which involves the interruption of both the interpretation of the current dialogue model, and perhaps of the ANS. Then, both the DM and the ANS have to be resumed when the spontaneous request has been attended, but from the context that was left after the interruption was handled.

Conversely, the coordination also involves conditions in which the representational behavior takes precedence over the reactive one. For instance, if the robot is engaged in an explanation task it may need to put on hold the APOS to avoid spontaneous distractions,

and restore it when the explanation task has been accomplished. Another condition is when none of the expectations of the current situation are met, and the system has to load and execute a recovery dialogue model. For this, the system may need to suspend both the ANS and the APOS, direct all of its attention towards placing itself in context, and resume both of these when the context has been restored. Here again, the ANS has to resume the navigation task that was performing before the interruption, but from the context (i.e. position and orientation) that was left after the contingency was handled.

Finally, these generic protocols are defined in the coordinator, which controls their execution independently of the dialogue models representing the application task.

4   The robots Golem and Golem-II+

Over the last few years we have been developing the basic structure of IOCA: its dialogue model specification, interpretation theory, and programming environment. We first produced the Golem robot that was able to guide a poster session about our research projects through a spoken Spanish conversation. We also produced several applications to illustrate the integration of language, vision and navigation with Golem (e.g., [Aguilar and Pineda, 2010]). Next, we produced the application "Guess the card: Golem in Universum". It is a multimodal application in a fixed platform in a permanent stand of UNAM's science museum Universum in which the user plays a game with the system through a spoken Spanish conversation supported with computer vision and the display of images [Meza *et al.*, 2010]. Next, we presented the robot Golem-II+ which is also able to guide a poster session, but in addition to the original system, it is capable of interpreting pointing gestures expressed by the user during the interaction, illustrating the coordination between language, vision and motor behavior [Avilés *et al.*, 2010]. All of these applications have been developed using the basic representational loop only. We have also developed and tested the basic APOS algorithms with very promising results [Rascón *et al.*, 2010]. Videos of these systems are available at http://leibniz.iimas.unam.mx/~luis/. At the moment, we are incorporating and testing the extension of IOCA with reactive behaviors in the robot Golem-II+, to model the different test scenarios of the RoboCup@home competition.

References

1. Allen, J.F., Core, M.G.: Draft of DAMSL: Dialog Act Markup in Several Layers Annotation Scheme. Department of Computer Science. Rochester University (1997)
2. Allen, J.F., Byron, D.K., Dzikovska, M., Ferguson, G., Galescu, L., Stent, A.: Toward Conversational Human-Computer Interaction. AI Magazine, 22(4):27–38. Winter (2001)

3. Aguilar, W., Pineda, L.A.: Integrating Graph-Based Vision Perception to Spoken Conversation in Human-Robot Interaction. J. Cabestany et al. (Eds.): IWANN 2009, Part I. LNCS 5517, pp. 789–796. Springer-Verlag Berlin Heidelberg (2009)
4. Avilés, H., Alvarado, M., Venegas, E., Rascón. C., Meza, I., Pineda, L.: Development of a Tour-Guide Robot Using Dialog Models and a Cognitive Architecture. IBERAMIA 2010, LNAI, Vol. 6433, Springer-Verlag. Berlin Heidelberg, pp. 512 – 521 (2010)
5. Avilés, H., Sucar, E., Pineda, L., Mendoza, C.: A comparison of dynamic naïve Bayesian classifiers and Hidden Markov Models for gesture recognition, *Journal of Applied Research and Technology* (to appear).
6. Chong, H.Q., Tan, A.H., Ng, G.W.: Integrated cognitive architectures: a survey. Artificial Intelligence Review, 28:103—130 (2007)
7. Clark, H., Schaefer, E.F.: Contributing to Discourse. *Cognitive Science*, 13:259–294 (1989)
8. Levinson, S.C.: Pragmatics. Cambridge University Press, Cambridge, UK (1983)
9. Mann, W.C., Thompson, S.: Rhetorical Structure Theory: Towards a functional theory of text organization, Text 8(3), pp. 243—281 (1988)
10. Meza, I., Salinas, L., Venegas, E., Castellanos, H., Chavarria, A., Pineda, L.: Specification and Evaluation of a Spanish Conversational System Using Dialogue Models. IBERAMIA 2010, LNAI, Vol. 6433, Springer-Verlag, Berlin Heidelberg, pp. 346 – 355 (2010)
11. Pineda, L., Estrada, V., Coria, S., Allen, J.: The obligations and common ground structure of practical dialogues, Inteligencia Artificial, *Revista Iberoamericana de Inteligencia Artificial*. Vol. 11 (36), pp. 9-17 (2007)
12. Pineda, L.A.: Specification and Interpretation of Multimodal Dialogue Models for Human-Robot Interaction, in Artificial Intelligence for Humans: Service Robots and Social Modeling, G. Sidorov (Ed.), SMIA, México, pp. 33–50 (2008)
13. Pineda, L., Meza, I, Salinas, L.: Dialogue Model Specification and Interpretation for Intelligent Multimodal HCI. A. Kuri-Morales and G. Simari (Eds.): IBERAMIA 2010, LNAI, Vol. 6433, Springer-Verlag. Berlin Heidelberg, pp. 20–29 (2010)
14. Rascón, C., Avilés, H., Pineda, L.: Robotic Orientation towards Speaker in Human-Robot Interaction. IBERAMIA 2010, LNAI, Vol. 6433, Springer-Verlag, Berlin Heidelberg, pp. 10–19 (2010)
15. Tulving, E.: Memory systems: episodic and semantic memory. In: E. Tulving and W. Donaldson (Eds.), Organization of Memory. New York: Academic Press. pp. 381-403 (1972)
16. Richard, T., Vaughan, B., Gerkey, P., Howard, A.: On device abstractions for portable, reusable robot code. In Proc. of the IEEE/RSJ Intl. Conf. on Intelligent Robots and Systems (IROS), pages 2121-2427. Las Vegas, Nevada (2003)

Visual Data Combination for Object Detection and Localization for Autonomous Robot Manipulation Tasks

Luis A. Morgado-Ramirez, Sergio Hernandez-Mendez, Luis F. Marin-Urias,
Antonio Marin-Hernandez, and Homero V. Rios-Figueroa

Department of Artificial Intelligence, Universidad Veracruzana, Sebastian Camacho No. 5,
91000, Xalapa, Ver., Mexico
lamr22@gmail.com, smendez234@hotmail.com, luisfelipe@ieee.org,
{anmarin,hrios}@uv.mx

Abstract. For mobile robot manipulation, autonomous object detection and localization is at the present still an open issue. In this paper is presented a method for detection and localization of simple colored geometric objects like cubes, prisms and cylinders, located over a table. The method proposed uses a passive stereovision system and consists in two steps. The first is colored object detection, where it is used a combination of a color segmentation procedure with an edge detection method, to restrict colored regions. Second step consists on pose recovery; where the merge of the colored objects detection mask is combined with the disparity map coming from stereo camera. Later step is very important to avoid noise inherent to the stereo correlation process. Filtered 3D data is then used to determine the main plane where the objects are posed, the table, and then the footprint is used to localize them in the stereo camera reference frame and then to the world reference frame.

1   Introduction

Automatic and robust detection and spatial localization of objects under no specific or controlled conditions, i.e. unlike of assembly lines or structured environments, is one of the most challenging tasks for computer vision. There are many problems where the use of these sort of solutions can improve the performance of automatic systems, e.g. in autonomous mobile robot manipulators or unknown scene analysis. On this work we focus mainly on mobile robot manipulation scenarios but the approach presented can be adapted to other complex environments.

For autonomous mobile robot manipulators is really a challenge to locate and detect objects on scenes. The applications for these kinds of task vary from folding clothes to environment mapping and so on. Typically the problem of mobile manipulators is decomposed on three stages: a) object detection and localization, b) approach planning and c) finally correct grasping. On this work we focus on the first of the three mentioned stages.

Commonly to detect and localize objects in such scenarios active sensors are used, e.g. active stereovision systems or time of flight (TOF) sensors. In active stereovision

the use of a monocular video camera and a known laser pattern (e.g. straight lines or a matrix of points) is used to recover 3D information from images captured from the camera [1]. On the other side, the use of sensors like LIDARs or TOF cameras, avoid the computation of 3D information as it is returned directly from the sensor and are a very good and robust source of data. As active sensors the consumption of energy is high and it is important to avoid having multiple sensors of the same kind on the same environment. For example having many robots doing their respective tasks on the same environment could be a problem if they use active sensors.

The use of passive stereovision is an alternative to deal with such a problem, however the accuracy of the 3D reconstruction is sometimes reduced. Accuracy on stereovision systems depends on many factors, e.g. a good calibration, the selection of internal parameters of the stereovision process (maximal disparity range, size of disparity window, etc.), the correct choice of lenses for specific tasks, etc.

The main purpose of this work is to allow an autonomous mobile robot to locate simple geometric objects as the ones showed on Fig. 1 (child's toys), in order to be able, on a continuation of this work, to manipulate them.

Fig. 1. Simple Geometric textured objects used in our experiments.

To reach mentioned objects the robot should be at a closer distance of them. Condition that poses some problems, for example, when the objects are closer to the minimal disparity plane, the stereovision correlation process induces many errors (Fig. 2). Moreover, if the size of the objects relative to the image is small, then the correlation window should be reduced to avoid finding false correlation values, however, this compromise the stereo vision accuracy.

On Fig. 2b is showed the results of a 3D visualization process of the recovered 3D information from a single cube in the image. As we can see on Fig. 2a, the results of disparity plane induce errors from which is not possible to recover 3D shape with the desired accuracy to induce form, in this case perpendicular planes belonging to the object. The main factor that induces these errors is the position of the camera relative to the plane where are posed the objects, in this case the table. A tilted camera produce that disparity planes, that are parallel to the image plane, will be not enough

to describe the planes of objects that are not parallel to these planes. Then errors are induced creating larger deformations.

On Fig. 2b are showed some segmented objects where it is possible to see the problem relative to correlation process, as we can see many wrongly matching pixels on the neighborhood of the objects are considered as part of them.

When the objects in the scene are bigger these errors can be neglected, however when it is desired that mobile robots could manipulate commonly humans objects this is not the case. Bigger objects will be more difficult to manipulate by only one anthropomorphous arm.

<table>
<tr><td>(a)</td><td>(b)</td></tr>
</table>
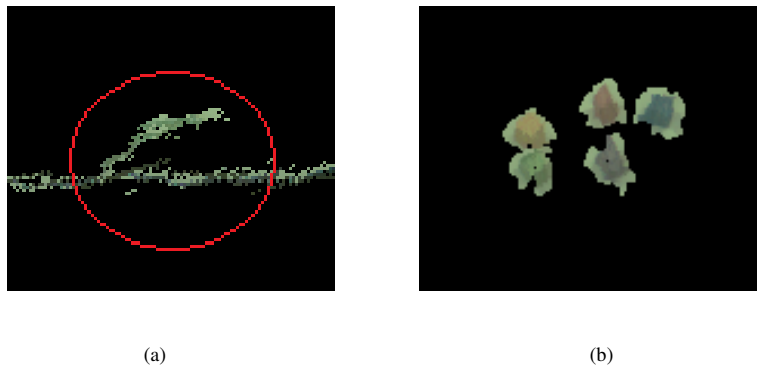
Fig. 2. Stereovision common problems, a) form induced from the correlated data does not match the form of the real object, b) some mismatched pixels create false data, which interpreted with truthful data deforms the objects.

This paper is organized as follow; on next section we analyze some recent related works. On section three and four we present the proposed approach, beginning with the object detection, followed by the object localization method, respectively. On section five we present the results, and finally on section six our conclusions and future work.

2   Related Work

The problem of object detection and localization for autonomous mobile robot is an active research field. As a direct result there are many approaches to deal with such a problem. As it has been exposed previously, many of these works use active sensors, together with CAD models in order to detect known objects and localization. For example in [2] CAD models are used in combination with an efficient hierarchical search computed offline to guide the exhaustive pose estimation.

In [3] it is presented a method for object detection using GPU computation in order to accelerate commonly object detection algorithms usually very slow and impractically to be used on mobile robot manipulation. There are some other approaches that use shapes descriptors, as for example in [4] where these descriptors are used in combination with a TOF sensor in order to recover 3D localization of the

objects detected. In [5] shape descriptors are also used to detect transparent objects detection.

In [6] passive stereo data has been used also in combination with CAD models in order to match known objects. Ulrich et al. in [7] propose a method for 3D model selection from a database over Internet.

There are some approaches to deal with object recognition when 3D points acquire from different sensors. For example in [8] Boyer et al. propose a robust sequential estimator to adjust surfaces of noisy data that included outliers. To eliminate outliers, the detected edges and smooth regions extracted and adjusted the areas determined by the AIC criterion. Takeda and Latombe in [9] considered a special case where the problem can be reduced to a problem in one dimension of a line as a set and compute a maximum likelihood solution.

In this paper, we present an alternative to geometric object detection and localization based only on visual characteristics, without the use of active sensors. The proposed method works at 18 Hz, speed which fast enough to deal with mobile robot manipulation tasks and allowing dynamic object localization, very important for visual servoing used in accurate grasping.

3   Object detection

The methodology proposed for object detection combines two kinds of visual information. On one side a color segmentation procedure is applied to the original images in order to get the regions where the colored objects are. On a second step borders in image are obtained. Both, visual information are merged together as a characteristics level fusion to get a robust object detection method.

3.1   Color Segmentation

Image color segmentation is the decomposition of an image on the colored component parts with the same color attributes. For human beings is a very easy task, however for computer vision systems robust color segmentation is still a challenge. Human beings are able to combine different sources of visual information as texture, gradients, or different tonalities to recover the dominant color of a given object.

For autonomous computer vision systems are not always easy to define the way that all that information could be merged. For example in Fig. 1, are showed some objects that we want to be detected, as we can see, they have texture, and different color tonalities.

The first step in the proposed approach is to convert image to a normalized color space. The result of this process is to eliminate color variations from reflections, shadows or not equal illumination as it is showed on Fig. 3a. However at this stage is very difficult to make a good color segmentation, because as a result of the normalize color process the color space is reduced.

In order to detect easily colors a luminance increase is applied to the resulting image as it is showed on Fig 3b.

A color space reduction is then applied to the processed image in order to cluster similar colors as humans do easily, that is, many green tonalities are grouped together as only green color (Fig 4).

Image color space reduction is obtained applying the following formula:

$$RS_c = \frac{C}{D_v^2} \text{ , with } C \in \{R, G, B\} \tag{1}$$

with RS_c the new color component and D_v the reduction factor for the cubic color space.
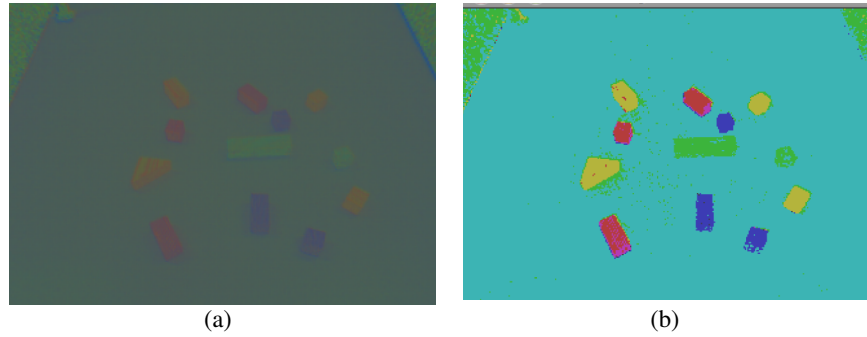
Fig. 3. a) Normalized color space and b) luminance adjustment to separate colors.

In figure Fig. 4a are shown the results for the color space reduction where it is applied a color labeling in order to distinguish more easily the colors. As we can see in this figure, there are still some holes in the objects as well as some colors that do not belong correctly to the segmented object.
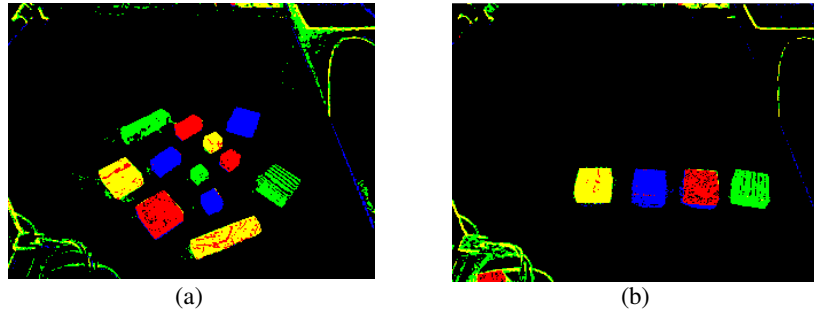
Fig. 4. Two images where reduce space color segmentation is applied.

3.2 Edge Detection

Combination of color segmentation with edge detection allow us to delimit object as well as assign colors to the regions where color has not been detected or it has been wrongly detected.

We use a simple canny edge detector that was the one that gives us best results as it is showed on figure 5. Even so, edge detectors can be used isolated to delimited objects, mainly edge detectors because edge detectors are sensible to illumination conditions given different edges in a sequence of images which correspond most of the time to shadows that are more or less perceive by the camera.

(a)   (b)
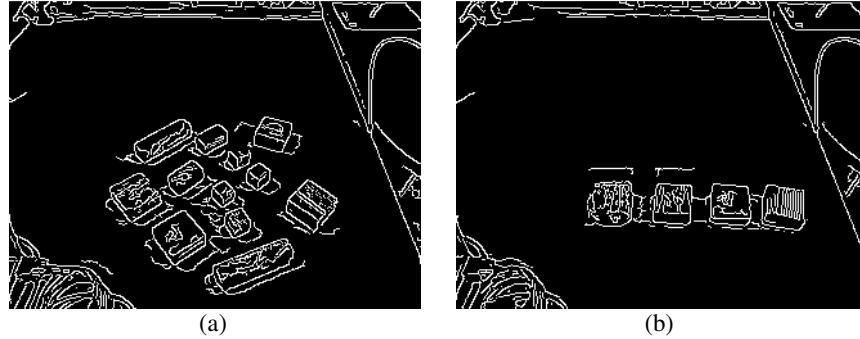
Fig. 5. Canny edge detector applied to the original images.

3.3   Object Detection Data Fusion

Data fusion at this stage is done with the following procedure.

Be *C* the color label of a given pixel and *P* the percentage of similar colored neighbor pixels, then:

```
Add all the edges to a list L.
While L is not empty do
  If the pixel u in L belongs to a given color label C then
    Add u to a region C
    For each neighbor pixel v of u do
      If v belong to the same region C insert v in L
      If not, label as visited pixel.
```


(a)   (b)
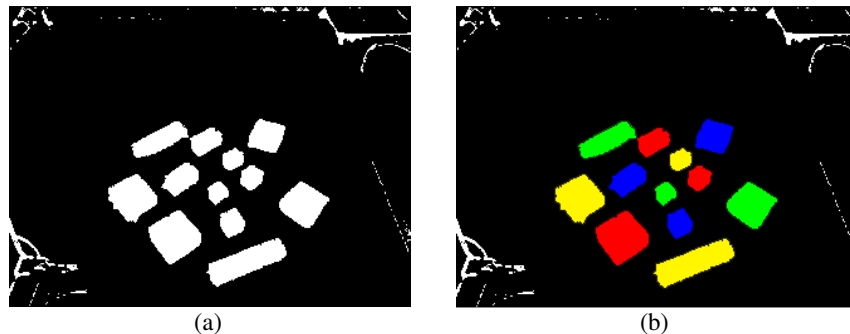
Fig. 6. a) Binary mask obtained by the fusion of color segmentation and edge detection, and in b) Color object labeled.

With this procedure we obtain a binary mask that determines the colored objects as the images showed on Fig. 6a. Finally, dominant label on the object is assigned to the entire segmented region as it is showed on Fig. 6b.

At this stage we have detected colored objects in the scene, now is necessary to localize these objects on the camera reference frame.

4   Object Localization

In order to avoid the problems with the noise produced by the stereovision correlation process as is has been showed on Fig. 2b, we use the object segmentation mask fig. 6 to recover 3D information only on the regions where the objects has been detected Fig. 7a. However, as the objects are small, a very near the minimal disparity plane the shape of the 3D form does not correspond to the real object form as has been described in Fig. 2a.

In order localize objects; we assume that all objects are over a table and as it has been said, all these objects are very simple geometric forms. So, the shape of the footprint in the surface of the table, give us information about the position and orientation of a given object. The problem here is the to find the plane equation corresponding to the table in order to project all the 3D segmented points on this surface to recover their footprint and then their position in the camera reference frame, and then to the world or manipulator reference frame.

As we have seen on Fig. 2a, disparity data has a lot of noise, so is not possible to recover flat surfaces belonging to the up side plane of the objects. In order to deal with this problem we have applied a RANSAC algorithm to find the best plane that fits to our objects and then with the bounding box of the 3D points belonging to the objects in the recently calculated plane, we have move the plane to the bottom of this bounding box.

Then the 3D points belonging to the objects are projected over this plane that correspond to the table plane Fig. 7b.

(a)   (b)
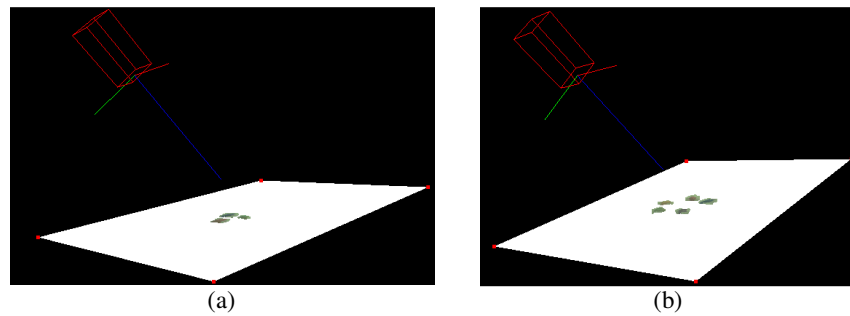
Fig. 7. Projection of 3D seemed points over a fitting plane that correspond to the table plane.

5   Results

In order to get a confidence measure we have compared the results of the proposed methodology for color image segmentation with the ground truth (Fig. 8) of the coor segmented objects and we have obtained a rate of 90% of matched pixels with an average of 2% of false positives and a 8% of true negatives matches.

(a)	(b)
(c)	(d)
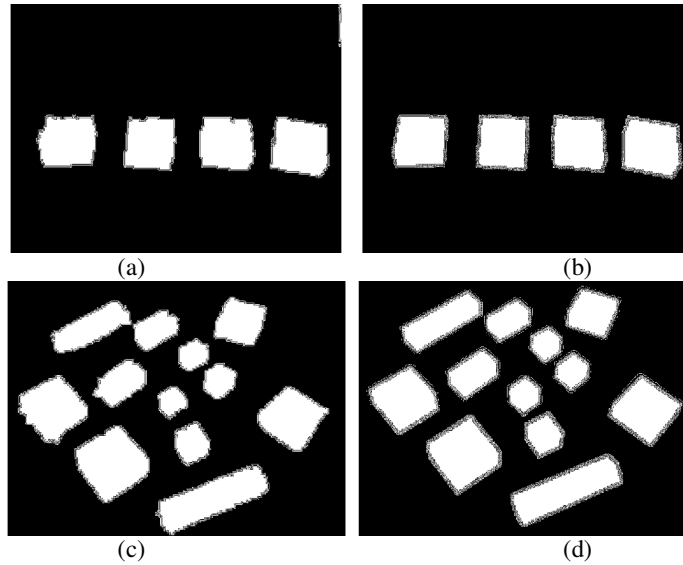
Fig. 8. a) and c) examples of color object segmentation mask and b) and d) corresponding ground truth.

We have estimated a maximal error of 1 cm on the projection of 3D footprint center considered as the location of the objects. Many tests under different light conditions were evaluated to validate the results of the proposed methodology without varying the described accuracy.

6   Conclusions

We have presented a method for simple geometric colored object detection based on the fusion of different visual characteristics. The proposed works at a frame rate of 18 hz, making it ideal for robotics applications where computing time is crucial. The mask obtained by the color segmentation process is used as a noise filter in order to avoid errors on the stereo correlation process that produces bad objects localization estimations. The method can be applied continuously in order to give to a manipulation robot the active state of the world.

Fusion data structure will be used in future works in order to match edges from both images coming from the stereo camera in order to get a more robust object detection and localization.

References

1. Quigley M., Batra S., Gould S., Klingbeil E., Le Q. V., Wellman A., Ng A. Y.: High-accuracy 3d sensing for mobile manipulation: Improving object detection and door opening, in IEEE International Conference on Robotics and Automation (2009)
2. Ulrich M., Wiedemann C., Steger C.: Cad-based recognition of 3D objects in monocular images. In International Conference on Robotics and Automation 1191–1198 (2009)
3. Coates A., Baumstarck P., Le Q. V., Ng A. Y.: Scalable learning for object detection with gpu hardware. In *IROS* 4287–4293 (2009)
4. Marton, Z.; Pangercic, D.; Blodow, N.; Kleinehellefort, J.; Beetz, M.: General 3D modeling of novel objects from a single view. Intelligent Robots and Systems (IROS), 2010 IEEE/RSJ International Conference, 3700–3705 (2010)
5. Fritz M., Darrell M., Black M., Bradski G., Karayev S.: An additive latent feature model for transparent object recognition," in *NIPS*, S. for Oral Presentation (2009)
6. Hillenbrand U.: Pose clustering from stereo data. In Proceedings VISAPP International Workshop on Robotic Perception – RoboPerc (2008)
7. Klank, U.; Zia, M. Z., Beetz, M.: 3D model selection from an internet database for robotic vision. Robotics and Automation. ICRA '09. IEEE International Conference, 2406–2411 (2009)
8. K.L Boyer, M.J. Mirza, and G. Ganguly, The robust sequential estimator: a general approach and its application to surface organization in range data, IEEE Trans. Pattern Anal. Machine Intell., vol. 16, no.10, 987-1001 (1994)
9. H. Takeda and J-C. Latombe, Maximum likelihood fitting of a straight line to perspective range data. IEICE Trans., vol.J77-D-II, no.6, 1096-1103 (1994)

Mobile Robot SPLAM for Robust Navigation

Abraham Sánchez[1], Alfredo Toriz[2], Rene Zapata[2], and Maria Osorio[1]

[1] Benemérita Universidad Autónoma de Puebla, Computer Science Department,
Puebla, Mexico
[2] Montpellier Laboratory of Informatics, Robotics, and Microelectronics (LIRMM),
UMR 5506 - CC 477
161 rue Ada, Montpellier, France
alfredo.torizpalacios@lirmm.fr, zapata@lirmm.fr, asanchez,
aosorio@cs.buap.mx

Abstract. This paper describes a simultaneous planning localization and mapping (SPLAM) methodology, where a mobile robot explores the environment efficiently and also considers the requisites of the simultaneous localization and mapping algorithm. The method is based on the randomized incremental generation of a data structure called Sensor-based Random Tree, which represents a roadmap of the explored area with an associated safe region. A continuous localization procedure based on B-Splines features of the safe region is integrated in the scheme.

1 Introduction

SLAM (Simultaneous Localization And Mapping) is a challenging problem in mobile robotics. SLAM approaches are used simultaneously with classic exploration algorithms [1]; however, results obtained with SLAM algorithms strongly depend on the trajectories performed by the robots, while classic exploration algorithms do not take into account the uncertainty about the localization of the robot when it travels through unknown environments, making harder the construction of the map, when the robot's position is unknown, generating useless and inaccurate maps. With the integrated exploration or SPLAM (simultaneous planning localization and mapping), the robot explores the environment efficiently and also considers the requisites of the SLAM algorithm [2], [3].

An integrated exploration method is introduced in [3] to achieve the balance of speed of exploration and accuracy of the map using a single robot [3]. Freda et al. [2] use a sensor-based random tree (SRT). Recently, a novel laser data based SLAM algorithm using B-Spline as features has been developed in [4]. Extended Kalman filter (EKF) is used in the proposed BS-SLAM algorithm and the state vector contains the current robot pose together with the control points of the splines. The observation model used for the EKF update is the intersections of the laser beams with the splines contained in the map. In our proposal, we did not use the EKF but and integrated exploration based approach, called SRT-B-Splines. In this method, the tree is expanded, while the configurations for the coverage near the frontiers of the robot, that is a new candidate, are selected.

These configurations belonging to the new candidates are evaluated considering the reliability of the expected observable features in those points.

The basics of the B-splines are briefly presented in Section II. The proposed approach to solve the simultaneous planning localization and mapping problem is detailed in Section III. Simulation results are discussed in Section IV. Finally, conclusion and future work are detailed in Section V.

2   B-Splines

Most shapes are simply too complicated to define using a single Bézier curve. A spline curve is a sequence of curve segments that are connected together to form a single continuous curve. A knot vector is a list of parameter values, or knots, that specify the parameter intervals for the individual Bézier curves that make up a B-spline. The purpose of the knot vector is to describe the range of influence for each of the control points [6]. Let a list $t_0 \leq t_1 \leq t_2 \leq \ldots \leq t_{m-1} \leq t_m$ of $m + 1$ non-decreasing numbers, such that the same value should not appear more than k times, $k =$ order of the B-spline. We define the i-th B-spline function $N_{ik}(t)$ of order $k(= k - 1$ degree) as:

$$N_{i1}(t) = \begin{cases} 1 & \text{if } t_i \leq t \leq t_{i+1}, \\ 0 & \text{otherwise.} \end{cases} , \ k = 1 \tag{1}$$

$$N_{ik}(t) = \frac{t - t_i}{t_{i+k-1} - t_i} N_{i,k-1}(t) + \frac{t_{i+k} - t}{t_{i+k} - t_{i+1}} N_{i+1,k-1}(t), \ k > 1 \tag{2}$$

Let the next properties:

1. $N_{ik}(t) > 0$ for $t_i < t < t_{i+k}$
2. $N_{ik}(t) = 0$ for $t_0 \leq t \leq t_i, t_{i+k} \leq t \leq t_{n+k}$
3. $\sum_{i=0}^{n} N_{ik}(t) = 1 \quad t \in [t_{k-1}, t_{n+1}] \quad$ normalizing property

Given a set of $n + 1$ control points $d_i(i = 0, ..., n)$ and a knot vector $T = [t_0, t_1, ..., t_{m-1}, t_m]$ one can define a B-spline $X(t)$ of order k as:

$$X(t) = \sum_{i=0}^{n} d_i N_{ik}(t) \tag{3}$$

where $N_{ik}(t)$ describes the blending B-spline function of degree $k - 1$ associated with the knot vector T.

The simplest method of fitting a set of data points with a B-splines curve is the global interpolation method [6]. The spline fitting problem is, given a set of data points $D_0, D_1, \ldots, D_n$ which correspond to an unknown curve, find the B-spline function to approximate the data points.

3   The SPLAM Approach

Several techniques have been proposed so far to tackle the SLAM problem. The main difference between them concerns basically with the environment representation and the uncertainty description [5]. A wide variety of localization and mapping techniques relies on environment representations consisting of a set of characteristics elements detectable by the robot's sensory system (feature-based maps). Lines and segments are commonly used as features. They can be effectively extracted from range scans and then exploited for localization and/or mapping purposes.

In the integrated exploration approach, the robot simultaneously creates a map of its environment and finds a location in such environment (i.e., the robot takes local decisions on how to move in order to minimize the error of its estimated positions and the positions of the marks). The strategy adopted for the exploration process is called SRT (Sensor Based Random Tree) [5], [8], and is based on the construction of a data structure that represents the roadmap of the explored area with an associated security region (SR); each node tree ($\mathcal{T}$) consists of a robot's position and its associated local security region (LSR) that is constructed through the perception of the robot system. It carries out a continuous localization process based on the extraction of environmental characteristics (curves or lines), these features are compared with the new curves that are extracted from the LSR of the current position. The algorithm implemented for the integrated exploration is described in [9].

The exploration of unknown environments requires an additional functionality because the odometric information reported by the robot, in most cases is not accurate, resulting in inaccurate maps useless for future navigations. The localization function implemented, uses B-spline curves to represent the frontier between the free regions and the obstacles in a complex environment. The proposed algorithm assumes that the robot's initial position is well located and, consequently, the first observation of the environment has a perfect location. Once the robot has moved from a position q_{last} to a position q_{curr}, the new position of the robot is obtained by adding to the last located position, the increment $\triangle x, \triangle y$ and $\triangle \theta$ reported by the robot's odometric system. After this position is estimated, the robot will collect the information of the surrounding environment for the localization process.

The raw data collected by the sensor can not be directly used in the localization process, due to errors inherent to the measurement system used (laser sensor). In our case, we got an equivalent error of $\pm 1\%$ of the measured distance, that will be optimized using the method of least median square (LMS Least Median Square). The decision to use this method is based on a comparative study of different methods proposed in the literature, including RANSAC and its variants (MSAC and NAPSAC), and Least Squares. The minimum is defined as $\min M = med(r_i^2)$, where $r_i (i = 1, ..., n)$ are the residuals of the control points d_i and their corresponding points on the curve: $r_i = |d_i - d_i N_{i,p}(t_k)|$. The treatment of the laser readings will be described in the data segmentation

process. Before the processed data can be used by the localization algorithm, they need to undergo several processes, see Fig. 1:

- FIRST SEGMENTATION. An analysis of the relative position of consecutive data points is performed. The aim is to detect points close enough that belong to the same obstacle.
- SECOND SEGMENTATION. The obtained segments in the first segmentation are again subjected to testing for consecutive points whose angle is below a certain threshold. The objective of this segmentation is to detect corners and curves with high curvatures.
- SETTING. Each of the obstacles of the second segment are adjusted to the B-Spline grade 3 that form its control polygons.
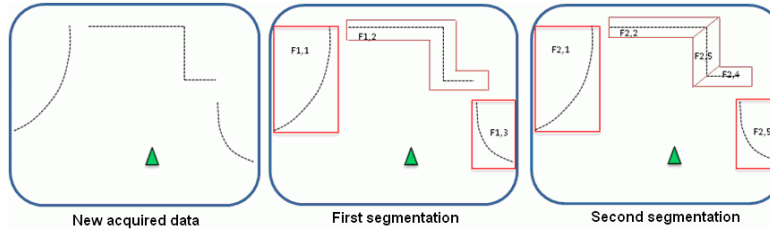
Fig. 1. The segmentation process.

The first segmentation is performed using the adaptive clustering concept, which consists of dividing a dataset into subsets (clusters) such that the data from the same subset share some common characteristic. In adaptive clustering, the membership to a measured point in the subset depends on the distance between the objects and the laser and on the calculation of different values of the discriminant $D_{threshold}$. The clustering process used in this part is based on the classic criteria of Dietmayer [10], whose operation can be explained in the Fig. 2. Pa and Pb represent two consecutive points detected by the laser, while ra and rb are the distances of these points to the coordinates origin. Given the triangle $OPaPb$, where ra and rb are known and α is the angular resolution of the laser, we can apply the cosines theorem to calculate the distance between Pa and Pb:

$$rab = \sqrt{ra^2 + rb^2 - 2rarb\cos(\alpha)}$$

Because the scanner used in our experiments have an angular resolution $\alpha = 0.061$, a very small value according to Dietmayer, it is possible to simplify the calculation of rab assuming that $rab \approx |ra - rb|$. The criteria used to form the clusters is that, if the distance between Pa and Pb is less than $rab \leq C_0 + C_1 \cdot \min\{ra - rb\}$, where $C_1 = \sqrt{2(1 - \cos(\alpha))}$, then Pb belongs to the same cluster than Pa. Otherwise, the points Pa and Pb belong to different clusters. The constant C_0 represents a noise adjustment in the laser measures.
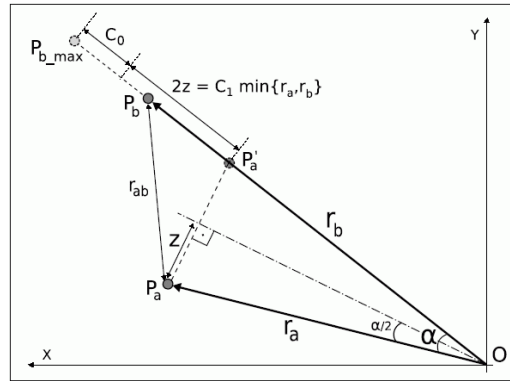
Fig. 2. Illustration of the Dietmayer's clustering criterion.

The other constant, C_1, takes a value not explained by Dietmayer, but, that can be explained using the Fig. 2, where it can be appreciated that $\min\{ra, rb\} = ra$, therefore:

$$C_1 \cdot \min\{ra, rb\} = ra \cdot \sqrt{2(1 - \cos(\alpha))} = 2 \cdot ra \cdot \sqrt{\frac{1 - \cos(\alpha)}{2}}$$

On the other side, the variable named z in the Fig. 2 will take the value:

$$z = ra \cdot \sin(\frac{\alpha}{2}) = ra \cdot \sqrt{\frac{1 - \cos(\alpha)}{2}}$$

Finally, we get $2z = C_1 \cdot ra$; which means that C_1 or ra is the distance between the points Pa and Pa', being Pa' a point on the segment OB located at the same distance from the origin than Pa. On the other hand, knowing that $rb > ra$ is satisfied in the Fig. 2, then:

$$rab = rb - ra \leq C_0 + C_1 \cdot ra$$
$$rb \leq ra + C_0 + C_1 \cdot ra$$

This means that if we add the distances $C1 \cdot ra$ and C_0 to the point Pa', we obtain the point Pb_{max} that corresponds to the maximum distance that point Pb can be moved in order to form part of the same cluster that the point Pa. As mentioned above, the second segmentation has the objective of detecting straight lines that form corners and high curvature loops. To achieve this objective we used the work by Pavlidis and Horowitz named "Split and Merge" [11]. The algorithm has two phases. The first phase is recursive, and consists in dividing the available segments into smaller ones, while the second is used to merge segments that are almost collinear. In Fig. 3, one can see a practical example of the algorithm.

Due to the nature of the method, we can make particular segments of untreated data corresponding to a specific cluster, that is, the method allows us to
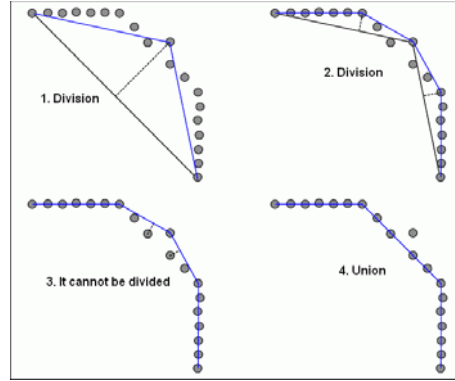
Fig. 3. The split and merge algorithm.

easily identify straight lines but at the same time if the result is a series λ_{min} of non-collinear segments smaller than D_{min} threshold, then we can safely say that the robot is approaching a curve. Thus, the treatment to be given to the data is as follows:

– **Segments of straight lines**. Let $\min M = med(r_i^2)$, where $r_i(i = 1, ..., n$ are the residual of the points to the line $r_i = |y_i - mx_i - b|$. To calculate M, one can use the algorithm proposed by David M. Mount et al., [12].
– **Curves**. Let $\min M = med(r_i^2)$, where $r_i(i = 1, ..., n$ are the residual of the points to the line $r_i = |d_i - d_i N_{i,p}(t_k)|$. This operation is performed by approximating a cubic B-Spline to the points d_i. Once obtained the residuals, there will be a correction, moving the points d_i with larger residuals, a distance heuristically selected, to the B-Spline.
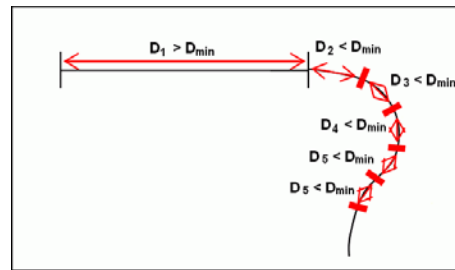
Fig. 4. Segmentation of lines and curves on a cluster by using the split and merge algorithm. D_1 is considered a straight line and the segments D_2, ..., D_5 curves.

Once the data from the sensor are segmented, a process of data association is performed. The first association is crude, and the control points of each segment

obtained in the segmentation process are compared with the control points in the map, using the following criteria:

$$\min(dist(X_{m,i}, X_{o,j})) < d_{min}, i = 1, ..., n_m, j = 1, ..., n_0$$

Where $X_{m,i}$ and $X_{o,j}$ are the control points of the splines, on the map and observed, respectively, n_m and n_0 are the number of control points of the splines on the map and observed, $dist(X_{m,i}, X_{o,j})$ represents the Euclidean distance between the control points, and finally d_{min} is the parameter that will regulate if the points are or not related. If no spline in the map is close enough to a detected spline in order to be related, then this new object is added to the map, once the robot's position has been located. By contrast, if a spline is associated with a map's feature, it is necessary to obtain a concordance between its points, as follows:
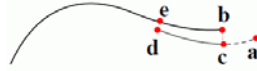
Fig. 5. Concordance between curves.

- One of the ends of the curve is considered point a.
- The closest point between the spline on the map and the point a is calculated (point b).
- If b is one of the endpoints of the spline on the map, then, the point nearest to b in the spline is calculated and named point c, if not, point a is associated with point b.
- The process is repeated starting in the other end of the spline (point d in the Fig. 5, that is associated with the point e on the spline in the map.
- Due to the B-splines property, the length of the curves can be known, and segments e-b and d-c can be adjusted to have the same length. If the difference of the lengths is greater than threshold l_{max}, the extreme elements of the larger curve are eliminated to adjust its size.

Once the curves of the estimated position and the curves of the environment are associated, it is necessary to conduct a final verification of the association by getting the distance from each end of each curve to the other as shown in the Fig. 6:

4   Experimental Results

A simulated robot and the real Pioneer P3DX robot equipped with front and rear bumper arrays, a ring of eight forward ultrasonic transducer sensors (range-finding sonar) and a Hokuyo URG-04Lx laser range finder were used in the experiment. The Pioneer P3DX robot is an unicycle robot. The LIRMM laboratory
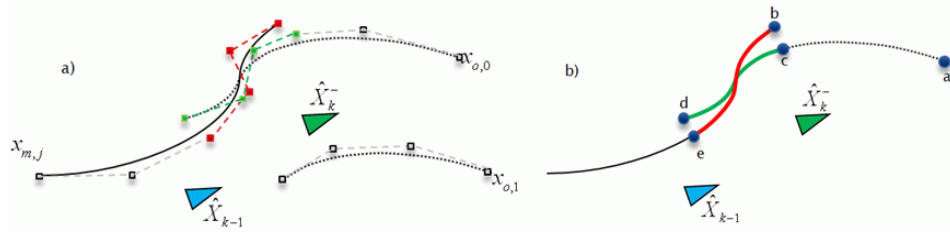
Fig. 6. Two association forms: a) association crude, b) association fine.

environment was used in the experimental and simulation tests (the environment had several corridors). Figure 7 shows the two final maps: in the leftside, the map obtained without a localization process and only with odometric estimates; in the rightside, the map obtained with the proposed approach. Comparing the two final maps, it can be said that the robot did not use the localization process, and collided frequently with the obstacles, as can be appreciated in the left image. Figure 8 shows the odometry errors versus the errors obtained with the proposed approach.
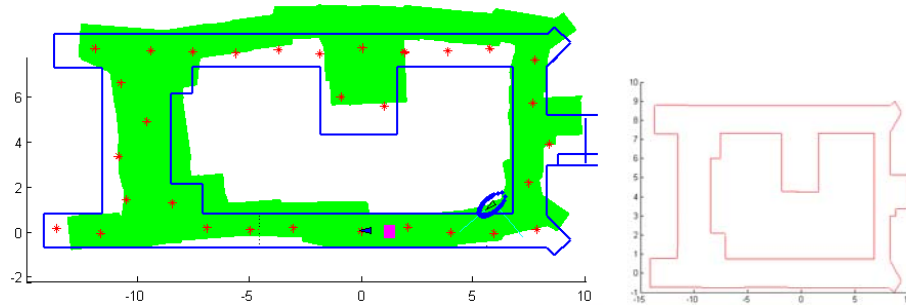
Fig. 7. Final map obtained only with odometric estimates and final map obtained with the SPLAM approach.

For the association process, the basic procedure proposed in [4] was retaken, but with a new functionality derived from the properties of the B-splines, i.e., we ensure that these new curves and those belonging to the environment have the same lengths. This new feature enabled better and more accurate association of the data collected with the sensor than the association obtained with the basic method originally proposed. The geometric properties of the final regions of the curves was considered to make a final association checking with the distances of the points a the end of the curves of the environment and the estimated position in order to verify their similitude. This exhaustive verification is necessary because the nature of the proposed localization method. It can be said that the
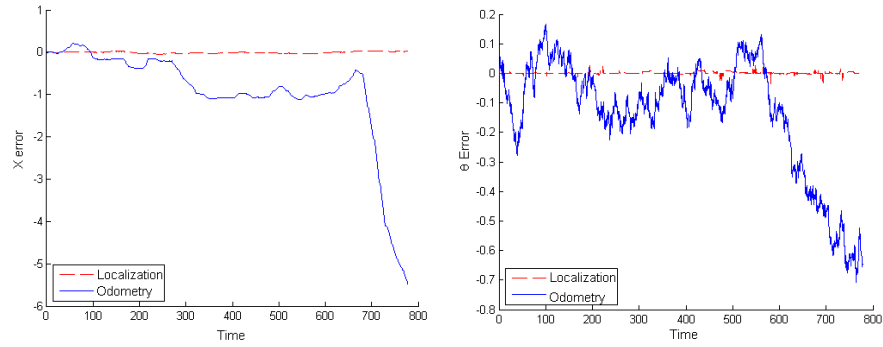
Fig. 8. X, θ errors for the odometry and the proposed approach.

approach presented in this paper, makes a good use of the parametric representation of the environment characteristics at the time of the data association.

The localization capability of a mobile robot is central to basic navigation and map building tasks. The two main instances of mobile robot localization problem are the continuous pose maintenance problem and the global localization also known as 'robot kidnapping' problem. Global position estimation is the ability to determine the robot's position in an a priori or previously learned map, given no information other than that the robot is somewhere in the region represented by the map. Fulfilling all these properties, our method can solve the kidnapping problem in a robust form, as can be seen in Fig. 9.
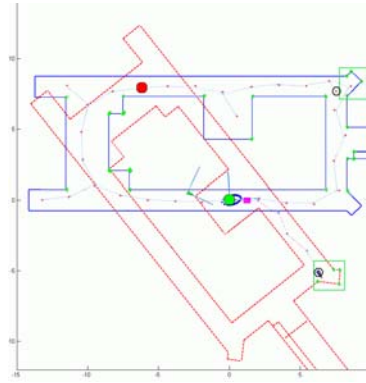
Fig. 9. Snapshot showing the execution of the proposed kidnapping strategy.

5   Conclusions and Future Work

Most of the early SLAM work was point-feature based. The main drawback with point-feature based SLAM is that measurements acquired from typical sensors did not correspond to the feature points in the environment. After the raw sensor data is acquired, post processing is required to extract point features. This process may potentially introduce information loss and data association error. Furthermore, in some situation, the environment does not have enough significant structure to enable point features to be robustly extracted from them.

As a conclusion, we can mention that we have developed a robust SPLAM tool that is not limited to environments with linear features. The localization method is perfectly suited to the new curves that can be increasingly seen in everyday's life. The theory and implementation of the B-splines was a powerful tool in our approach, and can be adapted to environments where the previous methods considered only simple descriptions.

As future work, we have considered the challenge of working with an extension of our proposal to the case of integrated exploration with multiple robots, which will take to us to the search of a solution to the multi-robot localization problem.

References

1. S. Thrun, W. Burgard and D. Fox, "Probabilistic robotics", *The MIT Press*, (2005)
2. L. Freda, F. Loiudice and G. Oriolo., "A randomized method for integrated exploration", *IEEE Int. Conf. on Intelligent Robots and Systems*, (2006) 2457–2464
3. A. A. Makarenko, S. B. Williams, F. Bourgante and H. F. Durrant-Whyte., "An experiment in integrated exploration", *IEEE Int. Conf. on Intelligent Robots and Systems*, (2002) 534–539
4. L. Pedraza, G. Dissanayake, J. Valls Miro, D. Rodriguez-Losada, and F. Matia, "Extending the limits of feature-based SLAM with B-Splines", *IEEE Transactions on Robotics*, Vol. 25, (2009) 353–366
5. A. Garulli, A. Giannitrapani, A. Rossi and A. Vicino, "Mobile robot SLAM for line-based environment representation", *IEEE European Control Conference. CDC-ECC*, (2005) 2041–2046
6. F. Yamaguchi, "Curves and surfaces in computer aided geometric design", *Springer-Verlag*, (1988)
7. G. Oriolo, M. Vendittelli, L. Freda and G. Troso, "The SRT method: Randomized strategies for exploration", *IEEE Int. Conf. on Robotics and Automation*, (2004) 4688–4694
8. J. Espinoza L., A. Sánchez L. and M. Osorio L., "Exploring unknown environments with mobile robots using SRT_Radial", *IEEE Int. Conf. on Intelligent Robots and Systems*, (2007) 2089–209
9. A. Toriz P., A. Sánchez L., R. Zapata and M. Osorio L., "Building feature-based maps with B-splines for integrated exploration". *LNAI 6433*, (2010) 562–571
10. K. C. Dietmayer, J. Sparbert and D. Streller, "Model based object classification and object tracking in traffic scenes from range images", *Proc. of the IV IEEE Intelligent Vehicles Symposium*, (2001) 25–30

11. T. Pavlidis and S. L. Horowitz, "Segmentation of plane curves", *IEEE Transactions on Computers*, Vol. C-23, No. 8, (1974) 860–870

12. D. M. Mount, N. S. Netanyahu, K. Romanik, R. Silverman and A. Y. Wu, "A practical approximation algorithm for the LMS line estimator", *Journal Computational Statistics & Data Analysis*, Vol. 51, Issue 5, (2007)

A Similitude Algorithm through the Web 2.0 to Compute the Best Paths Movility in Urban Environments

Christian J. Abrajan[1], Fabian E. Carrasco[1], Adolfo Aguilar[1], Georgina Flores[1], Selene Hernández[1], and Paolo Bucciol[2]

[1] DSC, Instituto Tecnológico de Puebla,
Av. Tecnológico 420, Maravillas 72220, Puebla, Mexico
[2] French-Mexican Laboratory of Informatics and Automatic Control,
Ex Hacienda Sta. Catarina Mártir s/n, 72820 S. Andrés Cholula, Pue., Mexico
{christian.abrajanf,node.fecc,adolforico2,kremhilda,
hdezrod}@gmail.com
bucciol@ieee.org

Resumen In this paper we present a similitude algorithm based on fuzzy relations to support the movement of a user of the Urban Public Transportation System (UPTS) in the Puebla City. The algorithm computes the best paths in order to support and to optimize the user mobility within urban environments based on three QoS metrics: spatial distance, security and number of transfers. The algorithm feedback uses the knowledge gained through the Web 2.0 to allow the user to query and to exchange experiences. This virtual system incorporates: a decision algorithm of the best paths, search algorithms and fuzzy relations algorithms of the UPTS, in order to benefits local and foreign travelers of the Puebla City or cities with similar characteristics.

Key words: Fuzzy Classification, Similarity Relations, Public Transportation, Shortest Path Algorithms, Shortest Path Optimization, Personal Safety, Web 2.0.

1. Introduction

In this paper a set of algorithms to find the best mobility paths using the Urban Public Transportation System (UPTS) in the City of Puebla is proposed. The objective of our approach is to support the UPTS user in order to provide the best transfer options with respect to: the shortest distance, the lowest cost (number of transfer) and the higher level of security. Our approach is supported on Web 2.0, enabling users to access and exchange knowledge taking advantage of interoperable standards. Our work is based on a novel approach to find the best path between starting and destination points of UPTS users. The path search and selection algorithm choose the best path based on road safety constraints and on a fuzzy classification algorithm, with the ultimate goal to improve the safety of the UPTS users. In Puebla, as happens in major cities, personal safety

is of utmost importance to visitors and residents. Helping them to choose the safest mobility path is therefore one of the primary goals that a modern public transportation system has to achieve. However, path selection algorithms for public transportation systems are actually based on only two types of metrics: temporal (time to reach the destination) and spatial metrics (distance to reach the destination). The case of the Puebla city is even worse. Information on the public transportation system is provided by means of leaflets sold in newspapers stores. Moreover, such information is generally inconsistent and vague. For this reason, UPTS users take decisions on their mobility paths based on intuition and incomplete information, often wasting more resources than needed (such as time and money) and putting into risk their physical safety. The proposed framework has the objective of providing information on the possible mobility paths between various locations in the city, taking into consideration the urban bus routes and safe transfer points. The remainder of this paper is organized as follows: Section 2 presents the state of the art. The theoretical framework is discussed in Section 3. Section 4 describes the architecture of the virtual web platform. Section 5 presents the path search and classification algorithms. Section 6 presents the simulation testbed and the results of the simulation. Finally, Section 7 concludes the paper.

2.   State of the Art

2.1.   Other Similar Applications of Fuzzy Classifications Algorithms

Fuzzy classification is used in several applications like medicine [3][4], urban remoting sensing [5], intrusion detection systems [6], among other. Some classifiers are based on several approaches, some of them are: fuzzy rules [7][8], evolutionary algorithms [6], maximum–likehood classification [5] and neuro–fuzzy models [9]. In this paper, a fuzzy classifier based on similarity relations is used to select from a set of paths that meet desired characteristics (spatial distance and number of transfers) those which meet certain restrictions (such as security level).

2.2.   Similar Works

Páginas Amarillas:[3] Páginas amarillas is a Spanish site that has a section called *Callejero* that focuses on helping visitor and citizens of Spain. It provides information on traffic and allows real-time viewing of traffic webcams.
ViaDF:[4] ViaDF is a route planning web site for the public transportation system in México City, Distrito Federal. The system minimizes the path cost between two points based on the information of the whole public transportation network (Metro, Metrobus, bus) in the city.

---

[3] http://callejero.paginasamarillas.es
[4] http://www.viadf.com.mx/

EL UNIVERSAL:[5] El Universal is a national newspaper that has developed a software tool for anonymous complaint via Internet when threats to personal safety, such as assaults, occur. The site of EL UNIVERSAL uses the Google Maps API [10] to show the place where the threat occurred, with the long-term goal of raising public awareness and preventing more threats in dangerous locations.

3. Theoretical Framework

3.1. *K* Shortest Path

"The K shortest paths"means K loopless paths from the origin to the sink that have the shortest lengths, and "the Kth shortest path"means the last of "the K shortest paths."[2]

The K-th Shortest Path Problem consists on the determination of a set $\{p_1, \ldots p_k\}$ of paths between a given pair of nodes when the objective function of the shortest path problem. That is, not only the shortest path is to be determined, but also the second shortest, the third shortest, and so up to the K-th shortest path.

3.2. Fuzzy Classification

The fuzzy classification could be based on Fuzzy Equivalence Relations. A fuzzy relation, $\underset{\sim}{R}$, on a single universe X, maps elements of X to X through the Cartesian product, where the strength of the relation between (x_1, x_2) ordered pairs of X is measured with a membership function $\mu_{\underset{\sim}{R}}(x_1, x_2) \in [0, 1]$. The Cosine Amplitude [1] is a useful similarity method to assing values to a fuzzy relation when a set of m data samples, $X = \{x_1, x_2, ..., x_m\}$, should be compared with each other. If each of the m data samples, x_i, is characterized by a set of n attributes, $x_i = \{x_{i_1}, x_{i_2}, ..., x_{i_n}\}$, the Cosine Amplitud method computes r_{ij} as

$$r_{ij} = \frac{\|\sum_{k=1}^{n} x_{ik}x_{jk}\|}{\sqrt{\left(\sum_{k=1}^{n} x_{ik}^2\right)\left(\sum_{k=1}^{n} x_{jk}^2\right)}}, \tag{1}$$

where $i, j = 1, 2, ..., m$ and $0 \leq r_{ij} \leq 1$; the resulting fuzzy relation $\underset{\sim}{R}$ is reflexive ($\mu_{\underset{\sim}{R}}(x_i, x_i)$=1) and symmetric $\mu_{\underset{\sim}{R}}(x_i, x_j) = \mu_{\underset{\sim}{R}}(x_j, x_i)$). In order to ensure that $\underset{\sim}{R}$ is an equivalence relation, the transitivity, given by

$$\mu_{\underset{\sim}{R}}(x_i, x_j) = \lambda_1 \text{ and } \mu_{\underset{\sim}{R}}(x_j, x_k) = \lambda_2, \text{ then } \mu_{\underset{\sim}{R}}(x_i, x_k) \geq min\{\lambda_1, \lambda_2\}, \tag{2}$$

is achieved by at most $m - 1$ fuzzy max–min composition of $\underset{\sim}{R}$, where the fuzzy max–min composition of two fuzzy relations $\underset{\sim}{R}$ and $\underset{\sim}{S}$, $\underset{\sim}{T} = \underset{\sim}{R} \circ \underset{\sim}{S}$, is computing by $\mu_T(x_1, x_3) = max_{x_2 \in X}(min(\mu_R(x_1, x_2), \mu_R(x_2, x_3)))$.

---

[5] http://www.eluniversal.com.mx/graficos/graficosanimados10/EU_mapa/mapa.html

Now, if $\underset{\sim}{R}$ is a fuzzy equivalence similarity relation, the data relationed in $\underset{\sim}{R}$ can be classified applying a Lambda–Cut[1] (λ–cut) as follows: given a λ, where $0 \leq \lambda \leq 1$,

$$R_\lambda = \left\{ x | \mu_{\underset{\sim}{R}}(x) \geq \lambda \right\}, \tag{3}$$

then R_λ contains the equivalence classes of the data samples X.

4.   Web 2.0-based Virtual Web Architecture

The use of Information and Communication Technologies (ICT) is a very promising field to solve the routing issues (or at least minimize their impact) of public transportation systems. On one side, it aims to obtain information on the safety of the UPTS system through its most active and dynamic resource, that is, their users. On the other side, it aims to assist UPTS users in the planning of their mobility paths based on safety constraints. Through the design of an ad-hoc web 2.0-based virtual web architecture we propose to improve the information exchange processes between the users of public transportation systems and the correlated governmental agencies such as Secretaria de Comunicaciones y Transportes, Procuraduría General de Justicia, Instituto Nacional de Estadística, Geografía e Informática. The main goal of the platform is twofold: (i) to ease the feedback procedures from the users and (ii) to provide standardized mechanisms to take advantage of the feedback information in the UPTS users' path selection processes.
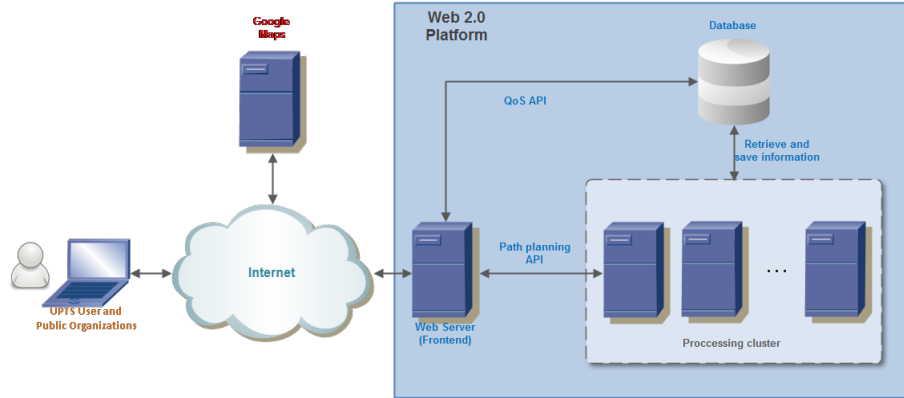
Figura 1. Architectural diagram of the proposed web platform.

The global architecture of the virtual web platform (see figure 1) is composed of:

Web services provider The web services provider is the system front-end to the user. It guarantees the correct service execution through two main API's: the Quality of Service API and the SafeTraveler API.

Algorithm 1 Yen's Algorithm that generates all shortest paths.

Input: s source, t target, P adjacency matrix.
Output: Q paths.
 1:      For every arc $u - v$ on P:
 2:ăăă ăRemove $u - v$ and all nodes preceding u in P from graph.
 3:ăăă ăă$P'_1 \leftarrow$ subpath from s to u in P.
 4:ăăă ăă$P'_2 \leftarrow$ shortest path from u to t in modified graph.
 5:ăăă ăă$P' \leftarrow$ append P'_2 to P'_1
 6:ăăă ăăAdd P' to Q.
 7:ăăă ăăRestore graph.

Processing cluster The processing cluster performs the system processing tasks. In particular, it pre-processes the user queries and executes the real-time path selection algorithms.

Database Within the database the pre-processed information on the most queried paths is stored. This information is constantly updated with the results of the new queries.

Traveler This is the user that will (i) query and (ii) share information with the system.

The platform also includes web 2.0-based mechanisms such as polls and fora (not shown in the figure) to easily obtain feedback from the UPTS users on the quality of the public transportation systems, and interfaces (Web Services) to public organizations to share information related with the UPTS system.

5. Search and Classification Algorithms of Public Transport Path

5.1. Yen's Algorithm

Algorithm of Y. Yen [2] was used to find the shortest routes to reach a destination.

Yen's algorithm calculates new paths from start node s to target node t based on a path P as follows in algorithm 1.

The algorithm of Yen has a time complexity of: $O(kn(m + nlogn))$ with n the number of nodes and m the number of arcs. [11]

5.2. Transfer Algorithm

The general complexity of the algorithm 2 is: $O(\prod_{i=0}^{Nt}(2Nr * (Nn/2^i))$
where:
Nt: Number of transfers Nr: Number of routes Nn: Número of nodes to go
For the case study, we have $Nt = 2$
$O(Nn^3 * Nr^3)$
where Nr is a small value.

Algorithm 2 Algorithm that generates the possible transfer options at UPTS for a road and number of transfers given.

Globals: *Rutas*, m lists of nodes of the UPTS paths,
        Path, list of n nodes with the path from source A to destination B
Input: *indice*, current index of *Path* list
        results, array of k triplets that contain $Rutas_x$, $Path_{abordo}$, $Path_{descenso}$
        transbordos, transfer number allowed
Output: R, l type-*results* arrays that contain the possible transfers
        Base Case If $indice = Path_B$ add *results* to R and return
        Pruning Case If $transbordos = 0$ return
        Search Recursive Case For each $r \in Rutas$
        identify those containing a $(Rutas_{r,i}, ..., Rutas_{r,i+n})$
        list equals to $(Path_{indice}, ..., Path_{indice+n})$,
        where $n \geq 1$, it means, selecting all lists with more than one element,
        creating for each list a triplet $Rutas_r, Path_{indice}, Path_{indice+n}$ in *results*.
        Finally, the $TransferAlgorithm(indice + n, results, transbordos - 1)$ is called.

Algorithm 3 Algorithm that computes the equivalence classes of a data sample.

Input: X, $m \times n$ sample data matrix of m paths from A to B,
        each one of n attributes
        λ, the restriction of classification of m paths
Output: R_λ, $m \times m$ equivalence classes matrix of the m paths
        1. Compute the similarity matrix $\underset{\sim}{R}$ using (1)
        2. Verify if $\underset{\sim}{R}$ is transitive in accordance with (2)
        3. If $\underset{\sim}{R}$ is not an equivalence relation
        then compute $\underset{\sim}{R} = \underset{\sim}{R} \circ \underset{\sim}{R}$ at most $m - 1$ times
        4. Compute the equivalence class matrix R_λ using (3)

5.3.   Fuzzy Classification Algorithm

In order to compute equivalence classes of the paths resulting from the transfer algorithm 2, the algorithm 3 is presented. This algorithm applies the Cosine Amplitude method (step 1) to compute the similarity among the paths given by algorithm 2. In steps 2 and 3 the similarity matrix obtained is transformed into an equivalence relation matrix applying the max–min composition. Finally, in accordance with a restriction level (λ) with respect to safety, distance and transfer numbers given by user, in the step 4 a defuzzification process (λ–cut) is applyed to equivalence relation matrix, obtaining the classification of paths that allow a user to move from point A to point B in Puebla City using UPTS.

Since the complexity of steps 1, 2, 3 and 4 of the Algorithm 1 is $O(mn^2)$, $O(m^3)$, $O(m^4)$ and $O(m^2)$, respectively, the time complexity of algorithm 1 is $O(m^4)$, where m is the paths number from A to B.

6. Results

In the following example (Figure 2), 21 reference points in a part of the City of Puebla are listed in the Table 1. The entry data required by the Virtual System are: origin, destination and security parameters.
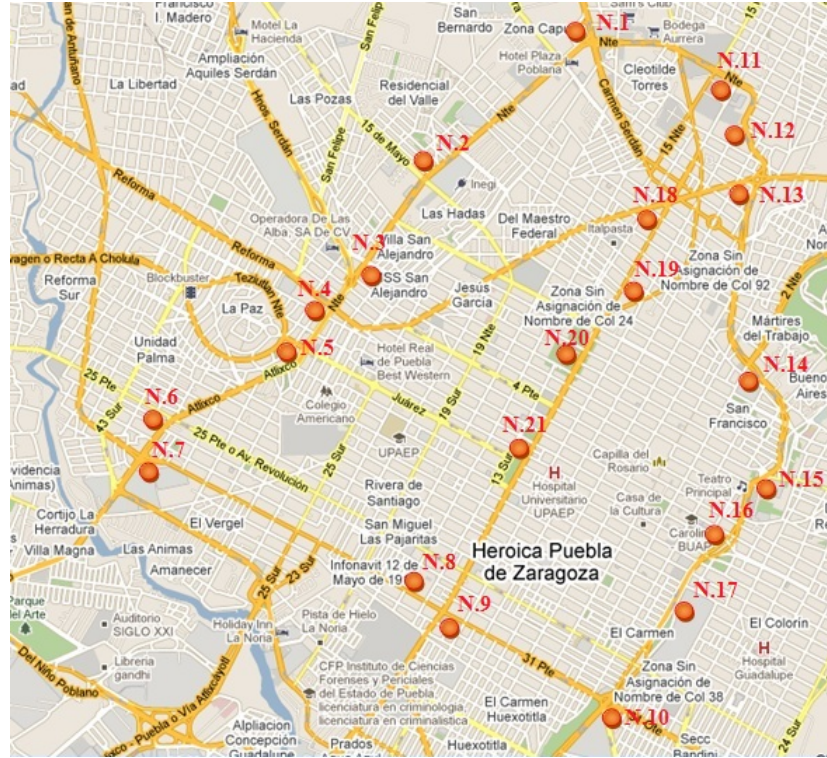
Figura 2. Nodes in the graph

The routes and the nodes shown in Table 2 are done by bus lines. This list of nodes follow a defined sequence as mentioned in the Table. Boardings and transfers the UPTS user needs to make to complete his journey, from the origin to a destination, as well as the route to take, are calculated using the information of the routes given in the graph in Figure 2.

In some cases the list in Table 2 includes 0's just to have the same length in each line of the route.

For example: a user needs to reach from the origin node 1 (CAPU) to the destination node 10 (Pza. Dorada). To do so, he has up to 6 possible routes (k-shortestPath) and a maximum of 3 transfers to make.

The obtained results are shown in Table 3 where: **Path** *n*: is a numeric sequence which identifies each node, and the order that needs to be followed to go

Cuadro 1. List of Nodes in the graph.

Nodo	Nombre	Nodo	Nombre
1	CAPU	12	Karts
2	Pza. San Pedro	13	China Poblana
3	H. San Alejandro	14	H. San José
4	Reforma	15	Centro Convenciones
5	Fuente Los Frailes	16	Reforma y Blvrd. 5 Mayo
6	25 pte y TELMEX	17	CENCH
7	31 pte Marriot	18	Diagonal y 11 Nte
8	Hosp. Universitario	19	Casa del Abue
9	31 pte y 11 sur	20	Museo Ferrocarril
10	Pza. Dorada	21	Paseo Bravo
11	Soriana		

Cuadro 2. List of Routes.

Route	Way
R1	1 - 2 - 3 - 4 - 5 - 6 - 7 - 8 - 9 - 10 - 0 - 0 - 0 - 0 - 0 - 0 - 0
R2	10 - 9 - 8 - 7 - 6 - 5 - 4 - 3 - 2 - 1 - 0 - 0 - 0 - 0 - 0 - 0 - 0
R3	1 - 11 - 12 - 13 - 14 - 15 - 16 - 17 - 10 - 0 - 0 - 0 - 0 - 0 - 0 - 0- 0
R4	10 - 17 - 16 - 15 - 14 - 13 - 12 - 11 - 1 - 0 - 0 - 0 - 0 - 0 - 0 - 0 - 0
R5	8 - 7 - 6 - 5 - 4 - 3 - 2 - 1 - 11 - 12 - 13 - 14 - 15 - 16 - 17 - 10
R6	1 - 11 - 18 - 19 - 20 - 21 - 9 - 0 - 0 - 0 - 0 - 0 - 0 - 0 - 0 - 0 - 0
R7	9 - 21 - 20 - 19 - 18 - 11 - 1 - 0 - 0 - 0 - 0 - 0 - 0 - 0 - 0 - 0 - 0
R7	15 - 20 - 21 - 0 - 0 - 0 - 0 - 0 - 0 - 0 - 0 - 0 - 0 - 0 - 0 - 0
R8	21 - 20 - 15 - 0 - 0 - 0 - 0 - 0 - 0 - 0 - 0 - 0 - 0 - 0 - 0 - 0
R9	20 - 21 - 4 - 5 - 6 - 0 - 0 - 0 - 0 - 0 - 0 - 0 - 0 - 0 - 0 - 0
R10	6 - 5 - 4 - 21 - 20 - 0 - 0 - 0 - 0 - 0 - 0 - 0 - 0 - 0 - 0 - 0

Cuadro 3. Results of k-shortest path and transfers.

Path 1:	$1-11-12-13-14-15-16-17-10$			Weight:	$20u$
Sol 1:	$3-1-10$	Sol 2:	$5-1-11$ $3-11-10$	Sol 3:	$5-1-12$ $3-12-10$
Sol 4:	$5-1-13$ $3-13-10$	Sol 5:	$5-1-14$ $3-14-10$	Sol 6:	$5-1-15$ $3-15-10$
Sol 7:	$5-1-16$ $3-16-10$	Sol 8:	$5-1-17$ $3-17-10$	Sol 9:	$6-1-11$ $3-11-10$
Sol 10:	$6-1-11$ $5-11-12$ $3-12-10$	Sol 11:	$6-1-11$ $5-11-13$ $3-13-10$	Sol 12:	$6-1-11$ $5-11-14$ $3-14-10$
Sol 13:	$6-1-11$ $5-11-15$ $3-15-10$	Sol 14:	$6-1-11$ $5-11-16$ $3-16-10$	Sol 15:	$6-1-11$ $5-11-17$ $3-17-10$
Path 2:	$1-2-3-4-5-6-7-8-9-10$			Weight:	$24u$
Sol 1:	$1-1-10$				
Path 3:	$1-2-3-4-21-9-10$			Weight:	$26u$
No solutions for Path 3 with 3 transfers.					
Path 4:	$1-11-18-19-20-15-16-17-10$			Weight:	$28u$
Sol 1	$6-1-20$ $9-20-15$ $3-15-10$				
Path 3:	$1-11-18-19-20-15-16-17-10$			Weight:	$30u$
No solutions for Path 6 with 3 transfers.					
Path 6:	$1-11-18-19-20-21-9-10$			Weight:	$30u$
Sol 1:	$3-1-11$ $6-11-9$ $1-9-10$	Sol 2:	$5-1-11$ $6-11-9$ $1-9-10$	Sol 3:	$6-1-9$ $1-9-10$

from the origin node to the destination node in each of the routes.

Weight: is the path weight given in "u" units.

Sol n: contains a group of (R, O, D) triplets, where R indicates the route to board, O is the bus stop R, and D is either a bus stop to transfer or the destination. It is worth mentioning that the order of the triplets in the result list is the sequence in which the buses need to be boarded.

The 20 found solutions are mapped obtaining a $m \times n$ matrix.

Given the following $m \times n$ matrix $X = [X1 \ \ X2]$, of $m = 20$ (columns) paths from A (CAPU) to B (Pza. Dorada), each one of $n = 5$ security levels: total, high, medium, low and poor (rows):

$$X1 = \begin{bmatrix} 0 & 0,33 & 0 & 0 & 0 & 0 & 0 & 0 & 0,33 & 0,25 \\ 0 & 0 & 0 & 0 & 0 & 0 & 0 & 0 & 0 & 0 \\ 0,50 & 0,33 & 0,67 & 0,67 & 0,67 & 0,33 & 0,33 & 0,33 & 0,33 & 0,50 \\ 0 & 0 & 0 & 0 & 0 & 0,33 & 0,33 & 0,33 & 0 & 0 \\ 0,50 & 0,33 & 0,33 & 0,33 & 0,33 & 0,33 & 0,33 & 0,33 & 0,33 & 0,25 \end{bmatrix},$$

$$X2 = \begin{bmatrix} 0,25 & 0,25 & 0,25 & 0,25 & 0,25 & 0 & 0 & 0,25 & 0,25 & 0 \\ 0 & 0 & 0 & 0 & 0 & 0 & 0 & 0 & 0 & 0 \\ 0,50 & 0,50 & 0,25 & 0,25 & 0,25 & 0,50 & 0,50 & 0,50 & 0,50 & 0,67 \\ 0 & 0 & 0,25 & 0,25 & 0,25 & 0 & 0,25 & 0 & 0 & 0 \\ 0,25 & 0,25 & 0,25 & 0,25 & 0,25 & 0,50 & 0,25 & 0,25 & 0,25 & 0,33 \end{bmatrix},$$

the Algorithm 3 computes the equivalence classes of Table 4. When $\lambda = \{0,9, 0,91\}$ the method computes two equivalence classes, grouping the 1-12 and 16-20 paths in the equivalence class 1: the paths with more unsafe transfers at a higher rate; and groupint the 13-15 paths in the equivalence class 2: the paths with a smaller proportion of unsafe transfers. In accordance with these results, the paths of the equivalence class 2 are preferable to the paths of the equivalence class 1.

Cuadro 4. Equivalence Classes Obtained by Fuzzy Classification Algorithm

λ	Class 1	Class 2	Class 3	Class 4	Class 5	Class 6	Class 7
0.90,0.91	1-12, 16–20	13-15	–	–	–	–	–
0.92,0.93, 0.94	1,3-5, 16,20	2,9-12, 18,19	6-8, 17, 13–15	–	–	–	–
0.95,0.96, 0.97,0.98,0.99	1,16	2,9	3-5, 20	6-8	10-12, 18,19	13-15	17

Doing a similar analysis as above, in Table 4, when $\lambda = \{0,92, 0,93, 0,94\}$, the Algorithm 3 computes three equivalence classes: the first class comprises the paths with medium security transfers at most; the second class comprises the paths with safe, fairly safe and unsafe transfers at the same rate; most of the third class paths have a balance of medium security, low security and unsafe

transfers. View of these results, the paths of the second equivalence class are preferable.

Finally, when $\lambda = \{0,95, 0,96, 0,97, 0,98, 0,99\}$, there are seven equivalence classes and the most recommended are first the fifth class and second the third class, because in the fifth class paths most of their transfers have medium security, and the third class paths have medium security transfers in greater proportion than unsafe transfers. All other classes are less desirable because the transfers with low security and unsafe are significant.

7. Conclusions

One of the main characteristics of the cities in developing countries is insecurity in certain urban areas. This Web platform designed to improve the integrity of UPTS traveler.

Mexico City and developing countries with similar characteristics, using a network of public disorderly public transport, which requires the traveler a precise knowledge of the public transport routes, safe areas for transfers and potential career options to ensure their integrity during their trip.

The creation of a social network based on the concepts of Web 2.0 provide greater speed in the exchange of experiences among travelers, with these preferences stored to support future travelers.

The connection of this site via Web Services, provides mechanisms for the exchange of knowledge among end users (travelers) and the opportunity that other sites use this service, incorporating the platform into the cloud computing.

Tackling a complex problem with a fuzzy classification algorithm provides a new approach to research to automatically find the path between two points, considering fuzzy parameters and the integrity of travelers.

Despite being a cubic algorithm, the pre-processing routes, helps to reduce the dimension of the problem. The use of robust computational architecture and parallelization of these, improves performance.

Referencias

1. Ross, J.: Fuzzy Logic with Engineering Applications. John Wiley & Sons (2004)
2. Yen J.:Finding the K shortest loopless paths in a network. Management Science (1977)
3. Sun, R., Wang, Y.; Atrial Arrhythmias Detection Based on Neural Network Combining Fuzzy Classifiers. Advances in Neural Networks 4492, 284–292 (2007)
4. Keles,A., Hasiloglu, A.S., Keles, A., Aksoy, Y.: Neuro-fuzzy classification of prostate cancer using NEFCLASS-J. Computers in Biology and Medicine, vol. 37, issue 11, 1617–1628 (2007)

5. Shackelford, A.K., Davis, C.H.: A hierarchical fuzzy classification approach for high-resolution multispectral data over urban areas. IEEE Transactions on Geoscience and Remote Sensing, vol. 41, issue 9, 1920–1932 (2003)
6. Özyer, T., Alhajj, R., Barker, K.: Intrusion detection by integrating boosting genetic fuzzy classifier and data mining criteria for rule pre-screening. Journal of Network and Computer Applications 30(1), 99–113 (2007)
7. Sánchez, L., Couso, I., Corrales, J.A.: Combining GP operators with SA search to evolve fuzzy rule based classifiers. Information Sciences 136, 175–191 (2001)
8. Evsukoff, A.G., Costa, M.C.A, Ebecken, N.F.F.: High Performance Computing for Computational Science–VECPAR 2004. LNCS 3402, 63–96 (2004)
9. Ozturk, A., Arslan, A., Hardalac, F.: Comparison of neuro-fuzzy systems for classification of transcranial Doppler signals with their chaotic invariant measures. Expert Systems with Applications 32(2), 1044–1055 (2008)
10. API Google MAPS.: Google Maps API Family., available at `http://code.google.com/apis/maps/index.html`
11. Vanhove, S., Fack, V.: Fast Generation of Many Shortest Path Alternatives, Belgium

Author Index
Índice de autores

Editorial Board of the Volume
Comité editorial de volumen

Felix F. Gonzalez-Navarro
Rafael Guzman Cabrera
Hartmut Haehnel
Jin-Kao Hao
Yasunari Harada
Pitoyo Hartono
Rogelio Hasimoto
Jean-Bernard Hayet
Donato Hernandez Fusilier
Oscar Herrera
Ignacio Herrera Aguilar
Joel Huegel
Michael Huhns
Dieter Hutter
Pablo H. Ibarguengoytia
Mario Alberto Ibarra-Manzano
Héctor Jiménez Salazar
Moa Johansson
W. Lewis Johnson
Leo Joskowicz
Chia-Feng Juang
Hiroharu Kawanaka
Shubhalaxmi Kher
Ryszard Klempous
Mario Koeppen
Vladik Kreinovich
Sergei Kuznetsov
Jean-Marc Labat
Susanne Lajoie
Ricardo Landa Becerra
H. Chad Lane
Reinhard Langmann
Bruno Lara
Yulia Ledeneva
Ronald Leder
Sergio Ledesma-Orozco
Yoel Ledo Mezquita
Eugene Levner
Derong Liu
Weiru Liu
Giovanni Lizarraga
Aurelio Lopez
Omar Lopez
Virgilio Lopez
Gabriel Luque
Sriram Madurai
Tanja Magoc
Luis Ernesto Mancilla
Claudia Manfredi
J. Raymundo Marcial-Romero
Antonio Marin Hernandez
Luis Felipe Marin Urias

Urszula Markowska-Kaczmar
Ricardo Martinez
Edgar Martinez-Garcia
Jerzy Martyna
Oscar Mayora
Gordon Mccalla
Patricia Melin
Luis Mena
Carlos Merida-Campos
Efrén Mezura-Montes
Gabriela Minetti
Tanja Mitrovic
Dieter Mitsche
Maria-Carolina Monard
Luís Moniz Pereira
Raul Monroy
Fernando Martin Montes-Gonzalez
Manuel Montes-Y-Gómez
Oscar Montiel
Jaime Mora-Vargas
Eduardo Morales
Guillermo Morales-Luna
Enrique Munoz de Cote
Angel E. Munoz Zavala
Angelica Munoz-Melendez
Masaki Murata
Rafael Murrieta
Tomoharu Nakashima
Atul Negi
Juan Carlos Nieves
Sergey Nikolenko
Juan Arturo Nolazco Flores
Paulo Novais
Leszek Nowak
Alberto Ochoa O.Zezzatti
Iván Olier
Ivan Olmos
Constantin Orasan
Fernando Orduña Cabrera
Felipe Orihuela-Espina
Daniel Ortiz-Arroyo
Mauricio Osorio
Elvia Palacios
David Pearce
Ted Pedersen
Yoseba Penya
Thierry Peynot
Luis Pineda
David Pinto
Jan Platos
Silvia Poles
Eunice E. Ponce-De-Leon

Volodimir Ponomaryov
Edgar Alfredo Portilla-Flores
Zinovi Rabinovich
Jorge Adolfo Ramirez Uresti
Alonso Ramirez-Manzanares
Jose de Jesus Rangel Magdaleno
Francisco Reinaldo
Carolina Reta
Carlos A Reyes-Garcia
María Cristina Riff
Homero Vladimir Rios
Arles Rodriguez
Horacio Rodriguez
Marcela Rodriguez
Katia Rodriguez Vazquez
Paolo Rosso
Jianhua Ruan
Imre J. Rudas
Jose Ruiz Pinales
Leszek Rutkowski
Andriy Sadovnychyy
Carolina Salto
Gildardo Sanchez
Guillermo Sanchez
Eric Sanjuan
Jose Santos
Nikolay Semenov
Pinar Senkul
Roberto Sepulveda
Leonid Sheremetov
Grigori Sidorov
Gerardo Sierra

Lia Susana Silva-López
Akin Sisbot
Aureli Soria Frisch
Peter Sosnin
Humberto Sossa Azuela
Luis Enrique Sucar
Sarina Sulaiman
Abraham Sánchez
Javier Tejada
Miguel Torres Cisneros
Juan-Manuel Torres-Moreno
Leonardo Trujillo Reyes
Alexander Tulupyev
Fevrier Valdez
Berend Jan Van Der Zwaag
Genoveva Vargas-Solar
Maria Vargas-Vera
Wamberto Vasconcelos
Francois Vialatte
Javier Vigueras
Manuel Vilares Ferro
Andrea Villagra
Miguel Gabriel Villarreal-Cervantes
Toby Walsh
Zhanshan Wang
Beverly Park Woolf
Michal Wozniak
Nadezhda Yarushkina
Ramon Zatarain
Laura Zavala
Qiangfu Zhao

Additional Reviewers

Árbitros adicionales

Aboura, Khalid
Acosta-Guadarrama, Juan-Carlos
Aguilar Leal, Omar Alejandro
Aguilar, Ruth
Arce-Santana, Edgar
Bankevich, Anton
Baroni, Pietro
Bhaskar, Pinaki
Bolshakov, Igor
Braga, Igor
Cerda-Villafana, Gustavo
Chaczko, Zenon
Chakraborty, Susmita
Chavez-Echeagaray, Maria-Elena
Cintra, Marcos
Confalonieri, Roberto
Darriba, Victor
Das, Amitava
Das, Dipankar
Diaz, Elva
Ezin, Eugene C.
Figueroa, Ivan
Fitch, Robert
Flores, Marisol
Gallardo-Hernández, Ana Gabriela
Garcia, Ariel
Giacomin, Massimiliano
Ibarra Esquer, Jorge Eduardo

Joskowicz, Leo
Juárez, Antonio
Kawanaka, Hiroharu
Kolesnikova, Olga
Li, Hongliang
Lopez-Juarez, Ismael
Montes Gonzalez, Fernando
Murrieta, Rafael
Navarro-Perez, Juan-Antonio
Nikodem, Jan
Nurk, Sergey
Ochoa, Carlos Alberto
Orozco, Eber
Pakray, Partha
Pele, Ofir
Peynot, Thierry
Piccoli, Maria Fabiana
Ponomareva, Natalia
Pontelli, Enrico
Ribadas Pena, Francisco Jose
Rodriguez Vazquez, Katya
Sánchez López, Abraham
Sirotkin, Alexander
Suárez-Araujo, Carmen Paz
Villatoro-Tello, Esaú
Wang, Ding
Yaniv, Ziv
Zepeda, Claudia